

REPORT OF THE FIFTH SCAR ANTARCTIC GEODESY SYMPOSIUM

INTERNATIONAL COUNCIL FOR SCIENCE
SCIENTIFIC COMMITTEE ON ANTARCTIC RESEARCH

SCAR Report
No 23, April 2005

Contents

SCAR Working Group on Geodesy and Geographic Information	
Report of the Fifth SCAR Antarctic Geodesy Symposium, Lviv, Ukraine, 14–17 September, 2003	1
Appendices	83

Published by the
SCIENTIFIC COMMITTEE ON ANTARCTIC RESEARCH
at the
Scott Polar Research Institute, Cambridge, United Kingdom

CONTENTS

Page

INTRODUCTION

PAPERS PRESENTED AT THE SYMPOSIUM

<i>Valery Lytvynov, Gennadi Milinevsky, Svetlana Kovalenok, Elena Chernysh, Rudolf Greku:</i> Ukraine National Antarctic Program: Geodesy Activity	1
<i>John Manning:</i> The Evolution of the GIANT Program	1
<i>Gary Johnston, John Manning, John Dawson, Paul Digney:</i> Geodesy Activities in PC Mega	7
<i>Hannu Koivula, Jaakko Mäkinen:</i> Geodetic Activities at Finnish Antarctic Research Station Aboa	10
<i>Andrzej Pachuta:</i> An Outline of Polar Expeditions of the Scientists from Warsaw University of Technology	13
<i>Olexandr Dorozhynskyy, Volodymyr Glotov:</i> Photogrammetrical Investigations of the Antarctic Coast	14
<i>Alexander V Prokopov, Yeugeniy V Remayev:</i> Tropospheric Delay Modeling for GPS Measurements in Antarctica	14
<i>Jan Cisak:</i> Overview of the Research on the Atmospheric Impact on GPS Observation in Polar Regions	15
<i>Fedir Zablotskyj, Alexandra Zablotska, Natalya Dovhan:</i> An Analysis of Contribution of the Troposphere and Lower Stratosphere layers to forming of the Tropospheric Delay Wet Component	23
<i>Alexander Prokopov, Alla Zanimonska:</i> The Second Order Refraction Effects for GPS Signals Propagation in Ionosphere	25
<i>I. Shagimuratov, A. Krankowski, L. W. Baran, J. Cisak, G.Yakimova</i> Storm-time structure and dynamics of the ionosphere obtained from GPS observations	28
<i>I. Shagimuratov, L. W. Baran, A. Krankowski, J. Cisak, I. Epishov:</i> Development of TEC fluctuations in Antarctic ionosphere during storm using GPS observations	32
<i>P. Wielgosz, I. Kashani, D. Grejner-Brzezinska, J. Cisak</i> Regional Ionosphere Modeling Using Smoothed Pseudoranges	37
<i>Svetlana Kovalenok, Gennadi Milinevsky, Maksim Moskalevsky, Vladimir Glotov,</i> <i>Korniliy Tretjak, Rudolf Greku, Yury Ladanovsky, Pavel Bahmach</i> Argentine Island Ice Cap Geodesy Survey for Climate Change Investigation	41
<i>Yaromyra Kostetska, Lyubov Yankiv-Vitkovska</i> On the Influence of the Solar Activity on the Results of GPS Measurements	41
<i>E Dongchen, Zhou Chunxia, Liao Mingsheng</i> Application of SAR Interferometry in Grove Mountains, East Antarctica	42
<i>E Dongchen, Li Fei, Zhang Shengkai, Jiang Weiping:</i> The Establishment of GPS Control Network and Data Analysis in the Grove Mountains, East Antarctica	46
<i>Richard D. Sanchez:</i> Positional Accuracy of Airborne Integrated Global Positioning and Inertial Navigation Systems for Mapping in Glen Canyon, Arizona	50
<i>A. Capra, F. Mancini, M. Negusini, G. Bitelli, S. Gandolfi, P. Sarti, L. Vittuari, A. Zanutta</i> VLNDEF Network for Deformation Control and as a Contribution to the Reference Frame Definition	57
<i>P.Sarti, J.Manning, A.Capra, L.Vittuari:</i> A Project on Local Ties and Co-locations in Antarctica	57
<i>Alexandr Yuskevich:</i> Accomplishment of Topographic–Geodetic Research Works in Antarctica	58
<i>Y.M Zanimonskiy:</i> On the Randomization of GNSS Solutions	58
<i>K.R.Tretyak:</i> Optimization of Geodynamic Network on the Argentina Islands Neighbouring to Vernadsky Antarctic Station	58

REPORT OF THE FIFTH SCAR ANTARCTIC GEODESY SYMPOSIUM

CONTENTS

	Page
<i>G. Bitelli , A. Capra, F. Coren, S. Gandolfi, P.Sterzai</i> Geoid Estimation on Northern Victoria Land	59
<i>A. Marchenko, Z. Tartachynska, A. Yakimovich, F. Zablotzkyj:</i> Gravity Anomalies and Geoid Heights derived from Ers-1, Ers-2, and Topex/Poseidon Altimetry in the Antarctic Peninsula Area	60
<i>Gennadi Milinevsky:</i> Tidal Observations at Faraday/Vernadsky Antarctic Station	64
<i>J. Krynski, Y.M. Zanimonskiy:</i> Current Results on the Investigation of GPS Positioning Accuracy and Consistency	64
<i>Rudolf Greku, Ksenya Bondar, Victor Usenko:</i> Application of the Planetary Geodesy Methods (the Geoid Theory) for the Reconstruction of the Earth's Interior Structure in the Western Antarctic	71
<i>Rudolf Greku, Gennady Milinevsky, Yuriy Ladanovsky, Pavel Bahmach, Tatyana Greku:</i> Results of GPS, Ground Photogrammetry, Echosounding and ERS Interferometric Surveys During Ukrainian Antarctic Expeditions	74
<i>M. Jia, J. Dawson, G. Luton, G. Johnston, R. Govind, J. Manning:</i> Crustal Motion in East Antarctica Derived from GPS Observations	76
<i>Valentyn Maksymchuk, Yury Gorodysky, Ihor Chobotok, Valentyna Kuznetsova:</i> Recent Geodynamics of the Earth's Crust in the Region of Antarctic Station "Academic Vernadsky" due to Results of Tectonomagnetic Investigations	81
<i>Yu.V. Kozlenko, I.N. Korchagin, V.D. Solovjov:</i> Gravity Studies of the Western Antarctic Region – New Possibilities in Geophysical Modelling	82
 APPENDICES	
1. List of Participants	83
2. Symposium Programme	84
3. List of Papers	86

Report of the

FIFTH ANTARCTIC GEODESY SYMPOSIUM 2003
Lviv, Ukraine, 14-17 September, 2003

INTRODUCTION

This fifth SCAR Antarctic Geodesy Symposium (AGS03) was held at the University "Lviv Polytechnic", Lviv. It was attended by 38 participants, which included representatives of nine SCAR countries. (See list of attendees in Appendix 1).

The activities included a welcome reception for participants at the Assembly Hall of the University "Lviv Polytechnic", a walking tour of the University and a symposium dinner held at Oles'ko Castle.

The symposium commenced with opening addresses from the University Administration, SCAR Geosciences SSG, Ukrainian Antarctic Centre and the Public Geodetic Service of Ukraine. They were followed by an overview of the Ukraine National Antarctic Program by Dr Milinevsky from the Ukrainian Antarctic Centre detailing geodesy activity in the Argentine Island archipelago.

The program included 36 presentations and a GIANT Business meeting (see Program in Appendix2). It contained a strong focus from Ukraine and Polish scientists on atmospheric studies related to GPS. Dr Milinevsky presented the history and status of the tide gauge at the Faraday/Vernadsky Antarctic station which was installed in 1947 and provides an important record of long term sea level variation due to climate change.

Professor E Dongchen from China confirmed in his paper that Interferometric Synthetic Aperture Radar is potentially a very useful technique to be utilized in Antarctica for measuring ice surface elevation providing it is well controlled with GPS positions.

Australia presented a background paper on the Evolution of the GIANT program, the recent field activity during the very successful Prince Charles Mountains Expedition of Germany and Australia (PCMEGA) and preliminary tectonic motions from their continuous GPS stations in Antarctica

Italy presented activities and impressive results from their Victoria land Deformation network (Dr Alessandro Capra) and Dr Sarti proposed to upgrade local geodetic ties at collocated sites to improve the Antarctic and global reference frames.

Dr Alexander Yuskevitch from Russia summarised the methods of the fundamental astronomic geodetic network (FAGN) and the on going development of the high precision geodetic network (H-PGN).

Dr Mullins presented details of the status of development of continuous remote GPS stations by the United States in the Trans Antarctic Mountains, which are designed to run through the Antarctic winter.

Dr Schenke from the Alfred Wegner Institute, Germany, gave details of the coordination of Antarctic bathymetric data and the IHO project for coordination of data in the Southern ocean.

The symposium concluded with a GIANT business meeting. Dr Capra summarised progress against milestones of the program set during the XXVI SCAR in Shanghai in 2002. A joint proposal from Italy and Australia was endorsed to study and to improve the stability of the Terrestrial Reference Frame over Antarctica as the basis for precise measurement of small tectonic motion. The need to identify suitable projects for the International Polar Year 2007/2008 was noted. A proposal by Italy to host a further symposium in the series (2005) was unanimously endorsed.

It was a most a successful event which was extremely well hosted by the University Lviv Polytechnic and the Ukrainian Antarctic Centre.

Most participants provided final versions of their papers or abstract summaries and these are published in this report.

John Manning,
Convenor, GIANT

Ukraine National Antarctic Program: Geodesy Activity

Valery Lytvynov(1, Gennadi Milinevsky(1, 2), Svetlana Kovalenok(1), Elena Chernysh(1), Rudolf Greku(3)

(1) Ukrainian Antarctic Centre, 16, Tarasa Shevchenka blvd, 01601, Kyiv, Ukraine;

(2) Kyiv National Shevchenka University, 6, Glushkova av, 04022, Kyiv, Ukraine;

(3) Institute Geology Sciences, 22, Gonchara st, 01054, Kyiv, Ukraine E-mail: antar@carrier.kiev.ua

Abstract

The meteorology and climate, hydrology, upper atmosphere physics and geospace researches, ozone layer, seismic and acoustic measurements, glaciology, environment, biology investigations have been provided at the Vernadsky Ukrainian Antarctic station within seven years. The important tasks of Ukrainian National Research Program are the Antarctic Peninsula region GPS geodesy survey, and small ice cap monitoring as indicators of the long-term climate changes. The program of the GIS development for the Argentine Island archipelago and adjacent Antarctic Peninsula region (GIS project «Argentina Islands-Antarctic Peninsula») has been recently started. The main objectives of the GIS project are:

- (1) the high precision geodesic stations network creation in the vicinity of Ukrainian Antarctic Vernadsky station on the base GPS-positioning data;
- (2) the retrieval of the hidden regularities and anomalous events in combined system land-ice-ocean-atmosphere-ionosphere. Within 2001/2003 seasons high precision coordinates of geodetic survey marks were measured and local geodetic network was created for Vernadsky station 30x10 square km area. The season permanent GPS-survey at the SCAR-2002 site on Galindez Island within the framework of the GIANT project was started at Vernadsky in 2002. The GPS observation was carried out at the site for 15 days in 2002 and

2003. The registration coordinates accuracy in 2002 was 1-2 millimeters. More than 300 GPS points have been determined for positioning of different geophysical measurements on islands. Galindez ice cap and adjusted to Vernadsky region part of Antarctic Peninsula ice streams mapping have been made using the ERS radar interferometer data. Echo sounding of the Argentine archipelago's seabed in the shallow unsurveyed area (within the framework of the IBCSO project) has been provided in the Vernadsky region since 1997. Determination of detailed local geoids with the altimeter data of the Bellingshausen Sea has been carried out within the framework of the project ANTEC

In the second part we describe the long term plans of the FGI for the deformation studies in Queen Maud Land. Basis for the time series are the absolute gravity measurements performed in 1994 and 2001 with JILAg-5 absolute gravimeter showing a slight increase in gravity. Absolute gravity measurements will be continued in the next summer season using the new FG5 gravimeter. To control the attraction of the near-field ice masses we will survey the time variation in ice topography with RTK. At the same time the permanent GPS station will provide continuous GPS-time series. We plan to keep on repeating the absolute measurements at Aboa and to extend the measurements to other sites in Queen Maud Land.

The Evolution of the GIANT Program

John Manning Geoscience Australia

John.manning@ga.gov.au

Abstract

The SCAR GIANT (Geodetic Infrastructure of Antarctica) program was established in 1992 to provide a common geodetic framework over Antarctica as the basis for recording of positional related science.

For the past ten years this has been an active program and there are nine elements in the current 2002-2004 program :

- Permanent Geoscientific Observatories;
- Epoch Crustal Movement Campaigns;
- Physical Geodesy;
- Geodetic Control Database;
- Tide Gauge Data;
- Atmospheric Impact on GPS Observations in Antarctica;
- Remote Observatory Technologies

- Ground Truthing for Satellite Missions; Geodetic Advice on positioning limits of special areas in Antarctica

The development and status of each sub element within the over arching GIANT program is discussed and access to data highlighted.

1. Historical Background

GIANT is the acronym for the Geodetic Infrastructure of Antarctica program of the Scientific Committee for Antarctic Research (SCAR). SCAR was formed at The Hague in February 1958. It evolved from a Special Committee on Antarctic Research which was established by the International Council for Science (ICSU) to coordinate the scientific research of the twelve nations who were active in Antarctica during the International

SCAR WORKING GROUP ON GEODESY AND GEOGRAPHIC INFORMATION

Geophysical Year in 1957-58. The ongoing objective of SCAR is to promote scientific collaboration in Antarctic research.

At the first SCAR meeting in 1958 Cartography, as it was known then, was part of Working Group 2 (along with Geology, Glaciology and Morphology). At the III SCAR meeting in September 1959 Cartography met as a Working Group in its own right. The following year at IV SCAR in September 1960, a Permanent Working Group on Cartography was established. The Chief Officer was General Laclavère from France. The name was subsequently changed at V SCAR in October 1961 to the Working Group on Geodesy and Cartography. The Working Groups Chief Officer was B P (Bruce) Lambert from Australia. Since then the Chief Officer position has been held by Australian representatives from the National Mapping Division. In 1988, at XX SCAR in Hobart, the name of the group was changed to the Working Group on Geodesy and Geographic Information (WG-GGI) to better reflect its total scope of activity.

From its inception the working group encouraged compatible mapping of the Antarctic continent and established a set of recommendations and standing resolutions as mapping standards. Initially it recommended the use of the Hayford 1924 International spheroid as the basis for mapping and geodetic computations. The essential role of Geodesy within the working group at that time was the provision of control for exploration and mapping. This has since evolved to include the monitoring of the current tectonic motion of the continent and its linkage to other continents.

Since the formation of the WG-GGI at V SCAR in 1961 group meetings were usually held at the time of the SCAR meetings and all activities were the responsibility of the Chief Officer. At the XX SCAR meeting in Hobart in 1988 the modus operandi was changed from this single responsibility in producing a growing number of products, with a greatly increased work load. A more distributed arrangement was identified, which was reinforced at a special meeting hosted by Germany in Frankfurt in June 1990 as an alternate venue to the SCAR meeting that year. At the subsequent XXII SCAR meeting at Bariloche in 1992, Drew Clarke from Australia was elected Chief Officer and the operational aspects of the WG-GGI was completely reviewed changing from a focus on mapping standards and individual national activities, to a theme based structure with distributed project responsibilities. The Geodetic Infrastructure of Antarctic program was identified as GIANT at the meeting. Since that time the overall WG-GGI program has further evolved into two major umbrella streams each with an overall coordinator:

- Geodesy (GIANT)
- Geographic Information

This structural grouping proved successful and both streams initiated projects and produced products which were increasingly became available through the web site

as Internet technology developed.

Event	Location	Date
AGS 98	Santiago University, Santiago	July 1998
AGS 99	Polish Academy of Science, Warsaw	14-16 July 1999
AGS 01	Arctic and Antarctic Institute, St Petersburg	
AGS 02	Land Information New Zealand, Wellington	
AGS03	University Lviv Polytechnic, Ukraine	15-17 th September 2003

Table 1 List of SCAR Antarctic Geodesy Symposia

The concept of a business meeting at the time of the SCAR week working of working group meetings directly before the main SCAR meeting, and a specialist interperiod meeting was developed. This commenced with the USGS hosting a workshop in Flagstaff immediately before the Boulder IUGG meeting in 1995. This approach was further developed when Chile proposed and hosted a specialist Antarctic Geodesy Symposium (AGS) in Santiago immediately before the Concepcion XXV SCAR. There have now been four AGS symposia as in Table 1 above culminating in this fifth AGS03 event in Lviv Ukraine. This series of meetings has provided an important continuity of face to face contact whilst focusing on program milestone for individual projects in the GIANT program.

At the XXVI SCAR meeting in Shanghai in 2002 the long standing and successful WG-GGI (including GIANT) was merged with other SCAR working groups to form the Geoscience Scientific Standing Science Group (GSSG) and as such lost its direct reporting stream to the SCAR Executive Committee. The WG-GGI was renamed the Geospatial Information Group of Experts (GIG) with the intention to broaden its scope to also include Geophysical network information. In the new structure GIANT continues as the coordinating program for SCAR Antarctic Geodesy but as a sub program within GIG, which in turn is a sub group of GSSG. GIANT continues also to contribute expertise and resources to the SCAR Antarctic Neotectonics (ANTEC) program. It is cross linked with the International Association of Geodesy regional sub commission on Antarctica as the GIANT convener is also the co-chair of the IAG sub commission on Antarctic Geodetic networks.

Until the 1960s the positioning of geographic features on the Antarctic continent and measurement of baselines to other continental land masses was still only achievable by local triangulation surveys within Antarctica and astronomical observations. Triangulation chains were difficult to establish due to the need for multi station visibility for angle observations. The networks which were established were limited to the immediate vicinity of the base stations, or as small local area triangulations in isolated mountain areas. It was impossible to connect these local triangulations.

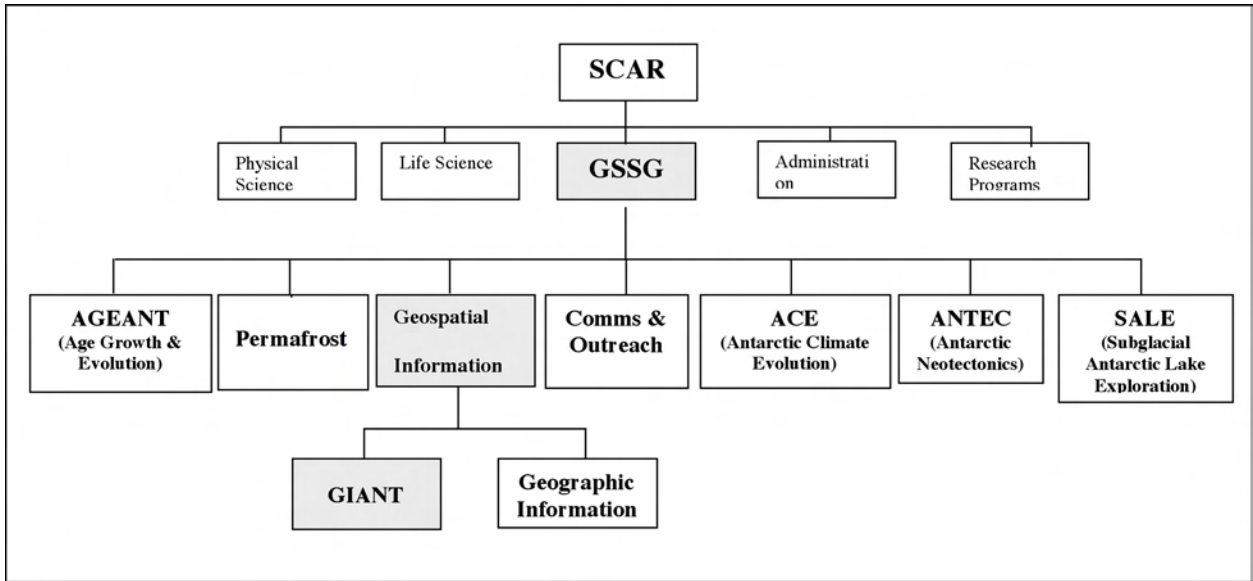
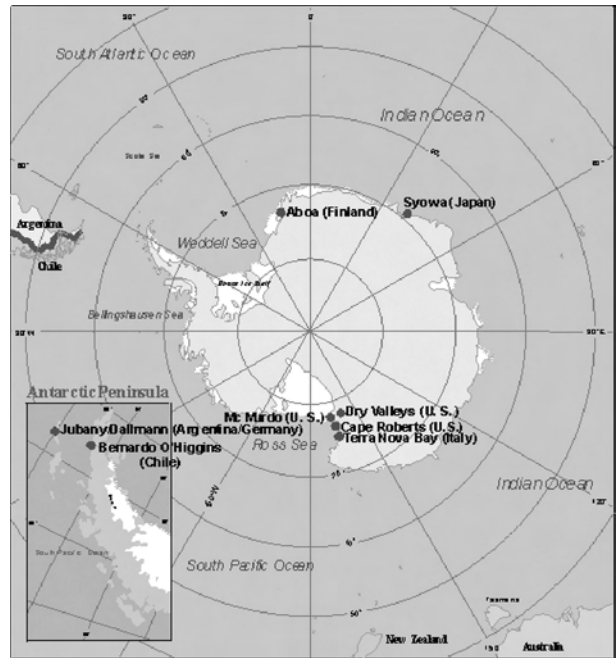
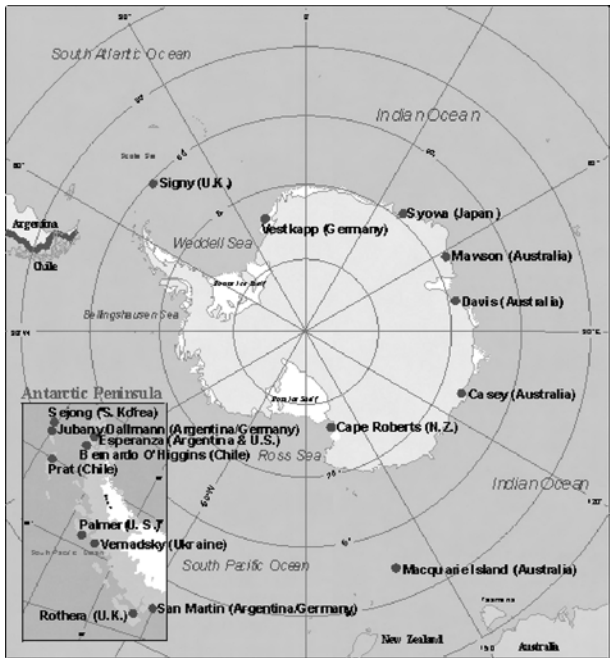


Figure 1: Structure of the Geoscience Standing Group (GSSG)



2. Technical Background : The progression to space geodesy

Optical and microwave electronic distance measuring (EDM) techniques were introduced to the Antarctic continent in the mid sixties, which enabled trilaterations, and large traversing loops, rather than pure triangulation to be undertaken, producing expanded but still isolated geodetic networks. This remained unchanged until the advent of man made satellites, although several over snow survey traverse connections between mountain features were carried out using EDM techniques.

With the advent of man made satellites, space geodesy was applied to address the problem of intra continental connection and to accurately determine the coordinates of some Antarctic stations in a global reference frame. In 1969 the global astro-triangulation PAGEOS program occupied Antarctic sites at McMurdo, Mawson, Palmer

Figure 3 Absolute gravity sites

and Casey, photographing passive satellites against a star background. In the 1970s active microwave positioning from satellites proved more useable than the PAGEOS optical photographic approach and firstly Transit Doppler and later GPS became available on global scale. The improvement in positional accuracies achievable from the different geodetic techniques is summarised in Table 1.

The early Antarctic space geodesy programs were the initiatives of individual countries as part of more extensive global programs, and no coordinated international geodetic program existed on the Antarctic continent. In 1976 the SCAR WG-GGI began to look at the possibility of linking the individual national geodetic networks by Doppler techniques and work commenced on gathering the extent of each nation's geodetic networks with view to a joint

Period	Technique	Baseline accuracy
1950s	Positional Astronomy	+/- 200metres
1969-70s	Satellite/Stellar photography (PAGEOS)	10 metres
mid 1970s	TRANSIT Doppler	3-5 metres
late 1980s	GPS	1-2 metre
1990	VLBI	1 decimetre
1995	GPS	1 decimetre
2000	GPS	Several centimetres
2003	GPS, enhanced VLBI	Sub centimetre

Table 1: Positional accuracy progression in Antarctica sites

approach, but due to logistic limitations no overall plan was implemented to link the individual networks.

In the late 1980's the application of the GPS military navigation system emerged as a civilian geodetic tool with a potential for Antarctica. The XXth meeting in 1988 endorsed a proposal by Australia to test the developing GPS technique for mapping control and potential applications in monitoring crustal motion. This pilot study was undertaken in two phases:

- Feasibility observations January 1990
- Test observations in January 1991

Station	Observing Authority	Receiver Type	Location
McMurdo	USGS	WM102	S77 51 E166 41
Davis	AUSLIG	Trimble 4000SLD	S68 34 E77 58
Law	AUSLIG	Trimble 4000SLD	S69 23 E76 23
Mawson	AUSLIG	WM102	S67 36 E62 53
Dovers	AUSLIG	WM102	S70 14 E65 51
Hobart	U. TAS	MiniMac	S47 48 E147 26
Orroral	AUSLIG	TI4100 Gesar	S35 38 E148 56
Yaragadee	AUSLIG	TI4100 Gesar	S29 02 E115 21
O'Higgins	IFAG	TI4100 Navigator	S63 19 E57 54
Punta Arenas	IFAG	TI4100 Navigator	S53 09 E71 00
Wellington	DOLIS	Trimble 4000SLD	S41 16 E174 47

Table 2: GPS observational sites 1990

Despite problems encountered the trial clearly showed that baseline accuracies in the order of one metre over intercontinental distances were possible even with the low number of GPS satellite available at the time (Govind et al 1990).

With the success of these feasibility studies the WG-GGI initiated an ongoing series of summer GPS epoch surveys. These were coordinated by Reinhard Dietrich from Germany (Dietrich 1996), (Dietrich, 2001) and the sites occupied are shown in Figure 4. All epoch data is archived at University of Dresden as an ongoing collection for science research (Dietrich@ipg.geo.tu-dresden.de).

Despite their success, the GPS campaigns were logistically costly and it was difficult to arrange the simultaneous occupation of all sites, being subject to different logistic arrangements. Consequently in 1993 permanent GPS sites were installed to provide fundamental fiducial stations to link epoch surveys together. The permanent stations were:

- McMurdo
- Mawson

- Amundsen-Scott (ice station)
- Casey
- Davis
- Macquarie Island (1995)

This was a significant technological advance as it provided a potential continuous time series of observations and a network of key sites which could be used as a control framework for subsequent occupations at different times. In 1994 permanent GPS trackers were also installed at :

- O'Higgins
- Syowa
- Kerguelen

Since that time permanent GPS trackers contributing continuous data to world data bases on a daily basis have been established at SANAE (1999) and Palmer. Other annual download GPS base stations are operating at Terra Nova bay, Maitri, Dumont Durville, Cape Roberts, Belgrano and Zhong Shan.(see figure 5)

The technology to power GPS equipment at unattended remote Antarctic observatory sites during the sunless winter is under current development with varying degrees of success. Ideally this requires remote power and satellite data retrieval strategies. The Australian National University has deployed 4 stations in the vicinity of the Prince Charles Mountains in East Antarctica and continues development for regular satellite downloads from some of those sites. Japan is trialling a remote site on an island some 30 km from Syowa and USGS is trialling annual download from remote sites at Finger Point, Mt Fleming and Cape Roberts (collocated with a remote operating tide gauge). This remote operation technology is not quite proven and needs further development to be ready for the international polar year in 2007.

3. The Geodetic Infrastructure of Antarctica

At the XXII SCAR in 1992 the results of the SCAR GPS Antarctic Project 1990-92 were assessed and it was decided to extend the GPS projects to develop collocation network of other techniques such as VLBI, Absolute Gravity, DORIS and tide gauges. This was collectively identified as the Geodetic Infrastructure for Antarctica (GIANT) the coordinating program for Geodesy.

The ongoing GIANT program objectives are to:

- Provide a common geographic reference system for all Antarctic scientists and operators.
- Contribute to global geodesy for the study of the physical processes of the earth and the maintenance of the precise terrestrial reference frame
- Provide information for monitoring the horizontal and vertical motion of the Antarctic.

Since 1992 the GIANT program has been revised and endorsed at each major SCAR conference on a two yearly basis. The components of the current program are:

3.1 Geodesy program (GIANT)

There are nine projects in the program as shown at www.scar-ggi.org.au/geodesy/giant.htm and are summarised as:

1. Permanent Geoscientific Observatories

Project Leader: Australia - Mr John Manning

Goal: To develop an infrastructure of permanent geoscientific (ie. seismologic, geomagnetic, geodetic and gravimetric) stations to bring all individual networks to a common datum, and to provide geoscientific information for the global monitoring and analysis of natural earth processes

2. Epoch Crustal Movement Campaigns

Project Leader: Germany - Prof Reinhard Dietrich

Members: Italy, Chile, Japan, China, Australia, USA

Goals:

1. To densify the geodetic infrastructure established from the permanent observatories; and
2. To develop a deformation model for surface movement vectors within a common Antarctic reference frame.

3. Physical Geodesy

Project Leader: Italy - Prof Alessandro Capra

Members: Germany, Australia, Russia, USA, Japan, Canada

Goal: Compilation and analysis of physical geodesy data, for the development of a new high resolution Geoid for the Antarctic.

4. Geodetic Control Data Base

Project Leader: Australia - Mr Glenn Johnstone

Members: Germany, UK, USA

Goal: Maintain the master index for Antarctic positional control, including all levels of accuracy

5. Tide Gauge Data

Project Leader: Japan - Dr Kazuo Shibuya

Members: Australia, China, Germany, New Zealand, Italy, Russia, USA (Amos), UK (Woodworth), other specialists as required

Goal: To consolidate the collection of and access to Antarctic tide gauge information

6. Atmospheric Impact on GPS Observations in Antarctica

Project Leader: Poland - Dr Jan Cisak

Members: Germany, Italy, USA, Australia (IPS), Norway, China, IGS

Goal: To understand the ionospheric and tropospheric impact of the atmosphere on the quality of GPS observations in Antarctica

7. Remote Observatory Technologies

Project Leader: USA - Mr Larry Hothem

Members: Japan (GSI), Australia, Italy, Netherlands (Swartz)

Goal: Identify technology and monitor developments for the deployment of geophysical and geodetic measurement sensors, and ancillary support equipment, at unattended

remote (no existing infrastructure for power, shelter and communications) Antarctic localities.

8. Ground Truthing for Satellite Missions

Project Leader: Germany - Prof Reinhard Dietrich

Members: Italy, Australia, USA (U of Texas)

Goal: To ensure new satellite missions are integrated with the Antarctic geodetic system

9. Geodetic Advice on positioning limits of special areas in Antarctica

Project Leader: Chile - Tnt Col Rodrigo Barriga

Members: Germany, Australia, USA

Goal: To provide advice to SCAR, through the Geoscience Standing Scientific Group on the geodetic aspects of protected area definitions.

One of the complex elements in The GIANT program is the development of the ellipsoid to geoid separation values to obtain heights above sea level from GPS or altimeter observations. An accurate determination of the Antarctic geoid continues to be severely hampered by the scarcity of gravity information, especially the interior of the continent. Australia produced early versions of the Antarctic Geoid based on GEM and OSU gravity data sets, which are available on the web site. In 1996 NIMA produced EGM96, a new global Gravity data model which however still suffers from lack of Antarctic gravity data. A grid of geoidal separation values based on EGM96 is available NIMA web site and which can be used to on line interpolate a separation value for any location (<http://www.nima.mil/GandG/egm96/intpt.htm>)

Whilst these earth gravity models still are inadequate for extensive Antarctic research, long wave gravity models from the CHAMP and GRACE satellite are beginning to become available and will improve the situation. Medium wave length gravity however is also required and this can be produced from airborne gravity. The experience from the successful aero gravity activities of Denmark and the United States of America in Greenland and the Arctic Ocean offer a technique to dramatically improve this aspect of the Antarctic gravity data set and provide the base for the subsequent computation of the geoid within the GIANT Geoid project. Ultimately terrestrial gravity will be integrated by introduction of precise Absolute gravity at origin sites to produce a continental wide gravimetric framework.

GIANT also provides important geodesy input to two other major activities:

- ANTEC, and
- ITRF

3.2 The Antarctic Neotectonics Group of Specialists ANTEC.

This group of specialists was established following the SCAR XXV meeting in Concepcion with three GIANT representatives. The ANTEC objectives are intertwined with the need for a precise geodetic framework over

Antarctica in the establishment of remotely operated sites away from the manned coastal stations and the integration with other geodetic techniques.

3.3 The International Terrestrial Reference Frame (ITRF)

Antarctica is important in the context of global geodesy. In the past global models have heavily relied on observations from Northern Hemisphere sites and the results do not always fit in the Southern Hemisphere or represent the best global picture. Antarctic space geodetic observatories have provided data to rectify this imbalance. Some continuous GPS sites make their data available to the International GPS Service (IGS) using satellite data retrieval systems. Data from continuous GPS sites in Antarctica were used in ITRF 2000 primary determinations (Altamimi 2001) and the epoch surveys have also been processed by Dietrich (2001) as densification of the global reference frame. This results in a network of official published IERS coordinates (with velocities) for Antarctic rock sites which can be used by any scientists in the Global reference frame. Through the GIANT program SCAR has accepted the recommendation that all geodetic networks in Antarctic should be computed in the ITRF 2000 reference frame using The GRS80 ellipsoid.

4. Conclusions

There has been considerable international cooperation in Antarctic Geodesy since SCAR was formed in 1958. The GIANT program was identified in the SCAR 1992 meeting and has evolved as the coordinating program for all SCAR Antarctic geodesy. With advent of man made satellites Geodesy has advance significantly linking isolated geodetic networks and monitoring tectonic motion.

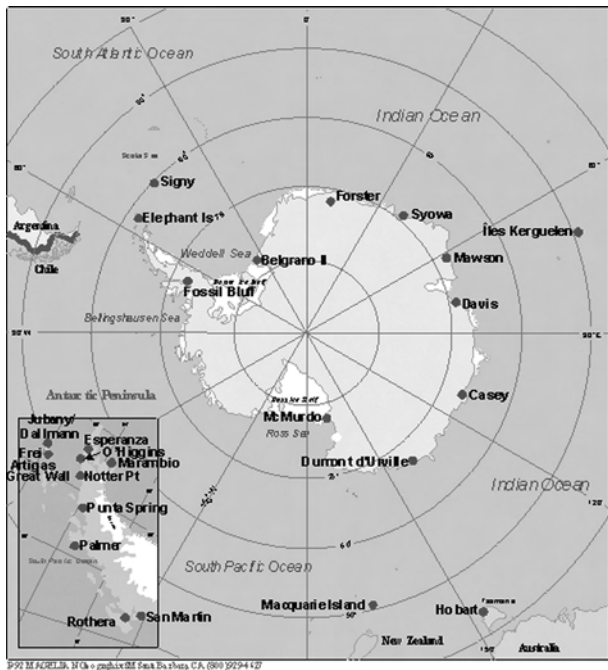


Figure 4. GAP1995 Observational Sites

A number of permanent GPS receivers have been installed in Antarctica and data is increasingly being retrieved by satellite transmission from these sites. This fiducial network of GPS points, augmented by VLBI and other techniques, forms the basis for an integrated geodetic infrastructure as the basis for all scientific spatial data. Data from these sites in Antarctica are of ongoing importance to global geodesy, especially in the determinations of precise orbits and the integration of different observational techniques. These sites provide a stable platform for combining summer epoch campaigns, densifying the ITRF network across Antarctica.

The application of space geodesy technology now enables a more comprehensive study of crustal movements within Antarctica and its relationship to other fragments of the ancient Gondwanaland. GIANT is making a significant contribution to the work of other Antarctic earth scientists such as the newly formed ANTEC group of specialists which is concerned with developing a better understanding of the crustal dynamics of Antarctica.

To meet the continual advancing requirement for accuracy for studying Antarctic geodynamics stresses, GIANT will expand the geodetic network to provide a very stable Antarctic reference frame for geodynamics and become involved in aerogravity campaigns to supplement satellite gravity data in order to improve the geoid.

5. References

Dietrich, R. (1996) 'The geodetic Antarctic Project GAP95 – German Contributions to the SCAR 95 Epoch Campaign', Deutsche Geodatische Kommission, Munchen, Germany 1996
 Dietrich, R. (2001) 'Present Status of the SCAR GPS Epoch Campaigns Report of the Second SCAR

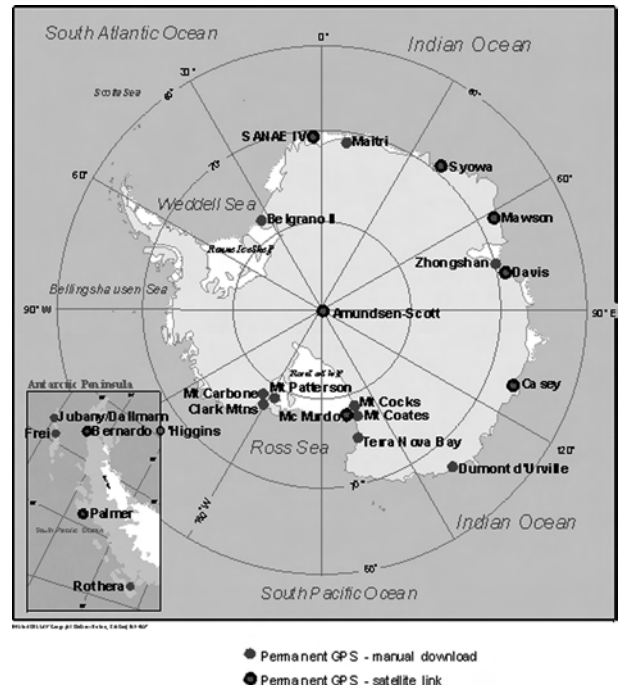


Figure 5. Continuous GPS sites

REPORT OF THE FIFTH SCAR ANTARCTIC GEODESY SYMPOSIUM

- Antarctic Geodesy Symposium*, Polish Academy of Sciences, Warsaw 14-16 July 1999 in *SCAR Report 20, May*, Scientific Committee on Antarctic Research, Cambridge
- Govind, R., Morrison, T., and Manning, J. (1990) 'Antarctic GPS Pilot Project - A Status Report.' Paper presented to SCAR Working Group Symposium, IFAG Frankfurt, June 1990.
- Kurihara, N., Kondo, T., Takahashi Y., Takahashi F., and Ejiri, M. (1991) 'The Results of the test VLBI experiments with Syowa Station in Antarctica and its future plans.' paper presented to the Chapman conference on Geodetic VLBI; Monitoring Global Change. Washington DC.
- Lambert, B.P. (1975) 'Geodetic Surveying in Antarctica 1970-1974; Report to the International Association of Geodesy. SCAR Working Group on Geodesy and Cartography. Canberra
- Manning, J., (1999) 'The SCAR Geodetic Infrastructure of Antarctica' Report of the Second SCAR Antarctic Geodesy Symposium, Polish Academy of Sciences, Warsaw 14-16 July 1999 in *SCAR Report 20, May*, Scientific Committee on Antarctic Research, Cambridge
- Manning, J., and Morgan, P. (1992) 'Antarctica - Where is it, and where is it going.' *The Australian Surveyor* vol 37 (1) pp 5-12, March 1992
- Manning, J., Morrison, T. and Murphy, B. (1990) 'The Transition to GPS: Australian Experience in Antarctica with Satellite Positioning.' Proceedings XIX FIG International Congress, Commission 5 pp 296-311, FIG, Helsinki.
- Morgan, P., and Tiesler, R. (1991) First Epoch Baselines between Antarctica and Australia - January 1990. ' *Australian Journal of Geodesy, Photogrammetry and Surveying*, December 1991

Geodesy Activities In PCMEGA 2003

Gary Johnston¹, John Manning¹, John Dawson¹, Paul Digney²
and Michael Baessler³

1. Geoscience Australia
2. Formerly Geoscience Australia
3. Institut fuer Planetare Geodaesie, Dresden University of Technology, Germany

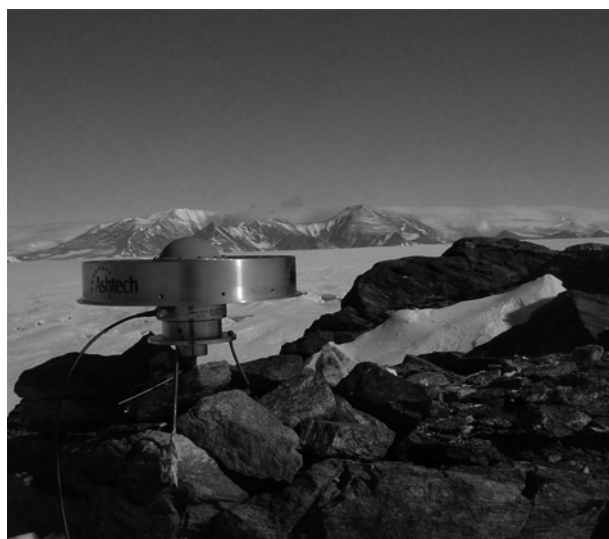


Figure 1. GPS point on Seavers Nunatak looking south East to Mt Menzies

Abstract

During the Antarctic summer 2003/2004 a major Geodetic Geological Geophysical expedition to the southern Prince Charles Mountains was undertaken jointly between Germany and Australia. This project was termed PCMEGA.

The joint expedition studied geochronology and

metamorphism of the area. Extensive airborne gravity and ice radar survey flights were undertaken over the ice cap to the immediate south of the mountains. Aeromagnetic transects over the Southern PCMs were also flown.

As part of the structural investigation of the area several first epoch GPS sites were established, together with occupations on previously established geodetic survey points, and a number of new mapping control were surveyed. An ice field calibration site for ICESAT, at a satellite crossover point near Mt Cresswell, was surveyed using kinematic GPS and a DORIS beacon was deployed on the glacial stream of the Lambert Glacier.

The GPS points were subsequently processed and the precision achieved on the first epoch occupations assessed. Additionally a GPS point on the nearby Grove Mountains was reoccupied for the third summer in a row to provide information to the ANTEC program from this part of East Antarctica. The preliminary results of these occupations will be presented in this paper.

1. Introduction

In the Austral summer of 2002-3 a geodesy team participated in the Prince Charles Mountains Expedition of Germany and Australia (PCMEGA). The expedition's objective was to undertake a geological and geophysical survey of the Southern Prince Charles Mountains in East Antarctica, including terrestrial and airborne gravity surveys, aeromagnetics, an ice radar survey and the enhancement of the geodetic network. The geodesy component was undertaken by a team consisting of surveyors from Australia (Geoscience Australia) and Germany (Dresden University of Technology).

2. Historical Background

The Prince Charles Mountains (PCM's) were first sighted as distant horizon features on the trimetrogon aerial photographs of the 1947-48 United States Operation Highjump. It was first reached by ground parties from Mawson in 1954 and then explored with aircraft support in the second half of the 1950s, when aerial photography was flown and controlled by sparse astronomical position fixes for reconnaissance mapping.

From the late 1960s the application of distance measuring equipment and the transition to use of helicopter support in the summer enabled a terrestrial geodetic network to be gradually developed through the northern and southern Prince Charles Mountains. This network, known as the Australian Antarctic Geodetic Network (AAGN), was established using angles and distances. It was later extended to the east and the west. By January 1976 the geodetic network stretched continuously from Davis to Molodezhnaya. This was a major feat but the positional accuracy suffered from a lack of traditional azimuthal control in poorly conditioned geometric figures, as it was difficult to observe Laplace azimuths in the summer daylight.

With the development of early satellite positioning techniques several Doppler Satellite fixes were observed in the Northern Prince Charles in 1988 and the next year surveyors' trialled the use of GPS for Antarctic geodesy. This quickly became the standard technique used for positioning during summer expedition projects. To provide a framework for these summer campaigns permanent GPS base stations were established at Casey, Davis, Mawson and Macquarie Island from 1993 onwards.

In 1995 and 1997 positional upgrades were observed with GPS at some geodetic network sites in the Southern PCM's. These were relatively short occupations on tripods but produced key tie points and significant improvements were achieved in the absolute accuracy of the geodetic network. Observations continued in 2000/01 along the northeastern edge of the Amery Ice shelf thus strengthening the single line traverse connection to Davis.

From 2000 Geoscience Australia entered into a multi year project under the Australian Antarctic Science Advisory Committee (ASAC) process. The Objectives of this project (ASAC 1159) are:

- To establish a reference framework for understanding the horizontal and vertical motion of Antarctica;
- Provide ANTEC with GPS data relating to vertical and lateral motions of east Antarctica (2001-2005); and
- Accurately co-ordinate points to update and strengthen the existing terrestrial based Australian Antarctic Geodetic Network, thus providing the geodetic infrastructure for all science programs as the positional basis for all geospatial data.

3. PCMEGA 2003

The primary geodetic objective was to obtain accurate ITRF2000 coordinates and gravity values on a network of points across the southern PCM's (SPCM's). This was done by:

- Running GPS base stations at Wilson Bluff, Mt Creswell and the Grove Mountains for high precision positions and to support the aircraft GPS positioning;
- Extending the geodetic framework in the SPCM's with GPS observations at Burke Ridge, Mt Borland, Mount Twigg, and other outcrops;
- Observe GPS at new monuments adjacent to existing geodetic network stations elsewhere; and
- Observing terrestrial gravity at all sites visited.

In addition other tasks completed were

- The establishment of a small ICESAT calibration range at a crossover point near Mt Creswell using kinematic GPS techniques;
- The deployment of DORIS near the Lambert Glacier grounding zone to measure ice flow velocities;
- The measurement of ice flow velocities adjacent to the Wilson Bluff Camp (NE end of the Bluff); and
- Photo-control surveys for satellite imagery at ten sites for the Australian Antarctic Division Mapping program

All GPS observations were taken on rock mounted antenna mounts (see Figure 1 for example) which eliminated the uncertainty of using tripod setups. Where existing AAGN points existed on the feature the new mark was placed adjacent to it and connected using terrestrial survey techniques allowing the adjustment of the AAGN network onto the new GPS control. Where no existing AAGN points were present the site was chosen for optimum stability and ease of access. Subsequent re-adjustment of the AAGN using these new points and the connections to the existing control has resulted in significant improvements in the accuracies of the network throughout the area.

More importantly the new GPS network bridges the Lambert Glacier with a number of sites either side of the main stream and a good latitudinal distribution as well (Figure 2).

The observational strategy of running three continuous trackers in the vicinity of the survey while the shorter seven day occupations occurred has resulted in very high coordinate precisions, even on the shorter occupations. Figure 3 and 4 illustrate the daily coordinate repeatability's achieved. Figure 3 shows one of the longer occupations at Mt Creswell and Figure 4 shows Harbour Headland which is one of the shorter occupations.

This first epoch observation at the network of new geodynamic style points has established the framework

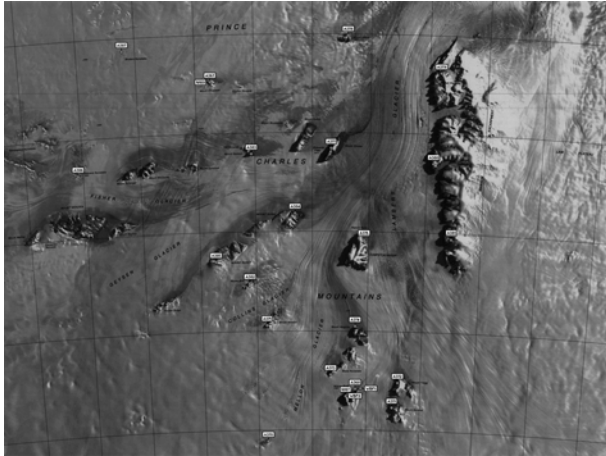


Figure 2. Distribution of GPS sites in the Southern Prince Charles Mountains

for future tectonic studies in the region. Subsequent observations on these points will allow a structural investigation of the region, and may give some insight into the processes which formed the Lambert Graben.

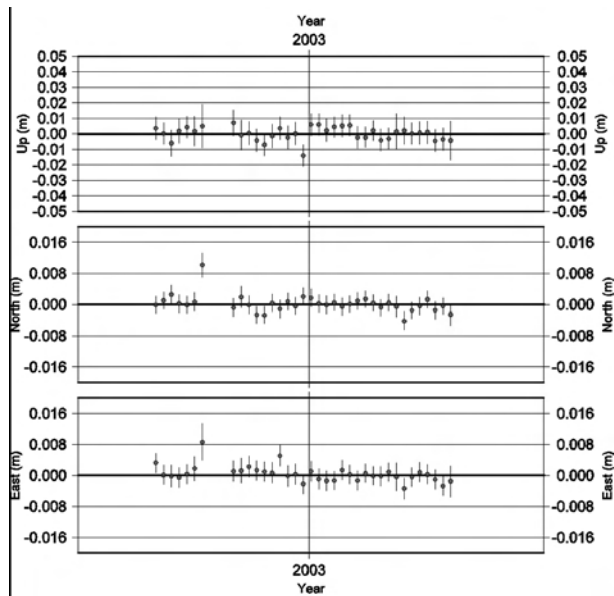


Figure 3. Aus367 (Mt Creswell) time series

Additionally, a GPS point on rock in the nearby Grove Mountains was reoccupied for a third summer in a row to provide horizontal movement information to the ANTEC program from this part of East Antarctica. The results of these occupations indicates that the horizontal motion is consistent with the east Antarctic plate, but a small differential vertical motion on this inland site compared to the coastal margin as represented by the IGS sites of Mawson and Davis is present. Figure 5 illustrates the time series for the Grove Mountains site. The continuation of this time series with longer observational spans will improve the understanding of this feature.

Relative gravity observational loops were taken between Davis and Mt Creswell, as well a Mt Creswell and Mawson. These loops were later extended to all

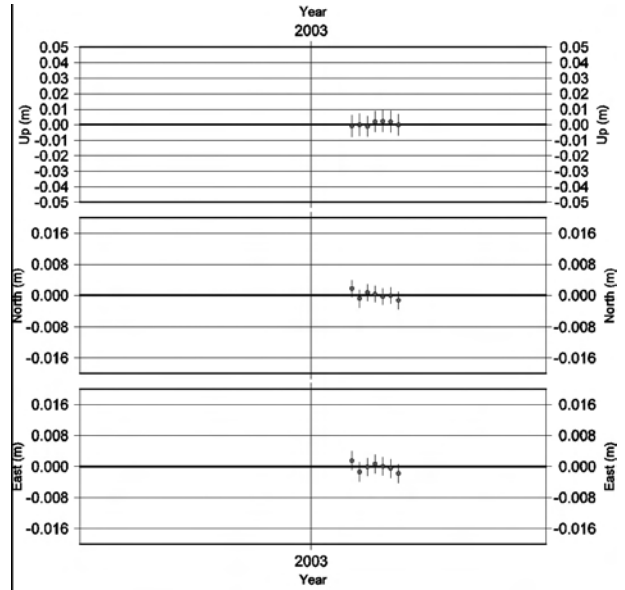


Figure 4. Scatter plot of AUS380 (Harbour Headland) results

sites visited in the area so that gravity values can be computed relative to the fundamental gravity stations and Davis and Mawson. Most points were visited twice for redundancy.

The secondary tasks completed will not be discussed here, but will be recorded at more length in a full technical report being prepared at Geoscience Australia.

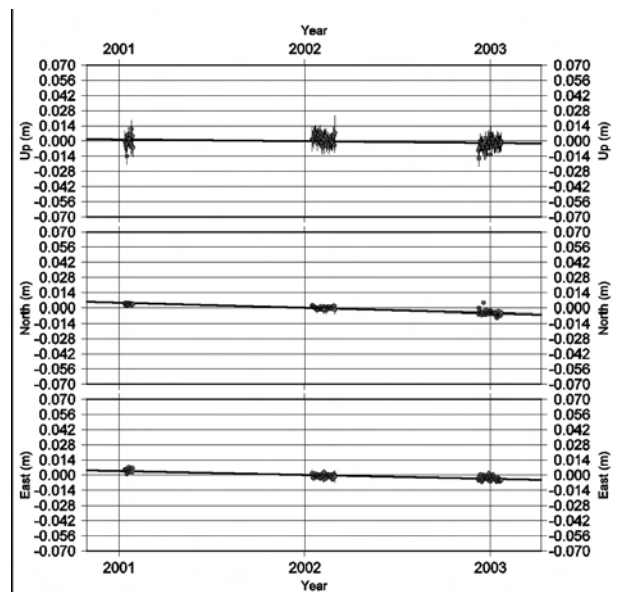


Figure 5. AUS351 (Grove Mountains) time series

4. Conclusions

The 2002-03 PCMEGA campaign was an unprecedented success for all disciplines of Geoscience studied. While extremely fortuitous weather conditions certainly contributed to the success of the campaign, the logistical and organisational support provided by the Australian Antarctic Division contributed more.

The geodesy program established 23 new geodynamic

style GPS points with a resultant coordinate precision in the order of 1-2mm horizontal and 2-3mm vertical. Many of these were also connected to the existing AAGN network allowing significant improvements to it. Gravity

observations were also taken adjacent to these points enhancing the usability of the gravity values. They can now be used for ground control of airborne or satellite gravity missions.

Geodetic Activities At Finnish Antarctic Research Station Aboa

Hannu Koivula and Jaakko Mäkinen

Finnish Geodetic Institute P.O.Box 15, FIN-02431 Masala, Finland

Hannu.Koivula@fgi.fi

Abstract.

We summarise geodetic activities at the Finnish Antarctic research station Aboa since 1989. In 1989–1992 a regional gravity network was established. Absolute gravity measurements were performed in 1994 and 2001. In 2003 a permanent GPS station was installed. In the future we plan to maintain the GPS time series, and to perform absolute-gravity measurements at other sites in Queen Maud Land, too.

Geodetic Activities at Aboa 1989–2001

The Finnish Antarctic Research Station Aboa (73°02' S, 13°25' W) in Western Queen Maud Land (Fig. 1) on the nunatak Basen was built in 1988–1989. It is a summer station and has not been occupied every year. The Finnish Geodetic Institute (FGI) has taken part in five of the ten Finnish scientific Antarctic expeditions (FINNARP) organized so far. Here we summarise shortly the activities of the first four of them. For more information see Ollikainen and Rouhiainen (1990), Jokela *et al.* (1993), Virtanen *et al.* (1994), Mäkinen (1994, 2001).

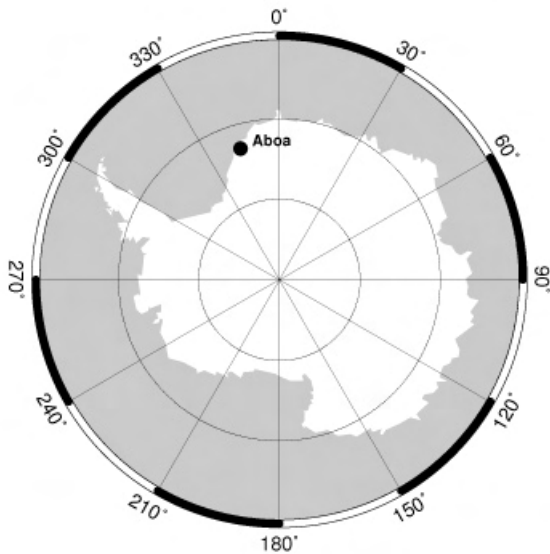


Figure 1. Finnish Antarctic Research station Aboa is located at 73°02' S, 13°25' W in Western Queen Maud Land.

Finnarp89 (1989/1990) and Finnarp91 (1991/ 1992).

A regional gravity survey covering 10000 km² was measured using Worden Master and LaCoste&Römberg

gravimeters, with 493 points at the spacing of 5 km. Snowmobile and helicopter transport, and GPS positioning were used. The Aboa reference station was tied to the International Gravity Standardization Network 1971 through station no. 43846J in Montevideo. A set of benchmarks was built around Aboa and measured with static GPS to create a local coordinate system. Snow accumulation and ice motion were studied on stake lines. A concrete pier was constructed on solid basaltic rock for future absolute gravity measurements.

Finnarp93 (1993/1994) and Finnarp2000 (2000/ 2001)

Absolute gravity was measured by the second author with the JILAg-5 of the FGI in January 1994 and in January 2001. The results (Fig. 2) show an apparent gravity change of $+9\pm 7 \mu\text{gal}$ (one-sigma) over 7 years. The change is thus not statistically significant. In 2001, the 5.5 km stake line of Sinisalo *et al.* (2003) was re-surveyed by GPS for snow surface elevations, and density of the top 0.5 m layer sampled. A similar local survey within 100 m of the absolute site was performed with tachymeter. The GPS station at the neighbouring Swedish base Wasa was occupied during the SCAR epoch 2001 and 2002 GPS campaigns.

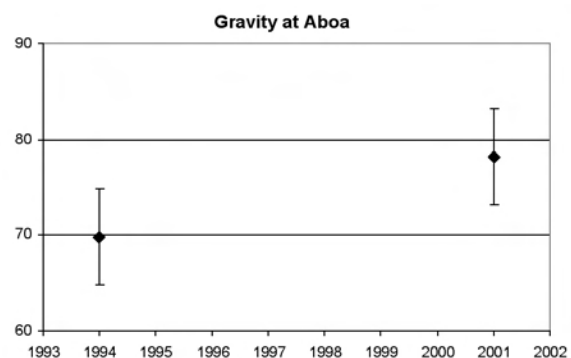


Figure 2. The results of two absolute gravity measurements in 1994 and 2001 show a slight increase in gravity.

Geodetic Activities at Aboa in 2002/2003

The first part of the season was mainly dedicated to the refurbishment of the Aboa station. Finnish Geodetic Institute sent the first author to Aboa for the latter part of the season. His main task was to install a permanent GPS station close to the absolute gravity hut.

Permanent GPS station.

The Aboa permanent GPS station became operational on January 31, 2003 at 10:10 UT. The station (Fig 3) is unoccupied most of the year so the power consumption of the GPS receiver is an essential issue. We chose a Javad EURO80 GDA receiver, which has a power consumption of 1.8–2.4 W only. We collect both code and phase data with 30 s observing interval and store it on a 512MB Compact Flash memory card. Both the receiver and memory card are specified for temperatures down to -40°C . The electronics of the receiver are sealed into a box and it was estimated that the heat produced by the receiver keeps the temperature in the box 20 degrees higher than the outside temperature. This should be sufficient, as temperature measurements at Aboa do not have records below -50°C . The memory card will be changed annually during austral summer expeditions by geodesists or any other research or logistics personnel available.

As an antenna platform we use a 1.5 m high steel grid mast that was anchored to basaltic rock with 1 m long screw bars (Fig. 4). The antenna is Ashtech choke ring (ASH701945C_M) with conical Ashtech snow radome. The receiver itself is located in the absolute gravity hut 15 m from the antenna mast.

The power is taken from a Ni-Cd battery pack (24V/1100Ah) located 100 m from the receiver at the main building of the base. During the field season the batteries are charged by diesel generators. When the station is not occupied the batteries are charged by four 50W solar panels, which are on test use. The batteries alone are able to keep the receiver running through the dark period of the austral winter. Finnarp logistics will install in the next season 26 solar panels of 100W each, and 3 wind generators for shared use of all the research facilities at Aboa.

The permanent GPS station is mainly used for long coordinate time series to support deformation studies, but data are also available for any other geodetic purposes in the area.

RTK Service.

When the Aboa station is occupied the GPS station offers also the RTK correction signal. It is sent using a Satelline-3As/d Epic radio modem (10W) with 430.15 MHz frequency. The RTK correction is available for

Table 1. The coordinates of the benchmarks on Basen. WASA was fixed to it's ITRF96 epoch 1997.1 coordinates by Dietrich et al. (2001)

Point Name	Coordinates			Sigmas (mm)		
	Latitude	Longitude	Height (m)	s(N)	s(E)	s(U)
900001	73°02'28.81537"S	13°24'05.69716"W	495.157	0.2	0.2	0.6
910023	73°02'29.94509"S	13°24'26.36215"W	482.557	0.2	0.1	0.6
910024	73°02'22.87693"S	13°24'32.74326"W	490.790	0.2	0.2	0.6
900032	73°02'37.59744"S	13°24'23.98902"W	467.352	0.8	0.4	1.9
ABOA	73°02'37.57989"S	13°24'25.68634"W	468.640	0.2	0.2	0.7
WASA	73°02'34.22900"S	13°24'50.52273"W	466.396	0.0	0.0	0.0

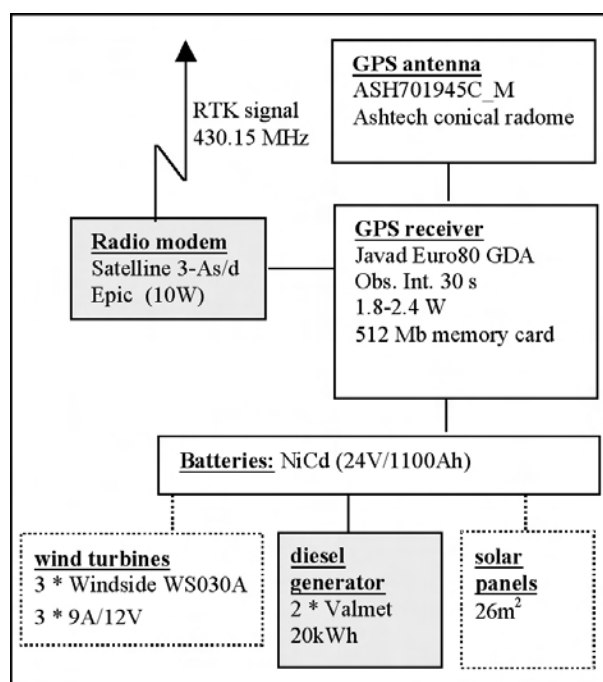


Figure 3. The components of the permanent GPS-station at Aboa. Grey boxes indicate components that are used the year around and keep the station operational in winter. White boxes indicate components used only when the station is occupied. Dotted lines indicate future components that are a part of a larger plan to support logistics and research facilities.

any researcher working in the area, to obtain accurate coordinates within 20–30 km from the station.

SCAR 2003 Epoch GPS Campaign.

We did GPS measurements on the Swedish point WASA that has participated in several SCAR epoch GPS campaigns (<http://www.tu-dresden.de/ipg/FGHGIPG/Aktuell-Dienste/scargps/database.html>). The 2003 campaign was performed between January 20 and February 10, in 2003. We did measurements from January 26 until the end of the campaign using Ashtech_Z receiver and choke ring antenna (ASH700936A_M). We have also data from the permanent GPS station starting from January 31. In the future the data from the permanent GPS station will be contributed to the SCAR epoch campaign database.

Local Geodetic Network.

During the Finnarp91 expedition a local geodetic coordinate system was created around Aboa. We re-measured all points located on Basen including the new GPS station. Static GPS measurements were performed with two Ashtech Z-XII receivers and choke ring antennas (ASH700936A_M) using 30 s observing interval. The baselines varied between 15 and 460 m and sessions from a few hours to 24 hours. In the adjustment we fixed the WASA coordinates to those in ITRF96, epoch 1997.1 published by Dietrich *et al.* (2001). The results were processed with Pinnacle software and are shown in Table 1.

Local snow and ice.

RTK will be used by the FGI to support absolute gravity measurements. The snow and ice topography around the gravity point is surveyed using RTK. The density of snow and ice is determined by drilling. From repeated measurements we can estimate the variation in the attraction of the near field ice and snow masses. During this season the 5.5 km stake line was re-built, samples drilled and coordinates measured with RTK. The local tachymetric survey of 2001 was repeated with RTK. While there was no absolute gravity observation in 2003 this will help to estimate annual variability.

Research rationale, future plans

With the repeated absolute gravity observations and with the permanent GPS station we strive to detect gravity change and contemporary crustal motion. They could be caused by past and present-day changes in the ice mass balance. Reconstructions of the last glacial cycle in the Antarctic are not well constrained by observational evidence, and differ appreciably both in ice volumes and in the timing of the deglaciation. Neither is the present-day mass balance well known. Thus there is considerable interest in collecting new observations related to past or present changes of the Antarctic ice mass. For predictions of gravity and vertical rates based on a number of scenarios of the ice mass balance see James and Ivins (1998).

The elevation change of the Antarctic from 1992 to 1996 was mapped by Wingham *et al.* (1998) using satellite radar altimetry. In the drainage basin around Aboa an average annual change of $+4.4 \pm 1.1$ cm is indicated. However, many 1° by 1° squares lack data due to the terrain inclination limitations of the ERS altimetry. Currently, the change in the ice surface elevation is being mapped by ICESAT/GLAS, and in the future by the CRYOSAT mission. Contemporary change in total mass (ice + mantle flow due to post glacial rebound) is surveyed by GRACE.

Additional information is obtained by observing the deformation of the solid Earth. GPS provides information on vertical and horizontal motion, while gravity is sensitive to both vertical motion and changes in density distribution. GPS is indifferent to the underlying causes, but for a given amount of vertical motion, the gravity change depends



Figure 4. The antenna mast of the Aboa GPS station

on the mechanism: The response of the Earth to present deglaciation is elastic and for a typical regional load the ratio of gravity change to vertical motion is $-0.27 \mu\text{gal}/\text{mm}$ (James and Ivins, 1998). The response to the past deglaciation ("post glacial rebound") is viscous mantle flow to restore the isostatic balance and the corresponding ratio is about $-0.16 \mu\text{gal}/\text{mm}$ (Wahr *et al.*, 1995). Combining GPS and repeated absolute gravity one thus could, in principle, not only determine total vertical motion, but also separate it into the post glacial rebound signal, and a signal showing present-day variation in ice mass.

In addition to the gravity change due to deformation of the solid Earth, the change in ice mass causes a change in gravity through the direct attraction. The Aboa absolute site is on bedrock, but model calculations show that a surface layer at a distance 15...1000 m from it has a (vertical) attraction of about 25% of the corresponding Bouguer sheet. This is of the same size than the deformation effect of the corresponding regional surface layer, and the near-field mass variation need not reflect the regional average. Thus the variation in the attraction by the local ice mass could overshadow the deformation effects we are looking for, and must be monitored separately.

We propose to continue both GPS and absolute gravity observations, and extend the latter to other sites in Queen Maud Land. The plan (Fig. 5) for the summer 2003/2004 includes absolute-gravity measurements at the bases Aboa (Finland), Sanae IV (Republic of South Africa) and Novolazarevskaya (Russia), using the recently acquired absolute gravimeter FG5 no. 221 of the FGI. At Aboa we will survey the snow topography with RTK, to control the

attraction of the near-field ice/snow masses. At the same time the permanent GPS station at Aboa will provide a continuous time series of coordinates.

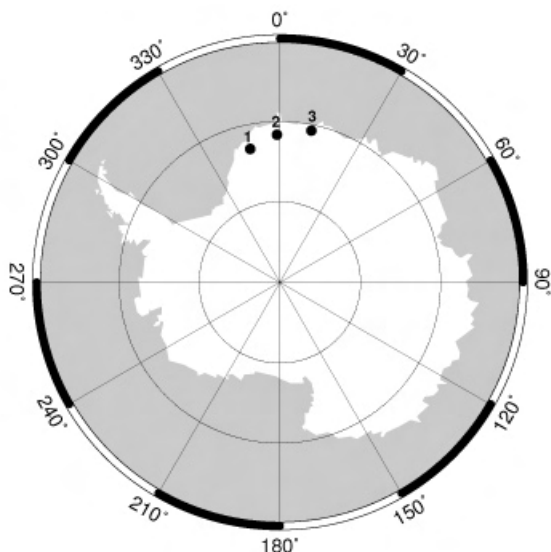


Figure 5. Measurement plan for the absolute gravity for the next field season. 1 is Aboa (FIN), 2 is Sanae IV (RSA) and 3. is Novolazarevskaya (RU).

References

- James, T.E. and E.R. Ivins (1998): Predictions of Antarctic crustal motion driven by present-day ice-sheet evolution and by isostatic memory of the Last Glacial Maximum. *J. Geophys. Res.* 103 (B3), pp. 4993–5017.
- Jokela, J., M. Ollikainen, P. Rouhiainen, H. Virtanen (1993): The gravity and GPS survey in Western Queen Maud Land, Antarctica, 1989–1992. *Rep. Finn. Geod. Inst.* 93:6. 46 p.
- Mäkinen J. (1994): *Determination absolute gravity at the Finnish Antarctic base Aboa in 1994*. Joint Symposium of the International Gravity Commission and the International Geoid Commission, Graz, Austria, September 11–17, 1994. Program and Abstracts (Ed. H. Sünkel).
- Mäkinen J. (2001): *Absolute gravity measurements at the Finnish Antarctic base Aboa in 1994 and 2001*. IAG International Symposium on Recent Crustal Movements (SRCM'01), Helsinki, Finland, August 27–31, 2001. Abstracts (Ed. M. Poutanen).
- Ollikainen, M. and P. Rouhiainen (1990): *Experiences on gravity measurements and GPS positioning in the Antarctic*. Proc. 11th general Meeting Nordic Geodetic Commission, Copenhagen 7–11 May 1990, pp. 435–441.
- Sinisalo, A., A. Grinsted, J. Moore, E. Kärkäs and R. Petterson: (2003). Snow accumulation studies in Antarctica with ground penetrating radar using 50, 100 and 800 MHz antenna frequencies. *Annals of Glaciology* 37. (in press).
- Virtanen, H., J. Jokela, M. Ollikainen and P. Rouhiainen (1994): *Gravity measurements in Antarctica by Finnish expeditions 1989–1992*. FINNARP Symposium, Ministry of Trade and Industry, Antarctic Reports of Finland 4, pp. 28–31.
- Wahr, J., D. Han and A. Trupin (1995): Predictions of vertical uplift caused by changing polar ice volumes on a viscoelastic Earth. *Geophys. Res. Letters* 22, pp. 977–980.
- Wingham, D.J., A.J. Ridout, R. Scharroo, R.J. Arthern and C.K. Shum (1998): Antarctic elevation change 1992 to 1996. *Science* 282, pp. 456–458.

An Outline of Polar Expeditions of the Scientists from Warsaw University of Technology Andrzej Pachuta

Warsaw University of Technology, Institute of Geodesy and Geodetic Astronomy,
00-661 Warsaw, Pl. Politechniki 1, Poland
E-mail: pachuta@gik.pw.edu.pl

Abstract

Active exploration of polar area by scientists from Warsaw University of Technology began in the late fifties of the XX century. On the occasion of the III International Geophysical Year Jerzy Fellmann took part in the Spitsbergen Expedition. He has measured the movement of Werenskiöld glacier in the area of Hornsund Fiord by photogrammetric methods. The most valuable and spectacular achievement of the first Polish geodetic Antarctic expedition to the Dobrowolski Station on Bunger Oasis was done by Janusz Sledzinski and Zbigniew Zabek during the Antarctic summer 1958/1959. They established the gravimetric point and the direct connection of this point to the Polish gravimetric network. Further geodetic studies at the A.B. Dobrowolski Station were carried out during the Antarctic expedition organized by Polish Academy

of Sciences in 1978/1979. The geodetic network and gravimetric measurements have been made by Andrzej Pachuta. The first geodynamic expedition with students' participation was organized to the Spitsbergen by Faculty of Geodesy and Cartography in the summer 1988. Andrzej Pachuta and Ryszard Preuss led this expedition. Dariusz Osuch, Piotr Wypych, Jarosław Kutyna, Artur Gustowski were the student participants. During this expedition Zdzisław Kurczynski and Stanisław Dabrowski made the photogrammetric measurements in fiord Hornsund. The second geodynamic expedition to the area around fiord Hornsund in Spitsbergen was organized in summer this year. Zdzisław Kurczynski manages the expedition. Artur Adamek, Michał Sagan and Małgorzata Piskorz are the students from the Warsaw University of Technology participating in this expedition.

Photogrammetrical Investigations of the Antarctic Coast

Olexandr Dorozhynskyy, Volodymyr Glotov

National University "Lvivska Politechnica", Lviv, Ukraine

Abstract

Changes of the Antarctica coast and the contiguous islands covered with the ice occur in the time with different rate and depend from whole range of factors, foremost from climatic environment. Determination of such quantitative changes, in other words the changes of surface topography, can be effectively solved by photogrammetric methods.

Authors have proposed the conception of the navigation-digital photogrammetry (O. Dorozhynskyy, 1997) and its application for concrete physiographic conditions. It is developed the technology of the terrestrial navigation-digital photogrammetry which based on the use of digital camera (for obtaining of the digital images of the shore line and glaciers), GPS-device (fixation of the spatial location of the surveying points and investigated objects points) and digital photogrammetric stations (creation of orthophotomaps of the shore line and frontal plans of the rocky shores).

Photogrammetric method has been completely tested

in the field conditions (V.Glotov, 2002, 2003) during two seasonal Antarctic expeditions on Ukrainian station "Academic Vernadsky". There have been produced about 1200 digital images which give rich materials for further researches.

The following previous results has been obtained:

- photogrammetric method of investigation of the kinematic processes (changes of ice cover and deformation of the shore line of Antarctic coast) is effective, objective and precise tool for quantitative evaluation of changes on such territories;
- creation of digital cartographic materials is a good basement for application of GIS-technologies for the analysis of spatial changes and systematic storage of data about kinematics of phenomenon will allow for direction of other branches to obtain the information for solution of their specific tasks, namely forecasting of glaciers changes.

Tropospheric Delay Modelling for GPS Measurements in Antarctica

Alexander V. Prokopov, Yeugeny V. Remyev

Kharkov State Research Institute of Metrology, Mironositskaya st. 42, 61002 Ukraine

E-mail: NIL1@metrology.kharkov.ua

Abstract

The accuracy of tropospheric delay modelling for polar regions was investigated. Ray tracing technique and data of radio sounding for Antarctic meteorological stations accessible in the Internet (<http://weather.uwyo.edu/upperair/sounding.html>) were used in researches. The results show that the errors of known methods of determination of tropospheric corrections for GPS are much higher for Antarctica than for middle latitudes. For example, errors of methods [1,2] for Mirnyj station are 3...4 times above than for USA and Europe.

The effect of the significant contribution of a wet component in delay of a signal at heights above tropopause predicted for Antarctica by F.D.Zablotskyj [3] is confirmed.

On the basis of the IROA method [1] the preliminary version of regional (Antarctic) model for determination of delay from ground meteorological data is developed. The testing which has been carried out by the ray tracing technique with the use of yearly sets of radio sounding profiles obtained for Mirnyj station showed: the accuracy of the developed model in a range of zenith angles 0° ... 80° is 1,5 ... 2,5 time higher than accuracy of known models.

The obtained results shows the need for further researches with the aim of increasing the accuracy of tropospheric delay models by taking into account the peculiarities of spatial distributions of atmospheric parameters in polar regions.

References:

- [1] Prokopov A. and Remyev Ye., New approach to the problem of determination of atmospheric refractivity corrections for space geodetic applications». *Reports on Geodesy*, 2000, No 9 (55), P.43-4.
- [2] Davis J.L, Herring T.A., Shapiro I.I., Rogers A.E.E. and Elgered G. Geodesy by radiointerferometry: Effects of atmospheric modelling errors on estimates of baseline length.// *Radioscience*. – 1985. – Vol. 20. – No. 6. P.1593 – 1607.
- [3] Zablotskyj F.D. On atmospheric influences on astrogeodetic measurements in Polar Regions: *SCAR Report* - May 2001// Publ/ Scientific Committee on Antarctic Research at Scott Polar Research Institute. - Cambridge (United Kingdom). - 2001. - 120. - P. 50 - 55.

Overview of the Research on the Atmospheric Impact on GPS Observation in Polar Regions

Jan Cisak

Institute of Geodesy and Cartography, Warsaw, Poland.

jcisak@igik.edu.pl

Abstract

Polar region is one of the best test areas on the Earth for research. The increased, in last years, number of permanent GPS stations there, provides a large amount of data and possibility to create a representative database.

Recent research developments within the framework of the project "Atmospheric impact on GPS observations in Antarctica" are presented in the paper. The effects of both ionospheric and tropospheric disturbances on GPS solutions are discussed. The GPS data, usually those provided by permanent GPS station arrays are commonly used to investigate the structure and dynamics of ionosphere. First results of the project concerned the influence of ionosphere over the Arctic and Antarctic regions on repeatability of co-ordinates of vectors of different length during the quiet and disturbed ionosphere (ionospheric storms).

The new approach of data analysis was conducted. It is based on the analysis of GPS solutions obtained from the overlapped segments of data. Time series of GPS solutions based on the processing overlapped data segments allow for investigation of atmospheric impact on GPS measurements in a new dimension. Such a series can be considered as a record of the process of variations of vector components during varying atmospheric disturbances. The experiments performed concerned the investigation of the response of the measuring system to ionospheric storms as well as the response of the measuring system to tropospheric disturbances.

The two-stage influence of ionosphere, as the fluctuation on local inhomogeneous ionosphere and the refraction on regional inhomogeneous ionosphere, makes ambiguity resolution difficult and causes the errors in vector final solutions. The deep study of the problem should lead to the rejection of bad solutions. It has also been found that the analysis of correlations gives the possibility to correct the horizontal components of the vector obtained using commercial as well as the Bernese software. Similar analysis was performed when looking for the correlation of vector solution and tropospheric data. The results obtained using the Bernese software are not correlated with the tropospheric delay. The repeatability of the vertical component of the vector obtained using commercial programmes is substantially improved after introducing the correction.

1. Introduction

A considerable progress observed in the geodynamic research is the result of a development in measuring techniques (Manning, 2001). The qualitative results on crustal movements presented in some publications

(Dietrich *et al.*, 2001, Dietrich *et al.*, 2002) seem, however, to be at the level of their accuracy determination. A realistic estimation of the potential of the experiment is thus necessary to avoid false conclusions describing non-existent occurrences (artefacts), especially when the experiment is difficult or very expensive.

That is exactly the case of the experiments conducted in Antarctica. Seasonal changes of atmospheric conditions frequently make impossible to perform widespread continuous (yearly) GPS observations. On the other hand, those seasonal changes can cause periodic biases in data acquired, as well as periodic deformations of the Earth's crust. Besides data acquired at the growing number of Antarctic IGS permanent stations (recently about 15 stations) there is a large set of data provided by GPS Epoch Crustal Movement Campaigns (<http://www.geoscience.scar.org/geodesy/giant.htm>) organized for a number of years under the umbrella of SCAR GIANT (Geodetic Infrastructure of ANTArctica) program. About 50 Antarctic stations participated in those campaigns that took place during Antarctic summer only. The question arises whether the seasonality of those campaigns influences the results obtained, and if so, how that influence could be quantitatively evaluated.

The main goal of the GIANT program project on the atmospheric impact on GPS observations in Antarctica is to investigate the atmospheric impact on the quality of GPS observations in Antarctica, and possibly to develop recommendations for future Antarctic GPS campaigns, data post-processing strategies and modelling GPS solutions.

The GPS data, usually those provided by permanent GPS station arrays, are commonly used to investigate the structure and dynamics of the ionosphere (Baran *et al.*, 2001a; Feltens and Jakowsky, 2001) as well as to investigate the troposphere (Kruczyk, 2002). During the realisation of the project it was impossible to concentrate on the atmospheric impact only and separate it from the study of the atmosphere. The results of the investigations of the ionosphere as well as of the troposphere are the output of the project too. The bibliography at the end of the paper includes the majority of publications that summarize the results obtained in the framework of the GIANT project.

2. Project background

The GIANT program project on the atmospheric impact on GPS observations in Antarctica, coordinated by Poland, has been created at the XXVI SCAR meeting in Tokyo in 2000. The Polish project, financed by Polish Scientific Committee, named "The investigation of atmospheric impact on the results of the precise geodetic measurements

with GPS technique in polar conditions” was established in the Institute of Geodesy and Cartography (grant No 8T12E 045 20) in March 2001. J Cisak – the project leader, reported the first results of the international project to the projects coordinators meeting in Siena in July 2001. One week later the Third Antarctic Geodesy Symposium AGS’01 took place in St. Petersburg. One session of the Symposium was devoted to the problem of the atmospheric impact on GPS technique of measurements. The proceedings of the Symposium were published in SCAR Report, No 21, January 2002, publication of the Scientific Committee on Antarctic Research, Scott Polar Research Institute, Cambridge, UK. As the result of the Symposium, an efficient cooperation between SCAR WG on Geodesy and Geographic Information and IGS IONO WG (Feltens and Jakowsky, 2001) has been established. J. Cisak was invited to take part in the workshop of the IONO WG of IGS that was held in Darmstadt, in February 2002. Some results of the project as well as the SCAR WG GGI activity were presented and published in the special issue of the workshop. The new achievements in the project were presented at the International Workshop on “Atmospheric impact on GPS observations focused on Polar Regions”, 15 May 2002, Warsaw, Poland. The papers and presentations of the workshop are placed on the web page of the SCAR Geoscience Standing Group: <http://www.geoscience.scar.org/geodesy/warsaw/index.htm>. The next interim report of the state of the project was presented to the international geodetic community at the WG GGI meeting during the XXVII SCAR, Shanghai, China, July 2002. The papers with the attempt to correct the final GPS solutions for the Antarctic vectors were presented at the AGS’02, Wellington, New Zealand, December 2002 (Cisak *et al.*, 2002)

<http://www.geoscience.scar.org/geodesy/ags02/index.htm> and at the Poland – Italy geodetic meeting, Bressanone, Italy, April 2003 (Cisak *et al.*, 2003c). The project is still running. Everybody is very welcome to contribute to it. The final report is to be prepared and presented at the next SCAR Symposium in Bremen, 2004.

3. Ionosphere

3.1. Influence of non-homogeneity of ionosphere in polar region on the results of GPS measurements

The non-homogeneity of the atmosphere in the Polar Regions is an important factor when considering the influence of ionosphere for the determination of coordinates by use of GPS technique. It has various forms of different range.

The most spectacular form of the non-homogeneity of the atmosphere is the main ionospheric trough, which is the large-scale structure of lowering electron concentration. The concentration of the electrons in the area of ionospheric trough can be even ten times smaller than outside that area. The width of such zone, along the meridian, can reach 2-3 degrees of arc. The latitudinal gradients of the electron concentration in such area can significantly differ

from those in quiet ionosphere and can lead to erroneous determination of phase ambiguities (Baran *et al.*, 2001b; Baran *et al.*, 2001c).

The other forms of the non-homogeneity of the ionosphere in Polar Regions are the bubbles with dimension of a few hundreds or even a thousand kilometres. The electron concentration inside the bubbles can exceed the concentration outside it by a factor 10 to 100. The edges of that type of non-homogeneity are characterized by large gradients.

The non-homogeneities of the atmosphere in the range of tens of kilometres can substantially affect GPS measurements and the accuracy of GPS solutions. The intensity of those non-homogeneities during the magnetic storms can grow up to several times, and cause substantial fluctuation of GPS signal phases (Epishov *et al.*, 2002). Such fluctuations can be observed even in the latitudes below 60°.

During the occurrence of large electron concentration gradients the ionospheric refraction can strongly affect the determination of ambiguity and result in growing errors of GPS solutions. The correlation between the growth of unsolved ambiguities and variations in TEC values due to ionospheric storms is clearly visible when calculating vectors from GPS data in Polar Regions; it leads to erroneous determination of vector components (Cisak *et al.*, 2002c; Cisak *et al.*, 2003a). The GPS signal passing through the area of electron concentration changes demonstrates phase fluctuations that can result in loss of lock to satellites what further affects continuity in phase recording.

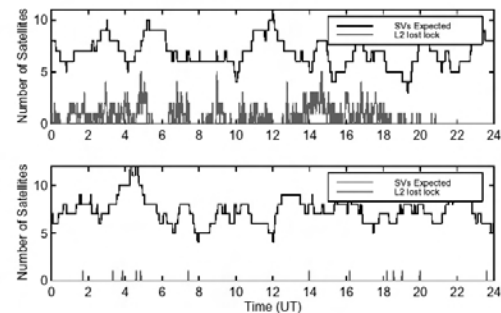


Fig. 3.1.1. The number of satellites with a loss of lock on L2 against the number of satellites observed

Fig. 3.1.1 (Stewart and Langley, 1999) presents the comparison of the number of satellites for which a loss of lock on L2 occurred with the number of satellites visible in Fairbanks (Alaska) during high activity of ionosphere in 27 August 1998 (upper graph) and for quiet ionosphere in 13 December 1998 (lower graph).

The influence of the electron concentration changes, resulting as the refraction of signal path and its differential lengthening with respect to different frequencies (Fig. 3.1.2) causes the second order refraction errors. Thus, the use of L3 combination does not completely remove the ionospheric effect from GPS solutions. For modelling and estimation of those effects the model errors of one

layer model can be used (Zanimonskaya and Prokopov, 2001).

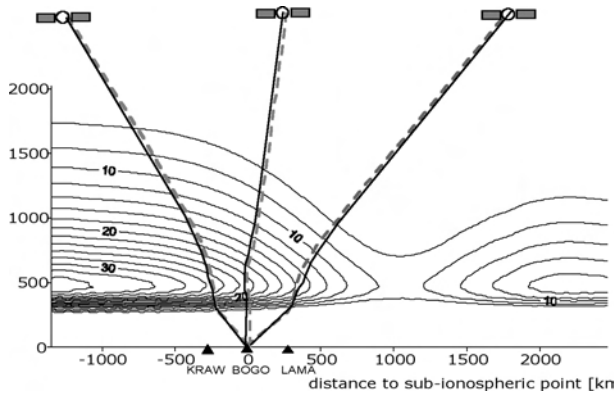


Fig. 3.1.2. Refraction of the signal path during the ionospheric trough. The dot-lines correspond to lower frequency signal (L2) and continuous lines - higher frequency (L1). The contour lines correspond to the electron density in units 10^4 el/m^3

Incorrectness of the ionosphere modelling using single layer approximation results in non-linearity in both TEC and pseudo-range determination (Brunner and Gu, 1991; Zanimonskaya and Prokopov, 2001). That non-linearity affects also other parameters, e.g. TZD (Krynski *et al.*, 2002b) and vector components.

Similarly to optical systems the effect of non-homogeneity of the ionosphere is proportional to the measure of non-homogeneity itself.

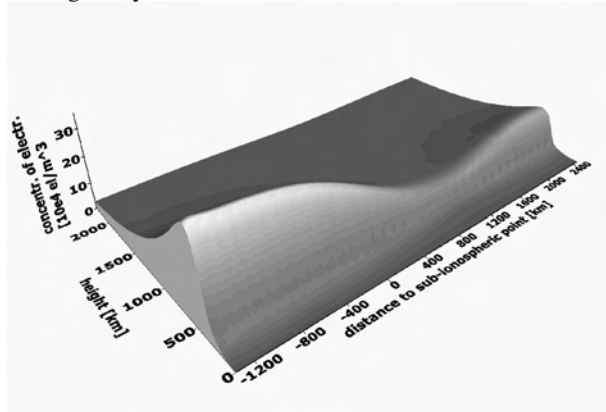


Fig. 3.1.3. 3D distribution of electron density during the ionospheric storm in 13 September 1999

Fig. 3.1.4 shows the errors of the pseudo-range estimation from L3 combination, during the transition of the signal through the inhomogeneous structures of ionosphere of different size. In the compartments of inhomogeneous ionosphere of the shape of lens the largest divergence of electron contents from not violated ionosphere was considered equal to $5 \cdot 10^5 \text{ m}^{-3}$. The dimension of inhomogeneous structures of the ionosphere in the cases shown in Fig. 3.1.2 and Fig. 3.1.3 is about 1000 km and electron density change is $2 \cdot 10^5 \text{ el/m}^3$. Taking into account data from Fig. 3.1.4, those ionospheric disturbances affect pseudo-range by about 3 cm. It results in systematic errors in GPS solutions, mainly through the erroneous ambiguity determination.

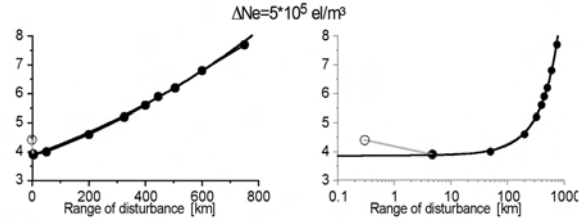


Fig. 3.1.4. Dependence of the second order errors in pseudo-ranges on the dimension of inhomogeneous elements of ionosphere with fixed maximum of electron density changes

3.2 Dependence of variations in vector components from the electron concentration in ionosphere for the Antarctic GPS stations.

Seasonal changes of atmospheric conditions frequently disturb the continuity in tracking GPS satellites (during all seasons). Those changes can cause periodic errors in GPS solutions and suggest the periodic movements of the Earth's crust, what naturally is an artefact. Besides an increasing number of permanent Antarctic stations, for several years the periodic GPS Epoch Crustal Movement Campaigns (Detrich, and Rülke, 2002) have been conducted. More than 50 stations take part in those campaigns. They are organized during the Antarctic summer only. It is questionable whether the results of one-season campaigns reflect the real changes in the stations co-ordinates and indicate the actual crustal movements. The first results of investigation of the influence of ionosphere on GPS solutions, obtained in the framework of this project were presented at the Antarctic Geodesy Symposium AGS'01 in St. Petersburg in July 2001 (Krankowski *et al.*, 2001a). Data from the second part of February 1999 acquired at several stations of Northern Hemisphere and several Antarctic stations were used in the analysis (Table 3.2.1.).

Table 3.2.1. Vectors and their lengths examined in the analysis

Baseline	Distance [km]	Baseline	Distance [km]
Onsala-Metsahovi	784	Onsala - Ny-Alesund	2387
Onsala-Kiruna	1250	Onsala - Thule	3622
Onsala-Tromso	1406	O'Higgins - Arctowski	132
Onsala-Hoefn	1640	Davis - Mawson	636
Onsala-Reykjavik	1956	Davis - Casey	1397

Table 3.2.1. Vectors and their lengths examined in the analysis

All vectors were determined using the Bernese v.4.2. software with use of QIF strategy (Quasi Ionosphere Free) from 24h, 12h and 6h sessions. Dispersion in vector components (from 5 solutions) reaches the level of 20 cm when sub-daily sessions were processed, while for 24h sessions the dispersion do not exceed 7 cm. The maximum differences were obtained for observations collected from 12:00 – 18:00 UT, when TEC shows the large dynamics of changes. Similar large differences occurred for long vectors (over 650 km) as well as for short ones, e.g. Arctowski - O'Higgins (132 km). For the stations in

Northern Hemisphere (vector Onsala – Metsahovi) the differences were significantly smaller. This experiments and results obtained were encouraging to look for the confirmations of the results with use of the larger statistic material and with using new research methods.

GPS data from several permanent IGS Antarctic stations (Fig.3.2.1) were analysed, separately those from summer and from winter seasons. The Bernese v.4.2 software with QIF ambiguity resolution strategy was used to process the data in daily sessions with 23h overlap. (Cisak *et al.*, 2003).

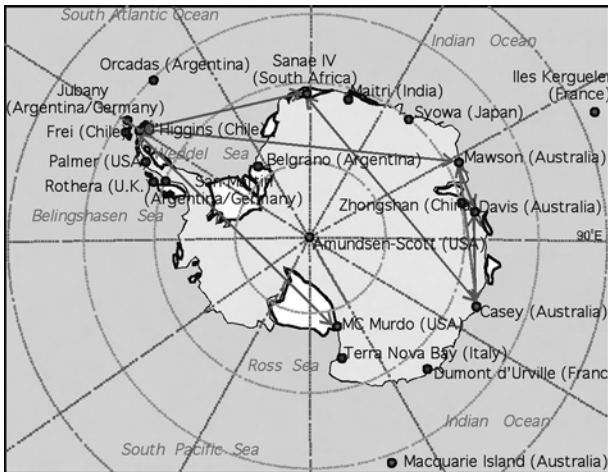


Fig. 3.2.1. The map of Antarctic permanent GPS stations and analysed vectors

The Ionosphere Working Group of the International GPS Service publishes the global maps and arrays of TEC values, given in function of latitude and longitude with 2h temporal resolution. Annual variations of TEC values for 2001 obtained from IONEX data by calculating daily averages over Antarctic Davis (DAV1) and European Borowa Gora (BOGO) stations as well as the Ap index representing in linear scale a measure of geomagnetic activity are presented in Fig. 3.2.2.

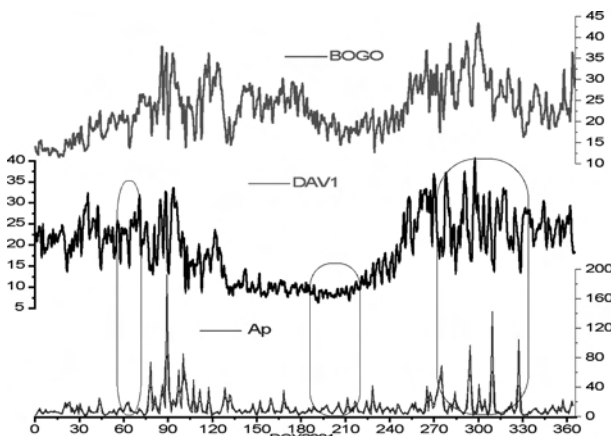


Fig. 3.2.2. Annual variations of diurnal mean TEC over DAV1 and BOGO stations obtained from IONEX data and the Ap index

Seasonal variations of the ionosphere are clearly visible in the graph; it is especially distinct over the Antarctic station Davis.

Data of particular interest correspond to time intervals that have been marked on the graph (Fig. 3.2.2). The first data set corresponds to the vicinity of 64DOY2001 when the occurrence of ionospheric storm was detected in the analysis of time series of GPS solutions of vectors between EPN stations (Zanimonskiy *et al.*, 2002). The third data set covers the period of extremely active ionosphere that took place in October and November 2001. The impact of the atmosphere on GPS solutions of vectors was carefully analysed for that period (Cisak, *et al.*, 2002). The lowest electron concentration and the lowest geomagnetic activity in 2001 occurred in July. Thus the July 2001 data (second data set marked in Fig.3.2.2) was included to the analysis. Averaged solutions for lengths and vertical components of vectors between selected Antarctic permanent GPS stations for the chosen data sets are given in Table 3.2.2.

Table 3.2.2.

Vector	Vector length [m]			
	March (9 days)	July (30 days)	Oct. (30 days)	Nov. (30 days)
MAW1-DAV1	636437,6895 ±0,0005	636437,6893 ±0,0002	636437,6885 ±0,0003	636437,6873 ±0,0003
DAV1-CAS1	1397636,0179 ±0,0007	1397636,0193 ±0,0003	1397636,0141 ±0,0005	1397636,0134 ±0,0005
MAW1-CAS1	2028197,5492 ±0,0017	2028197,5484 ±0,0004	2028197,5446 ±0,0007	2028197,5424 ±0,0008
Vertical component [m]				
MAW1-DAV1	44,4544 ±0,0011	44,4482 ±0,0006	44,4522 ±0,0006	44,4521 ±0,0006
DAV1-CAS1	22,5020 ±0,0018	22,4934 ±0,0010	22,5054 ±0,0009	22,5065 ±0,0009
MAW1-CAS1	22,5109 ±0,0026	22,4911 ±0,0013	22,5139 ±0,0012	22,5096 ±0,0010

Differences between the average lengths and vertical components of the vectors calculated during the period of the unstable and quiet ionosphere (July 2001) are given in Table 3.2.3. Variations of the solutions shown in Table 3.2.2. for different seasons are quite substantial. In most cases they exceed their accuracy estimated by using a common error propagation procedure. The differences obtained (Table 3.2.3.) were interpreted by means of statistical analysis of correlations of GPS solutions for vector components, and by means of parameters from the processing with the Bernese software, i.e. $_2$, number of ambiguities resolved, number of single differences used in the solution, internal accuracy parameters, etc. with ionospheric data from IGS IONO-WG (IONEX) and also with the data received directly from IONO-WG, kindly provided by Dr. Manuel Hernandez-Pajares.

Table 3.2.3.

Vector	Difference in vector length [mm]			
	March (9 days)	July (30 days)	Oct. (30 days)	Nov. (30 days)
MAW1-DAV1	0,2±0,5 1,1±0,5	0,0 ±0,2 0,0 ±0,2	-0,8±0,3 0,4±0,3	-1,9±0,3 -0,7±0,3
DAV1-CAS1	-1,5±0,7 2,5±0,7	0,0 ±0,3 0,0 ±0,3	-5,2±0,5 -0,3±0,5	-5,9±0,5 -0,9±0,5
MAW1-CAS1	0,8±1,5 3,7±1,6	0,0 ±0,4 0,0 ±0,4	-3,8±0,7 -0,1±0,7	-6,0±0,8 -2,3±0,8
Difference in vertical component [mm]				
MAW1-DAV1	6,1±1,1	0,0 ±0,5	4,1±0,6	3,8±0,6
DAV1-CAS1	8,6±1,8	0,0 ±0,9	11,8±0,9	13,2±0,8
MAW1-CAS1	19,8±2,3	0,0 ±1,2	22,8±1,2	18,5±0,9

The problem concerns the errors, resulting from non-linearity of calculating algorithms and from second order effects of signal propagation in the ionosphere. The non-linearity of the algorithms used for the data processing of satellite observations was widely discussed in the literature (e.g. Tiberius, 1998). The weak non-linearity causes the

known effect of detection, i.e. the conversion of variations of process parameters or random input signals into biases in output results. For determination of metrological properties of measurement system the qualitative and quantitative assessment of conversion of random error into systematic error is needed. The growth of random errors of GPS observations during the ionosphere's storm (Baran et al., 2002) can be used as a signal for testing the hypothesis of the detection.

The second order effects of the ionosphere can also be considered as the source of non-linearity in the process of solving ambiguities. The existence of other sources of non-linearity cannot be excluded but the complex technology, instrumentation, software, mathematical and physical models of different sources of disturbances of GPS signal make the description of the phenomena quite difficult.

Polar regions, in particular the Antarctic - a continent being the extensive international research laboratory, are suitable test areas for investigating ionosphere's effects on GPS solutions. During the Antarctic winter the diurnal changes of electron concentration are insignificant. It is due to a low and almost not varying altitude of the Sun over the region. The changes in electron concentration over Antarctic are caused mainly by geomagnetic activity. The Antarctic winter in 2001 was exceptionally quiet in the sense of geomagnetic activity as compared with other years. The results of GPS positioning from that winter can thus be considered as reference in studying the ionosphere's impact on GPS solutions obtained in other years as well as in different seasons. Overlapping sessions of 24-hour were processed to smooth random errors in GPS solutions and to eliminate short-term biases. The TEC data from IONEX files was respectively averaged over 24h with 1h temporal resolution (Fig. 3.2.2).

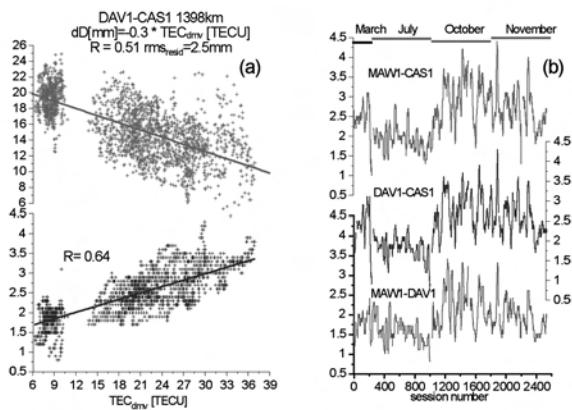


Fig. 3.2.3. Variations of vector length and uncertainty of ambiguity estimation versus TEC (a), and time series of uncertainties of ambiguity estimation for the periods investigated (b)

Fig. 3.2.3a shows the relationship between DAV1-CAS1 vector length (dD) and diurnal average of TEC (upper graph) as well as the relationship between the uncertainty of ambiguity estimation in the vector calculation and diurnal average of TEC (lower graph). Diurnal average of

TEC presents stronger correlation with the uncertainty of ambiguity resolution (correlation coefficient of 0.64) than with vector length (correlation coefficient of 0.51).

Due to a regional scale of dynamics of the ionosphere in Antarctica, the ionospheric disturbances affect similarly GPS data acquired at the investigated stations. Thus the GPS vector solutions obtained with the Bernese software are practically free of TEC differences between the stations. It should also be noted that the time series of uncertainties of ambiguity resolution do not substantially differ for different vectors and do not depend on their length (Fig.3.2.3b). The same conclusions are drawn from the analysis of GPS solutions for EPN vectors.

The obtained results indicate the dependence of ambiguity resolution on the state of ionosphere. Crucial role in both performed quantitative and qualitative analysis played the use of time series of GPS solutions based on overlapped sessions (Krynski and Zanimonskiy, 2002). Correlations shown in Fig. 3.2.3 indicate a possibility of modelling the ionospheric effects on GPS solutions. For example, the solutions for vector length could get corrected by using the regression model of $dD = k(TECdmv)$ based on TEC data. For DAV1-CAS1 vector of 1398 km, the correction equals to +3 mm/10TECU. Generally, the unstable ionosphere causes shortening of vector length obtained from GPS solution. The vector lengths corrected with the model are shown italic in Table 3.2.3. Introducing the corrections resulted in the decrease of seasonal dispersion in both October and November data and made them more similar to the July data when the ionosphere was quiet. Although in most cases the applied corrections improve the obtained results, there are exemptions when the procedure does not seem suitable (Table 3.2.3). They might happen due to relatively small amount of data processed as well as larger and more irregular disturbances of the ionosphere.

4. Troposphere

4.1 Dependence of variations in vector components from the Total Zenith Delay for the Antarctic GPS stations.

Time series of vector components obtained with the

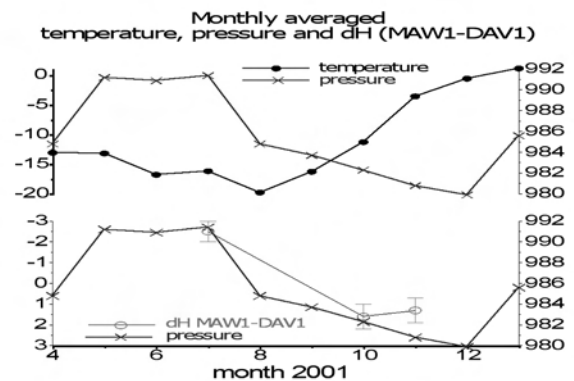


Fig.4.1.1. Annual variations of monthly averages of temperature, atmospheric pressure as well as vertical component of the MAW1-DAV1 vector

Bernese v.4.2 software for daily sessions of GPS observations from a number of permanent stations acquired in July, October and November 2001, were used to investigate the impact of varying meteorological conditions on GPS solutions. Analysed data correspond to the periods substantially distinguished in terms of dynamics of the atmosphere. Variations in monthly average of temperature, atmospheric pressure as well as vertical component of the MAW1-DAV1 vector are given in Fig. 4.1.1.

Variations in vertical components of the vectors defined by pairs of investigated GPS permanent stations in Antarctica are correlated with seasonal variations of atmospheric pressure. Similar conclusion was already drawn from the analysis of GPS solutions and meteorological data in mid-latitudes (Haefele and Kaniuth., 2001).

Tropospheric impact on GPS measurements is described in terms of tropospheric delay. To increase reliability of results obtained, tropospheric delay data from two independent sources was considered in the analysis. First, the Tropospheric Zenith Delay (TZD), available on IGS web pages, in the form of time series with 1h temporal resolution was considered. Second, the TZD data derived from radio sounding over the majority of permanent GPS stations in Antarctica, also in the form of time series but with 12h temporal resolution. The results obtained with use of both data sources were close to each other at the acceptable level.

Time series of atmospheric pressure and TZD at the Antarctic GPS stations (Fig. 4.1.2) as well as correlation of TZD and atmospheric pressure variations with vertical components of respective vectors (Fig. 4.1.3) were analysed.

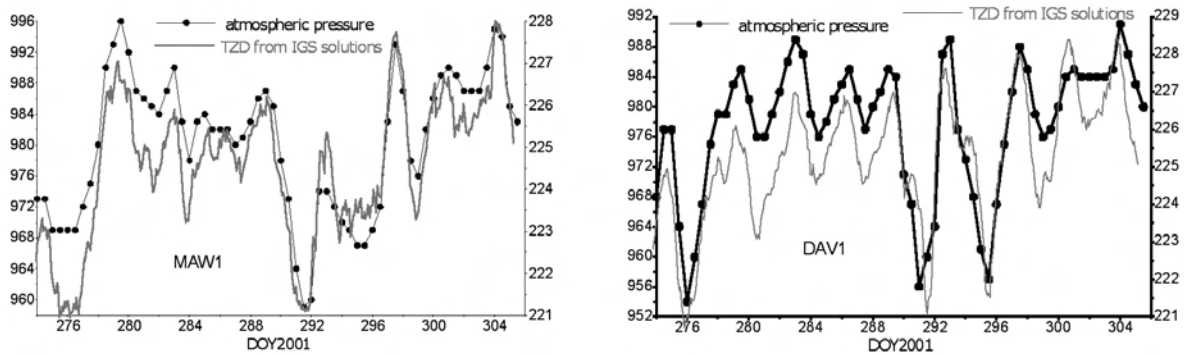


Fig. 4.1.2. Variations of atmospheric pressure and TZD for Mawson (a) and Davis (b) stations

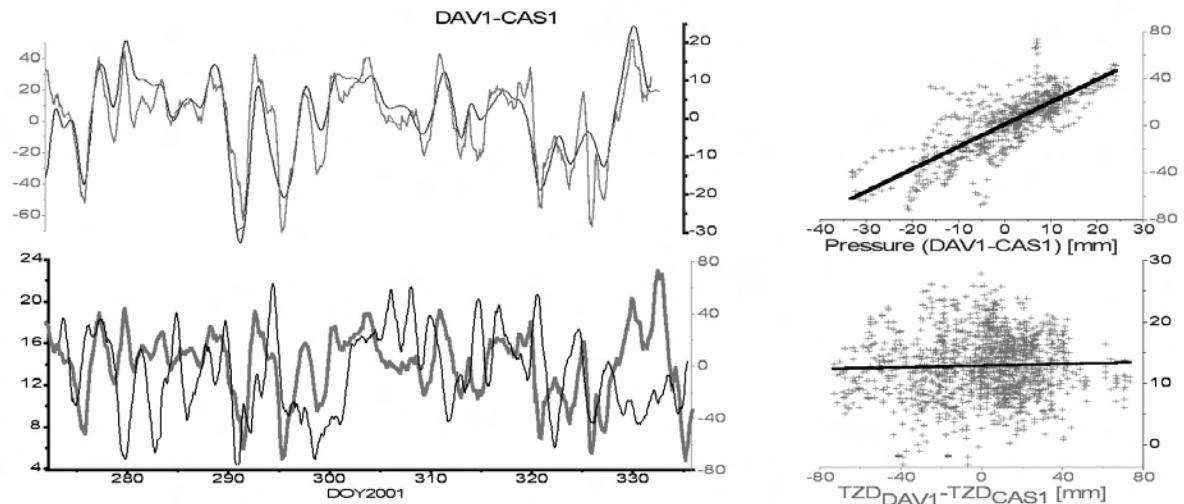


Fig. 4.1.3. Variations of differential TZD versus variations of atmospheric pressure and GPS-derived vertical component of DAV1 – CAS1 vector

No significant effect of variations of troposphere on GPS solutions observed (Fig. 4.1.3) proves sufficient modelling of troposphere in the Bernese v.4.2 software when computing vectors of a few hundred kilometres length and longer; GPS solutions obtained are practically free

of the tropospheric effect.

In case of commercial programmes used to process GPS data, the experiments conducted with EPN data indicate correlation of GPS-derived vector components with TZD. Correlation coefficients derived could efficiently be used to correct GPS solutions obtained with commercial software. It applies not only to GPS solutions for mid-latitude stations but also for those in Polar Regions.

5. Conclusions

The non-modelled delays of GPS signal when passing the atmosphere affect GPS solutions for station positions and vector components and result in variations in time series of such solutions. To improve GPS solutions with no better models of atmosphere, corrections to the computed vector components, calculated using correlation analysis, could be applied. Data from Antarctic GPS stations are especially suitable for modelling such correlation functions and determining their parameters due to a distinct seasonal variability of ionosphere in Polar Regions.

The results discussed in the paper focus on the analysis of the impact of ionospheric disturbances on variations of vector lengths obtained at high latitudes from GPS data. Variations of GPS solutions for lengths of vectors are commonly explained in terms of non-modelled variations of the ionosphere. Besides their direct effect on GPS solutions, they affect them indirectly by violating the mechanism of integer ambiguity resolution. Correlation analysis conducted using data sets from chosen Antarctic stations shows a possibility of using simple empirical models for partial eliminating the non-modelled in GPS processing software effects of ionosphere. Modelling ionospheric effects on the results of GPS data processing requires further research with use of larger data samples. GPS solutions corrected with such empirical models seem more suitable for geodynamics research.

The results of the research on the tropospheric impact on GPS solutions show seasonal dependence of height differences between Antarctic stations from changes of atmospheric pressure. Modelling the satellite signal passing through the troposphere in the Bernese v. 4.2 software seems satisfactory. No correlation between vector components obtained using the Bernese software and Total Zenith Delay was found. The analysis of time series of GPS solutions based on EPN data, obtained using commercial software shows the possibility of using empirical models to partially eliminate from GPS solutions the non-modelled in processing GPS data effects of troposphere – similarly to the ionospheric one.

Acknowledgements

The paper summarizes the results of the research conducted at the Institute of Geodesy and Cartography (IGiK), Warsaw, and at the University of Warmia and Mazury (UWM), Olsztyn. The research was partially supported by the Polish State Committee for Scientific Research (Research Project No 8 T12 E045 20). The author expresses his gratitude to all contributors to the project – particularly to Prof. W. Baran, Dr. A. Krankowski, Dr. P. Wielgosz from UWM, Dr. I. Shagimuratov from IZMIRAN, Kaliningrad, Russia, Prof. J. Krynski from IGiK, Dr. Y. Zanimonskiy from the Institute „Metrologia” Kharkov, Ukraine, who temporarily works at IGiK, and to Dr. Manuel Hernandez-Pajares from the Technical University of Catalonia, Spain, for processing and kind submission of high temporal

resolution ionospheric data. Some fragments of the paper as well as some figures are with the approval of the authors taken from the publications cited in bibliography.

Bibliography

- Baran L.W., Shagimuratov I.I., Wielgosz P., Yakimova G.A., (2001a): *The structure of high-latitude ionosphere during September 1999 storm event obtained from GPS observations*, EGS 2001, CD.
- Baran L.W., Shagimuratov I.I., Wielgosz P., (2001b): *Structure of the ionosphere during disturbance and effects GPS positioning*, IAG Report 2001 Scientific Assembly, Budapest, 2-7 September 2001.
- Baran L.W., Krankowski A., Shagimuratov I.I., (2001c): *Influence of Ionosphere on Repeatability of Vectors Co-ordinates Determination*, IAG 2001 Scientific Assembly. Budapest, 2-7 September 2001.
- Baran L.W., Rotkiewicz M., Shagimuratov I.I., (2001d) *Ionospheric Effects And GPS Positioning*, IAG 2001 Scientific Assembly. Budapest, 2-7 September 2001.
- Baran L.W., Ephishov I.I. and Shagimuratov I.I., (2001e): *Ionospheric Total Electron Content Behaviour During November 1997 Storm*, *Phys.Chem.Earth (C)*, 2001, Vol. 26, No 5, pp. 341-346.
- Baran L.W., Ephishov I.I., Shagimuratov I.I., (2001f): *Spatial Correlation of Ionosphere During Storm Derived from GPS Measurements*, *Bull. Pol. Ac. Sc.: Earth Sci.*, Vol. 49, No 2, pp. 151-164, Warsaw, December 2001.
- Baran L.W., Shagimuratov I.I., Ephishov I.I. Wielgosz P.A., Krankowski A., (2002a): *The response of the ionosphere over Europe to the geomagnetic storm on March 31, 2001*, EGS, Nice, April 2002, ST023; EGS02-A-01063; ST2-1WE5P-023.
- Baran L.W., Rotkiewicz, M., Wielgosz, P., Shagimuratov, I.I., (2002b): *Ionospheric Effects During a Geomagnetic Storm*, *Vistas for geodesy in the New Millennium*. International Association of Geodesy Symposia, 125, Springer-Verlag Berlin Heidelberg New York 2002, pp. 291-296.
- Baran L.W., Shagimuratov I.I., Aleshnikova M.V., Wielgosz P., (2002c): *Latitudinal Variations of TEC over Europe Obtained from GPS Observations*, 34th COSPAR Scientific Assembly, Houston, USA, 10-19 October 2002, Abstracts, CD, The New Face of Space - The World Space Congress - 2002.
- Brunner F.K., Gu M., (1991): *An Improved Model for Dual Frequency Ionospheric Correction of GPS Observations*, *Manuscripta Geodaetica*, 16, pp. 205-214.
- Cisak J., (2002a): *Overview of the SCAR/WG-GGI/ GIANT Activities as an Introduction to the Workshop*, Paper presented at the International workshop on “Atmospheric impact on GPS observations focused on polar regions”, 15 May 2002, Warsaw, Poland.

- Cisak J., (2002b): *Atmospheric Impact on GPS Observations in Antarctica* - Project of GEODESY/GIANT program of SCAR WGGGI Report 2000 – 2002, Presentation on WGGGI meeting of XXVII SCAR.
- Cisak J., Krynski J., Zanimonskiy Y.M., (2002): *Variations of Ionosphere Versus Variations of Vector Components Determined from Data of IGS Antarctic GPS Stations – New Contribution to the GIANT Project* “Atmospheric Impact on GPS Observations in Antarctica”, Paper presented at the AGS-02, Wellington, New Zealand, http://www.scar-ggi.org.au/geodesy/ags02/cisak_ionosphere_gps.pdf
- Cisak J., Krynski J., Zanimonskiy Y.M., Wielgosz P., (2003a): *Variations of Vector Components Determined from GPS data in Antarctic. Ionospheric Aspect in New Results Obtained within the Project* “Atmospheric Impact on GPS Observations in Antarctica”, Paper presented at the scientific conference, 22-23 January 2003, Lviv, Ukraine.
- Cisak J., Krynski J., Zanimonskiy Y., Wielgosz P., (2003c): *Study on the Influence of Ionosphere on GPS Solutions for Antarctic Stations in the Framework of the SCAR Project* „Atmospheric Impact on GPS Observations in Antarctica”, Paper presented at the 7th Bilateral Meeting Italy-Poland, Bressanone, Italy, 22-23 May 2003.
- Dietrich R., Dach R., Engelhardt G., Ihde J., Korth W., Kutterer H.-J., Lindner K., Mayer M., Menge F., Miller H., Mueller C., Niemeier W., Perlt J., Pohl M., Salbach H., Schenke H.-W., Schoene T., Seeber G., Veit A., Voelksen C., (2001): ITRF coordinates and plate velocities from repeated GPS campaigns in Antarctica - an analysis based on different individual solutions, *Journal of Geodesy*, Number 74, pp. 756-766, Springer Verlag, Germany.
- Dietrich R., Rülke A., (2002): The SCAR GPS Campaigns in the ITRF2000, *SCAR Report, No 21*, January 2002, Scientific Committee on Antarctic Research, Scott Polar Research Institute, Cambridge, UK.
- E Dongchen, Cheng Xiao, Zhou Chunxia, (2002): *GPS Meteorology in Antarctica*, Paper presented at the AGS-02, Wellington, New Zealand, http://www.scar-ggi.org.au/geodesy/ags02/dongchen_gps_meteorology.pdf
- Ephishov I.I., Shagimuratov I.I., Wielgosz P., Cisak J., (2002): *Phase Fluctuations of GPS Signals at High Latitude Ionosphere During the Storm, EMC2002*, Proceedings of XVII International Wrocław Symposium and Exhibition on Electromagnetic Compatibility, pp. 37-42, 2002.
- Feltens J., Jakowsky N., (2001): The International GPS Service (IGS): Ionosphere Working Group activities, *SCAR Report*, Publication of the Scientific Committee on Antarctic Research, Scott Polar Research Institute, Cambridge, UK.
- Góral W., (1997): Numerical estimation of differential refraction correction in GPS measurements. *Reports on Geodesy*, Warsaw U. of Tech., Institute of Geodesy and Geodetic Astronomy, No 5(28), pp. 181-187.
- Haefele P., Kaniuth K., (2001): *Analysis of Time Series of GPS Height Estimates with Regard to Atmospheric Pressure Loading*, Paper presented at the IAG International Symposium on Vertical Reference Systems, 21-23 February 2001, Cartagena, Colombia.
- Krankowski A., (2002): *Modelling of the Ionosphere in Polar Regions*, Paper presented at the International workshop on “Atmospheric impact on GPS observations focused on polar regions”, 15 May 2002, Warsaw, Poland
- Krankowski A., Baran L.W., Shagimuratov I.I., (2001): *Influence of the Northern ionosphere in positioning precision*, Abstract XXVI General Assembly EGS, Nice, France 25-30 March 2001.
- Krankowski A., Baran L.W., Shagimuratov I.I., Cisak J., (2002a): *Influence of Ionosphere in Antarctic Region on GPS Positioning Precision*, Collection of Papers and Viewgraphs of IGS/IAACs Ionosphere Workshop, ESOC Darmstadt, Germany, 17-18 January 2002.
- Krankowski A., Baran L.W., Shagimuratov I.I., Cisak J., (2002b): Influence of Ionosphere in Arctic and Antarctic Regions on GPS Positioning Precision, *SCAR Report, No 21*, January 2002, Publication of the Scientific Committee on Antarctic Research, Scott Polar Research Institute, Cambridge, UK.
- Krankowski A., Baran L.W., Shagimuratov I.I., (2002c): Influence of the northern ionosphere on positioning precision, *Physics and Chemistry of the Earth*. 2002, Vol. 27, No 5, pp. 391-395.
- Kruczyk M., (2002): *Tropospheric Delay in GPS Permanent Networks – a Tool for Atmosphere Research*, Paper presented at the International Workshop on “Atmospheric impact on GPS observations focused on polar regions”, 15 May 2002, Warsaw, Poland.
- Krynski J., Zanimonskiy Y., (2001): Contribution of Data from Polar Regions to the Investigation of Short Term Geodynamics. First Results and Perspectives, *SCAR Report, No. 21*, January 2002, Publication of the Scientific Committee on Antarctic Research, Scott Polar Research Institute, Cambridge, UK.
- Krynski J., Cisak J., Zanimonskiy Y.M., Wielgosz P., (2002a): *Variations of GPS Solutions for Positions of Permanent Stations – Reality or Artefact*, Symposium of the IAG Sub commission for Europe (EUREF) held in Ponta Delgada, Portugal, 5-7 June 2002, EUREF Publication No 8/2, Mitteilungen des Bundesamtes für Kartographie und Geodäsie, Frankfurt am Main (in print).
- Krynski J., Zanimonskiy Y.M., Cisak J., Prokopov A.V., Zanimonskaya A.E., Wielgosz P., (2002c): *Global Ionospheric Impact on the Satellite Navigation System Errors (in Russian)*, Proceedings of the Conference in Kharkov State University, Kharkov, Ukraine, 3 October 2002.

- Manning J., (2001): The SCAR Geodetic Infrastructure of Antarctica, Report from the Second SCAR Antarctic Geodesy Symposium, Warsaw, July 1999, *SCAR Report No. 20*, pp 22-30, SCAR, Cambridge.
- Manning J., Cisak J., (2002): Overview of the SCAR/WG-GGI/GIANT activities within the project on the Atmospheric Impact on GPS Observations in Antarctica and possible fields of cooperation with IGS/Iono WG. Proceedings of IGS/IAACs Ionosphere Workshop, Darmstadt, 17-18 January 2002
- Mendes V.B., Prates G., Santos L., Langley R., (2000): *An Evaluation of Models for the Determination of the Weighted Mean Temperature of the Atmosphere*. Proceedings of The Institute of Navigation 2000 National Technical Meeting, Anaheim, CA, U.S.A., 26-28 January 2000; pp. 433-438.
- Poutanen M., Koivula H., Ollikainen M., (2001): *On the Periodicity of GPS Time Series*, Proceedings of IAG 2001 Scientific Assembly, 2-7 September 2001, Budapest, Hungary.
- Prokopov A.V., Remayev Ye.V., (2001): *Integral Ray Optics Approximation in the Electromagnetic Waves Theory and its Applications for Atmospheric Delay Modelling in GNSS Measurements*, Proceedings of IAG Assembly, Budapest, 2001.
- Schaer S., (1999): *Mapping and Predicting the Earth's Ionosphere Using the Global Positioning System*, PhD Thesis, Astronomical Institute, University of Berne.
- Shagimuratov I.I., Baran L.W., Tepenitsyna N.J., Ephishov I.I., (2002a): *Variations of TEC during ionospheric storm in September 1999 Obtained from GPS Observations*, Proceedings of the XX Conference on Propagation of Radio Waves. Niznij Novgorod, 2-4 July 2002, Niznij Novgorod, pp. 123-124 (in Russian).
- Shagimuratov I.I., Baran L.W., Wielgosz P., Yakimova G.A., (2002b): The structure of mid- and high-latitude ionosphere during September 1999 storm event obtained from GPS observations, *Ann. Geophys.* 20, 1-6, 2002.
- Wielgosz P., (2002): *Use of Deterministic Ionospheric Component in GPS Observations Processing*, Paper presented at the International workshop on "Atmospheric impact on GPS observations focused on Polar Regions", 15 May 2002, Warsaw, Poland.
- Wielgosz P., Grejner-Brzezinska D., Kashani I., (2003): *On High-Resolution TEC Derivation from Regional GPS Networks: Feasibility Study*, Paper presented at 2003 IEEE AP-S Symposium and USNC/CNC/URSI National Radio Science Meeting, Columbus, Ohio.
- Ulyanov Y., Zanimonska A., Zanimonskiy Y., (2000): *Correlation of Surface Temperature with Average Temperature of Troposphere in Radioacoustic Sounding Data* Paper presented at the Second International Workshop on "Satellite Navigation in CEI Area" Olsztyn 3-4 July 2000.
- Zablotskiy F., (2002) On Determination Precision of Tropospheric Delay at the Antarctic Coast Stations, *SCAR Report, No. 21*, January 2002, Publication of the Scientific Committee on Antarctic Research, Scott Polar Research Institute, Cambridge, UK.
- Zanimonskaya A., Prokopov A., (2001): Estimation of the Second Order Refraction Effects in the Ionosphere Models for GPS Applications (in Ukrainian), *Geodesy, Cartography and Photogrammetry*, Lviv, No 61, pp. 24-29.
- Zanimonskiy Y., Krynski J., Cisak J., (2002): *Correlation of the Atmospheric and Geodetic time Series of GPS Results. Impact, coincidence or artefact?* Paper presented at the International Workshop on "Atmospheric impact on GPS observations focused on polar regions", 15 May 2002, Warsaw, Poland.

An Analysis of Contribution of the Troposphere and Lower Stratosphere Layers to Forming of the Tropospheric Delay Wet Component

Fedir Zablotskiy, Alexandra Zablotska and Natalya Dovhan
National University "Lviv Polytechnic"
Chair of Geodesy and Astronomy

Abstract

An estimation was made of the most influential layers of the lower atmosphere into quantity formation of the wet component of zenith tropospheric delay in summer in the Antarctic regions as well as in the West and South-West regions of Ukraine.

The Central Antarctica Region is distinguished especially inasmuch as an extratropospheric part of the wet component and is there dominating in the total value of wet component.

An analysis of the most widely used Saastamoinen and

Hopfield analytical models assigned for the determination of the wet component was realized.

The lower (neutral) atmosphere is one of the main error sources which reduces essentially an accuracy of GPS measurements. The error caused by the neutral atmosphere effect (tropospheric delay) has two components – dry and wet ones.

The total tropospheric delay is expressed as:

$$d_{trop} = d_d^z \cdot m_d + d_w^z \cdot m_w,$$

where d_d^z and d_w^z are zenith dry and wet components

respectively; m_d, m_w are mapping functions of the components of zenith tropospheric delay at zenith angles $Z > 0^\circ$.

On the whole it may be defined either by vertical profiles of the meteorological parameters measured at the moment of GPS measurements or by the way of modelling of such profiles. The first way is pretty unwieldy, expensive and inefficient.

The second one presents as a rule the generally averaged vertical profiles in the form of analytical models and resolves to determine the first component of tropospheric delay with relatively high accuracy. A determination of the second component is a problem task as the wet component forecasting is very complicated because of the difficulty of the establishment of water vapour quantity in the lower atmosphere. Therefore the error of the determination of the wet component amounts to several tens of millimetres even in the zenith zone.

The cause of unsatisfactory precision of the determination of the wet component of zenith tropospheric delay in polar regions by means of existing analytical models consists in the following. In general it is accepted that the value of water vapour pressure drops to zero at the boundary of troposphere and tropopause and therefore an air humidity profile for the determination of water vapour pressure is recommended to take into consideration to the upper boundary of troposphere. Practically all analytical models for the determination of the wet component are constructed on that ground. This approach satisfies to some extent the reality for low and middle latitudes. At high latitudes and first of all in Antarctic Region both the stratification itself and the structure of the lower atmosphere differ essentially.

Though the value of the wet component of zenith tropospheric delay is here significantly less than in the middle latitudes, the essential part of it, namely about 20%, concentrates in the lower stratosphere of the Antarctic coast zone. It should be noted that the differences of air temperatures at the altitude of 17 km above sea level average -16° in summer period between Odesa and Mirnyj stations and -15° between Odesa and Heise Island (the Central Arctic) stations. Thus as a result of the establishment of the "warm" lower stratosphere in polar regions during the summer period, a considerable proportion of water vapour mass part accumulates here and that is what forms a certain increase of water vapour partial pressure and the value of zenith tropospheric delay wet component accordingly.

Table 1
Average quantitative characteristics (%) of the wet component of zenith tropospheric delay and of the water vapour pressure in the different atmospheric layers at the stations

Wet component d_w^z			Vapour pressure e		
0.04-2 km	2 km- H_{TROP}	H_{TROP} - H_U	H_{TROP}	H_U	
48.4	30.2	21.4	8.12	25.21	52.8
60.4	38.9	0.8	10.92	24.00	63.7

The averaged percentage of the wet component d_w and the water vapour partial pressure e in three high atmospheric layers of Mirnyj and Odesa stations for summer period are shown in table 1.

The values H_{TROP} characterize the upper boundary of troposphere and the values H_U – the upper boundary of relative humidity sounding.

As it is obvious, the value of the wet component of zenith tropospheric delay which is formed by extratropospheric layers of atmosphere exceeds 20% at Mirnyj station and amounts to 0.8% only at Odesa station. According to table 1 a close correlation between the distribution of the wet component of zenith tropospheric delay and water vapour partial pressure is observed.

As long as the aim of our paper was to make an estimation of the most influential layers of the lower atmosphere into quantity formation of the wet component of zenith tropospheric delay in summer period we chose additionally 14 vertical profiles obtained from aerological sounding for each station:

- Mirnyj – Antarctic Coast Zone;
- Vostok – the Central Antarctica;
- Lviv - the West region of Ukraine;
- Odesa - the South-West region of Ukraine.

At the same time the atmospheric models were made up for the vertical profiles with the measurements of the relative humidity not less than up to the altitude of 24 km above sea level (the mean isobaric surface corresponds to 30 hPa).

A special attention was devoted to the Central Antarctica where the extremely low temperatures cause a very small content of water vapour in the air. Thus, the average monthly surface quantity of water vapour pressure at Vostok station amounts to only 0.25 hPa for January and declines to 0.03 hPa at the upper boundary of the troposphere.

Table 2
Averaged meteorological parameters and parts of the wet component of zenith tropospheric delay d_w (mm)

H_0 km	P_0	t_0	U_0	d_w 850	d_w 700	d_w 500	d_w H_{TROP}	d_w 30	d_w total.	δd_w (SA)	δd_w (HO)
O d e s s a											
0.04	1010.4	18.8	77	84.6	51.6	30.8	8.4	1.4	176.7	10.1	8.8
L v i v											
0.33	976	17.8	77	68.8	54.6	36.5	12.3	2.4	174.7	22.1	18.7
M i r n y j											
0.04	983.8	-4.2	73	16.1	11.7	8.3	2.4	7.9	46.4	10.2	-0.7
V o s t o k											
3.49	633.0	34.5	70	-	-	3.1	2.2	14.1	19.4	16.1	13.6

Notice: P_0, t_0, U_0 - atmospheric pressure (hPa), air temperature ($^\circ$) and relative humidity (%) at the station level H_0 ;

d_w - part of the wet component of zenith tropospheric delay in the atmospheric layers "station level – 850 hPa", "850 – 700 hPa", "700 – 500 hPa", "500 hPa – upper boundary of the troposphere", "upper boundary of the troposphere – 30 hPa";

$d_w^{(total)}$ - total value of the wet component of zenith tropospheric delay;

δd_w (SA) and δd_w (HO) – differences between the total value of the wet component of zenith tropospheric delay obtained by means of the aerological profile and the total value of the wet component calculated after Saastamoinen - Hopfield models.

In addition, we give the results (table 2) which characterize the percentage part of the wet component of zenith tropospheric delay in the above mentioned atmospheric layers.

Table 3.

Table 3

Averaged parts of the wet component of zenith tropospheric delay in the atmospheric layers

Station	H_0 - 850 hPa	850- 700 hPa	700- 500 hPa	500 hPa - H_{trop} 30 hPa	H_{trop} - 30 hPa
Odessa	47.9	29.3	17.4	4.6	0.9
Lviv	39.4	31.2	21.0	7.0	1.4
Mirnyj	34.8	25.2	17.9	5.2	16.9
Vostok	-	-	16.0	11.3	72.7

As it is obvious from the data of tables 1-3, the two lower layers of troposphere “station level – 850 hPa” and “850 – 700 hPa” import about 70% into the total quantity of the wet component in the middle latitudes. The next layer “700 – 500 hPa” adds another almost 20%. Hence, the three lower layers of the troposphere import about 95% of the wet component into the total quantity of it at Odessa station and over of 90% - at Lviv one.

The contribution of these layers at the Antarctic coast zone decreases to 80%, and in the Central Antarctica it amounts to only 16%.

On the basis of our investigations the following should be noted for the summer period:

- in the middle latitudes a predominant mass of the atmospheric water vapour is located in the lower half of the troposphere. The part of the wet component of zenith tropospheric delay amounts to 5.5% and 8.4% in the layers of the atmosphere

between 500 and 30 hPa at the Odessa and Lviv stations accordingly;

- at the high latitudes and especially in Antarctica the water vapour is pushed up into higher layers of the atmosphere. At the same time this process increases with displacement from the coast zone to the central part of the continent. So the part of the wet component of zenith tropospheric delay makes up in the atmospheric layers from 500 to 30 hPa 22.1% at Mirnyj station and 84% (!) at Vostok one;
- the existing analytical models, as it is shown in table 2, do not provide a high accuracy of determination of the wet component of zenith tropospheric delay.

Conclusions

The extratropospheric contribution to the formation of the total value of the wet component of zenith tropospheric delay is very essential in polar regions and first of all in Antarctica in contrast to the middle latitudes. For more precise account of the wet component of tropospheric delay influence on the results of GPS measurements in summer period in polar regions it is necessary to include to the total humidity the extratropospheric part of it up to the about 25 km height. This value may be modelled on the basis of detailed analysis of the lower atmosphere stratification by means of aerological data of the polar stations at which the permanent GPS observations or the long GPS campaigns are already being carried out.

The Second Order Refraction Effects for GPS Signals Propagation in Ionosphere

A. Prokopov, A. Zanimonska

National Science Center “Institute of Metrology”

Mironositskaya st. 42, 61002, Kharkov, Ukraine

e-mail: nil1@metrology.kharkov.ua

When measuring on the Earth – Space satellite direction the radio signal experience the additional delay caused by the difference between the speed of light in vacuum and speed of signal propagation in medium and by refractive lengthening of the signal path while crossing the ionosphere and troposphere. To reduce the tropospheric effect the correction models are usually used. To reduce ionospheric effect dual-frequency methods are used besides the modelling. These methods are instrumental methods and they are based on the fact that ionosphere is a dispersive medium.

One of the weakness of existing dual-frequency methods is the fact that these methods use measuring equation obtained on the assumption that signals with different frequencies propagate along the same rectified trajectory. This means that the refractive effects of spatial separating of the ray paths with different carrier frequencies and their refractive lengthening due to bending are not take into

account. More over while deriving the equations the square root in the formula for refractive index of ionosphere was replaced by linear function of electron concentration (i.e. the higher order terms in the inverse power of frequency series expansion of the refractive index aren’t take into account) and the influence of the Earth’s magnetic field can be neglected.

Errors caused by effects mentioned above (which are usually called the second order effects) have been studied in [1, 2, 3] where it was shown that the total residual error at high values of electron concentration on big zenith angles run up to several cm

In general case the following mathematical model can be used for error calculation [3]:

$$\sigma_{sep} = \frac{f_2^2}{f_1^2 - f_2^2} \left[\Delta D_2 - \Delta D_1 + \Delta S_2 - \frac{f_1^2}{f_2^2} \Delta S_1 \right]$$

$$\sigma_{length} = \Delta D_1$$

where, σ_{sep} , σ_{length} - refractive errors caused by the separating effect of the ray paths and the lengthening accordingly (these formulas allow for all the second order effects mentioned above).

$$\Delta D_i = \int_{S_i} ds - L$$

$$\Delta S_i = \begin{cases} \int_{S_i} (n-1) ds & \text{-for phase measurements} \\ \int_{S_i} (\frac{1}{n}-1) ds & \text{-for code measurements} \end{cases}$$

n is the refractive index of ionosphere;

ΔD_i is refraction lengthening of a signal path with the frequency ;

ΔS_i is a delay of a signal with the frequency ;

S_i is a signal path with the frequency ;

s is a ray coordinate;

L is a distance from a receiver to a satellite along the straight line.

Errors σ_{sep} and σ_{length} were calculated for various frequencies f and zenith angles τ_0 (code measurements). Though these errors appear in the measurement equation with the opposite signs, the total error (the residual refraction error of the two-frequency method) at high values of electron concentration on big zenith angles can reach several sm. One can see it on the Fig. 1 where the data obtained with the use of the biexponential model of electron concentration profile are shown.

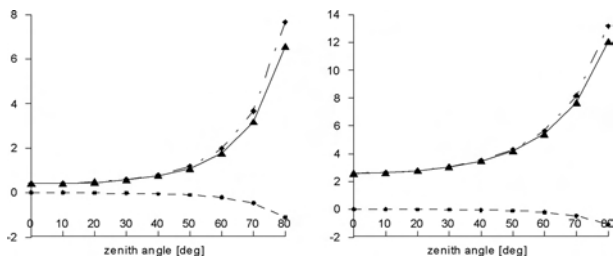


Fig. 1. The refraction errors of the two-frequency method for $N_m=5.106 \text{ cm}^{-3}$, $=1227.46 \text{ MHz}$, $=1575.60 \text{ MHz}$ (a solid line is for total effect, a dashed line is for lengthening effect, a dash-and-dot line is for space separation effect).

The left plot on Fig. 1 corresponds to the case when geomagnetic field is not taken into account. The right plot corresponds to the case with the following parameters of geomagnetic field: gyrofrequency is equal to 1.4 MHz and $\cos\theta=0.5$, where θ is the average angle between the satellite-receiver line and lines of the geomagnetic field.

When analyzed errors are essential special steps to calculate and exclude these errors from measurement results are necessary. Let's consider the theoretical base of the possible methods of such calculations.

Geometrical distance between a satellite and a receiver can be written as [1]:

$$L = S_1 + \Omega_1 \int_{P_1} N_e ds - k_1 \quad (1)$$

$$L = S_i + \Omega_i \int_{P_i} N_e ds - I_i - k_1 \quad (1a)$$

where (1) is written for the frequency f_1 , and (1a) is for the f_i ;

$$\Omega_i = \frac{C_x}{2f_i^2} \left(1 m \frac{C_y}{f_i} \overline{H_0 \cos\theta} + \frac{C_x}{4f_i^2} N_m \eta \right),$$

$$C_x = \frac{e^2}{4\pi^2 \epsilon_0 m}, \quad C_y = \frac{\mu_0 e}{2\pi m},$$

and the common symbols are used (N_e is the electron concentration; e, m are electron charge and electron mass; ϵ_0, μ_0 are permittivity and permeability in vacuum; H_0 is the amplitude of the geomagnetic field, $\overline{H_0 \cos\theta}$ is the average value of the geomagnetic field effect; η is the shape parameter: ,

$$\eta = \frac{\int_{P_1} N_e^2 ds}{N_m \int_{P_1} N_e ds}, \quad N_m \text{ is the maximum value of } N_e, \quad k_1 \text{ is identical with } \Delta D_1.$$

According to the estimations [1] the stated above formulas allow to take into account the second order effects in wide range of ionospheric conditions with an error not exceeding 1 mm.

As one can see there is an additional item I in the equation (1a) which is take into consideration the spatial separating effect of the ray paths P_1 and P_i . Basically, the equations (1), (1a) can be considered for any given frequencies f_1, f_2, K, f_n . Then, according to (1a), the unknowns are,

$$L + k_1, \overline{H_0 \cos\theta}, N_m \eta, \int_{P_1} N_e ds \text{ and } I_1 K I_n$$

Hence, in general case, the system of $n + 4$ equations is necessary to determine the geometric length of the trajectory $L+k_1$ between the satellite and the receiver (without the determination of the refractive lengthening k_1 , which needs a special examination). At the same time, according to the definition of I , the number of equations in the system is equal to $n + 1$. To bring the number of the equations in correspondence with the number of the unknowns the 2nd order expansion of I in terms of

$\frac{1}{f^2}$ at f_2 could be used:

$$I_i = I(f_i) = I(f_2) + \left(\frac{1}{f_i^2} - \frac{1}{f_2^2} \right) \frac{\partial I}{\partial \left(\frac{1}{f^2} \right)} \Big|_{f=f_2} \quad (2)$$

Under such approach the minimum number of the unknowns is equal to six and using (2) we've accordingly obtained the system of six equations:

$$L = S_1 + \Omega(f_1, \overline{H_0 \cos\theta}, N_m \eta) \int_{P_1} N_e ds - k_1 \quad (3)$$

$$L = S_2 + \Omega(f_2, \overline{H_0 \cos\theta}, N_m \eta) \int_{P_1} N_e ds - I(f_2) - k_1$$

$$L = S_i + \Omega(f_i, \overline{H_0 \cos\theta}, N_m \eta) \int_{P_1} N_e ds - [I(f_2)$$

$$+ \left(\frac{1}{f_i^2} - \frac{1}{f_2^2} \right) \frac{\partial I}{\partial \left(\frac{1}{f^2} \right)} \Big|_{f=f_2}] - k_1, i = 3 \text{ K } 6$$

Taking into account that Ω is a linear function of $\overline{H_0 \cos\theta}$ and $N_m \eta$ with the coefficients, depending on the frequency, the system can be written as:

$$L = S_1 + a(f_1) \int_{P_1} Neds + b(f_1) \overline{H_0 \cos\theta} \int_{P_1} Neds + c(f_1) N_m \eta \int_{P_1} Neds - k_1$$

$$L = S_2 + a(f_2) \int_{P_1} Neds + b(f_2) \overline{H_0 \cos\theta} \int_{P_1} Neds + c(f_2) N_m \eta \int_{P_1} Neds - I(f_2) - k_1$$

$$L = S_i + a(f_i) \int_{P_1} Neds + b(f_i) \overline{H_0 \cos\theta} \int_{P_1} Neds +$$

$$c(f_i) N_m \eta \int_{P_1} Neds - \left[I(f_2) + \left(\frac{1}{f_i^2} - \frac{1}{f_2^2} \right) \frac{\partial I}{\partial \left(\frac{1}{f^2} \right)} \right]$$

$$f=f_2] - k_1 \quad i = 3, 6$$

where

$$a(f) = \frac{C_x}{2f^2}, b(f) = m \frac{C_x C_y}{2f^3}, c(f) = \frac{C_x^2}{8f^4} \quad (4)$$

Then, the system is linear in relation to the unknowns,

$$L + k_1, \int_{P_1} Neds, \overline{H_0 \cos\theta} \cdot \int_{P_1} Neds, N_m \eta \cdot \int_{P_1} Neds,$$

$$I(f_2) \text{ and } \left. \frac{\partial I}{\partial \left(\frac{1}{f^2} \right)} \right|_{f=f_2}$$

and can be easily solved analytically. The obtained solution allows for the all second order effects by instrumental means, but it needs the measurements of pseudorange L_i on six different carrier frequencies.

The method considered above is instrumental. All the input information is gained from the measurements.

6-frequency systems aren't in plan for the near future, but developed in USA and Europa systems (GPS III and Galileo) are providing access for 3 carrier frequencies. Thus we consider a combined method of allowing for ionosphere impact. For that we leave 3 equations and 3 most important for our problem unknowns in system (3). The rest of the unknowns we determine on the base of GPS measurements instead of modelling (combined method).

While choosing the unknowns we take into account that there is a formula for I in [4]. Besides, the IAGA model is recommended for the calculation of H_0 . Thus, we have three unknowns

$$L, \int_{P_1} Neds \text{ and } N_m \eta$$

and the similar to (3) system:

$$L = S_1 + \Omega_1 \int_{P_1} Neds - k_1$$

$$L = S_2 + \Omega_2 \int_{P_1} Neds - I(f_2) - k_1 \quad (5)$$

$$L = S_3 + \Omega_3 \int_{P_1} Neds - I(f_3) - k_1$$

where

$$\Omega_i = \Omega(f_i, \overline{H_0 \cos\theta}, N_m \eta)$$

Having excluded $\int_{P_1} Neds$, we reduce the system (5) to the system of two equations:

$$S = \frac{1}{\Omega_2 - \Omega_1} (\Omega_2 S_1 - \Omega_1 S_2) - [k_1 - k_2] \quad (6)$$

$$S = \frac{1}{\Omega_3 - \Omega_1} (\Omega_3 S_1 - \Omega_1 S_3) - [k_1 - k_3]$$

where

$$k_i = I(f_i) \frac{\Omega_1}{\Omega_i - \Omega_1}, \quad i = 2, 3$$

and $[k_i - k_j]$ is calculated by the corresponding formula from [4].

Using (4), $\Omega_i - \Omega_1$ and $\Omega_i S_1 - \Omega_1 S_i$ will take the form:

$$\Omega_i - \Omega_1 = a(f_i) + b(f_i) \overline{H_0 \cos\theta} + c(f_i) N_m \eta -$$

$$a(f_1) - b(f_1) \overline{H_0 \cos\theta} - c(f_1) N_m \eta =$$

$$= (a(f_i) - a(f_1)) + (b(f_i) - b(f_1)) \overline{H_0 \cos\theta} +$$

$$(c(f_i) - c(f_1)) N_m \eta = a_{i1} + b_{i1} \overline{H_0 \cos\theta} + c_{i1} N_m \eta$$

$$\Omega_i L_1 - \Omega_1 L_i = (a(f_i) S_1 - a(f_1) S_i) + (b(f_i) S_1$$

$$- b(f_1) S_i) \overline{H_0 \cos\theta} + (c(f_i) S_1 - c(f_1) S_i) N_m \eta =$$

$$= A_{i1} + B_{i1} \overline{H_0 \cos\theta} + C_{i1} N_m \eta$$

According to (7) we get the solution from system (6)

$$L + [k_1 - k_2] = \frac{A_{21} + B_{21} \overline{H_0 \cos\theta} + C_{21} N_m \eta}{a_{21} + b_{21} \overline{H_0 \cos\theta} + c_{21} N_m \eta} =$$

$$\frac{A_{31} + B_{31} \overline{H_0 \cos\theta} + C_{31} N_m \eta}{a_{31} + b_{31} \overline{H_0 \cos\theta} + c_{31} N_m \eta} \quad (8)$$

there $N_m \eta$ is determined from the quadratic equation

$$(N_m \eta)^2 (C_{21} c_{31} - C_{31} c_{21}) + N_m \eta (ab_{31} C_{21} + AB_{21} c_{31} - ab_{21} C_{31} - AB_{31} c_{21}) + ab_{31} AB_{21} - ab_{21} AB_{31} = 0 \quad (9)$$

where

$$AB_{i1} = A_{i1} + B_{i1} \overline{H_0 \cos\theta}, \quad ab_{i1} = a_{i1} + b_{i1} \overline{H_0 \cos\theta}$$

Formula (8) and equation (9) give a solution which allow for second order refractive ionospheric effects on the base of the 3 frequency pseudorange measurements and models of geomagnetic influence and spatial separation of the ray paths.

In some cases it may be useful to choose different set of unknowns. For example, $L, \int_{P_1} Neds$ and $\overline{H_0 \cos\theta}$

when the last unknown is difficult to model (during the huge magnetic storms or near the magnetic poles). Following the discourse described above one can obtain the similar to (8) and (9) equations.

When $f_3 \rightarrow f_2$ and the second order items are neglected we have the passage to the limit of the standard dual-frequency method. Equation (9) is turning into the identity

$$ab_{21} AB_{21} - ab_{21} AB_{21} \equiv 0$$

and formula (8) is being reduced to the measurement equation of the currently used model [1].

For dual-frequency GNSS the allowing for the second order ionospheric effects by the instrumental or combined methods is impossible, since there is no resource to receive

the additional information (there aren't additional carrier frequencies). In this case it is possible to take advantage of the model approach. The entry values for the method of ionospheric error modelling, developed by us, are TEC (on which the parameters of analytical model of the electron concentration profile are determined) and a zenith angle (on which the value of the correction is determined using the obtained model). It is necessary to mark, that this method will not eliminate the refractive effect completely, since the value of TEC is determined with some error. Besides, the allocation of electrons in ionosphere could a little differ from a model, but this factor is not so essential as TEC.

Conclusions

Three approaches to solving the problem of modelling and elimination of the second order ionospheric errors are considered. That are instrumental approach (when all the information is gained from the measurement), model approach (when the independently defined refractive error correction is put in the results of the measurements) and combined one.

Storm-time Structure and Dynamics of the Ionosphere Obtained from GPS Observations

I.I. Shagimuratov (1), A. Krankowski (2), L.W. Baran (2), J. Cisak (3), G. Yakimova (1)

(1) WD IZMIRAN, Kaliningrad, RUSSIA

(2) Institute of Geodesy, Warmia and Mazury University in Olsztyn, POLAND, kand@uwm.edu.pl;

(3) Institute of Geodesy and Cartography, Warsaw, POLAND

Abstract.

The analyses of the structure of the ionosphere during the greatest storm in recent years, which took place on 31 March 2001 obtained by multi-stations technique using GPS observations of IGS and EPN network are presented. Storm-time changes of the ionosphere were analyzed via the TEC maps for American and European regions. The response of the ionosphere in the Antarctic area eliminates temporal TEC variations obtained over an individual station. High spatial resolution of TEC maps was realized using GPS observation from 80-100 European and American stations. The TEC maps were produced in latitudinal range of 40-75 with 15 min interval. Time-dependent features of the ionospheric storm were identified using the differential TEC maps based on the deviation of TEC during the storm in comparison to a quiet period. The response of TEC to geomagnetic storm consists of effects of both enhancement and depletion (positive and negative disturbances). A short-duration positive effect on the first stage of the storm was observed over Europe on subauroral ionosphere probably due to the auroral particle precipitation. The enhancement of TEC exceeds 150% compared to the quiet time. The negative effect took place during daytime on the first day of storm and lasted till next night.

These methods assumed to be useful for increase of accuracy of GNSS, both the systems which is now in use and the perspective multi-frequency ones (Galileo, GPS-III).

References.

- Min Gu, F. K. Brunner. An improved model for the dual frequency ionospheric correction of GPS observations// *Manuscripta geodetica*. – 1990. – Springer-Verlag. – pp.205 – 214.
- Bassiri S., Hajj G.A. Modelling the Global Positioning System Signal Propagation Through the Ionosphere// *TDA Progress Report 42-110*. – August 15, 1992. – pp. 92 – 103
- Zanimonska A., Prokopov A. The estimation of the second order refractive effects in Ionospheric models for GPS applications.// *National University "Lviv Polytechnic" (Ukraine): Geodesy, cartography and air photography*. - #61. – 2001. – pp. 24-29. (in Ukrainian)
- Min Gu, F. K. Brunner. Theory of two frequency dispersive range correction// *Manuscripta geodetica*. – 1990. – Springer-Verlag. – pp.357 – 361.

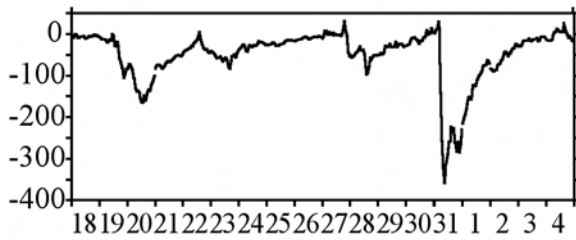
In the American sector the effect was more pronounced than over Europe. The essential changes of the ionosphere are observed on subauroral latitude, which we attribute to the occurrence of ionospheric trough and it developed during the storm. Maximal latitudinal gradients which occurred at the equatorial or polar walls of the trough depend on geophysical conditions. Over America the spatial distribution of TEC demonstrate the large scale structures, which probably can be associated with perturbations of the neutral winds. The strong storm effect took place over the Antarctic and Arctic regions also. During 31 March day time depression of TEC exceeded 200% daytime level of TEC in comparison to night TEC. The diurnal variations TEC over a high latitude station are essentially modified. In the auroral region in magnetic storm period the ionospheric different scale irregularities developed, which caused increasing intensity phase fluctuations of GPS signals. On the whole the results demonstrate complex storm patterns as a function of geophysical conditions, longitude, latitude and time.

Key words: Ionosphere, TEC, modelling of ionosphere

1 Introduction

Two severe geomagnetic storms took place on March 19

and March 31, 2001. The main phase of the first storm started about 11 UT on March 19. The Dst index reached its minimum value -160 nT at 13 UT on March 20 (Figure 1). Simultaneously K_p index amounted to 7 and $\Sigma K_p \approx 44$ (Figure 2). The second investigated storm started about 04 UT on March 31. The Dst index decreased sharply to -358 nT at 08:00 UT. The K_p index reached the value of 9 between 06:00 and 12:00 UT on March 31 (ΣK_p amounted of 61). The recovery phase took place after 09:00 UT on April 4, when Dst gradually returned to its regular level.



Days of March and April 2001
 Fig. 1. Dst index

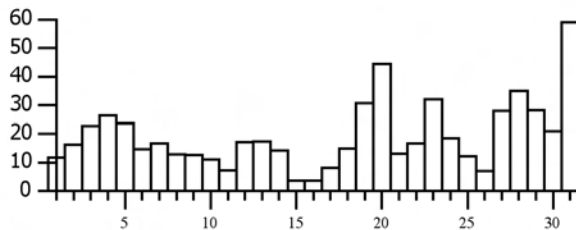


Fig.2. Variations of sum K_p during March 2001

2 Data source and estimation technique

The GPS data from IGS (International GPS Service) permanent network were used to obtain TEC changes on the global scale during both storms. A dense GPS network provided TEC measurements with high temporal and spatial resolution. The analyses of the storms were carried out over North America, Antarctica and Europe. To present the temporal and spatial variation of TEC during the storms, we created the instantaneous TEC maps. The data from over 80 European and 100 American GPS stations were used to create TEC maps. Precise dual frequency GPS phase measurements were used (Baran *et al.*, 1997).

While estimating TEC, the ionosphere was approximated as a single layer at a fixed height of 400 km above the Earth’s surface. The simple geometric factor was used to convert slant TEC into vertical one. A sun-fixed reference frame was used (local time/geomagnetic latitude). In order to produce TEC maps, the TEC measurements from all stations were fitted to a spherical harmonic expansion as functions of geographic latitude and longitude. The maximum degree/order of the spherical expansion was 16. The maps were derived with a 15-minute resolution.

3 Results

3.1 the storm on March 19, 2001

Over Europe, the storm started just after local noon on

March 19 (Figure 3). Storm-time effects occurred in TEC in the evening and during night, as the TEC increase at auroral and subauroral latitudes.

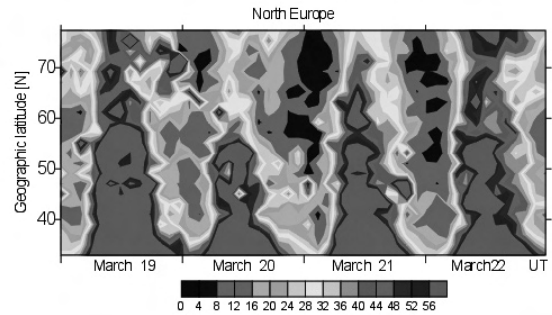


Fig. 3. Storm development over Europe

The analyses of TEC variations for the individual satellite passes show that during the driven phase of the storm, different scale irregularities developed at high latitudes. Patch-like structures with a strong TEC increase were observed. It is interesting, that similar structures but with decreased TEC were also observed (Baran *et al.*, 2002, Shagimuratov *et al.*, 2002).

During daytime on March 20, the negative effect occurred with a maximum at latitudes over 55°N. The weak negative effect took place also at latitudes under 40°N. The negative phase of the storm lasted through the next day (March 21) and the following night. The negative phase was mostly pronounced at latitudes over 50°-55°N.

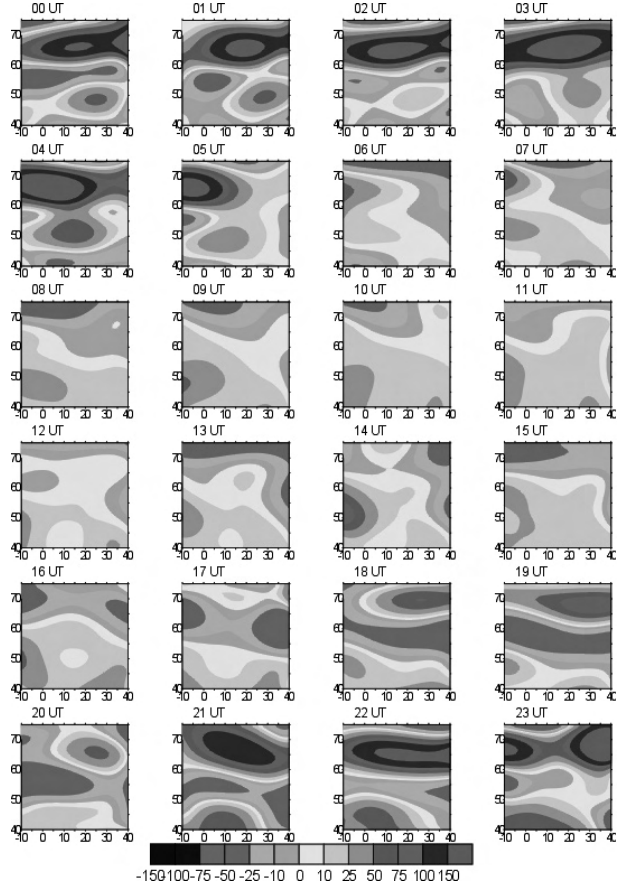


Fig.4a. The differential maps of TEC over Europe for March 19, 2001 (geographic coordinates).

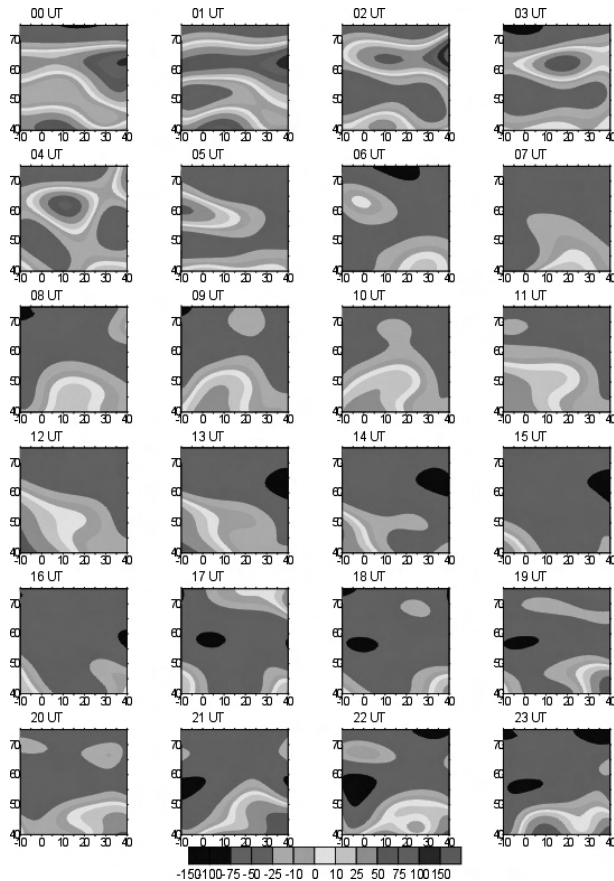


Fig.4b. The differential maps of TEC over Europe for March 20, 2001 (geographic coordinates).

On Figures 4a and 4b you can see the differential maps of TEC over Europe for March 19 and 20. Night time TEC increase took place on March 19/20 at auroral and subauroral latitudes. The increase reached 100-150%. The positive effect occurred also at latitudes below 50°N. The TEC depression, observed at latitudes about 55°N can be attributed to the effect of the midlatitude trough. On March 20, after 06:00 UT the negative effect prevailed over Europe and lasted until 06:00 UT on March 21.

3.2 the storm on march 31, 2001

Figure 5 presents storm development over North America region on March 31.

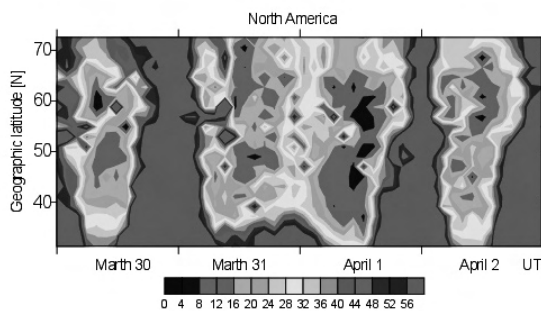


Fig. 5. Storm development over North America

Before the start of the storm the positive effect took place during the local daytime on March 31. The negative effect occurred during the following night and

TEC depression reached 75 %. The negative effect lasted through the following local day.

During the driven phase of the storm, large-scale structures of the increased TEC were observed in the ionosphere. The structures are related to the occurrence of the midlatitude trough and strong perturbations induced in the ionization processes, such as particle precipitation at high latitudes (Figure 6a and 6b).

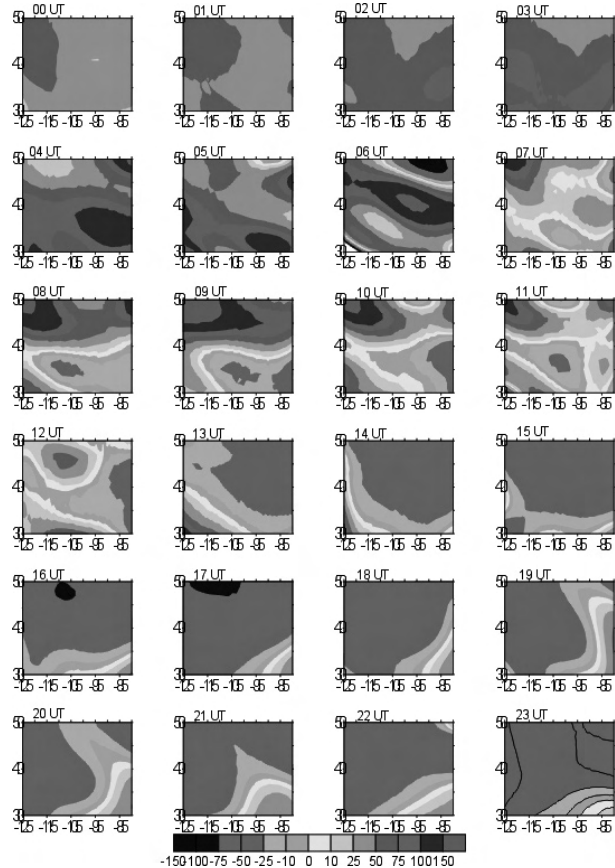


Fig.6a. Differential maps of TEC over North America for March 31, 2001 (geographic coordinates).

In the periods of geomagnetic storms (on March 19 and 31) the satellite/receiver biases of O'Higgins and McMurdo receivers increased sharply. On March 31 satellite/receiver biases reached the value of 4 meters at OHIG and MCM4, respectively (Figure 7).

Figure 8 presents diurnal variations of the TEC over single Antarctic stations for the period of storm of March 31, 2001. For a period of quiet day - 26 March 2001 the TEC values at Antarctic stations (Casey, Davis, Syowa, Sanae) reached the values of 30, 60, 50, 40 TECU, respectively. On March 31 2001 absolute TEC values decreased sharply to 15, 25, 18, 20 TECU, respectively.

4. Conclusion

The GPS observations of the IGS network were used to study the response of the ionosphere to two severe geomagnetic storms of March 2001 over European, North America, and Antarctic sectors. The following conclusions can be made:

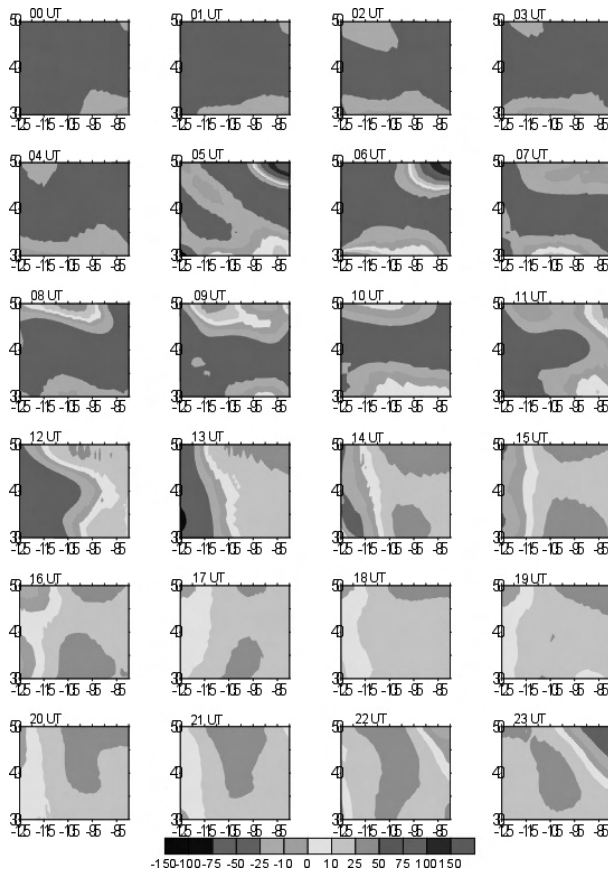


Fig.6b. Differential maps of TEC over North America for April 1, 2001 (geographic coordinates).

- The storm on March 19 was less intensive than the storm on March 31 (Dst = -160nT and Dst = -358, respectively).
- The storm on March 19 developed gradually. The driven phase of the first storm was prolonged but the storm of March 31 was of a short duration (only 4 hours).
- The main feature of both storms under investigation was a strong negative TEC effect. The TEC depression amounted up to 75-100%.
- The duration of the negative phase was longer for the weaker storm of March 19.
- The response of the ionosphere to both storms was more pronounced and longer over North America and Antarctica sectors than Europe.
- Both storms began with a positive phase. The maximum positive effect took place at auroral and subauroral ionosphere. The strong increase of TEC (~150%) at high latitudes can be attributed to the particle precipitation.
- The high deviation of TEC relative to quiet conditions gave rise to the displacement of the minimum of the midlatitude through.
- During the storms the intensive large-scale irregularities were observed at the auroral and subauroral ionosphere.
- The regional behaviour of the response of the ionosphere to the geomagnetic storms is clearly visible.

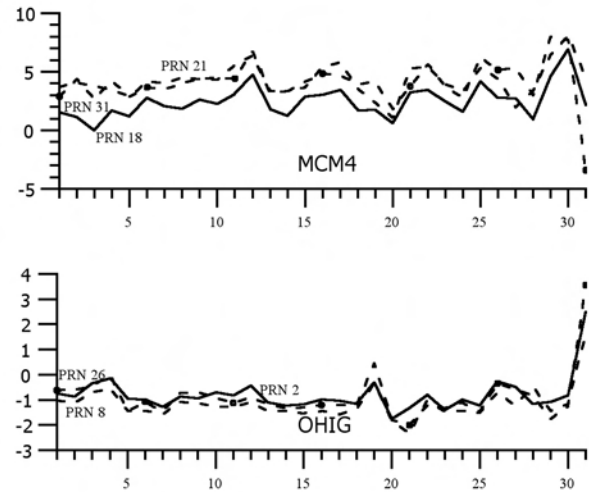


Fig.7 The satellite/receiver biases of OHIG and MCM4 receivers for March 2001

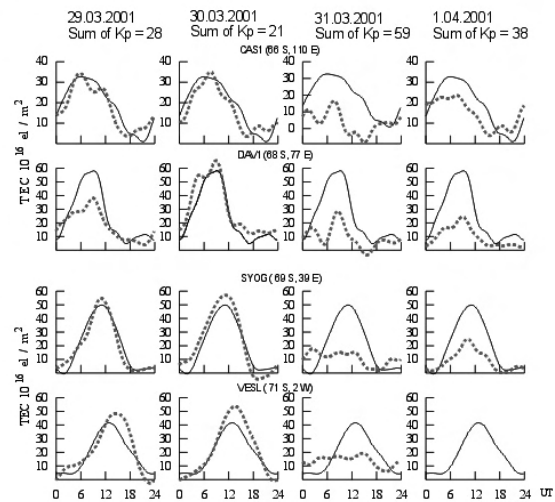


Fig.8 Diurnal variation of TEC over Antarctic stations for period 29 March -1 April 2001 (dashed line) and quiet day 26 March, 2001 (solid line)

Reference

Baran L.W., I.I. Shagimuratov, N.J. Tepenitsina, 1997, The use of GPS for Ionospheric Studies, *Artificial Satellites*, Vol.32, No 1, pp. 49-60.

Baran L.W., M. Rotkiewicz, P. Wielgosz, I. I. Shagimuratov; Ionospheric Effects During a Geomagnetic Storm, Vistas for geodesy in the New Millennium, *International Association of Geodesy Symposia*, Volume 125, Springer-Verlag Berlin Heidelberg New York 2002, pp. 291-296.

Frankowski, L. W. Baran, I. I. Shagimuratov; Influence of the Northern Ionosphere on Positioning Precision, *Physics and Chemistry of the Earth* 27 (2002), pp. 391-395, 2002 Elsevier Science.

Shagimuratov I.I., L.W. Baran, P. Wielgosz, G.A. Yakimova, The structure of Mid-and High-Latitude Ionosphere During September 1999 Storm Event Obtained from GPS Observations, *Annales Geophysicae* (2002) 20: pp. 655-661 European Geophysical Society 2002.

Development of TEC Fluctuations in Antarctic Ionosphere During Storm Using GPS Observations

I.I. Shagimuratov (1), A. Krankowski (2), L.W. Baran (2), J. Cisek (3), I.I. Ephishov (1)

(1) WD IZMIRAN, Kaliningrad, RUSSIA

(2) Institute of Geodesy, Warmia and Mazury University in Olsztyn, POLAND, kand@moskit.uwm.edu.pl;

(3) Institute of Geodesy and Cartography, Warsaw, POLAND

Abstract.

GPS observations of the Antarctic stations belonging to IGS network were used to study TEC fluctuations on high-latitude ionosphere during storms. Dual-frequency GPS phase measurements along individual satellite passes with 30 sec sampling interval were served as raw data. The ionospheric irregularities of different scale develop in the auroral, polar ionosphere. It is a common phenomenon which causes the phase fluctuations of GPS signals. We distinguished the variations of TEC related with the ionospheric structures of the spatial scale bigger than 200-300 km. At diagram of temporal variations of TEC along satellite pass the structure of TEC corresponds to the time scale bigger than 15-30min on the 4-6th hour duration of tracking satellite by individual stations. We attribute the variations of the time scale smaller than 15-30 min to TEC fluctuations related to small scale ionospheric irregularities. We used the rate of TEC index (ROTI) expressed in TECU/min as the measure of TEC fluctuations. The large scale ionospheric structures cause the increase of the horizontal gradients and difficulties of the carrier phase ambiguity resolution in relative GPS positioning. In turn the phase fluctuations can cause the cycle slips. At polar stations: MCM4, CAS1, DAV1 we detected the ionospheric structures of enhanced TEC bigger than 3-5 time relative background, while the TEC increased to 10-30 TECU in about 10-15min. The structures were observed during a storm as well as during moderate geomagnetic activity. The structures probably can be attributed to polar cap patches. At lower latitude station: OHIG during the storm can essentially increase the horizontal gradient which we attribute to the occurrence of the ionospheric trough and its storm-time dynamics.

The ROTI data was used to study the developments of phase fluctuations over the Antarctic ionosphere during geomagnetic disturbances. During storms the intensity of phase fluctuations increased. The occurrence of phase fluctuations was even detected during the active storm period of 31 March 2001 at middle latitude station OHIG located at 49 corrected geomagnetic latitude. The storm-time features in longitude and latitude development of phase fluctuations were obtained for the Antarctic region. The correlation between activity of phase fluctuations and magnetic field variation of Mawsen station was established.

Key words: Ionosphere, TEC, modelling of ionosphere

1 Introduction

The structure of the high-latitude ionosphere is very complicated and varied. Strong changes of the ionosphere occur during geomagnetic disturbances. The dramatic changes took place very frequently in the auroral and polar ionosphere. In this region the irregularities of differential scales are developed commonly which cause the fluctuations of total electron content. In the paper we distinguished two types of TEC fluctuations. In the first, the large scale fluctuations (LSF) of TEC which are caused by the ionospheric irregularities with scale bigger than 100-300 km. These ionospheric structures occurred as the deep spatial variations of TEC. The second type of fluctuations is the irregularities with size about ten kilometres which cause the phase fluctuations GPS signals. The small irregularities can coexist with large scale structures. In the report we present the analysis of the development of TEC fluctuations in March 2001. Two great geomagnetic storms took place on 20 and 31 March. The storm on March 31st was the severest one in the last decade. The Kp index reached maximal value of 9 and Kp made up 60. The Dst index reached maximum magnitudes with extremely high value about -360 nT. The geomagnetic conditions during March 2001 are presented in Figure 1 as variation of sum Kp index.

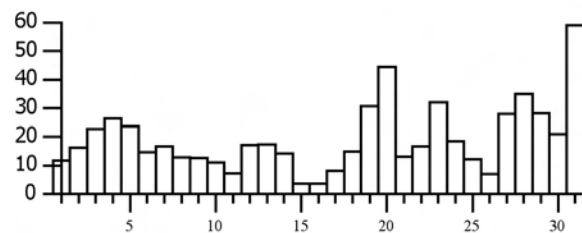


Fig.1. Variations of sum Kp during March 2001

2 The TEC data base

The GPS observations of the Antarctic IGS stations were used to study the development of TEC fluctuations in high-latitude ionosphere. The standard GPS measurements with 30 sec sampling provide the detection of the irregularities with size bigger than 6-10 km. In the Table 1 there are geographic and corrected geomagnetic coordinates of the stations. The broad longitudinal area of Antarctic stations enables to study the time development of TEC fluctuations.

The dynamics of the high-latitude ionosphere are controlled by the geomagnetic field. In the Table 1 you can see that geomagnetic latitudes are essentially different

from geographic one. So in Antarctic region we can choose from middle-latitude station – OHIG, auroral - SYOG, MAW1 to polar stations - MCM4, CAS1, DAV1.

Table 1. Antarctic IGS stations

Station	Geographic		Corrected Geomagnetic		MLT mid-night
	latitude	longitude	latitude	longitude	
OHIG	-63.32	-57.90	-48.93	12.23	03:47
CAS1	-66.28	110.52	-80.66	159.10	18:19
MCM4	-77.84	166.67	-79.95	325.00	07:07
PALM	-64.63	-64.05	-49.93	8.94	04:02
VESL	-71.67	-2.84	-61.67	43.56	01:46
SYOG	-69.01	39.58	-66.65	72.51	23:55
MAW1	-67.60	62.87	-70.68	91.49	22:39
DAV1	-68.58	77.97	-74.91	101.92	21:56

Table 1. Antarctic IGS stations

3 Large scale fluctuation of TEC

For the analysis of spatial and temporal changes of TEC during storm we used the high precision dual-frequency GPS phase measurements that provide more precise measurements of TEC than group delay ones. Phase ambiguities were removed by fitting phase measurements to the code data. After the above procedure the phase measurements contained satellite-receiver biases only. The

absolute TEC and the instrumental biases were estimated using the single site algorithm (Baran *et al.*, 1997). The biases were determined for every individual station using the GPS measurements for all satellite passes over station during 24 hour period. Using this procedure an absolute TEC for all satellite passes observed over single station during 24 hour period is calculated.

The spatial and temporal variations of TEC are clearly seen on the time variations of TEC along individual satellite passes. Figures 2a and 2b give an example of the TEC variations for individual satellite passes as observed from different stations during storm (dashed line) and quiet period (solid line). The vertical TEC in units of 10¹⁶ el/m² is plotted as a function of universal time (UT). This represents a part of diurnal TEC pattern sampled by satellites at these times. The spatial positions of satellites on figures also are presented (cross). Because the GPS satellites are on 12 sidereal hour orbits, the tracks repeat day by day (only the satellites arrive 4 min earlier each day). The plot approximately indicates that the satellites ionospheric trace for two days under consideration.

The series of large scale fluctuations (LSF) as enhancement of TEC are clearly shown on temporal patterns (Figures 2a and 2b). At the polar stations (CAS1, MCM4, DAV1) the TEC patterns demonstrate the great variability during disturbed as well as quiet days. During

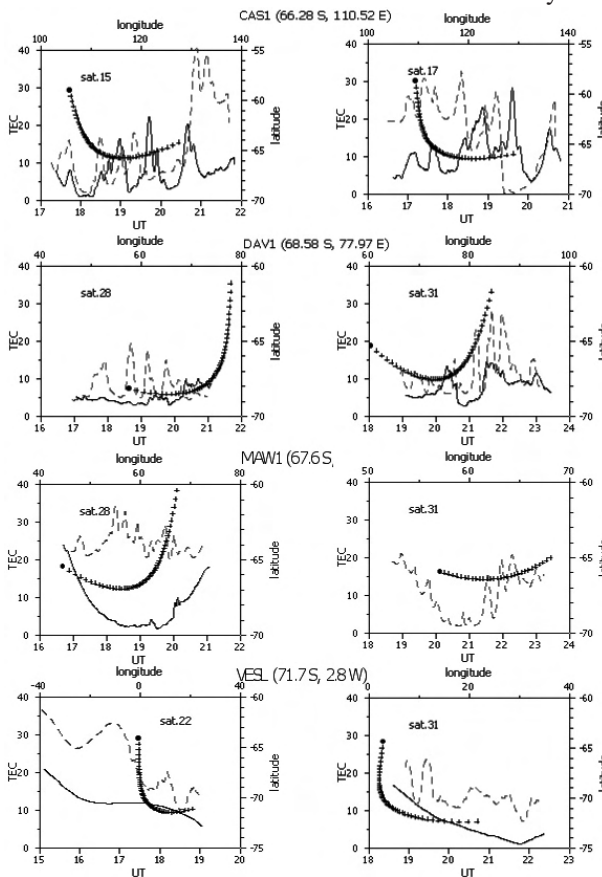


Fig.2a. TEC variations for satellites observed at different stations for during the storm (dashed line) and quiet period (solid line).

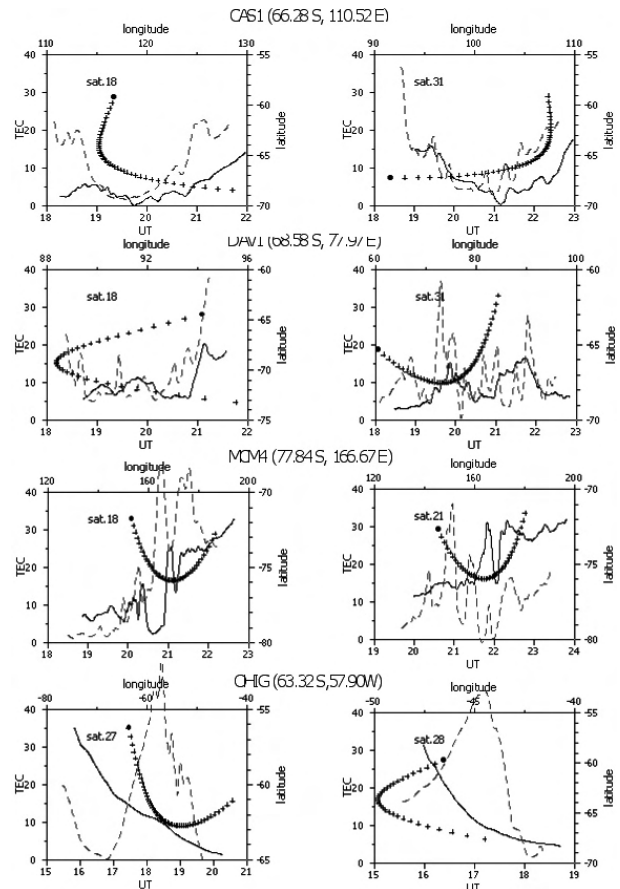


Fig.2b. TEC variations for satellites observed at different stations for during the storm (dashed line) and quiet period (solid line).

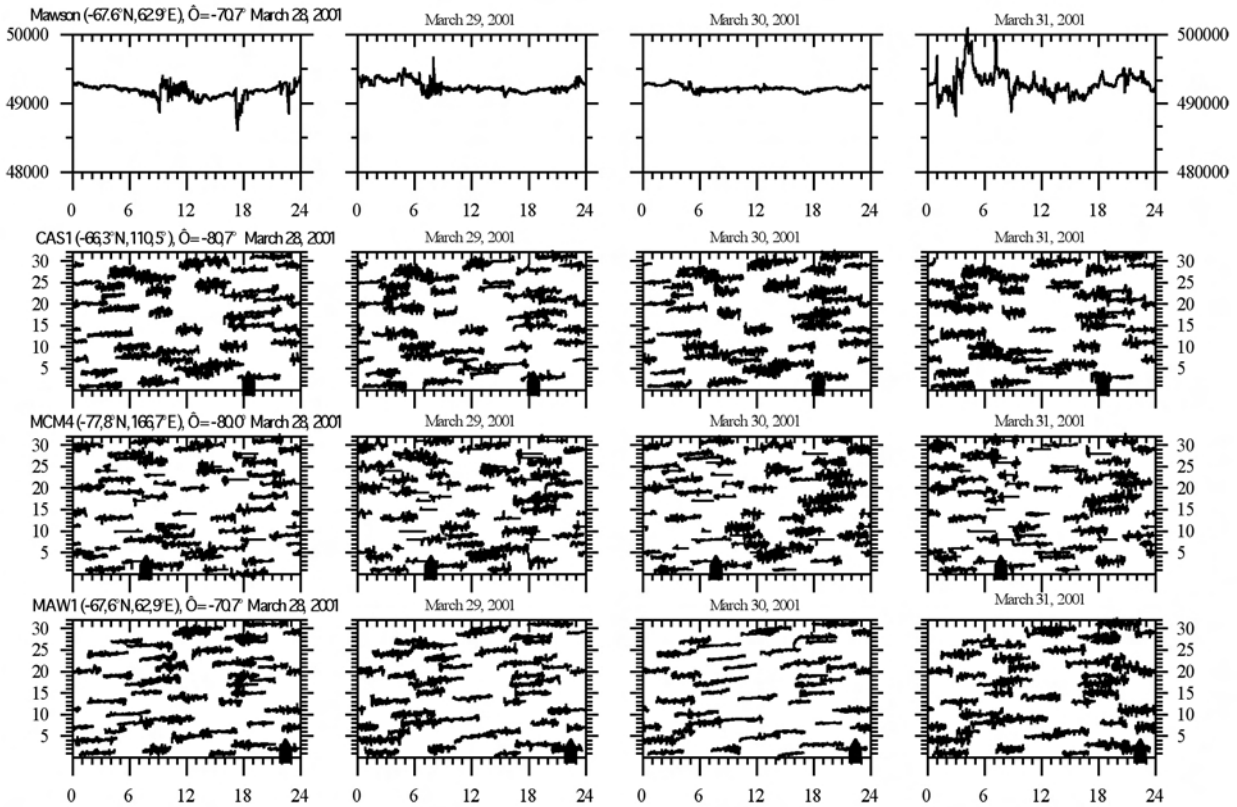


Fig.3. The Magnetic activity at Mawson and the phase fluctuations occurrence at different stations on March 28-31.

The plots show the phase fluctuations for individual satellites, the mark points out location of geomagnetic midnight storm the intensity of the fluctuations dramatically increased. The TEC increase of a factor of 2-8, the enhancement of TEC can exceed 10-20 TECU to relative phone. At lower latitudes the intensity LSF decreased. We attribute the TEC enhancement as occurrence of the polar cap ionospheric patches. These responses to F region plasma patch as the GPS ray encounter the patches structures (Weber *et al.*, 1984). Polar cap patches are large regions of enhanced F region plasma density observed travelling trough the ionospheric polar cap under the influence of the high-latitude convection (Pederson *et al.*, 2000). Discrete F region electron density is enhancement of a factor 2 or more. Patches are typically considered to be of the order of 100-1000 km in horizontal extent. The travelling speed of the patch is between 300-900 m-3 (Rodger *et al.*, 1999). Thus in the temporary pattern shown the variations of TEC along satellite passes the duration of occurrence of the patches can be 10 min or more.

The patterns of TEC fluctuation demonstrate the similar structures at spaced stations. It is well seen in Figure 2a for DAV1 and MAW1. Very similar portrait of the patch structures shows the TEC variation for PRN 15 and PRN 17 at CAS1 stations (top panel on Figure 2a) for March 2001. The time delays between the similar discrete structures correspond to a propagation velocity of the patch, and it is about 700 ms-1.

The deep variations of TEC are observed very frequently at polar stations. Analyses of data of MCM4 stations show that patch-like structures (about 90%

cases) were registered during March-April 2001 period. Over auroral station - VESL during quiet day the TEC demonstrates smooth run, during storm the LSF are often observed. The amplitudes of the TEC fluctuations in this region are smaller than on polar stations. At middle latitude station (OHIG) the large structures can be detected during the storm which we attribute to the occurrence of main ionospheric trough. In the time the horizontal gradients in the ionosphere over OHIG station increased. The sign storm time gradients can even be opposite to quiet geomagnetic conditions (Figure 2b).

4. Phase fluctuations of GPS signals

The TEC fluctuations, also called phase fluctuations, are caused by the presence of medium and small scale irregularities in the ionosphere. To estimate the phase fluctuations the dual-frequency phase measurements with 30 sec sample interval usually are used. The rate of TEC changes 1 min apart (ROT) is the source of the intensity of phase fluctuations study. The use of these relatively infrequent samples enables to study irregularity structures in the order of kilometres. When using ROT we avoid the problem of phase ambiguities.

As a measure of ionospheric activity we used also the Rate of TEC Index (ROTI) based on standard deviation of ROT (Pi *et al.*, 1997)

$$ROTI = \sqrt{\langle ROT^2 \rangle - \langle ROT \rangle^2}$$

ROTI has been estimated in 10-min interval.

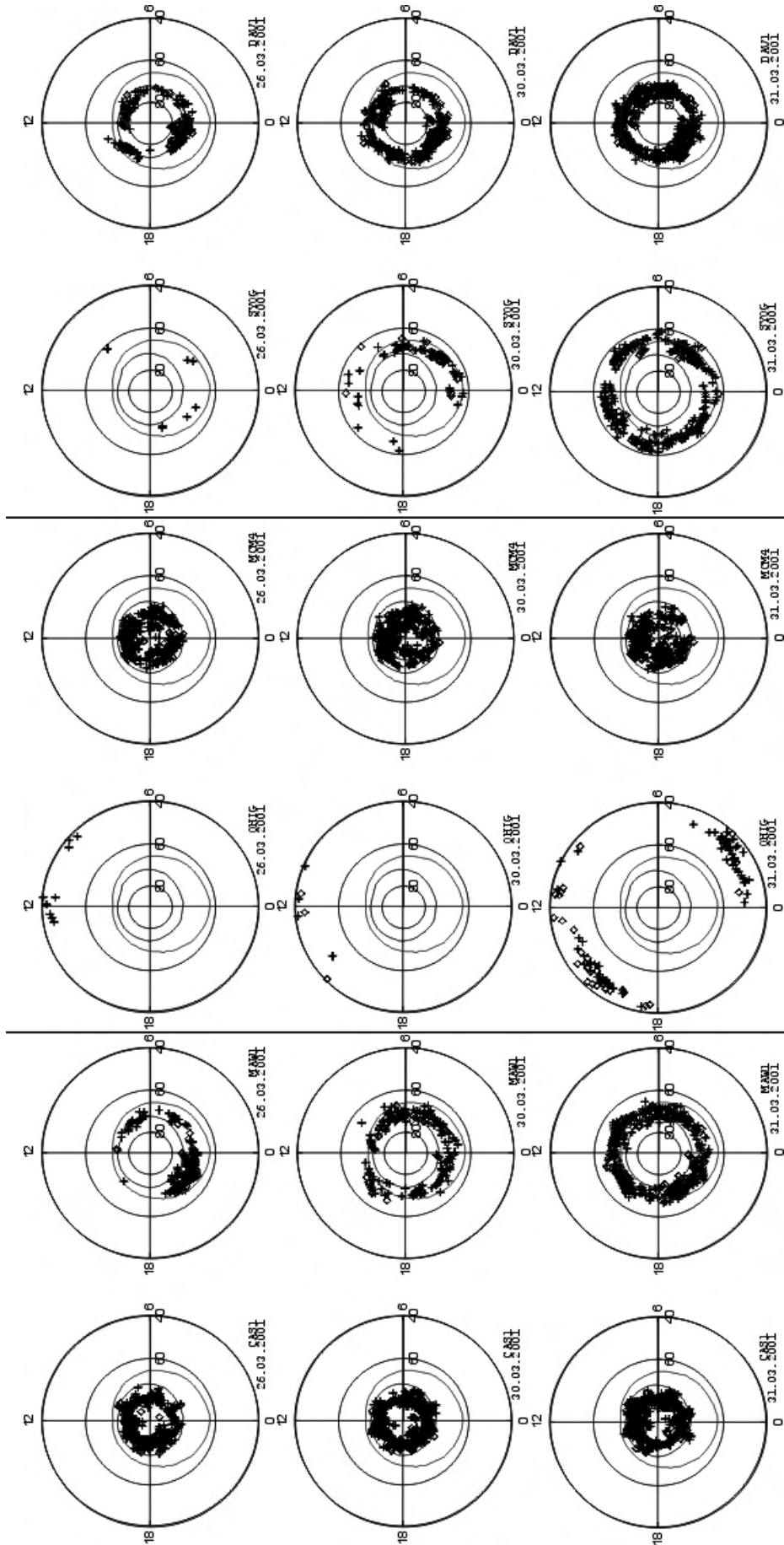


Fig.4a. Location of TEC fluctuations derived from GPS measurements in Geomagnetic local time and Corrected geomagnetic latitude for 26.03.2001, 30.03.2001 and 31.03.2001 on the different stations in south hemisphere. Intensity of fluctuations is indicated with following symbols: crosses represent fluctuations between 0.3 and 0.5 TEC/min, rhombs – bigger than 1.5 TEC/min.

Fig.4b. Location of TEC fluctuations derived from GPS measurements in Geomagnetic local time and Corrected geomagnetic latitude for 26.03.2001, 30.03.2001 and 31.03.2001 on the different stations in south hemisphere. Intensity of fluctuations is indicated with following symbols: crosses represent fluctuations between 0.3 and 0.5 TEC/min, rhombs – bigger than 1.5 TEC/min.

Fig.4c. Location of TEC fluctuations derived from GPS measurements in Geomagnetic local time and Corrected geomagnetic latitude for 26.03.2001, 30.03.2001 and 31.03.2001 on the different stations in south hemisphere. Intensity of fluctuations is indicated with following symbols: crosses represent fluctuations between 0.3 and 0.5 TEC/min, rhombs – bigger than 1.5 TEC/min.

The Figure 3 demonstrates the occurrence of the phase fluctuations (ROT) during 28-31 March 2001 with the most disturbed storm day - 31 March. The plot shows the variations of raw phase fluctuations for all satellites observed from Antarctic stations during 24 hour period. The top panel demonstrates the behaviour of variations of geomagnetic field at Mawson station. In the pictures the mark points out the location of the geomagnetic midnight. The maximum occurrence of phase fluctuations took place usually around local midnight (MN) (Aarons *et al.*, 2000), it is clearly seen at auroral stations (SYOG, VESL). In the same time the picture demonstrates that the developments of phase fluctuations are controlled by the geomagnetic activity. During the storm over Mawson station the development of phase fluctuation correlate with variations of geomagnetic field.

On polar stations the phase fluctuations all day are observed. On middle-latitude station - OHIG the fluctuations occurred only during storm day of 31 March. It is evident that during 31 March auroral oval for irregularities until middle latitudes was expanded.

The latitudinal occurrence of intensity of phase fluctuations depended on time is presented in Figure 4 (The polar coordinates – Corrected Geomagnetic Latitude (CGL) and Magnetic Local Time (MLT)). The intensity of the fluctuations with correspondence to the symbols is indicated. Figure 4a illustrates the exhibition of phase fluctuation over polar station - CAS1 and auroral one - MAV1. As Aarons showed, a dominant factor in the development of phase fluctuations during quiet period is the location of station relative to auroral oval. During quiet day of 26 March the maximal intensity is observed around magnetic local midnight. The geomagnetic storms modify the diurnal patterns of phase fluctuations extending the time of development and increasing their intensity. At polar site of CAS1 the weak intensity during storm increased more than at auroral station of MAV1. The developments of fluctuations over DAV1 station are more clearly controlled by geomagnetic activity. Figure 4b illustrates the exhibition of phase fluctuation over middle latitude station - OHIG and polar station - MCM4. In quiet and moderate magnetic activity at OHIG phase fluctuations are very weak and only in the most disturbed day 31 March the fluctuations occurred. It appeared during the greatest storms when the oval irregularities until middle latitudes are developed.

Figure 4c demonstrates the occurrence of phase fluctuations at lower (SYOG) and higher latitude edge of auroral oval. The intensity of fluctuations is essentially lower over SYOG than over DAV1 station. During storm day the fluctuations are registered the whole time, their intensity also markedly increased in the storm time.

5 Conclusion

The occurrence of TEC fluctuations depends on the geomagnetic latitude of a site. In the Antarctic region the difference between geomagnetic and geographic coordinates of site can be bigger than 10 degrees. So in the Antarctic region we can distinguish midlatitude, subauroral, auroral and polar stations.

Maximal TEC fluctuations took place at polar stations. The variations of TEC during storm reached 10-40 TEC. The enhancement of TEC exceeded 2-8 times a relative phone. Deep variations of TEC observed along individual satellite passes related to polar patches. They are transferred across line-of-sight of the receiver-satellite. The speed of the patches obtained from GPS observations was bigger than 700 m s⁻¹.

At lower latitudes the fluctuations of GPS signals are attributed to small and middle-scale irregularities. The intensity of phase fluctuations depends on geomagnetic activity. During maximal phase of storm on 31 March 2001 the fluctuations of moderate intensity were observed at middle latitude station of OHIG. The development of TEC strongly correlates with the geomagnetic field variations of Mawson station. The ionospheric gradients increased essentially during the storm. The irregular gradients sometimes exceed the regular ones. During the storm time it can cause the increasing of errors in determining phase ambiguities of GPS observations in the Antarctic region.

References

- Aarons J., Lin B., Mendillo M., Liou K., Codrescu M. Global Positioning System phase fluctuations and ultraviolet images from the Polar satellite, *Journal of Geophysical Research*, Vol 105, No A3, pp.5201-5213, 2000
- Baran L.W., Shagimuratov I.I., Tepenitsina, The use of GPS for ionospheric studies, *Artificial Satellites*, Vol. 32, No 1, pp.49-60, 1997
- Pedersen T.R., Fejer B.G., Doe R.A., Weber E.J., An incoherent scatter radar technique for determining two-dimensional horizontal ionization structure in polar cap F region patches, *Journal of Geophysical Research*, Vol. 105, No A5, pp. 10637-10655, 2000
- Pi X., Manucci A.J., Lindqwister, Ho C.M., Monitoring of global ionospheric irregularities using the worldwide GPS network, *Geophysical Research Letters*, Vol. 24, pp. 2283-2286, 1997
- Rodger A.S., Rosenberg T.J. Riometer and HF radar signatures of polar patches, *Radio Science*, Vol. 34, No 2, pp. 501-508, 1999
- Weber E.J., Buchau J., Moore J.G., Sharber J.R., Livingston R.C., Winningham J.D., Reinisch B.W., F layer ionization patches in the polar cap, *Journal of Geophysical Research*, Vol. 91, 12121, 1984

Regional Ionosphere Modelling Using Smoothed Pseudoranges

P. Wielgosz 1, 2, I. Kashani1, 3, D. Grejner-Brzezinska 1, Y. Zanimonskiy 4, J. Cisak 4

1. The Ohio State University; e-mail: wielgosz.1@osu.edu,

2. University of Warmia and Mazury in Olsztyn, Poland

3. Technion — Israel Institute of Technology

4. IGIK — Institute of Geodesy and Cartography, Warsaw, Poland

Abstract

This paper demonstrates the concept and some practical examples of the ionospheric total electron content (TEC) modelling using undifferenced phase-smoothed pseudorange GPS observations. After the smoothing process, the pseudorange observations are, in fact, equivalent to the carrier phase observations, where the integer ambiguities might be biased. The resulting TEC estimates were tested against the International GPS Service (IGS) TEC data for some American, European and Antarctic stations. The point-measurements of TEC were interpolated using the Kriging technique, in order to create TEC maps. The quality of the ionosphere representation was tested by comparison to the reference IGS Global Ionosphere Maps (GIMs).

Key words: GPS, Ionosphere, Kriging

1. Introduction

Spatial and temporal characteristics of the ionosphere are of primary interest in their own scientific context, but they are also of special interest to communication, surveillance and safety-critical systems, as they affect the skywave signal channel characteristics. The TEC is one of the important parameters in ionospheric research and one of the most important parameters in the trans-ionospheric radio propagation studies (Ma and Maruyama, 2001).

Today, GPS delivers large volumes of data suitable for continuous, near or real-time ionosphere monitoring during the disturbed and quiet geomagnetic conditions, and offers an attractive alternative to the traditional methods. Currently, the well established and commonly used GPS-derived GIMs provided by IGS have spatial resolution of 2.5° and 5.0° in latitude and longitude, respectively, and 2 hour temporal resolution (Feltens and Jakowski, 2002). Thus, although IGS supports the scientific community with quality GPS products, IGS GIMs cannot reproduce local, short-lasting processes in the ionosphere. In addition, the resolution of these products might not be sufficient to support high quality GPS positioning, especially in the presence of local ionospheric (Cisak *et al.*, 2003a).

The need to produce high-resolution regional ionosphere models, supporting navigation, static and kinematic positioning and space weather research, is commonly recognized (Komjathy, 1997). Gao and Liu (2002) pointed out that the interpolation methods might give better results, as compared to the mathematical function representation of TEC (e.g., spherical harmonics

expansion). Thus, in this paper we investigate the applicability of the Kriging interpolation/prediction method for TEC representation (Journel and Huijbregts, 1992). This paper presents some preliminary test results and the comparison with the IGS GIMs.

2. Methodology

The double frequency GPS phase and code observations, collected at the reference station network, were used in the approach presented here. The carrier phase observations are used to smooth the pseudoranges, as described by Springer (1999). The Differential Code Biases (DCBs) for satellites, denoted as Δb^k , are provided by IGS (ftp://gage.upc.es/pub/gps_data/GPS_IONO) and the DCBs for the receivers, Δb_i , are derived from the GPS receiver calibration performed using the BERNESE software (Hugentobler *et al.*, 2001). Next, the geometry-free linear combination of the un-differenced GPS observations is applied to derive the ionospheric delay related to the first GPS frequency (Schaer, 1999):

$$I_i^k = (\tilde{P}_{i,4}^k - c(\Delta b^k + \Delta b_i)) / \xi_4 \quad (1)$$

where:

- I_i^k - ionospheric delay
- $\tilde{P}_{i,4}^k$ - un-differenced pseudorange geometry-free linear combination (phase-smoothed)
- c - speed of light
- Δb^k - DCB of satellite k
- Δb_i - DCB of receiver i
- ξ_4 - coefficient converting ionospheric delay on P_4 to P_1

The relationship between the absolute TEC and the ionospheric delay is shown in the following formula (Schaer, 1999):

$$I_i^k = \pm \frac{C_x}{2} TEC f_1^{-2} = \xi_{TEC} TEC \quad (2)$$

where $\frac{C_x}{2} = 40.3 \times 10^{16} \text{ ms}^{-2}/\text{TECU}$

is the proportionality factor; $\xi_{TEC} = 0.162 \text{ m}/\text{TECU}$ is the ionospheric delay caused by 1 TECU on the first GPS frequency — f_1 .

For the TEC representation, a single layer model (SLM) was used. SLM assumes that all the free electrons are contained in a shell of infinitesimal thickness at altitude H . A mapping function converting slant TEC to the vertical one is needed as shown in (Mannucci *et al.*, 1993).

In order to create regional TEC maps, the Kriging method was used (Davies, 1986; Stanislawska *et al.*, 2000 and 2002). Kriging is an estimation and interpolation method applied in geostatistics, which uses the known sample values and a variogram to determine the unknown values at different locations/times. It utilizes the spatial and temporal correlation properties of the underlying phenomenon, and incorporates the measures of the error and uncertainty of the estimates. At each location, Kriging produces an estimate and a confidence bound on the estimate, the Kriging variance.

3. Numerical Tests

At the first stage of the numerical analysis, GPS observations from five CORS stations (COLB, SIDN, MCON, LEBA and PKTN) with the average separation of ~100km, located in the southern part of the State of Ohio, were selected. The 60 second sampling rate and the elevation mask of 20° were used in the processing. The vertical TEC values were obtained according to the methodology presented above using the MPGPS™ software (Wielgosz *et al.*, 2003). The data from the magnetically active day of April 29, 2003 were processed and analyzed. Figure 1 indicates that the active geomagnetic period started around 12:00 UT, and the Kp index reached the value of 6 between 18:00–21:00, which reflects a minor geomagnetic storm.

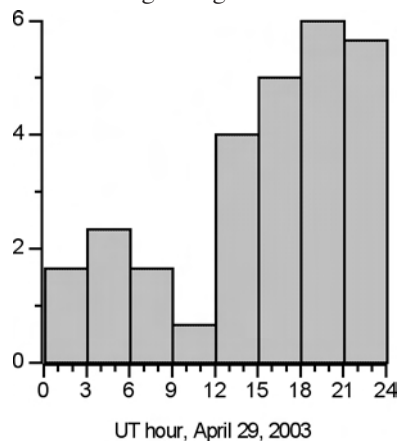


Figure 1. Kp index during the experiment.

The TEC values and the respective ionosphere pierce point (IPP) coordinates were calculated in geographic reference system (geographic latitude and longitude). Geographic reference frame was used to produce the epoch-specific instantaneous regional maps of the ionosphere. After analyzing the geographic location of IPPs for all the observational epochs, a region located between 35° – 45° north geographic latitude and 272° – 282° longitude was selected to produce the regional ionosphere maps. This area was covered by IPPs for most of the processed epochs; thus, the instantaneous ionosphere mapping was possible.

The TEC values obtained at the IPPs were interpolated using Kriging to create high-resolution instantaneous regional maps of the ionosphere. The results were analyzed and compared to the reference IGS maps, as described in

the following section. In order to compare the IGS TEC over different geographic regions, TEC was calculated using observations from the European IGS station, LAMA, and the Antarctic IGS station, CAS1. The results were compared to those obtained from the IGS GIMs. In the following, the TEC calculated using the MPGPSTM software is denoted as “OSU-TEC”.

4. Results And Analysis

The first analysis is concerned with the internal consistency of the model and the satellite/receiver DCB validation. The TEC values calculated from several CORS stations and GPS satellites were compared (Figure 2). It was shown that the TEC derived from the observations to each satellite is consistent between the neighboring stations, what confirms that the calibrated receiver DCBs are correct.

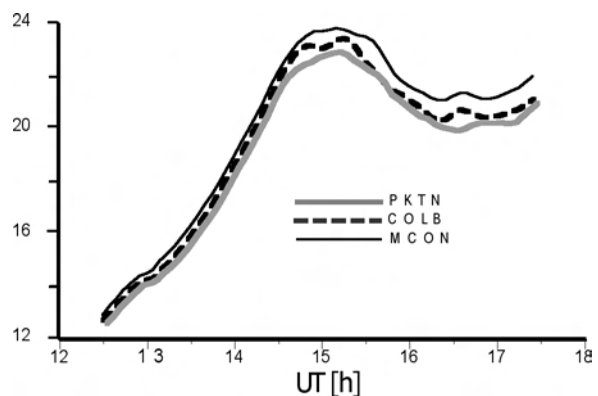


Figure 2. Comparison of the OSU-TEC observed to satellite PRN 04 from three CORS stations (COLB, PKTN and MCON) on April 29, 2003.

Figure 3 illustrates the examples of regional instantaneous ionosphere maps produced with the Kriging technique. For every map a semi-variogram was calculated and introduced to the interpolation process. The approach applied here allows a fast generation of the regional ionosphere maps, practically, for every observational epoch. Figure 3 illustrates the maps at the selected epochs. Notice that the local time for this region is –5 UT hours, and the maximum electron density, due to the geomagnetic disturbances, occurred for this area in the local evening. The resulting maps may allow detecting the local ionospheric phenomena, e.g. local TEC peaks of 1–3 TECU (Figure 3). The obtained ionosphere grid has the resolution of 0.08° in latitude and 0.12° in longitude. Such a dense TEC grid can be easily interpolated using simple linear interpolation and can be effectively used to support global navigation satellite systems (GNSS).

4.1 Comparison to IGS GIMs

In order to validate the instantaneous regional ionosphere maps, a comparison to IGS GIMs was performed. It should be noted that the IGS GIMs are a combination of GIMs provided by several analysis centres (ACs). All the ACs involved may use different approaches to the TEC derivation from GPS observations, as well as different TEC representation/modelling techniques. As it was mentioned

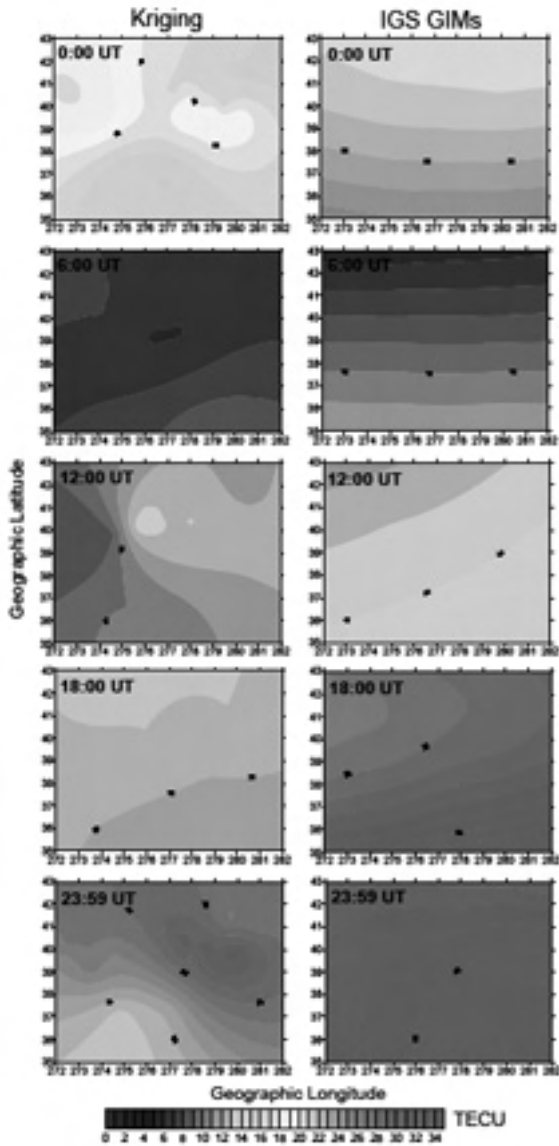


Figure 3. Comparison between the ionosphere maps derived using Kriging (OSU-TEC) and the IGS GIMs

in the introduction, the spatial resolution of the final IGS GIMs is 2.5° in latitude and 5.0° in longitude. For the comparison purposes, an area covering regional model was extracted from the IGS GIMs. Figure 3, right column, presents the example ionosphere maps for the selected epochs extracted from the IGS GIMs.

In general, the OSU-TEC is comparable to the IGS GIMs. It is noticeable, however, that GIMs' general TEC level is higher about 3–5 TECU, as compared to the maps generated using the Kriging method. This could be explained by the global nature of GIMs. IGS ACs often use TEC representation algorithms, which result in the model resolution comparable with the whole area of the region under investigation (Schaer, 1999). In addition, the sampling rate of the data sets and the network density used in the global and some regional models is much lower than the one investigated here. It should be noted that the investigated region is covered by only 8 GIM grid points.

This also explains why the TEC derived from GIMs is very smooth over the entire analyzed region. In contrast to GIMs, local features in the ionosphere represented by the regional models can be observed. However, some of these features might be caused by a clustered distribution of IPPs. Local distribution within the clusters, however, is more than sufficient. We believe that a regional model should correspond to a more accurate local ionosphere representation.

4.2 TEC comparison over different regions

The reasons for the above-mentioned systematic bias between the OSU-TEC and the IGS GIMs were further investigated using two additional data sets (OSU and IGS GIMs' TEC values at IPPs) for comparison of some permanent IGS stations in North America, Europe and Antarctica. First, the consistency of the results in time domain from both data sets was tested for the COLB station, as shown in Figure 4 (DOY 163/2003). This Figure displays a very similar diurnal TEC behaviour for both curves and a difference in the scale factor. This difference in scale is shown in Figure 5 and 6 by the means of direct comparison of both data sets.

Similar investigations were performed for the TEC data obtained from the international project "Atmospheric

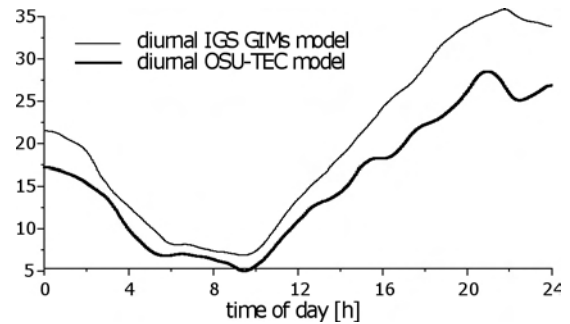


Figure 4. Diurnal TEC variations interpolated over COLB station derived from OSU-TEC and IGS GIMs, June 12, 2003.

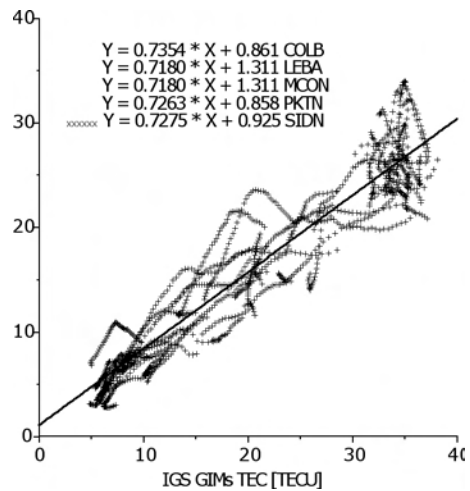


Figure 5. Comparison of the OSU-TEC variations for all satellites observed at SIDN station on June 12, 2003, to the TEC interpolated from the IGS GIMs (plot) and linear trends for the rest CORS stations (equations)

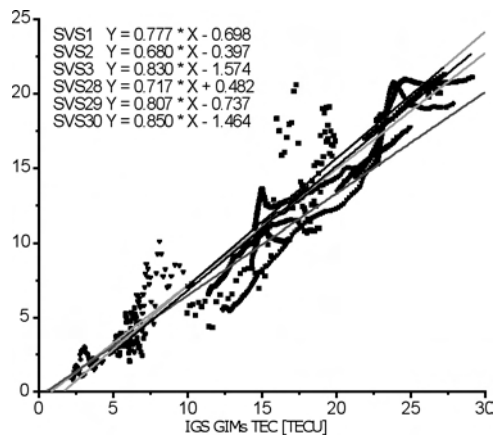


Figure 6. Comparison of the OSU-TEC variations for different satellites observed in COLB, LAMA and CASI data with the TEC interpolated from the IGS GIMs (June 12, 2003).

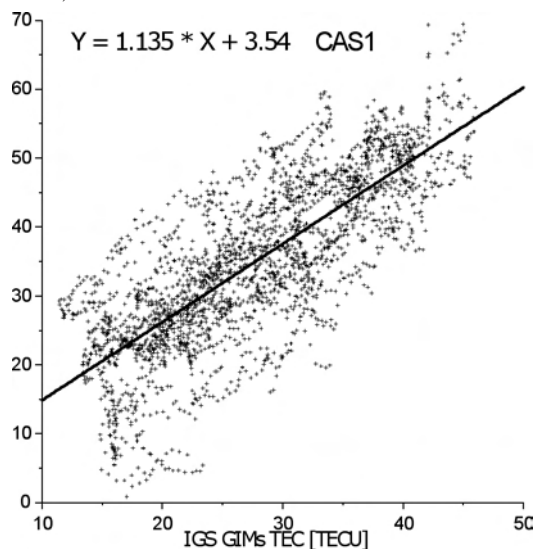


Figure 7. Comparison of TEC over the Antarctic CASI station derived from the UPC data with the TEC interpolated from the IGS GIMs (November 2001).

impact on GPS measurements in Antarctica” (Cisak *et al.*, 2003a and 2003b). Some of the results are shown in Figure 7. The TEC data with the 1-minute temporal resolution for some Antarctic stations were provided by Dr. M. Hernandez-Pajares from UPC (Hernandez-Pajares *et al.*, 1999). In that case, the earlier conclusion that the scale difference is caused by the very smooth character of the IGS GIMs seems to be confirmed.

5. Conclusions And Future Developments

The analyses presented here show that the TEC-recovery methodology, which takes the advantage of the phase-smoothed pseudoranges, is efficient, and enables generation of the real-time regional TEC maps, when applying the Kriging method. The primary advantages of the instantaneous regional ionosphere mapping presented here are the high temporal (one observational epoch) and spatial (0.08° in latitude and 0.12° in longitude) resolutions. Owing to the fact that DCBs do not change significantly during the course of a day, their values can be used even a

few days after the calibration. This may allow producing instantaneous TEC maps in near-real time. However, the systematic bias between both TEC estimation sets (OSU-TEC and IGS GIMs) needs to be further investigated.

Future studies will include the investigations of the behaviour of the selected ionospheric storms over the Antarctic region using the proposed approach. The impact of the ionospheric disturbances on the variations of the GPS vector components, at high latitudes, will be also investigated.

Acknowledgments

This work is supported by NOAA, National Geodetic Survey, NGS (project DG133C-02-SE-0759), and SOI — Survey of Israel (project 2002-11). Dr. Pawel Wielgosz is supported by the Foundation for Polish Science.

Some studies presented in this paper were performed in the framework of the SCAR Project “Atmospheric Impact on GPS Observations in Antarctica,” and were partially supported by the Polish State Committee for Scientific Research (Research Project No 8 T12 E045 20).

The authors are grateful to Dr. J Cisak for interesting discussion and presentation of this paper at the AGS03 in Lviv.

References

- Cisak J., Kryński J., Zanimonskiy Y.M., and Wielgosz P., (2003a), *Variations of Vector Components Determined from GPS Data in Antarctic. Ionospheric Aspect in New Results Obtained within the Project “Atmospheric Impact on GPS Observations in Antarctic”*, presented at 5th International Antarctic Geodesy Symposium — AGS’03, September 15–17, 2003, Lviv, Ukraine.
- Cisak J., Krynski J., Zanimonskiy Y., and Wielgosz P., (2003b), *Study on the Influence of Ionosphere on GPS Solutions for Antarctic Stations in the Framework of the SCAR Project “Atmospheric Impact on GPS Observations in Antarctic”*, Paper presented at the 7th Bilateral Meeting Italy—Poland, Bressanone, Italy, 22–23 May 2003.
- Davis, J.C., (1986), *Statistics and Data Analysis in Geology*, Second edition, John Wiley & Sons, New York, pp 383-386.
- Feltens. J. and Jakowski. N., (2002), The International GPS Service (IGS) Ionosphere Working Activity, *SCAR Report No. 21*.
- Gao, Y. and Liu, Z.Z., (2002), Precise Ionosphere Modelling Using Regional GPS Network Data, *Journal of Global Positioning Systems*, Vol. 1, No. 1: 18–24.
- Hugentobler. U., Schaer. S., and Fridez. P., (2001), *BERNESE GPS Software Version 4.2*, Astronomical Institute, University of Berne.
- Hernandez-Pajares. M., Juan, J.M., and Sanz, J., (1999), New approaches in global ionospheric determination using ground GPS data, *Journal of Atmospheric and Solar Terrestrial Physics*, Vol 61, pp 1237–1247.
- Journel, A.G., and Huijbregts, C.J., (1992), *Mining*

- Geostatistics*. Academic Press, New York, 600 pages.
- Komjathy, A., (1997), *Global Ionospheric Total Electron Content Mapping Using the Global Positioning System*, Ph.D. dissertation, Department of Geodesy and Geomatics Engineering Technical Report No. 188, University of New Brunswick, Canada, 248 pages.
- Ma, G., and Maruyama, T., (2002), A Comparison of GPS-derived TEC and foF2 over Japan, *Review of Radio Science: 1999–2002 URSI*, on CD-ROM, John Wiley and Sons.
- Mannucci, A.J., Wilson, B.D., and Edwards, C.D., (1993), *A New Method for Monitoring the Earth Ionosphere Total Electron Content Using the GPS Global Network*, Proceedings of ION GPS'93, pp. 1323–1332.
- Schaer S. (1999), *Mapping and Predicting the Earth's Ionosphere Using the Global Positioning System*, Ph.D. Thesis, Astronomical Institute, University of Berne, 205 pages.
- Springer T.A., (1999), *Modelling and Validating Orbits and Clocks Using the Global Positioning System*, Ph.D. dissertation, Astronomical Institute, University of Berne, Berne, Switzerland, 155 pages.
- Stanislawska, I., Juchnikowski, G., Hanbaba, R., Rothkaehl, H., Sole, G., and Zbyszynski, Z., (2000), COST 251 Recommended Instantaneous Mapping Model of Ionospheric Characteristics – PLES, *Phys. Chem. Earth (C)*, vol. 25, no. 4, pp. 291–294.
- Stanislawska, I., Bradley, P.A., and Juchnikowski, G., (2002), *Spatial correlation assessment of ionospheric parameters for limited-area mapping*, Proceedings of the XXVIIIth General Assembly of URSI, Maastricht, the Netherlands 17–24 August 2002.
- Wielgosz, P., Grejner-Brzezinska, D.A., Kashani, I., (2003), Regional Ionosphere Mapping with Kriging and Multiquadric Methods, *Journal of Global Positioning Systems*, Vol. 2, Issue 1.

Argentine Island Ice Cap Geodesy Survey for Climate Change Investigation

Svetlana Kovalenok (1), Gennadi Milinevsky (1, 2), Vladimir Glotov (3), Korniliy Tretjak (3), Rudolf Greku (4), Yury Ladanovsky (5), Pavel Bahmach(5)

(1) Ukrainian Antarctic Centre, 16, blvd Tarasa Shevchenka, 01601, Kyiv, Ukraine;

(2) Kyiv National Shevchenka University, 6, Glushkova av., 04022, Kyiv, Ukraine;

(3) National University Lvivska Politechnica; 12, Bandera st., 79013, Lviv, Ukraine;

(4) Institute Geology Sciences, 22, Gonchara st, 01054, Kyiv, Ukraine;

(5) ECOMM Co, 18/7, Kutuzov st., 01133, Kyiv, Ukraine

E-mail: antar@carrier.kiev.ua

Abstract

The geodesy survey of small island ice caps in Antarctic Peninsula region within the framework of the GIS project for the Argentine Islands archipelago has been started in 2002. The purpose of monitoring is the possible regional climate changes observation on shape, position, dynamics and future of archipelago small ice caps. The task was determined by the latest data of regional warming up to 5°C in the Faraday/Vernadsky area during the last century. The main objectives of the survey are creation of the large-scale digital maps (1:25,000 – 1:1,000) for the Argentina Islands region, producing the precision geodesic data for ice cap monitoring and the evolution model creation. The geomorphology monitoring of the ice caps is based on the GPS and photogrammetric survey. The changes of size, shape, deformation, moving velocity and the edge

position of ice caps on Argentine Islands archipelago shows the possibility to use the geodetic survey data of the ice cap for the regional climate variability study. The research is based on historical data ice cap observation of Galindez Island and other islands in the area. On the base the photogrammetric survey the large-scale digital map (1:1,000) of the Marina Point of Galindez Island was created. The data of fifty years meteorological observations and tide data at Faraday/Vernadsky station, long-term variability in sea-ice extent/thickness, monitoring of ozone layer and UV energy flow, hydrological measurements provided at Vernadsky, the upper atmosphere changes measurements over Antarctica, the botanical evidence of climate changes are the additional sources for the climate pattern of the Antarctic Peninsula.

About the Influence of the Solar Activity on GPS-Supervision

L. Yankiv-Vitkovska, Ya. Kostecka

National University Lvivska Politechnica, 79013, Lviv, St. Bandera, 12 Str.

E-mail: luba_y@ukr.net

Abstract

The state-of-the art review of influence of Solar activity on condition ionosphere is made which, in turn, influences of GPS-supervision. Is shown, that for specification of model

ionosphere it is necessary to find exacter connections between the phenomena occurring on the Sun, and condition ionosphere.

Application of SAR Interferometry in Grove Mountains, East Antarctica

E Dongchen(1), Zhou Chunxia(1), and Liao Mingsheng(2)

1 Chinese Antarctic Center of Surveying and Mapping, Wuhan University, Wuhan, 430079, P.R.China

2National Key Lab. For Information Eng. in Surveying, Mapping and Remote Sensing, Wuhan University, Wuhan, 430079, P.R.China,

Email: edc1939@public.wh.hb.cn

Abstract

Synthetic aperture radar interferometry has been proposed as a potential technique for digital elevation model (DEM) generation, topographic mapping, and surface motion detection especially in the inaccessible areas. Grove Mountains Area locates to the southwest of Princess Elizabeth Land, inland areas of east Antarctica. The topographical map of the core area (11×10 KM²) was printed after the field surveying with GPS and total station was finished under the atrocious weather conditions during the 16th CHINARE (Chinese National Antarctic Research Expedition) 1999/2000. This paper will present an experimental investigation of the ERS-1/2 SAR tandem data in 1996 on DEM generation of the Grove Mountains Core Area, analyse the data processing, and compare the DEM with the actual topographic form. It is confirmed that InSAR is a very useful technique to be utilized in Antarctica, and can be used to produce more products instead of dangerous field surveying.

Key words: Synthetic aperture radar interferometry, ERS-1/2 Tandem, GPS, DEM, Antarctica.

1. Introduction

Maps of Antarctica's interior remained mostly white blanks into the mid-1980s. Satellites using visible light had produced detailed surface images, but their angles of view excluded more than 1.2 million square miles poleward of about 82° south latitude. Then in 1997, the Canadian RADARSAT-1 satellite was rotated in orbit. With its synthetic aperture radar (SAR) antenna looking south

towards Antarctica, it permitted the first high-resolution mapping of the entire continent of Antarctica. In other areas of Antarctica, DEM and topographic mapping have been obtained by means of different methods or their integration such as synthetic aperture radar, radar altimeter, laser altimeter, radar echo sounding, GPS surveys, aerial photographs, and geodetic maps.

In 1998, China planned to take the first time expedition to Grove Mountains Area (see also Figure 1), which locates to the southwest of Princess Elizabeth Land, inland areas of east Antarctica. Adopting Landsat4 TM images, Chinese Antarctic Center of Surveying and Mapping (CACSM) had completed the colourful satellite image map of the Grove Mountains in the scale of the 1:100 000 in August 1998 to ensure the expedition route and navigation to Grove Mountains Area during the 15th CHINARE 1998/1999. Then the topographical map of the core area (see also Figure 2) was printed after the field surveying with GPS and total station was finished under the atrocious weather conditions during the 16th CHINARE 1999/2000.

However, in Antarctica, traditional mapping method is no longer a most efficient means to obtain the topographical maps or DEM in large areas especially in abominable

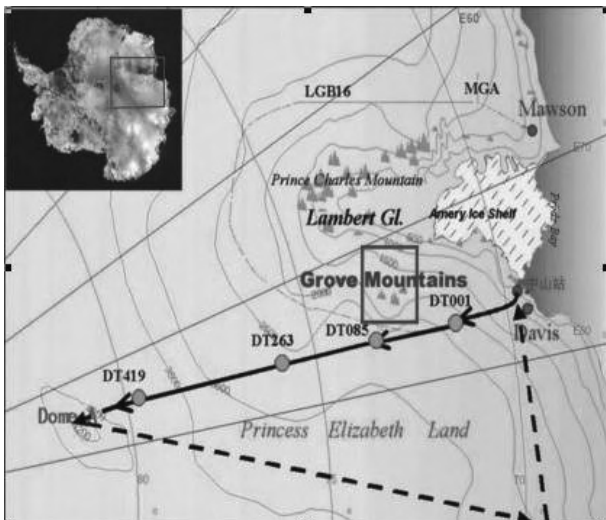


Figure 1: Grove Mountains, East Antarctica.

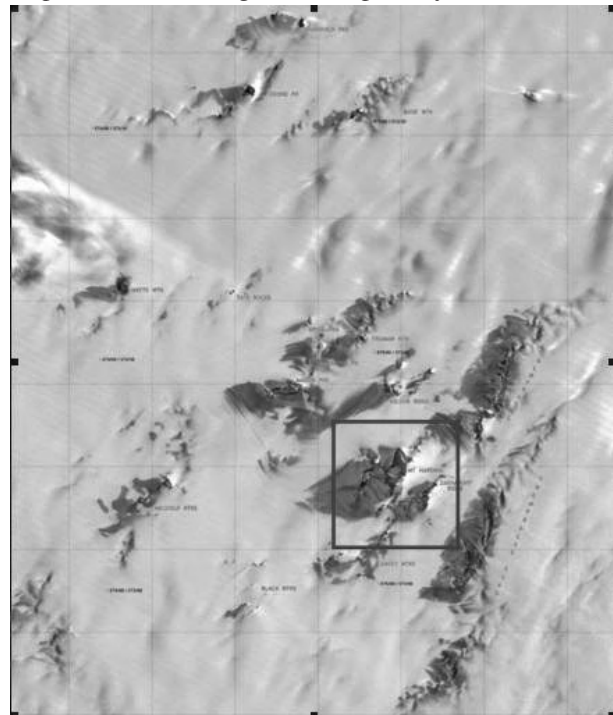


Figure 2: Grove Mountains Core Area.

environment. Synthetic aperture radar interferometry has been proposed as a potential technique for digital elevation model (DEM) generation, topographic mapping, and surface motion detection especially in the inaccessible areas. So we bought radar image data from ESA and a case study for DEM generation was done in Grove Mountains. In this paper, the primary experiment result based on ERS-1/2 tandem data is presented. Moreover, with the hard-won field surveying data, comparing and analyzing DEM generated by using tandem radar image data with DEM generated with the topographic points is carried out.

2. Methodology

The tandem operation of ERS-1 and ERS-2 satellites, with a short temporal baseline, put forward a better time correlation for DEM generation. It utilizes the two single look complex image of the same area to form interfere and further obtain the three dimension information. The principle to get height *h* is illuminated in the following geometry figure.

With reference to Figure 3, the height (*h*) is given by
$$h = H - r_1(\cos\xi\sqrt{1 - \sin^2(\theta - \xi)} - \sin\xi\sin(\theta - \xi)) \quad (1)$$
 where *H* is the flying height, ξ is the baseline tilt angle, θ is the side looking angle and related to the interferometric phase difference ϕ as follows:
$$\phi = \frac{4\pi}{\lambda}(r_2 - r_1) = \frac{4\pi}{\lambda}(B_x \sin\theta - B_z \cos\theta) \quad (2)$$
 where λ is the wavelength, *r*₁ and *r*₂ are the distances between the radar antennas and the scatterer.

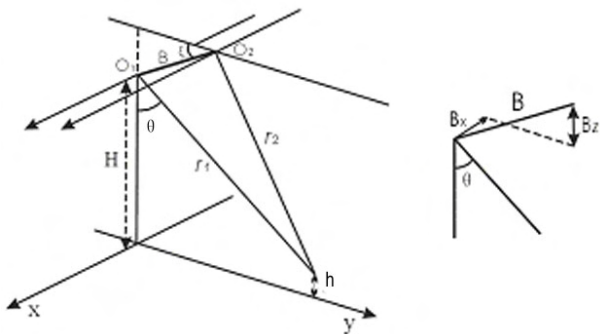


Figure 3: Geometry of SAR interferometry.

In this study, the interferometric SAR data processing mainly includes: (1) coregistration of the complex image data; (2) formation of the interferogram; (3) Phase unwrapping; (4) DEM generation. Indeed, baseline refinement, removal of flat earth, noise filtering, etc., are always indispensable to obtain a high-precision DEM.

DEM of Grove Mountains was generated by the ERS tandem data. Since we have DEM generated with the topographic points obtained during the field surveying, then we can perform a comparison.

3. Field Surveying

Grove Mountains Area, with bare peaks at inland areas of east Antarctica, is located to the south of the Zhongshan Station about 400 km. Its geographical extension is 72°40'– 73°10'S, 74°00'– 75°45'E, and the area is about 3200 km²; meanwhile, the core area extension is 72°50'54"– 72°56'20"S, 74°54'07"– 75°14'09"E, and its area is about 110 km². Grove Mountains is of typical inland character and also an ideal midway station place for

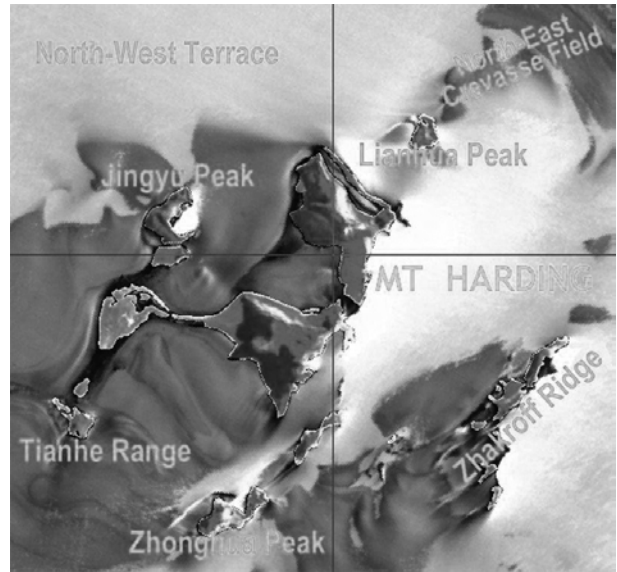


Figure 4: TM color satellite image map.

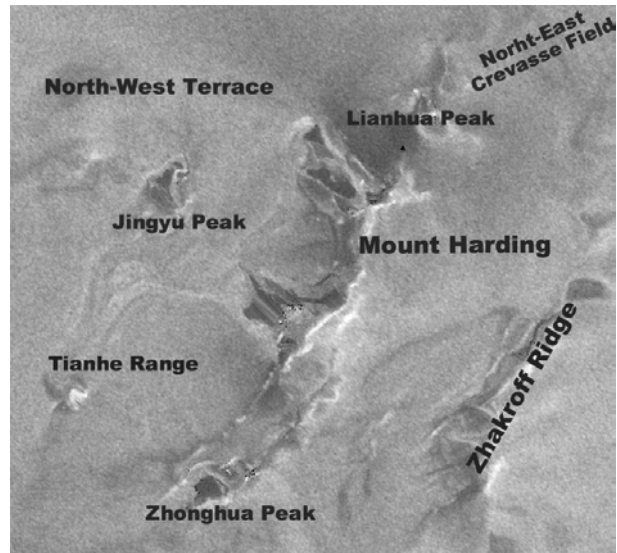


Figure 5: ERS-1 radar image.

expedition teams extending to the South Pole.

In the core area, there are two exposed mountains, many rock peaks, and detritus strips on the surface of the ice sheet with the altitude of 2000 meters, which has great topographical undulation and is densely covered by ice crack. The weather there is atrocious for it has blustery or milky weather half of a year and the average temperature is about thirty degrees below zero centigrade, which brings great difficulties for field surveying and operations.

TM colour satellite image map and ERS-1 radar image (1996/02/10) of the core area are illustrated in Figure 4 and Figure 5 respectively. In TM image map, ice face is in light green, blue-ice face is in blue green, horn and bare rocks are in brown. The Mount Harding, Zhakroff Ridge, Jingyu Peak, Tianhe Range, Zhonghua Peak, and Lianhua Peak can be easily interpreted from both of them, and the general position is coherent. Meanwhile some difference occurs inevitably because radar image and TM image are in different characters and the error exists.

In order to provide geologists with the topography of Grove Mountains, our geodetic surveyors has conducted the field surveying with GPS and total station and completed the mapping experiment in the Grove Mountains Core Area during the 16th CHINARE 1999/2000 summer expedition. The topographical map of the core area at the scale of 1:25 000 (see also Figure 6) was printed after the field surveying was finished in 31 days by two surveyors of CACSM under the atrocious weather conditions, and 14,300 topographical points were obtained through post-processing differential GPS (DGPS) technique and forward intersection method with total station. WGS-84 coordinate system and Transverse Mercator map projection are adopted. The center meridian is 75°E, and the vertical contour interval is 10 meters.

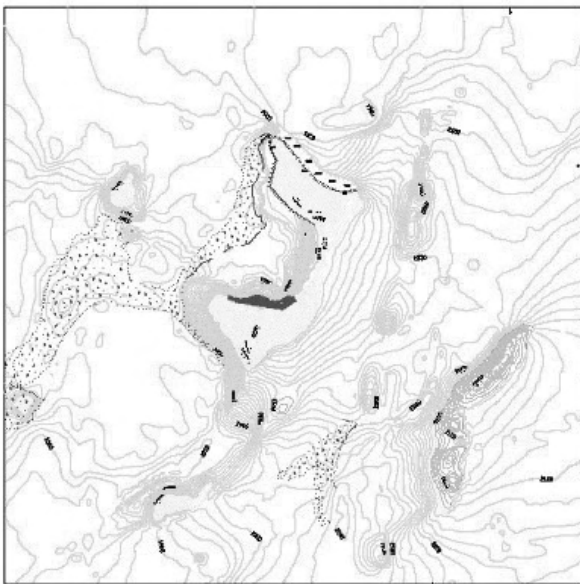


Figure 6: Topographical map of Grove Mountains Core Area.



Figure 7. Interferogram of the core area

4. Dem Generation With Insar And Data Interpretation

The information of the tandem single-look complex image pair is listed in Table 1. The perpendicular baseline is about 164m, and parallel baseline is about 94m. Baseline parameter plays a very important role in flat earth effect removal and geometric transformation from phase to elevation, so it is very important to adopting precise baseline parameter. In practice, baseline accuracy at centimetre level is the basic requirement for producing high-precision DEM. ESA attached five sets of orbit vector data at intervals of 4.2 seconds within the head file while distributing SAR image data. In this study, we adopted ERS-1/2 high precision orbits calculated and provided by Delft Institute for Earth-Oriented Space Research (DEOS).

Table 1. ERS-1/2 tandem data information

Satellite	Orbit	Track	Frame	Date
ERS-1	23910	375	5139	1996-02-10
ERS-2	04237	375	5139	1996-02-11

Table 1. ERS-1/2 tandem data information

Interferogram, which is defined as the product of the complex SAR values of the second image with the complex conjugate of the reference image, includes both the amplitude and phase information of SAR image pair. And it is the basis for DEM generation. Figure 7 shows the interferogram of Grove Mountains Core Area. After the fieldwork, we get to know that disordered blocks of rocks and snow cover on the tops of the mountains and peaks, which causes the discontinuous interferometric phase fringe of these areas.

Once the phase is unwrapped, an absolute phase is required to obtain the absolute pixel height. A point with known elevation in the scene can be used to provide an absolute elevation reference. In Grove Mountains, two geodetic control points and one are set on the top of Mount Harding and Zhakroff Ridge respectively, while it is impossible to find their location in radar image because the field GPS surveying was done in 2000 and the SAR images were acquired in 1996. And even if they are in the radar image, it is also difficult to find them. For the particular environment in this location, it's trouble to find feature points too. On the other hand, ice-sheet flowed and changed a lot in such a long period. So we could only find a relatively flat and stable area to appoint a point as the reference point. Area west to Mount Harding is relatively stable because of the blocking effect of Mount Harding. Meanwhile, with reference to the coherence of the core area (see also Fig. 8), which depends on the terrain conditions, the brighter means the better coherence. Generally speaking, the areas covered mostly by ice and snow to the west of the Mount Harding and Zhakroff Ridge have relatively better coherence. Other areas covered by ice and snows such as northwest terrace take



Figure 8: Coherence of the core area

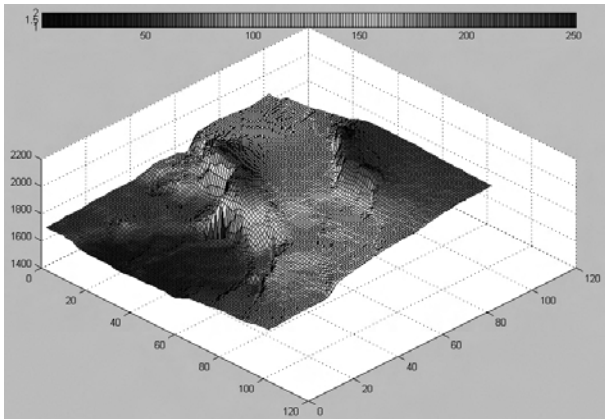


Figure 9: DEM generated by using tandem radar image data

second place. And coherence of the top of the mountains and peaks are the worst. A point to the west of Mount Harding with rough elevation of 1867 meters is selected as the reference point.

After phase unwrapping, the DEM was generated. In order to show intuitionistic vision, colour perspective model of the grid DEM is formed as Figure 9. In those areas of high topographic deviationism, the deviation is fairly large for the layover and shadow effect caused by side-glanced radar observing mode. Compared with the perspective model from the DEM generated with the topographical points obtained during the field surveying (see also Figure 10), the terrain tendency and the main terrain character are coincident. Red stands for the higher, and blue the lower. Mount Harding and Zhakroff Ridge are obvious in Figure 9 and Figure 10, while Jingyu Peak, Zhonghua Peak and Lianhua Peak are not exactly presented in Fig.9. Meanwhile, Fig.9 doesn't show the valley and lower terrain that can be clearly given in Fig.10. The details of the topography information in the two following figures exist differences and need more study and analysis.

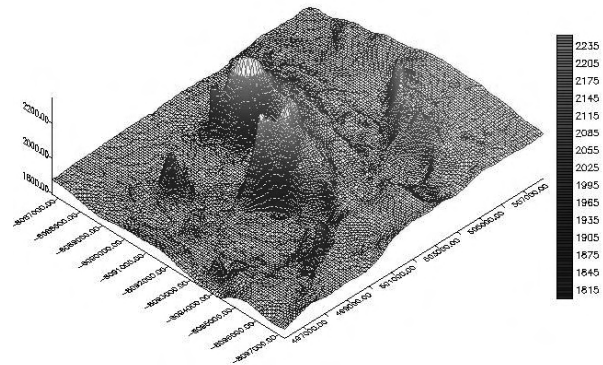


Fig.10. DEM generated with the topographic points obtained during the field surveying

Table 2. Results of the comparison of the two DEM

Terrain	Flat terrain		Hilly terrain
	Relatively stable	Flowing	
Mean	2.3m	13.7m	-61.9m
RMS	5.4m	20.3	89.3m

Table 2. Results of the comparison of the two DEM

From 1996 to 2000, changes in Grove Mountains may be caused by snow accumulation, ice-snow melting and ice sheet flowing, and ice sheet flowing is the main factor. However, according to the topographic feature, ice sheet flow and the coherence of the core area, relatively flat and stable areas can be found. It is more reasonable to assess the DEM difference in three different terrains listed in Table 2 than only to compare the whole area.

With the measured results listed in Table 2, the quality of DEM difference of the relatively stable areas is preferable, which confirms that InSAR is valid to be utilized in this area. For the flowing ice surface, the corresponding DEM difference gets larger, which is mainly caused by the changes in ice surface. The result is unsatisfied in the hilly terrains because of the surface of the mountains covered by snow and blocks of rocks, which brings noises and difficulties to obtain accurate height.

5. Conclusions And Future Activities

From the primary study and other researchers' study on DEM generation and topographic mapping, it could be shown that InSAR will be very useful to be utilized in Antarctica as a new mean for producing topographic products more effective instead of field surveying.

In order to obtain high-precision DEM, formation of the interferogram, phase unwrapping, and other crucial steps must be further studied to reduce the error. Band C can penetrate to the ice surface, but here this penetration effect to DEM generation is neglected. Moreover, we can analyse the properties of snow cover on InSAR phase and coherence, and the effect on DEM generation and mapping.

Scientists have been very interested in Antarctic ice sheet flow, ice sheet kinematic characteristics, and mass balance. InSAR can also be an effective tool in these research fields by adopting more pairs of radar image data.

During the 19th CHINARE 2002/2003, our researchers has set eight ground control points covering all Grove Mountains area, which will help us to utilize interferometric SAR image data or others to precisely produce the topographical map of the whole Grove Mountains area and extract the topographic information of Antarctic inland ice sheet.

References

- P.A. Rosen, I.R. Joughin, F.K. Li, S.N. Madsen, E. Rodriguez and R.M. Goldstein, "Synthetic Aperture Radar Interferometry", *Proceedings of the IEEE*, vol.88, no. 3, pp. 333-382, March 2000.
- G. Rufino, A. Moccia and S. Esposito, "DEM Generation by Means of ERS Tandem Data", *IEEE Trans. Geosci. Remote Sensing*, vol. 36, no. 6, pp. 1905-1912, Nov. 1998.
- M. Coltelli, G. Fornaro, G. Franceschetti, R. Lanari, G. Puglisi, E. Sansosti and M. Tesauro, "ERS-1/ERS-2 tandem data for digital elevation model generation", *IEEE Proceedings of IGARSS'98*, vol. 2, pp. 1088-1090, 1998.
- H.A. Zebker and R.M. Goldstein, "Topographic mapping from interferometric SAR observations", *J.Geophys. Res.*, vol. 91, pp. 4993-4999, 1986.
- H.A. Zebker, C.L. Werner, P. Rosen, and S. Hensley, "Accuracy of Topographic Maps Derived from ERS-1 Interferometric Radar", *IEEE Trans. Geosci. Remote Sensing*, vol. 32, no. 4, pp. 823-836, July 1994.
- M. Schwäbisch, M. Matschke, W. Knöpfle, and A. Roth, "Quality Assessment of InSAR-derived DEMs Generated with ERS Tandem Data", *IEEE Proceedings of IGARSS'96*, vol. 2, pp. 802-804, 27-31 May 1996.
- R.M. Goldstein, H.A. Zebker, and C.L. Werner, "Satellite Radar Interferometry: Two-Dimensional Phase Unwrapping", *Radio Science*, vol. 23, no. 4, July-August 1988.
- M. Schwäbisch, "Large Scale Interferometric DEM Generation using ERS Tandem Data: Example of the Czech Republic", *IEEE Proceedings of IGARSS'98*, vol. 3, pp. 1641-1643, 6-10 July 1996.
- K.E. Mattar, A.L. Gray, Marco W.A. van der Kooij and P.J. Farris-Manning, "Airborne Interferometric SAR Results from Mountainous and Glacial Terrain", *IEEE Proceedings of IGARSS'94*, vol. 4, pp. 2388-2390, 8-12 Aug 1994.
- R. Abdelfattah, J.M. Nicolas, M.R. Boussema, "Impact of Orbital Parameters on DEM Production by SAR Interferometry", *IEEE Proceedings of IGARSS'2000*, vol. 2, pp. 739-741, 2000.
- R. Goldstein, "Atmospheric Limitations to Repeat-Track Radar Interferometry", *Geophys. Res. Letters*, vol. 22, no. 18, pp. 2517-2520, 1995.
- K. A. Hogda, T. Guneriusen and I. Lauknes, "Synthetic aperture radar for DEM generation in snow-covered mountain terrain", *IEEE Proceedings of IGARSS'2002*, vol. 4, pp. 2193-2195, 2002.
- Shi Shiping, "DEM Generation using ERS-1/2 Interferometric SAR Data", *IEEE Proceedings of IGARSS'2000*, vol. 2, pp. 788-790, 2000.
- RADARSAT-1 Antarctic Mapping Project, http://www.asf.alaska.edu/4_4.html.

The Establishment of GPS Control Network and Data Analysis in the Grove Mountains, East Antarctica

E Dongchen(1), Zhang Shengkai(1), Yan Li(2) and Li Fei(2)

(1) Chinese Antarctic Center of Surveying and Mapping, Wuhan University, Wuhan, 430079, China

(2) School of Geodesy and Geomatics, Wuhan University, Wuhan 430079, China

Email: edc1939@public.wh.hb.cn

Abstract

In order to provide the satellite image map for the field expedition, during the 19th CHINARE (Chinese National Antarctic Research Expedition) 2002/2003 summer season, GPS control network was established in Grove Mountains, East Antarctica. Its geographical extension is 72° to 73°S, 73° to 76°E, and its area is about 8000km². In the inland ice sheet where the elevation is approximately 2000m, seven permanent GPS control marks were set with the support of helicopter and vehicles. Simultaneously observing with Zhongshan permanent GPS station, we constructed the geodetic network with these seven points by Trimble 4000ssi GPS receiver. Processed by the high-accuracy GPS software^o™GAMIT, the positioning precision is good enough to satisfy with the acquirement of cartography in this area.

Key Words geodetic network, satellite image, Grove Mountains, Antarctica

1. Background

Grove Mountains is located in Princess Elizabeth land in East Antarctica, about 400km inland from Zhongshan Station and 160km east of the Mawson Escarpment, it consists of a scattered group of mountains and nunataks. The range includes 73°-76°E, 72°-73°S, extending an area of 8000km². Grove Mountains has great topographical undulation and is densely covered by ice crevice, the weather there is atrocious [1]. The average temperature in January is -18.5°E which is 18°E lower than Zhongshan Station, and the average wind velocity is more than 10m/s [2]. So it has been one of our ideal midway station points

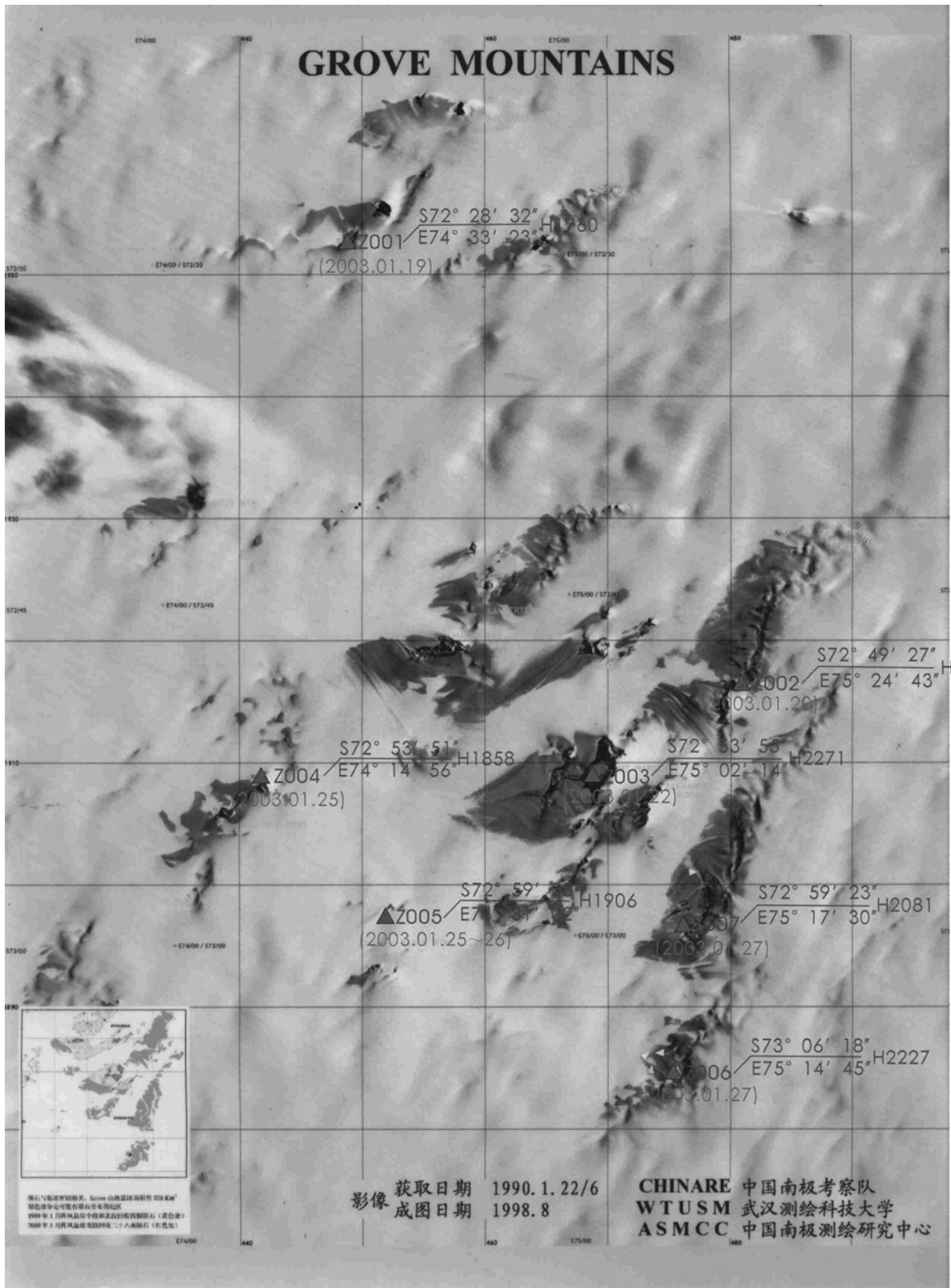


Fig.1: GPS control network in the Grove Mountains

(Note: the coordinates in Fig.1 are the approximate coordinates with single point positioning)

in the route from Zhongshan Station to eastern Antarctic ice-cover and in the expedition of Antarctic Pole Point.

During the 1998/1999 Antarctic summer season, the 15th CHINARE (Chinese National Antarctic Research

Expedition) first went to the Grove Mountains for research and expedition. During the 1999/2000 summer season, the 16th CHINARE carried out the second expedition in the Grove Mountains, the surveyors utilized the Differential

GPS technology and mapped the core area which covers 110 km² at the scale of 1:25000 [3]. In the summer 2002/2003, it is the third time that the 19th CHINARE went to the Grove Mountains, the surveyors established 7 permanent geodetic points in this area, collected data on those points with GPS receivers, and prepared for the topographic mapping with the satellite image.

Besides CHINARE, ANARE (Australia National Antarctic Research Expedition) and RAE(Russian Antarctic Expedition) also have been to the Grove Mountains several times since 1950s[4].

2. Geodetic surveys 2002/2003 in the Grove Mountains

During the 2002/2003 summer season, the 19th CHINARE carried out the third expedition in the Grove Mountains, the main tasks include: geodetic survey, meteorite collection, ice kinematics and geology expedition etc..

In order to provide the satellite image map for the field expedition, the surveyors established 7 permanent geodetic points in Cooke PK-the north section of the Gale Escarpment-Mount Harding-Melvold NTKS-Black NTKS-the south section of the Gale Escarpment and the Fig.2: GPS benchmark in the Grove Mountains



middle section of the Gale Escarpment, and the GPS control network is shown in Fig.1.

In January 19, 2003, the Z-9 helicopter flew from Zhongshan Station to the camp No.5 at the foot of the Mount Harding, then the helicopter flew to the Cooke PK for GPS observation and ice sampling etc... This is the first time that Chinese helicopter flew to the Grove Mountains under the furious weather conditions without foreign aids. On account of the long distance between Zhongshan Station and the Grove Mountains, the fuel carried by the helicopter can only maintain the single fly to the Grove Mountains, the helicopter had to be replenished the fuel so that it can fly back to Zhongshan Station. But the temperature in the Grove Mountains is so low that the helicopter couldn't close the engine, so the helicopter can only stay in the Grove Mountains for a short time.

Shortly after its arrival at camp No. 5, the helicopter carried the surveyors to Cooke PK. Because the wind near the foot of the Cooke PK is too violent, the helicopter had to land on ice far away. The permanent geodetic mark which carved Z001 was established on a nunatak to the

south of Cooke PK, the mark is illustrated in Fig.2 below. Only small amount of data were collected on this point because the helicopter had to fly back in an hour.

Except for Cooke PK, snow vehicles were utilized when collecting GPS data on other 6 points. On the apparent and flat solid bedrock, the surveyors used the impact drill to drill an aperture in the bedrock, then put the screw of the benchmark into the aperture and clung it with glue. After the benchmark was stable enough, the GPS antenna was mounted over the benchmark and began to collect data. About one hour's GPS data were collected on each point. The satellite cutoff angle was set to 15 degree and the sample interval was 15 second. After observation, photos were taken from different directions for the benchmark. GPS observation in the Grove Mountains is shown in Fig.3.



Fig.3: GPS observation in the Grove Mountains

The observation records are shown in table 1.

Table 1. GPS observation record in Grove Mountains (GPS observation time is GMT)

Point	Date	Start	Finish	Receiver Type	Antenna Type	Vert Antenna Height
Z001	2003.1.19	10:13:45	10:35:30	Trimble-4000SSI	4000SSE	0.200m
Z002	2003.1.20	08:54:15	09:55:45	Trimble-4000 SSI	4000SSE	0.243m
Z003	2003.1.22	11:20:45	12:38:15	Trimble-4000 SSI	4000SSE	0.200m
Z004	2003.1.25	16:23:15	17:24:00	Trimble-4000 SSI	4000SSE	0.243m
Z005	2003.1.25	18:46:15	19:46:30	Trimble-4000 SSI	4000SSE	0.200m
Z006	2003.1.27	11:35:45	12:38:00	Trimble-4000 SSI	4000SSE	0.200m
Z007	2003.1.27	15:56:15	16:57:15	Trimble-4000 SSI	4000SSE	0.200m

3. Data Processing

A high-accuracy GPS processing software package-GAMIT was utilized, and the data were processed on ULTRA2 workstation. GAMIT is a comprehensive GPS analysis package developed by MIT and Scripps for the estimation of three-dimensional relative positions of ground stations and satellites orbits. The software is composed of ARC-Model-SINCLN-DBCLN-CVIEW and SOLVE modules etc... [4].

The data were processed using IGS precise ephemeris in the ITRF 2000 Reference Frame, at epoch 2000 and the baseline was constituted with the Zhongshan permanent GPS station. The ephemeris precision is one of the most important factors in GPS data processing, and its influence on baseline processing can be given in the formula below:

$$\frac{|\Delta r|}{10|r|} = \frac{|\Delta b|}{|b|} - 4|r| \quad (1)$$

Where $|\Delta r|$ is the error of satellite orbit, r is the satellite

earth centre position vector, $|\Delta b|$ is error of the base line vector and b is the base line vector between the two stations [5].

The main limiting factors in GPS baseline processing are listed below:

- The satellite clock offset
- The receiver clock offset
- The influence of ionosphere refraction
- The influence of troposphere refraction
- The phase center correction of the satellite and receiver
- The tidal correction of the station

The quality of the data is also important for the precision and reliability of baseline. The data edit which included fixing the cycle slips and eliminating the remained residuals is the main job in processing data. When editing the data, run AUTCLN module firstly, which allows better handling of poor data and provides quality statistics for each station. Then CVIEW should be run to examine the phase residuals from the initial solution and to add instructions for deleting data to the AUTCLN command file and fix remaining small cycle slips interactively. After that, clean X-file can be drawn for baseline resolution [6].

Basing on the data edit, ARC-MODEL and SOLVE can be run sequentially. The coordinates of the control points are shown in table 2.

Table 2. The coordinates of the Grove Mountains control points

Point ID	Location	Coordinates		
		X (m)	Y (m)	Z (m)
Z001	Cooke PK	513123.2465	1857351.9446	-6061561.744
Z002	North of Gale Escarpment	476009.4087	1828996.9854	-6073542.7912
Z003	Mount Harding	485917.0248	1818191.2331	-6076090.8947
Z004	Melvold NTKS	510881.2294	1811322.8830	-6075661.3398
Z005	Black NTKS	499957.5196	1804891.3702	-6078525.0285
Z006	South of Gale Escarpment	473679.3826	1798618.4237	-6082789.418
Z007	Middle of Gale Escarpment	475350.6838	1810866.8957	-6078894.7289

Table 2. The coordinates of the Grove Mountains control points

The precision of the control points are listed in table.3:

Table 3. The precision of the control points

Point ID	X_m_	Y_m_	Z_m_
Z001	8.8486	10.1408	14.1732
Z002	0.0486	0.0414	0.0341
Z003	0.4087	0.1673	0.1505
Z004	0.0971	0.1793	0.1236
Z005	0.2774	0.1639	0.2417
Z006	0.0697	0.0441	0.0262
Z007	0.0373	0.0991	0.0877

Table 3. The precision of the control points

From table 3, the conclusion can be drawn that the precision of Z001 is poor because of the short observation time. Besides Z001 point, the other 6 points can satisfy the need of the satellite image mapping at the scale of 1:50000.

4. Conclusion and suggestions

The precision of the 6 points in the Grove Mountains

except for Z001 are high enough to satisfy the need of the satellite image mapping at the scale of 1:50000.

Because of the limitation of the logistic support, short term GPS data were observed at Z001 point. As a result, the precision of this point is too low to use. If it is possible, Z001 should be re-observed in next expedition and 2-3 points should be established in the north part of the Grove Mountains, so the geodetic network would be more equivalent.

2-3 points should be re-observed in next expedition so as to get multi-session repetitive data for analysis of the crustal movement and geodynamics. The control points in the Grove Mountains can be analyzed together with the points in Larsemann Hills and Amery Ice Shelf, this would be of great importance to the research of geodynamics and ice kinematics of east Antarctica.

Additionally, this geodetic network should be combined with the geodetic network made by Australia and Russia if possible, which would unify the geodetic network in the Grove Mountains and Lambert Glacier-Amery Ice Shelf System in east Antarctica.

Acknowledgements

Thanks to Dr. Jiang Weiping, Zhang Hongping and Liu Youwen from GPS Center of Wuhan University for the support of GPS data processing.

5. Reference

Sun JB *et al.* The Digital Mapping of Satellite Images Under No Ground Control and the Distribution of Landform, Blue Ice and Meteorites in the Grove Mountains, Antarctica. *Chinese Journal of Polar Science*, Vol.13, No.1, P. 21-31, 2001.

Cheng YJ, Lu LH, Bian LG The Weather Characteristic in Summer Season in the Grove Mountains, East Antarctic. *Chinese Journal of Polar Research*, Vol.11, No.4, 291-300,1999.

Peng WJ, Ding SJ, Chen CM The Application of Post Process DGPS Technology in the Topographic Mapping of Grove Mountains, Antarctica. *Chinese Journal of Polar Research*, Vol.13, No.4, P. 301-306, 2001.

Gary Johnston, Paul Digney, John Manning *Extension of the Australian Antarctic Geodetic Network in Grove Mountains*. AGS'01, 2001.

Cheng X, Zhang YM, E DC *et al.* The operation of GAMIT/GLOBK in PC. *Bulletin of Surveying and Mapping*, No.1, P. 4-6 2003.

Jiang WP, Liu JN, Ye SR The analysis of the System Error in Baseline Processing of GPS Deformation network. *Journal of Wuhan University*, Vol.26, No.3, P.197-199, 2001.

Wang QH, E DC, Chen CM Antarctic Traverses from Zhongshan Station to Dome-A and the Results Analysis for the GPS Points along the Expedition Route. *Geo-Spatial Information Science*, 5 (1): 31-36, 2001.

Positional Accuracy of Airborne Integrated Global Positioning and Inertial Navigation Systems for Mapping in Glen Canyon, Arizona

Richard D. Sanchez and Larry D. Hothem

Any use of trade, product, or firm names is for descriptive purposes only and does not imply endorsement by the U.S. Government.

Abstract

High-resolution airborne and satellite image sensor systems integrated with onboard data collection based on the Global Positioning System (GPS) and inertial navigation systems (INS) may offer a quick and cost-effective way to gather accurate topographic map information without ground control or aerial triangulation. The Applanix Corporation's Position and Orientation Solutions for Direct Georeferencing of aerial photography was used in this project to examine the positional accuracy of integrated GPS/INS for rough terrain mapping in Glen Canyon, Arizona. The research application in this study yielded important information on the potential of airborne integrated GPS/INS data-capture systems for deployment to Antarctica.

Introduction

Over the past decade, several publications have confirmed the potential of utilizing the Global Positioning System (GPS) and inertial navigation system (INS) technology for the direct observation of exterior orientation data (Schwarz, 1993; Ackerman, 1995; Skaloud, 1996). Increasingly, onboard GPS/INS data collection is part of the service offered by aerial companies. Many software systems can now access such data to reduce or eliminate the need for ground control points. In many cases, it is the enabling technology for the collection of light detection and ranging (lidar), synthetic aperture radar, and multibeam sonar data. It was not until recently that the remote sensing and photogrammetric mapping community gave serious attention to using integrated GPS/INS technology to measure camera attitude to an accuracy that permits photogrammetric mapping without conventionally determining the camera exterior orientation parameters from aerial triangulation. The process of direct observation of exterior orientation data with airborne integrated GPS/INS is often referred to as "direct measurement," "direct sensor orientation," "direct exterior orientation," and "direct geocoding." However, throughout this paper, the authors will refer to this process by the more widely used term "direct georeferencing."

Many earth science mapping applications, especially in rural or remote areas, can be realized more efficiently and economically with the reduction of ground control and tie point data. This can be achieved by direct georeferencing of the exterior orientation of an imaging sensor using an integrated system comprising a GPS receiver and an INS component. The GPS produces precise positions that are subject to errors arising from loss of satellite lock and

resolution of phase ambiguities. Information from the INS can be used to correct these errors while the GPS data are used to continuously calibrate the INS. Hence, when used together, the two components may provide an appealing solution to positioning and orientation problems in mapping applications. Nevertheless, the use of this technology is not without its own technical problems, and an understanding of its limits and usefulness is critical for addressing mapping applications. A crucial issue to mapping applications and direct georeferencing is the accuracy, scale, and consistency achievable by an integrated system.

Numerous documented GPS/INS-related field tests have been conducted over the years (Cramer, 1999; Cramer, Stallmann, and Haala, 2000). These tests were flown over well-surveyed sites and were carefully evaluated by private and public institutions in collaboration with Applanix Corp. The results from these tests, which measured the difference between the Applanix Position and Orientation Solutions for Direct Georeferencing (POS/DG)-computed camera orientation and the camera orientation obtained from aerial triangulation, demonstrated reliable performance. Although the difference of GPS/INS-derived omega, phi, kappa, (ω , Φ , κ) from aerial triangulation angles gives a good measure of GPS/INS performance, it does not allow the separation of GPS/INS errors from aerial triangulation errors (Hutton, Savina, and Lithopoulos, 1997). A better gauge of performance is to apply GPS/INS-derived values to the exterior camera orientation plus the camera interior report parameters using digital photogrammetric software and then to compare the accuracy of terrain mapping with the well-surveyed reference points visible in the image (Abdullah, 1997). The purpose of this project was to test the terrain-mapping accuracy of Applanix POS/DG in an area of rapidly changing relief using this approach.

Project Test Area

The regional location of the project area was in the southernmost part of Glen Canyon, a section of the Colorado Plateau and canyon lands of Arizona and Utah formed by the Colorado River (fig. 1). The marked change in relief in this area provided an excellent test for measuring the potential of GPS/INS for terrain mapping and ultimately providing agencies like the USGS's Grand Canyon Monitoring and Research Center (GCMRC) a continuous source of reliable data to study landscape and habitat changes along the Colorado River corridor. The canyon lands, which date back nearly 2 billion years on

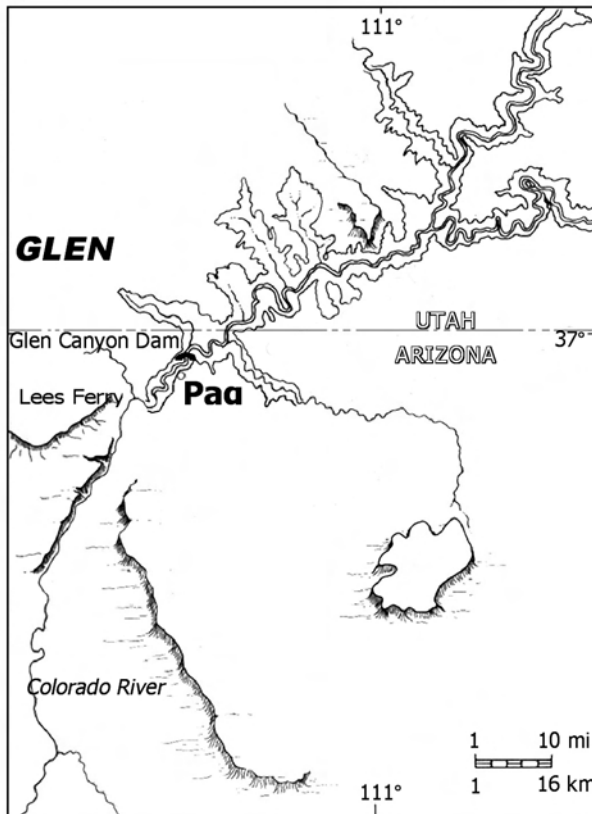


Figure 1. Project area is located between Page and Lees Ferry, Arizona.

the bottom and 250 million years at the top, are a rough succession of resistant beds forming deep, narrow gaps with vertical and overhanging cliffs separated by slopes and valleys carved out by the Colorado River beginning 5 to 6 million years ago (Zimmer, 2001). During 1869 to 1872, U.S. Army Major John Wesley Powell explored the Glen Canyon as part of the expedition of the Colorado River (Powell, 1875). As many a fisherman and passerby will affirm, the cliffs, river banks, and sandbars of the canyon offer nesting places to rock wrens, canyon wrens, peregrine falcons, ravens, and high-flying condors. Since the completion of the Glen Canyon Dam in 1963, the water temperature downriver averages 46° F (8° C) year round. This constant flow of clear, cold tail water, along with the introduction of trout and shrimp-like scuds, eliminated most of the native fish, such as the Colorado squawfish and the humpback chub (Ray Hall, U.S. Park Ranger, oral commun., September 26, 2001). The dam-regulated flows decreased the sediment supply and have affected the habitats of the endangered willow fly-catcher and Kanab ambersnail. The canyon's ecosystem and desert environment are also home to deer mice, pocket mice, packrats, spotted skunks, ringtail cats, gray foxes, beavers, bobcats, coyotes, jackrabbits, antelopes, squirrels, badgers, and mule deer. Seasonal wildlife includes a large population of ducks and some Canadian Geese. Plants such as joint-fir or Mormon Tea (*Ephedra*), Horsetail (*Equisetum L.*), salt cedar or Tamarix (*Tamarix gallica*), and varieties of cacti dominate the canyon ecosystem (Gaines, 1957).

Direct Georeferencing Concept

The determination of the exterior orientation parameters is a fundamental requirement for the geometric evaluation of terrestrial and remotely sensed images. Conventionally, this is accomplished by an indirect approach of applying a number of known ground control points and their corresponding image coordinates. Using a mathematical model for the transformation between object and image space, we can calculate the exterior orientation to relate the local image coordinates to the global reference coordinate system. This process is accomplished with the spatial resection of single images, a method that is generalized to an aerial triangulation of multiple frames or images (Skaloud and others, 1996). The photogrammetric collinearity equations are applied to connect overlapping images by means of tie points and to relate the local model coordinates to the global reference coordinate system through control points. Consequently, exterior orientation parameters for the perspective center of each image can be estimated as one group of the unknown parameters within a least squares adjustment.

In the direct approach, the GPS and the inertial measurement unit (IMU) provides measurement of the true physical position and orientation of the camera or sensor (Schwarz and others, 1993). Unlike the indirect approach of aerial triangulation, the exterior orientation parameters are determined independently of the camera or sensor. Before using the position and orientation components (GPS antenna and IMU) for sensor orientation, we must determine the correct time, spatial eccentricity, and boresight alignment between the camera coordinate frame and IMU. The calibration of the GPS/IMU and camera is vital since minor errors will cause major inaccuracies in object point determination.

System Configuration and Calibration

Sensor Configuration

The commercial airborne integrated GPS/INS used in this project is the POS AV 310 from Applanix Corp., Richmond Hill, Ontario, Canada. The POS AV-DG package comprises four main components: (1) a dual-frequency L1/L2 carrier phase embedded GPS receiver (NovAtel MiLLennium), (2) a POS IMU, (3) the POS computer system, and (4) the POS/DG postprocessing software. Several occupied geodetic monuments (Airport, T96, Davian, Signal Hill, Navajo Point, Flagstaff NCMN, and L404) along the canyon rim served as base stations. In addition, 11 aerial panel points with documented horizontal and vertical coordinates were placed along the flight corridor to test the accuracy of the POS/DG position and height information later. For the test, the POS IMU was rigidly mounted on a Wild RC30 aerial camera. The GPS antenna was centred above the camera on top of the fuselage of the National Oceanic and Atmospheric Administration's (NOAA) Cessna Citation jet. The integration of the collected POS/DG raw data was computed at the camera perspective center using the Applanix POS/DG Post Processing software.

Boresight Calibration

The spatial offsets between the different sensor components have to be identified to relate the position and orientation information provided by the GPS/IMU to the perspective center of the camera. The angular and linear misalignments between the POS IMU body frame and the imaging sensor are referred to as “boresight” components. Immediately after the actual fly-over of the Glen Canyon project area, the test flight for the boresight calibration was carried out over a well-surveyed range in the nearby Hopi Reservation. Aerial photographs were collected at a flying height of 1,524 m (5,000 ft) and a photographic scale of 1:10,000. Three rows of 7 targets consisting of 21 photographs with 60 percent forward and 30 percent side overlap were collected. The test range covered a 4.5- x 14.8-km (2.8- x 9.2-mi) area. Static GPS data were collected using several base stations (Airport, T96, Davian, Signal Hill, Navajo Point, Flagstaff NCMN, and L404) located near the test range to check for any systematic errors caused by different baseline length. To resolve the boresight transformation, the National Geodetic Survey (NGS) compared the GPS/IMU positioning/orientation results with the aerial triangulation solution. The NGS then used data from the POS/DG and aerial triangulation from the flight to resolve the fixed misalignment angles between the IMU and the camera.

Terrain Mapping

The NOAA carried out the overflight of the project area on September 6, 1999, at altitudes between 3,200 to 3,500 meters (10,500 to 11,500ft). The acquired misalignment angles from the Hopi Range test flight were applied to the POS/DG data, and the camera perspective center coordinates (in easting, northing, and elevation) and the camera orientation parameters (in angles ω , Φ , κ) were computed by Applanix. The POS/DG-computed data at camera perspective center, as well as the camera’s internal geometry and lens characteristics, were then applied by the USGS to geometrically correct the scanned aerial frames (4027 through 4032, see fig. 2) using the Softcopy Exploitation Tool Set (Socet Set) software (Socet Set® is a trademark of BAE Systems Solutions, Inc.).

Surveyed Reference Points

To synchronize with the POS/DG data collection and to know the precise grid coordinate of any point in the project area, a field team directed by the GCMRC placed 15 aerial panels along the corridor of the Glen Canyon before the overflight. Many of these panels were placed over old survey markers. To validate the positional accuracy of the panels, the U.S. Geological Survey (USGS) conducted static surveys of these old monuments in September 2001. The selected points were occupied for over 30 minutes at 5 second intervals using two Ashtech Z-12 receivers. Simultaneous collection from the Flagstaff (FST1) Continuous Operating Reference Station (CORS) at 5-second intervals provided the RINEX files (range and

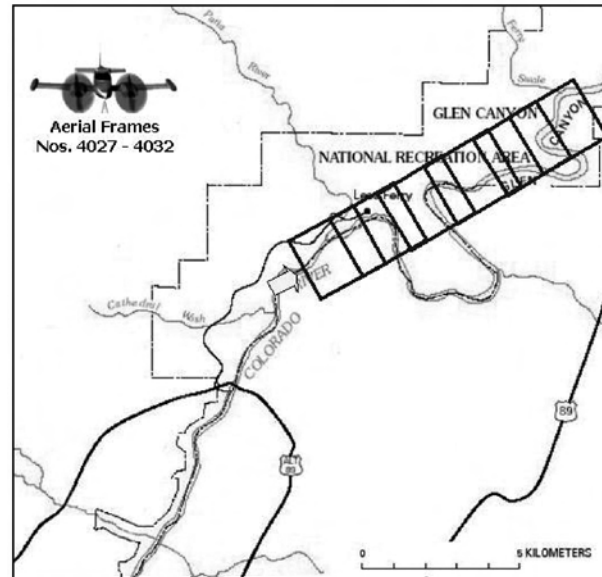


Figure 2. Coverage of aerial frames applied in the evaluation.

carrier phase or binary measurements, predicted orbital coordinates or ephemeris data, and site information files) used in the postprocessing with Ashtech Solutions version 2.5. Traditional setup of the antenna over the survey marker was used in these static surveys. For geodetic coordinates and details about each survey marker revisited, see appendix A of this report.

In addition to their use as panel points, the survey markers in the Lees Ferry area proved invaluable for checking the accuracy of auxiliary GPS instruments. The Ashtech Z12 GPS rover and the simultaneous collection of FST1 CORS produced post processed differentially corrected positions that were used in determining the horizontal and vertical accuracy levels of the auxiliary GPS instruments. Experimentation with an OmniSTAR Model 3000LR12 (an integrated RT-DGPS system for GPS observations and reception of broadcast range correction) produced differentially corrected positions with horizontal and vertical accuracies at the submeter level. The Rockwell PLGR II with PPS for point positions determined by autonomous methods produced horizontal and vertical accuracies in the decimetre-to-metre range. (See appendix B).

Comparison with Survey Reference Points

Three stereoscopic models were generated with Socet Set photogrammetric software using the POS/DG computed data and the camera’s report parameters (fig. 3).

In each stereomodel, a thorough examination for undesirable y-parallax or disparity was conducted by moving between the river corridor and the canyon rim of the interior and corners of the stereomodel, respectively. The results varied from negligible to excessive. In one model the effect of y-parallax made it difficult to perform reliable measurements. Absolute orientation was then examined using the horizontal and vertical coordinates of the visible panel point in the three models and the values

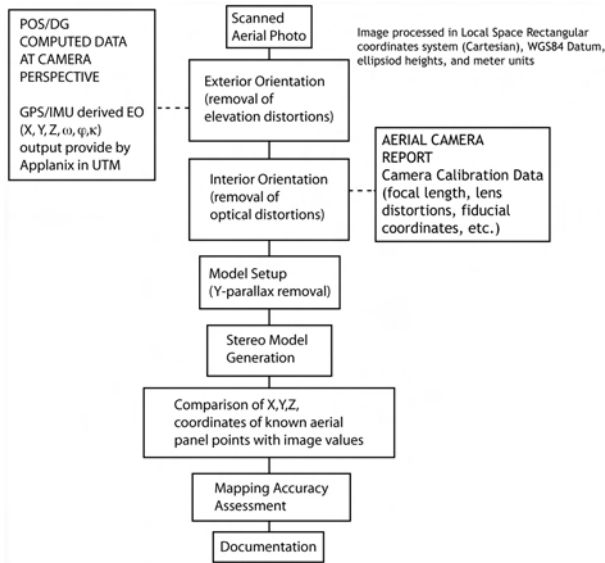


Figure 3. The flow process applied in this study for generating the stereomodels for testing the accuracy of Position and Orientation Solutions for Direct Georeferencing of aerial photographs.

of their corresponding surveyed reference positions. The difference between the logged surveyed reference positions and corresponding panel points displayed in the stereoimage were measured on the digital photogrammetric workstation. The difference was determined by subtracting the values of the panel point from the surveyed reference position. The measured panel point values in the stereoimage were roughly parallel to the ground level at an average vertical positional bias of +2.59 m. Figure 4 and table 1 show the results of the comparison of the panel point coordinates in the stereoimages against the values of the logged survey referenced positions.

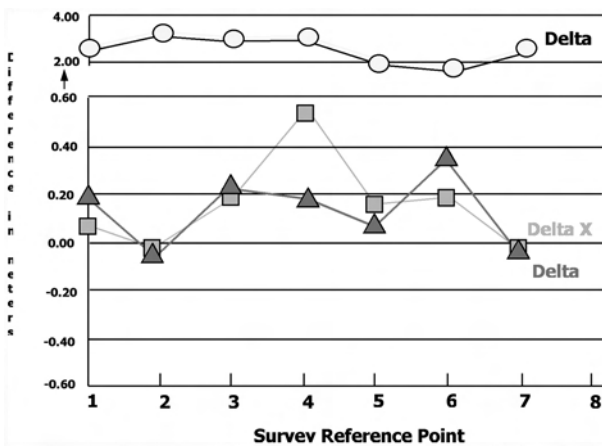


Figure 4. Difference, in meters, between coordinate values of ground-surveyed reference points and corresponding panel points measured on the digital photogrammetric workstation.

A comparison using the same ground-surveyed reference points shown above with Aeroscan ALMS lidar data collected by the GCMRC in late March 2000 at a flight altitude of 3,048 m (10,000 ft), with a pulse rate of 15 kHz and a scan rate of 13 Hz, showed a lower vertical positional

REF.	PANEL #	Delta X	Delta Y	Delta Z
1	6BC	+0.07	+0.19	+2.48
2	114	-0.02	-0.05	+3.28
3	115	+0.19	+0.24	+3.02
4	211	+0.56	+0.16	+3.11
5	212	+0.16	+0.08	+1.88
6	214	+0.19	+0.35	+1.78
7	G307B	-0.02	-0.03	+2.58
Average		+0.16 m	+0.14 m	+2.59 m

Table 1. Statistical rundown of the difference between the ground-surveyed reference points and corresponding panel points measured on the digital photogrammetric workstation.

bias (0.21 m to 0.55 m) than those found in the processed POS/DG of aerial photographs. Although there was some improvement in the vertical accuracy of the DG lidar system measurements, the lower vertical positional bias of the lidar data still does not meet accuracy standards for large-scale mapping and could result in significant errors in studies related to volume determination.

Discussion Of Results

Although the horizontal positioning results proved accurate, the higher than normal vertical positional bias results of this study do not meet National Mapping Accuracy Standards (NMAS) or American Society of Photogrammetry and Remote Sensing (ASPRS) accuracy standards for large-scale mapping. Other authors made comparable findings (for example, Cramer, 1999; Colomina, 1999; and Greening and others, 2000). Greening suggested 1:8,000 scale as the “lower limit below which airborne GPS errors can become relatively dominant to the point where a significant reduction in the number of ground control is not possible.”

Several factors may have contributed to the higher than normal vertical positional bias between the coordinate values of surveyed reference points and corresponding aerial panel positions in the image. The most demanding applications of large-scale airborne mapping, with required mapping accuracy at the 10- to 20-cm range, call for higher precision of the exterior orientation, which is largely dependent on the imaging sensor and flight altitude. In this study, a 153-mm calibrated focal length of the Wild RC30 and high-flying height of 3,200 to 3,500 m (10,500 to 11,500 ft) was used. In accordance with a typical soft C-factor (Light, 1999), a suggested minimum of 1,000 m (3,300 ft) flight altitude with the 153-mm focal length camera may have resulted in lower RMS values and achieved a higher precision desirable in large-scale mapping. Further, the aerial photographs flown separately for the boresight calibration were collected with the same camera, but at a flying height of 1,524 m (5,000 ft), which may have caused a shift in the Z value. The influence of ground position errors resulting from imaging sensors and flight altitudes have been dealt with in detail (Grejner-Brzezinska, 1999).

Another problematic concern of GPS/INS-derived position orientation data is the stereo-model residual parallax issue. During the setup of the stereomodels, it was found that the y-parallax varied significantly. In one of the models, the effect of y-parallax made it awkward to take reliable measurements. The y-parallax disparity took the form of an unusually high average difference between the coordinate values of surveyed reference points and corresponding panel points, as well as imperfect, out-of-focus three-dimensional images in the display of the digital photogrammetric workstation.

Several geodetic factors also may have contributed to the high RMS values in the exterior orientation solution. Because of the marked difference in canyon relief and changes in bedrock

Densities, there exists a “deflection of the vertical” (that is, an angle of departure of the gravity vector from the corresponding ellipsoidal normal). In the canyon area where there are marked geoidal undulations, the separation between the geoid and ellipsoid can vary rapidly and in a nonlinear manner.

Although the lidar data results were lower in vertical positional bias than those found in the processed POS/DG of aerial photographs, several factors may have played a part in their high elevation measurement. These factors range from the lidar processing algorithms to the source of beam. Factors originating from the source of the beam include problems with the

- 1) lever arm and GPS position,
- 2) INS gyros (drift and alignment),
- 3) laser frame (misalignment in INS),
- 4) scanning (mirror), and
- 5) range (timing, bias, noise). Any of these factors not being adjusted properly may have resulted in mismatched profiles and introduced elevation errors.

Recommendations

The higher than normal vertical positional bias results of this study did not meet large-scale mapping accuracy standards. It is important to keep in mind the limitations of airborne integrated GPS/INS mapping technology and to balance the criteria for its use against practical considerations of large-scale mapping in canyon-like or mountainous terrain. For the time being, precision large-scale mapping of 1:8,000 scale or better will require a combination of airborne GPS/INS and aerial triangulation to exploit the benefits offered by direct external orientation data and minimize potential mapping accuracy limitations.

Additional research is needed to examine the

- (1) influence on mapping accuracy of geodetic complexities in areas of marked changes in relief and the relationship of IMU performance to significant gravity anomalies and deflection of the vertical;
- (2) output of POS/DG computed data at camera perspective center in a Cartesian coordinate system

to replicate the true spatial geometry of the object space;

- (3) large scale mapping application of the “Total Orientation Procedure” concept (Colomina, 2000) for optimal sensor orientation using a combination GPS/INS and aerial triangulation;
- (4) adequate rigidity in the relationship between IMU and camera reference frame; and
- (5) accuracy limits of GPS-aided INS of LiDAR data for meeting NMAS and ASPRS standards

Acknowledgments

The authors would like to thank Herb Grossman, USGS-WRD (retired), who generously provided his time to help in conducting the fieldwork, and Raymond M. Hall, National Park Service, whose cooperation at Lees Ferry was outstanding. Also thanks for the offsite support provided by Mike Liszewski, GCMRC, Flagstaff, Ariz., Fidel Paderes, BAE, San Diego, Calif., and Mike Aslaksen, NGS-NOAA, Silver Spring, Md. The USGS provided the funding for this research project.

References

- Abdullah, Q., 1997, *Evaluation of GPS-Inertial Navigation System for airborne photogrammetry: ASPRS/MAPPS Softcopy Conference*, Arlington, Va.
- Ackerman, F., 1995., *Sensor and data integration - The new challenge: Integrated Sensor Orientation ISPRS Workshop*, Germany.
- Colomina, Ismael, 1999, *GPS, INS and aerial triangulation: What is the best way for the operational determination of photogrammetric image orientation?: ISPRS 2000*, v. 32, Muchen.
- Colomina, Ismael, 2000, *T.O.P. concepts for sensor orientation*, ISPRS 2000, v. 33, Amsterdam.
- Cramer, Michael, 1999, Direct geocoding: Is aerial triangulation obsolete; Fritsch/Spiller (eds.), *Photographic Week 1999*, Heidelberg, Germany, Wichmann Verlag, p. 59-70.
- Cramer, M., Stallmann, D. and Haala, N., 2000, Direct georeferencing using GPS/Inertial exterior orientations for photogrammetric applications; *International Archives of Photogrammetry and Remote Sensing*, v. 33, part B3, p. 198-205.
- Gaines, Xerpha, 1957, *Plants of the Glen Canyon: Plateau Technical Series*, Museum of Northern Arizona, v. 30., no. 2, p. 31-34.
- Greening, W.J. Trevor, Schickler, Wolfgang, and Thorpe, Anthony J. 2000, *The proper use of directly observed orientation data: Aerial Triangulation Is Not Obsolete*, ASPRS 2000 Proceedings, Washington, D.C.
- Grejner-Brzezinska, Dorota A., 1999, Direct exterior orientation of airborne imagery with GPS/INS system: Performance analysis, navigation: *Journal of the Institute of Navigation*, v. 46, no. 4, Winter 1999-2000, p. 261-270.

REPORT OF THE FIFTH SCAR ANTARCTIC GEODESY SYMPOSIUM

- Hutton, J., Savina, T., Lithopoulos, L., 1997, *Photogrammetric applications of applanix's position and orientation system*; ASPRS/MAPPS Softcopy Conference, Arlington, Va.
- Light, Donald L., 1999, C-Factor for softcopy photogrammetry; *Photogrammetric Engineering & Remote Sensing*, v. 65, no. 6, p. 667-669.
- Powell, J.W., 1875, *Exploration of the Colorado River of the West: 1869-72*, Washington, D.C., Government Printing Office.
- Schwarz, K.P., Chapman, M.A., Cannon, M.E., and Gong P., 1993, An integrated INS/GPS approach to the georeferencing of remotely sensed data: *Photogrammetric Engineering & Remote Sensing*, v. 59, no. 11, p. 1667-1674.
- Skaloud, J., Cramer, M., Schwarz, K.P., 1996, Exterior orientation by direct measurement of camera position and attitude: *ISPRS International Archives of Photogrammetry*, v. XXXI, part B3, Vienna, Austria.
- Zimmer, Carl, 2001, How old is it?: *Journal of the Nat. Geog Soc*, v. 200, no. 3, Washington, D.C., p. 78-102.

Appendix A

Field Record Summary – Glen Canyon 9/24-27/01

SITE NAME	COORDINATES ¹	SURVEY MARKER	STAMP MARKING
GCP 6BC	LAT: 36° 52' 28.66827" N. LON: 111° 33' 27.78332" W. ELLIP. HT: 939.401 meters MSL: 962.824 meters	92.5 mm in diameter brass survey marker	BUREAU OF RECLAMATION
GCP 211	LAT: 36° 51' 48.14314" N. LON: 111° 34' 37.31705" W. ELLIP. HT: 936.652 meters MSL: 960.055 meters	92.5 mm in diameter brass survey marker	U.S. COAST & GEODETIC SURVEY
GCP 212	LAT: 36° 51' 57.56024" N. LON: 111° 35' 12.31421" W. ELLIP. HT: 930.269 meters MSL: 953.664 meters	60 mm in diameter aluminum survey marker	BANNER INC.
GCP 214	LAT: 36° 51' 48.23613" N. LON: 111° 35' 55.43807" W. ELLIP. HT: 939.976 meters MSL: 963.352 meters	12.7 mm in diameter unthreaded rebar	NO STAMP MARKING
GCP 114	LAT: 36° 53' 11.18031" N. LON: 111° 31' 51.77007" W. ELLIP. HT: 951.340 meters MSL: 977.784 meters	92.5 mm in diameter brass survey marker	BUREAU OF RECLAMATION
GCP 115	LAT: 36° 53' 10.41023" N. LON: 111° 31' 10.30107" W. ELLIP. HT: 947.940 meters MSL: 971.383 meters	No survey marker; X 10x10 Bldr RL 9-mile	NO STAMP MARKING
GCP G307B	LAT: 36° 52' 28.89023" N. LON: 111° 34' 00.98043" W. ELLIP. HT: 935.380 meters MSL: 958.799 meters	No survey marker; photo location RL	NO STAMP MARKING

APPENDIX B
POSITIONAL COMPARISON
OF GROUND CONTROL POINT #214
(NAD83/GRS-80)

Ashtech Z-12* <i>(STATIC SURVEY)</i>	OmniSTAR LR12 <i>(RT-DGPS)</i>	Difference, in meters
Lat: 36° 51_ 48.23613_ N	36° 51 48.195 N	0.662
Long: 111°35_ 55.43807_ W.	111° 35 55.463 W.	-0.583
Ellip. Height: 939.976 m	939.692 m	-0.284



GCP #214

PLGR II <i>(PPS)</i>		
36° 51 48.15 N.		1.386
111° 35 55.60 W.		-3.779
945 m		-5.024

GCP #214 Old Coordinates <i>(Unknown method)</i>		
36° 51_ 48.23_ N		0.099
111° 35 55.44 W.		-0.045
939.280 m		-0.684

Processed Image Display Coordinates <i>(Socet Set Workstation)</i>		
36° 51_ 48.258_ N		-0.354
111° 35_ 55.446_ W.		-0.187
941.760 m		-1.784

* GPS static data collected at 5-second data rate on September 25, 2001; post-processed with corresponding RINEX file downloaded from NGS National FTS1 CORS Web Site

VLNDEF Network for Deformation Control and as a Contribution to the Reference Frame Definition

**A. Capra(2), F. Mancini(1), M. Negusini(3), G. Bitelli(1), S. Gandolfi(1), P. Sarti(3),
L. Vittuari(1), A. Zanutta(1)**

(1) DISTART – University of Bologna, Bologna, Italy;

(2) DAU – Polytechnic of Bari, Taranto, Italy;

(3) CNR - Istituto di Radioastronomia, Matera, Italy E-mail: a.capra@poliba.it

Abstract

VLNDEF (Victoria Land Network for DEformation control) Geodetic Program is within the activity of GIANT (Geodetic Infrastructure of Antarctica) SCAR (Scientific Committee on Antarctic Research) Program. Moreover the geodetic activities are established within the actions of ANTEC (ANTarctic NeoTEctonics) SCAR (Scientific Committee on Antarctic Research) Group of Specialists. During 1999-2000 and 2000-2001 Italian expeditions was established and completely surveyed a network of 27 stations, over an area of 700 km northward and 300 km westward. The average distance between vertexes is in a range of 70-80 km and covering the area from TNB (Terra Nova Bay Italian base) to the Oates Coast [1,2].

In 2002-03 campaign the repetition of the whole network has been made.

Due to the long connections involved, session duration of about 48 hours was initially planned; this duration was recently increased and session duration in 2002-03 campaign was around 7 days; in agreement with Scientific International Community guidelines and thanks to the increased storage capabilities, time series of about 20-50 days were also collected on selected vertexes.

In the area the TNB1 GPS permanent station is operating since the 1998 when it was installed in proximity of the Italian summer station at Terra Nova Bay [3]. Data collected during the survey operations over the VLNDEF points have been fully processed in the attempt to constrain solutions within a specific reference frame. A subset of TNB1 data have also been requested by the scientific community in the frame of the SCAR GPS epoch campaign

and in the realisation of the new International Terrestrial Reference Frame year 2000. Basically the TNB1 data processing is performed by means of the scientific Bernese GPS software Version 4.2. TNB1 Data are routinely processed in addition to 7 Antarctic IGS (International GPS Service for Geodynamics) permanent stations in order to strength the results within a specific ITRF. Results, integration with data from provided by other peri-antarctic GPS permanent stations and an attempt in the evaluation of the regional displacement are here presented.

Preliminary results of VLNDEF surveying repetition and deformation analysis are presented.

References:

- [1] Capra A., Gandolfi S., Mancini F., Sarti P., Vittuari L. -*VLNDEF project: geodetic contribution to geodynamics study of Victoria land, Antarctica. 2001.* Proceedings of Gravity, Geoid and Geodynamics GG2000 IAG symposium, Banff, Alberta, Canada, July 2000, 379-385.
- [2] Capra A., Gandolfi S., Mancini F., Sarti P., Vittuari L. -*VLNDEF project for crustal deformation control of Northern Victoria Land. 2002.* AGS '01 (Antarctic Geodesy Symposium), St.Petersburg, July 2001, *SCAR Report, 21*, 8-10.
- [3] Capra A., Gandolfi S. *Italian GPS permanent station in Antarctica (Terra Nova Bay- Victoria Land.* Proceedings of the workshop on the Italian GPS permanent network. F.Vespe & M.Fermi Eds., Matera, 10-11/4/97. ASI, Marzo 1999

A Project on Local Ties and Co-locations in Antarctica

P.Sarti(1), J.Manning(2), A.Capra(3), L.Vittuari(4)

(1) Institute of Radioastronomy - CNR, Italy;

(2) Geoscience Australia, Australia;

(3) Polytechnic of Bari - II Fac. of Engineering, Taranto, Italy;

(4) DISTART - University of Bologna, Italy E-mail: p.sarti@ira.cnr.it

Abstracts

Co-locations between Space Geodesy techniques are nowadays fundamental for global geodetic multi technique products (e.g.: ITRF, EOP). When co-locations involve tide gauges and other geophysical instruments, the importance of geodetic observatories increases, widening the research field and the scientific

perspectives. In order to be effective, co-locations must be accurately measured with efficient and comprehensive local ties performed with terrestrial measurements. Work is being done on this subject and a few methodologies have already been tested and presented. Geoscience Australia and the Italian Institute of Radioastronomy-

CNR have separately developed methodologies capable to produce SINEX files for co-located Space Geodesy techniques. The information contained in SINEX files is fundamental for a complete and rigorous approach to techniques combination.

These SINEX have been used or tested for ITRF2000 computation and results have been very encouraging. Starting from this positive experience and making use of the knowledge acquired on this topic, we have decided to start a new project in one of the most inaccessible and

unknown parts of planet earth: Antarctica. The quality of scientific information coming from this region has to be of the highest level and its quantity possibly increased: it is fundamental for a good understanding of global geophysical processes. With this presentation, we are reviewing the most recent situation that concerns the Antarctic co-locations and the amount and quality of information currently available. We are also presenting the joint Italian-Australian project on local ties that we hope will be soon part of the GIANT programme.

Accomplishment of Topographic-Geodetic Research Works in Antarctica

Alexandr Yuskevich,

Federal Enterprise "Aerogeodesiya", Saint-Peterburg, Russia

Abstract

During the period of 1995-1999 through the efforts of specialists from the 17 countries in accordance with the GIANT program, there had been created a global geodetic GPS network of Antarctica (ITRF) which included 45 points (ellipsoid WGS-84). At present, specialists of the Russian Federation have started the development works on the territory of Antarctica with the aid of satellite means and methods of fundamental astronomic-geodetic network (FAGN) and high-precision geodetic network (H-PGN). In the accomplishment of satellite observations, the two-frequency aligned (combined) receivers GLONASS/GPS "Javad" (USA) are used. Observations of fragments FAGN and HPGN are carried out using the network method of carrying out performances of simultaneous measurements on a great number of points. In addition to the points

situated on the territory of Antarctica, the observations are also carried out on the points situated in Moscow, St. Petersburg, Irkutsk, Khabarovsk. Simultaneously with the satellite observations on points FAGN and H-PGN, gravimetric observations are carried out. While creating FAGN and H-PGN their connection with the existing global GPS network was ensured. A preliminary processing of the results of satellite measurements is accomplished using software: Pinnacle, GPSurvey, Trimble GLoad. The catalogue of the coordinates of points FAGN and H-PGN is presented in the system ellipsoid WGS-84. The main aim of these research works is revealing tidal signals of GPS observations and determining exact coordinates, heights, speed of movement and deformation of glacier (ice) surface in the region under research.

On the Randomization of GNSS Solutions

Y.M. Zanimonskiy

E-mail: yevgen@online.kharkiv.com, yzan@poczta.onet.pl

Abstract

Time series of GNSS solutions are quite specific. The variations in it have a complex structure. Besides a random part they contain also components of a chaotic character as well as biases. Models errors, non-modelled effects and varying satellites configuration cause systematic variations in GPS solutions. The analysis of such time series indicates the existence of a number of periodic components and trends that are not modelled in data processing stage. In particular, periodic variations with dominating 12h and 24h periods are distinguished. Numerous changes (jerks) in satellite configuration occur

with a period of one sidereal day. They cause specific variations in time series of the components of computed vectors from GPS data. Variations in such a time series correspond rather to a chaotic process than a random one. Jerks can be suppressed by optimising the length of overlapping sessions and eliminating the disturbing results.

In this study a new method of suppressing the variations in GNSS solution due to changes in satellite configuration is presented. This realization of bootstrap method have been adapted to GNSS software.

Optimization of Geodynamic Network on the Argentina Islands Neighbouring Vernadsky Antarctic Station

K.R. Tretyak

National University "Lvivska Polytechnika"

Abstract

According to the results of paleomagnetic, magnetometric and geological-tectonic researches there are obtained

considerable differences in the tectonic structure of the archipelago Argentina islands. Geodetic methods, namely

local GPS-networks can add and provide with new information about modern geodynamics of the Antarctic Peninsula. Mainly it concerns to the territory of Argentina Islands contiguous to Ukrainian Antarctic station "Academic Vernadsky". With this purpose in the frame of seasonal 8-th Ukrainian Antarctic expedition (February-March 2003) in the district of Antarctic station "Academic Vernadsky" it was created the precise geodetic network of ambient islands by the join efforts of scientists of National University "Lvivska Politechnika" (K. Tretyak, V. Glotov) and Close Corporation "ECOMM" (J. Ladanovskyy, P. Bahmach). The network was developed not only with purpose to study the deformations and movements of the earth's crust on the territory of Antarctic peninsula but also for creation of control geodetic network for implementation of topographical-geodetic works on the station "Academic Vernadsky" which is located in the north part of Antarctic peninsula (south latitude $B=65015'$, western longitude $L=64015'$).

Created geodynamic network covers north-eastern contiguous in the radius of 15 kilometers islands and the part of continent. The network is based on 8 geodetic station. The centers of stations are seated in the basement of rocks. The eccentricities of antennas of the phase centers were determined simultaneously on the special hard base for receivers Leica SR-399, SR-9500 and Trimble 4600LS before the beginning of observations.

The measurements were implemented from 12 to 28 of February with use of three double frequency GPS-receivers (firm Trimble 4800 and firm Leica SR-399 and SR9500) and single frequency receiver Trimble 4600LS.

Receiver Trimble 4800 was working during all time on the station VER1 in the mode of temporary permanent station. Duration of vectors measurements varies from 2 to 12 hours depending on weather conditions and transport limitation. For increasing of trustworthiness and accuracy of determination of station coordinates in the measured vectors it were applied the correction of eccentricities of the phase centers of GPS-antennas and it was fulfilled a posteriori network optimization.

In the result of considering of eccentricities of the phase centers of GPS-antennas and a posteriori network optimization the maximum errors of determination of plane coordinates of stations decreases from 5,7mm to 4,3 mm, and mean error from 2,9mm to 2,4mm. Maximum error of altitude determination decreases from 7,3 to 5,5 mm, and mean error from 3,9 to 3,2 mm. In percentage ratio maximum errors decrease on 25% and mean errors on 15%. Optimized network is more homogenous according to the accuracy.

It should be mentioned that relative error of determination of vector of station displacement after implementation of equal according to accuracy next circle will be approximately $3 \cdot 10^{-7}$. Taking into account that values of velocity of the earth surface deformations in the plane and seismic not active regions is 10^{-7} 1/year and in mountain region is 10^{-6} - 10^{-5} 1/year, then already in the next year on the assumption of repeated measurements it can be obtained the reliable quantitative parameters of passing of modern deformation processes in this region. It will allow to improve the modern regional geodynamic model of the Antarctic peninsula.

Geoid Estimation on Northern Victoria Land

G. Bitelli (1), A. Capra(2), F. Coren(3), S. Gandolfi(1), P.Sterzai(3),

(1) DISTART – University of Bologna -V.le Risorgimento n.2 - 40136 Bologna, Italy;

(2) DAU – Polytechnic of Bari - V.Orabona n.4 - 70125 Bari, Italy;

(3) O.G.S. –Borgo Grotta Gigante 42/c- Sgonico, Trieste

E-mail: a.capra@poliba.it

Abstract

A program for local geoid determination through gravimetric measurements was started in Victoria Land [1], in an area located around the Italian base Terra Nova Bay. The program started an activity planned on a more extended area, with the aim to evaluate an high accuracy geoid for all northern Victoria Land.

Points distributed on a regular grid of $3.75'$ latitude and $15'$ longitude, corresponding to an average distance of 10 km, were measured in Mount Melbourne and Mount Murchison area. Moreover sparse points were measured around the planned grid.

The positioning of gravimetric stations has been made by precise GPS method in order to obtain a decimeter accuracy in coordinate determination. This accuracy,

overall for the height, is fundamental for high accuracy geoid estimation. The gravimetric closure has been made on IRGS (Italian Relative Gravity Station) located at Terra Nova Bay. Gravimetric data will be reduced using the DTM from BEDMAP project for the interior and using the DEM generated by INSAR surveying along the coast. Preliminary results of local geoid estimation are presented.

References:

- [1] Barzaghi R., Borghi A., Capra A., Gandolfi S. Analysis of Regional Geoid Estimation in Victoria Land. AGS'01 (Antarctic Geodesy Symposium), St.Petersburg, Luglio 2001, SCAR Report N.21, pp.6-8, January 2002.

Gravity Anomalies and Geoid Heights Derived from ERS-1, ERS-2, and TOPEX/POSEIDON Altimetry in the Antarctic Peninsula Area

A. Marchenko, Z. Tartachynska, A. Yakimovich, F. Zablotskyj
National University "Lviv Polytechnic", S. Bandera St., 12, Lviv, Ukraine
Email: march@polynet.lviv.ua

Abstract.

Gravity anomalies in the area between the Antarctic Peninsula and South America were determined using satellite altimetry observations of the Sea Surface Heights over this region. The satellite data applied in the analysis include ERS-1, ERS-2, and TOPEX/POSEIDON altimetry from 1992 to 2001. The solutions for gravity anomalies and geoid heights at (2'x4') and (3'x3') grid points, respectively, are evaluated by the Tikhonov regularization method. The estimation is based on the kernel functions described by singular point harmonic functions. Comparison with the independent KMS99 and KMS01 solutions of the Geodetic Division of the Danish National Survey and Cadastre was performed.

1. Introduction

This paper represents further continuation of the recent study by (Marchenko and Tartachynska, 2003) on the inversion of the Sea Surface Heights (SSH) into the gravity anomalies Δg in the closed region of Black sea and will focus here on the recovery of the gravity anomalies Δg and geoid heights N from the ERS-1, ERS-2, and TOPEX/POSEIDON altimetry (SSH) in the marine part of the region between the Antarctic Peninsula and South America. Computations of the gravity anomalies and geoid heights from the combination of ERS1, ERS2, and TOPEX/POSEIDON Sea Surface Heights (SSH) in the area at longitude from 60°W to 70°W and latitude from 60°S to 70°S are discussed, where the Ukrainian Antarctic station Vernadsky is located in the central part of the chosen region.

The following data sets corrected by CSL AVISO for different geophysical and instrumental effects are used:

- subset 1 represents 63660 ERS1 Sea Surface Heights corrected by AVISO and taken for the period from October 1992 to June 1996 of the ERS-1 mission;
- subset 2 represents 13'x3'119 values of the corrected ERS2 SSH taken for the period from April 1995 to September 2001 of the ERS-2 mission;
- subset 3 represents 361175 TOPEX-POSEIDON corrected SSH also extracted from the AVISO database and taken for the period from October 1992 to October 2001 of the TOPEX/POSEIDON mission.

The first 3'x3'E1E2TP solution for gravity anomalies and geoid heights is evaluated at the coordinates of the KMS2001 (3'x3') grid points over the marine part of studying area by means of the Tikhonov regularization method using kernel functions (analytical covariance functions) described by singular point harmonic functions.

The dependence of the regularization parameter on the variance of the studying field and the variance of the noise is considered. An optimal kernel function was adopted as the modified Poisson kernel or the so-called dipole kernel. The second 2'x4'E1E2TP solution at the coordinates of KMS1999 (2'x4') grid points was constructed especially for further comparison with the KMS1999 gravity anomalies inverted by FFT method in the Geodetic Division of the Danish National Survey and Cadastre from multi mission satellite altimetry data (see, Andersen and Knudsen 1998; Knudsen and Andersen, 1998). The comparison of 3'x3'E1E2TP geoid heights with KMS2001 3'x3' solution is analyzed.

2. Method

As before (Marchenko, and Tartachynska, 2003) the traditional "remove-restore" procedure was used to get the initial information δN for further determination of the gravity anomalies Δg :

$$\ddot{a}N = SSH - N_{EGM96}, \quad (1)$$

where SSH are the corrected Sea Surface Heights, assumed to be coincided with the geoid height N ; N_{EGM96} is the long wavelength part of N adopted according to the EGM96 gravity field model (360, 360).

Then the prediction of the residual gravity anomalies $\delta\Delta g_p$ and the residual geoid heights δN_p was estimated at some point P (preferably inside the studying area) applying the regularization method

$$\ddot{a}\Delta g_p = C_{\ddot{a}\Delta g, \ddot{a}N} (C + \alpha C_{nn})^{-1} \mathbf{I}, \quad (2)$$

$$\delta N_p = C_{\delta N, \delta N} (C + \alpha C_{nn})^{-1} \mathbf{I}, \quad (3)$$

where \mathbf{I} is the q -vector consisting in this case of the components δN_i ($i = 1, 2, \dots, q$); q is the number of the observations δN_i ; C is the $(q \times q)$ - covariance matrix of the residual geoid height δN ; $C_{\Delta g, \delta N}$ is the $(1 \times q)$ - cross-covariance matrix between $\delta\Delta g$ and δN ; $C_{\delta N, \delta N}$ is the $(1 \times q)$ - auto-covariance matrix of δN ; C_{nn} is the $(q \times q)$ - covariance matrix of the measurements noise \mathbf{n} ; α is the Tikhonov regularization parameter (Neyman, 1979; Moritz, 1980; Marchenko and Tartachynska, 2003).

Having the values (1) at some set of scattered points and the above covariance matrixes, the residual gravity anomalies $\delta\Delta g$ and the residual geoid heights δN can be estimated straightforward at chosen grid points by the regularization method. After solving this basic problem the predicted gravity anomalies Δg and geoid undulations N can be restored at the same grid by means of the EGM96 gravity field model

$$\Delta g = \Delta g_{EGM96} + \delta\Delta g, \quad (4)$$

$$N = N_{\text{EGM96}} + \delta N. \quad (5)$$

For further use of the relationships (2), (3) the following problems have to be solved:

1. The construction of the analytical covariance function $K(P,Q)$ of the anomalous potential T .
2. The choice of a suitable method for the computation of the regularization parameter α .
3. Preprocessing or prediction of 19959 regular distributed SSH values by the collocation method at 3'x3' grid points, because of a large total number (=557954) of observations.

The analytical covariance function or reproducing kernel $K(P,Q)$, described only by singular point harmonic functions (Marchenko and Lelgemann, 1998; Marchenko, 1998), is chosen in the following way

$$K_n(P,Q) = \left[\frac{GM}{R} \right]^2 \beta_n \sigma^{n+1} v_n, \quad \sigma = \frac{R_B^2}{r_P r_Q}, \quad (6)$$

where R is the Earth's mean radius; R_B is the Bjerhammar's sphere radius; r_P and r_Q are the geocentric distances to the external points P and Q ; GM is the product of the gravitational constant G and the planet's mass M ; v_n is the dimensionless potential of eccentric radial multipole of the degree n ; β_n represents some dimensionless coefficient. Expressions for the analytical auto-covariance function of geoid heights and cross-covariance function between gravity anomalies and geoid undulations (based on the covariance propagation) can be found in (Marchenko, 1998).

Note now that the traditional determination of the regularization parameter α in (2) or (3) according to (Tikhonov and Arsenin, 1974; Neyman, 1979) requires in the frame of a special iterative process the inversion of matrixes with a dimension equal to the number q of observations. So, when a number of observations are large we come to a time consuming procedure. As before (Marchenko, and Tartachynska, 2003) to avoid this difficulty another possible value of α is used

$$\alpha = 1 + \sqrt{1 + \text{Trace}(\mathbf{C}\mathbf{C}_{nn}) / \text{Trace}(\mathbf{C}\mathbf{C}_{nn})}, \quad (7)$$

leading to the estimation of α prior to the matrix inversion in (2) and (3).

Simplest illustration of possible values of the regularization parameter given by (7) can be made under several assumptions. First one, geodetic measurements of one kind only are considered. Second one, the matrix \mathbf{C}_{nn} can be represented as $\mathbf{C}_{nn} = d\mathbf{I}$ where d is the variance of a noise and \mathbf{I} is the unite matrix. Third one, the matrix \mathbf{C} can be described by the Dirac delta function and can be written as $\mathbf{C} = C_0\mathbf{I}$, where C_0 is the variance of a studying field. With these assumptions the expressions for the regularization parameter corresponded to (7) are found as

$$\alpha = 1, \quad (8)$$

$$\alpha = 1 + \sqrt{1 + \frac{C_0}{d}}. \quad (9)$$

In fact, the first root (8) corresponds in (2) and (3) to the least-squares collocation solution. The second root (9) corresponds to the relationship (7) under the adopted assumptions and can serve for the illustration of a possible dependence of α on the given C_0 and d . Note again that the formulae (7) and (9) represent only possible upper limit of α (Marchenko, and Tartachynska, 2003), which requires a further improvement of the considered estimation of α .

4. Results and conclusions

Removing the contribution of the geopotential model EGM96 (360,360) from altimetry data (SSH) the residual geoid heights δN were adopted as initial information. Then the empirical covariance function (ECF) of the residual geoid heights $\delta N = \delta \text{SSH}$ was constructed and approximated by the analytical covariance function (ACF) based on the radial multipoles potentials or ACF of the so-called point singularities (Marchenko and Lelgemann, 1998). As a result, the optimal degree $n = 1$ in the formula (6) was chosen from ECF approximation that corresponds to the dipole kernel function (Poisson kernel without zero degree harmonics). The optimal ACF has the following essential parameters: (a) the variance of the field $\text{var}(\delta N) = 0.1214 \text{ m}^2$; (b) the correlation length $\xi = 0.384$; (c) the curvature parameter $\chi = 4.074$.

Then to avoid a large total number of observations (=557954) the computation of the regular distributed SSH values at 19959 (3'x3') grid points by the collocation method was made before the application of the relationships (2) and (3), using the nearest scattered SSH values around every grid point within the radius search = 5' (mean value of applied SSH for the prediction is equal 47) and Gaussian covariance function on this step. Fig. 1 illustrates such regular SSH data distribution at 3x3 grid points where predicted SSH values are known. In the following this regular (3'x3') grid was adopted as initial information for the recovery of the gravity anomalies and geoid heights by the Tikhonov regularization method to obtain the solution 2x4E1E2TP at 27342 (2'x4') grid points and the solution 3x3E1E2TP at 2'x4'356 (3'x3') grid points filled all studying area.

According to the expressions (2), (3) and (7), the prediction of the residual gravity anomalies $\delta \Delta g$ and the residual geoid heights δN was done by the regularization method at the adopted grids points with the resolution (2'x4') and (3'x3'), completely filled all marine part of the studying area. Note that the regularization parameter consists the value $\alpha \approx 3.55$ computed according to (7). Statistics of the estimated δN and $\delta \Delta g$ and their accuracy are shown in Table 1.

Accuracy distributions are shown in Fig. 2 and Fig. 3. Fig. 4 and Fig. 5 illustrate the gravity anomalies and geoid heights computed by the regularization method and based on the adopted 19959 (3'x3') grid values SSH, obtained preliminary from ERS-1, ERS-2, and TOPEX/POSEIDON altimetry (see, Fig. 1).

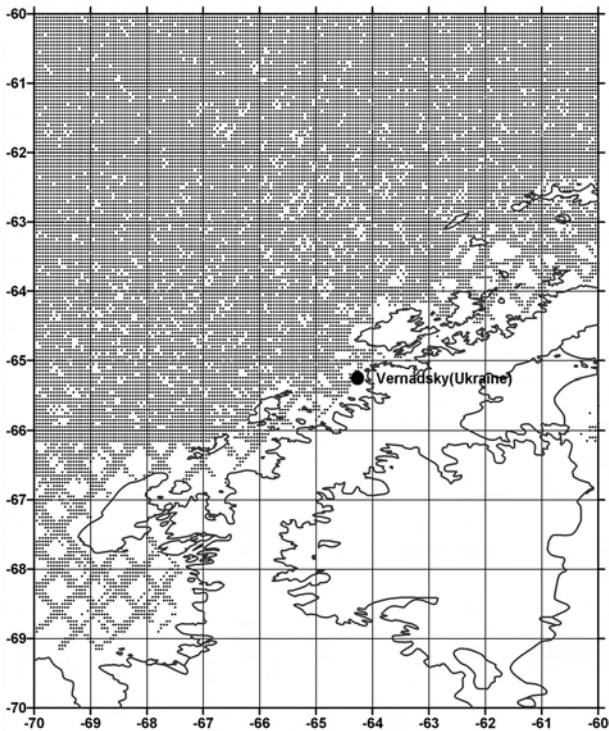


Fig.1. Distribution of the predicted at 19959 points SSH values of the (3'x3') regular grid

taticistics	δN , m, (3'x3') grid	$\delta\Delta g$, mGal, (2'x4') grid
finimum	-2.81	-90.48
faximum	0.30	44.22
fmean	-1.13	-15.81
tandard deviation	0.38	14.39

Table 1. Statistics of the predicted residual geoid heights δN and gravity anomalies $\delta\Delta g$ at (2'x4') and (3'x3') grid

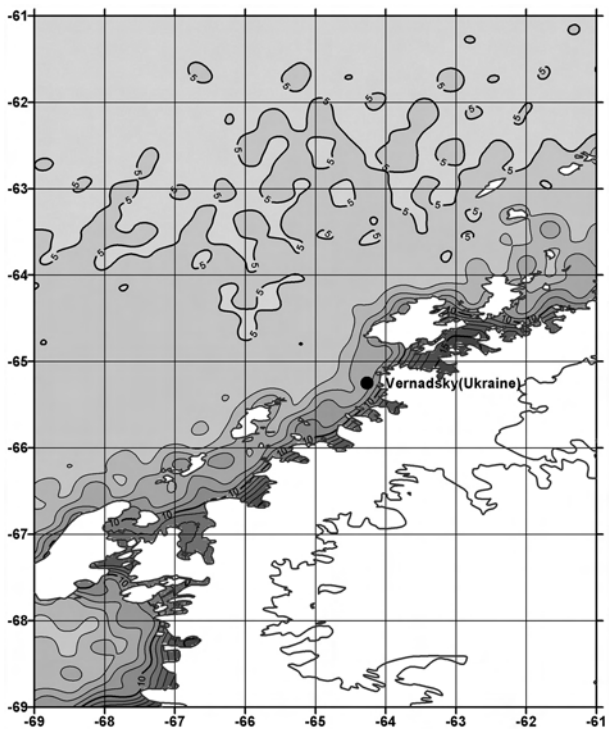


Fig. 2. Accuracy of the geoid prediction from ERS-1, ERS-2, and Topex/Poseidon altimetry. Contour interval: 0.01 m

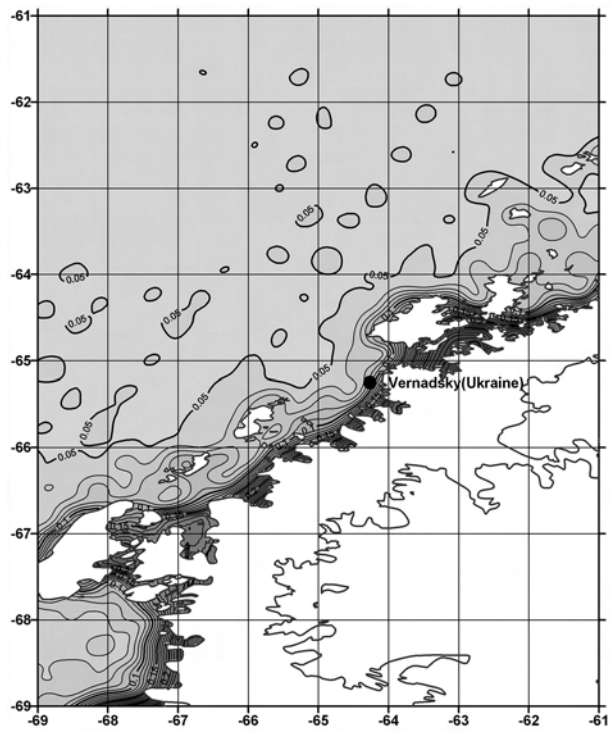


Fig.3. Accuracy of the gravity anomalies inversion from ERS-1, ERS-2, and Topex/Poseidon altimetry. Contour interval: 1 mGal

taticistics	3x3E1E2TP solution		2x4E1E2TP solution	
	N, m	σN , m	Δg , mGal	$\sigma \Delta g$, mGal
finimum	3.22	0.04	-112.06	3.91
faximum	20.39	0.34	100.64	16.44
fmean	12.45	0.05	5.18	4.63

Table 2. Statistics of the 2x4E1E2TP gravity anomalies and 3x3E1E2TP geoid heights restored at (2'x4') and (3'x3') grids, respectively, and their accuracy estimations

Table 3 illustrates the comparison of the constructed above 3x3E1E2TP geoid solution and 2x4E1E2TP gravity anomalies, obtained from ERS-1, ERS-2, and TOPEX/POSEIDON altimetry, with the (3) KMS2001 SSH and (2'x4') KMS1999 gravity anomalies derived also from multimission satellite altimetry data. Note here a good accordance of the 3x3E1E2TP and KMS2001 solutions in terms of the mean and standard deviations of the predicted geoid heights. Nevertheless, we get large differences between 2x4E1E2TP and KMS1999 gravity anomalies demonstrated by the Table 3 and Fig. 6. These discrepancies have rather a systematic character, which possibly connects with the initial data distribution (see Fig. 1). On the one hand, larger differences have located typically around islands and near the seashore where initial data may be absent and inverted gravity anomalies reflect mostly the results of the extrapolation. This conclusion has confirmed by the accuracy distribution of the geoid heights and gravity anomalies shown in the Fig. 2 and Fig. 3, respectively. On the other hand, such deviations may be caused by difference in the adopted methods of data processing. The Tikhonov regularization method was applied in this paper for the whole studying

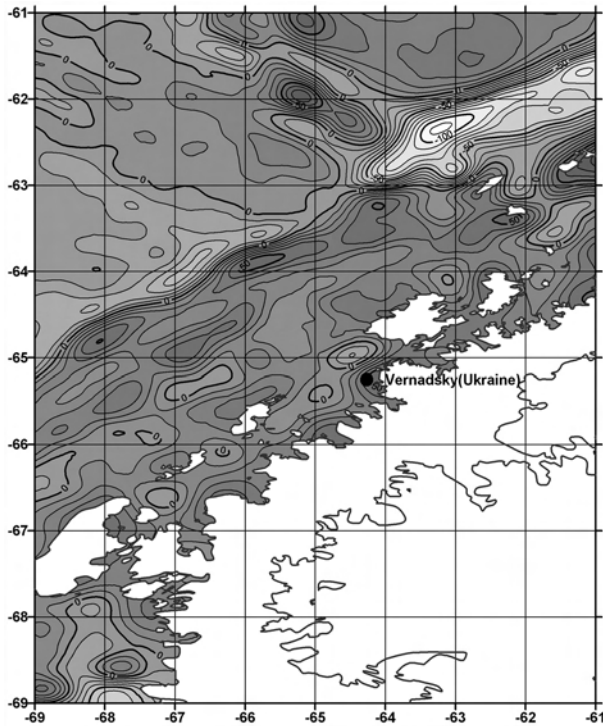


Fig. 4. Gravity anomalies inverted from ERS-1, ERS-2, and Topex/Poseidon altimetry. Contour interval: 10 mGal

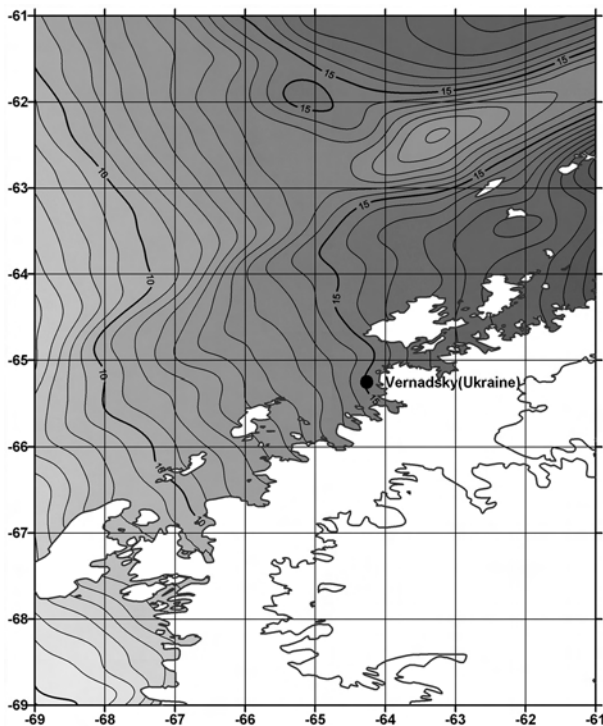


Fig. 5. Geoid heights from ERS-1, ERS-2, and Topex/Poseidon altimetry. Contour interval: 0.5 m.

geographical region without any separation to cells and based on the ERS-1, ERS-2, and Topex/Poseidon data. In the case of (2'x4') KMS1999 solution the inversion of gravity anomalies was done by "piecewise processing" of multimission satellite altimetry within every (1° x 5°) chosen rectangular cell using FFT method (Andersen and

Statistic	$N - N_{KMS2001}, m$	$\Delta g - \Delta g_{KMS1999}, mGal$
Minimum	-0.98	-89.46
Maximum	1.26	40.77
Mean	0.03	-14.95
Standard deviation	0.16	8.72

Table 3. Comparison of the predicted (3) geoid heights and (2'x4') gravity anomalies with the KMS2001 and KMS1999 solutions, respectively

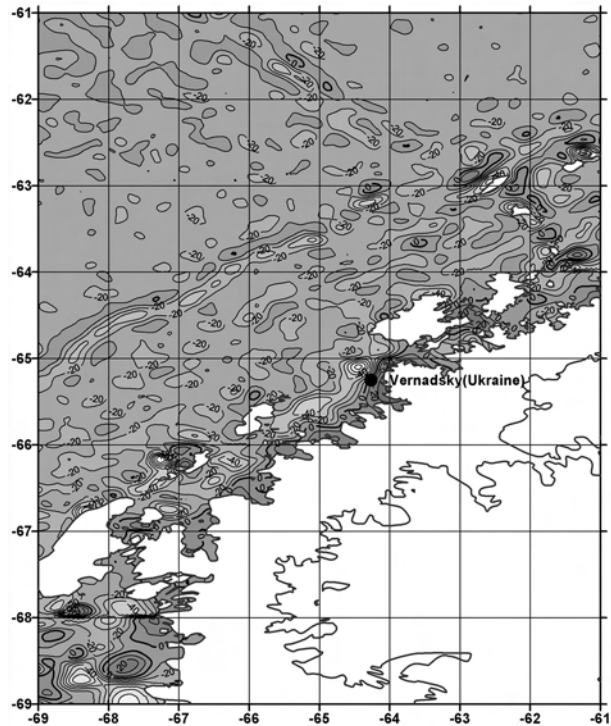


Fig. 6. Differences between (2'x4') inverted gravity anomalies and KMS2001 solution. Contour interval: 10 mGal

Knudsen 1998; Knudsen and Andersen, 1998). As a result, further improvement of the considered above solutions in the frame of the regularization method is expected after including gravimetry, GEOSAT altimetry, etc.. data.

Acknowledgments.

We are very much indebted to AVISO for their support in receiving the corrected SSH of ERS-1, ERS-2, and Topex/Poseidon altimetry used in this paper.

References

Andersen O.B. and P. Knudsen (1998) Global marine gravity field from the ERS-1 and GEOSAT geodetic mission altimetry. *Journal of Geophysical Research*, Vol. 103, No C4, pp. 8129-8137.

Knudsen, P., and O. B. Andersen (1998) Global marine gravity and mean sea surface from multimission satellite altimetry, in "Geodesy on the Move, Gravity, geoid, geodynamics and Antarctica", IAG scientific assembly, Rio de Janeiro, Brazil, Sept. 3-9 1997, Eds, Forsberg, Feissel and Dietrich., IAG symposia, 119, 132-138, Springer verlag, Berlin.

- Marchenko A.N. (1998) Parameterization of the Earth's Gravity Field. Astronomical and Geodetic Society, Lviv, Ukraine.
- Marchenko A.N. and Lelgemann D. (1998) A classification of reproducing kernels according to their functional and physical significance. *IGeS Bulletin*, No 8, Milan, pp. 49-52
- Marchenko A.N. and Tartachynska Z.R. (2003) Gravity anomalies in the Black sea area derived from the inversion of GEOSAT, TOPEX/POSEIDON and ERS-2 altimetry. *Bolletino di Geodesia e Scienze Affini*, ANNO LXII, n.1, pp. 50-62
- Moritz H. (1980) Advanced Physical Geodesy. Wichmann, Karlsruhe
- Neyman Yu. M. (1979) Variational method of Physical Geodesy. Nedra, Moscow, (in Russian)
- Tikhonov A.N. and V.Y. Arsenin (1974) Methods of solution of ill-posed problem. Nauka, Moscow, (in Russian)

Tidal Observations at Faraday/Vernadsky Antarctic Station

Gennadi Milinevsky(1, 2)

(1) Ukrainian Antarctic Centre, 16, Tarasa Shevchenka blvd, 01601, Kyiv, Ukraine; (2)

Kyiv National Shevchenka University, 6, Glushkova av, 04022, Kyiv, Ukraine E-mail: antar@carrier.kiev.ua

Abstract

The history and ongoing information on tide measurements at the Base F/Faraday/ Vernadsky Station, and future development of tide gauge are discussed. Faraday/ Vernadsky station has the longest time series of sea level changes in Antarctica. The British Antarctic Survey occupied a research station in the Argentine Islands from 1947 to 1996. The original hut was replaced in 1954 by a purpose - built geophysical observatory. The ownership of the Faraday Station was transferred to Ukraine in 6 February 1996, and renamed as "Akademik Vernadsky". Sea level observation is ongoing by the Ukrainian Antarctic Center. The station is equipped with an old float gauge and a more recent but simple technology pressure gauge provided by Proudman Oceanographic

Laboratory (POL, UK). Since 2000, ongoing hydrological measurements were started at the Vernadsky (profiles of sea temperature, salinity and oxygen). The tide measurements development lays in provision of an ongoing tide gauge data program at Vernadsky including maintenance of the POL equipment. Aid in the upgrade of tide gauge equipment and data communication mechanisms. Tide gauge at Galindez Island (65° 15' S, 64° 16' W) included in Global Sea Level Observing System Development in the Atlantic and Indian Oceans to monitor long-term sea level variations due to climate change. The Proudman Oceanographic Laboratory is currently collecting the Faraday/ Vernadsky tide gauge records.

Current Results on the Investigation of GPS Positioning Accuracy and Consistency

J. Krynski, Y.M. Zanimonskiy

Institute of Geodesy and Cartography, Modzelewskiego 27, PL 02-679 Warsaw, Poland;
e-mail: krynski@igik.edu.pl, yzan@poczta.onet.pl; Fax: +48 22 3291950, Tel.: +48 22 3291904

Abstract

Considerable progress observed in geodynamics research is mainly the result of development of measuring techniques. The qualitative results on crustal movements presented in some publications seem, however, to be at the level of their accuracy determination. A realistic estimation of the potential of the experiment is necessary to avoid false conclusions that may describe the non-existent occurrences (artefacts), especially when experiment is difficult or very expensive. Uncertainty of vector components estimation, obtained from processing GPS data using either commercial or scientific software, represents rather an internal consistency than the accuracy of positioning. The problem of reliable accuracy estimation of GPS positioning concerns all fields of surveying practice including GPS positioning for geodynamics.

The strategy of GPS solutions quality analysis based on the concept of overlapped sessions with optimum length and temporal resolution is presented. The strategy was verified with use of data from the Antarctic and European permanent GPS stations processed with both Bernese and Pinnacle software packages. Numerical examples are given.

Keywords: Global Positioning System (GPS) – Positioning accuracy – Statistical analysis

Introduction

It is well known that the solutions for vector components or coordinates obtained from processing precise GPS data from different observing sessions vary usually much

stronger than their precision estimate indicates. Standard deviations of GPS solutions provided by processing software reflect the internal consistency of data processed and the internal precision. In general they do not, however, indicate the actual accuracy of GPS positioning in the real scale (e.g. Dubbini *et al.*, 2003).

An extensive research is conducted to improve the precision of GPS solutions by using better models for GPS observations, and to improve the precision estimate (e.g. Teunissen, 2002). One approach is to study the variations of GPS solutions using data from permanent GPS stations. Time series of GPS solutions are particularly suitable for such investigations (Krynski and Zanimonskiy, 2002). The tools of statistical analysis and spectral analysis are useful to separate factors causing variations in GPS solutions and to estimate their magnitudes.

Time series of GPS solutions do not exactly represent a random process. The variations in GPS solutions have a complex structure. Besides a random part that is mainly due to observation noise they contain also components of a chaotic character as well as biases (Krynski *et al.*, 2002a). Model errors, non-modelled effects and varying satellite configuration, including multipath cause systematic variations in GPS solutions. In addition, due to non-linearity of the system, data noise generates biases in computed results. Missed cycles in integer ambiguity resolution and sudden changes in satellite configuration due to a rise of a new satellite or satellite's repair are the main sources of chaotic errors.

The choice of the method used to suppress disturbances in time series corresponds to their character, i.e. random or chaotic. Noise, external with respect to measuring system, is simply filtered out using the smoothing procedure that employs a rectangular window. The size of the window becomes a parameter to be determined. According to the classical procedure of time series processing, the optimum size of the window can be estimated at each filtering stage. The analysis of such time series indicates the existence of a number of periodic components and trends that are not modelled in data processing stage (Bruyninx, 2001; Poutanen *et al.*, 2001; Krynski *et al.*, 2002). Major part of the power spectrum of the variations is concentrated in diurnal and larger periods. In particular, periodic variations with dominating 12h and 24h periods (Krynski *et al.*, 2000) are distinguished. Few hours' long periods in the spectrum are most probably the artefacts (King *et al.*, 2002) caused by the effects that are dominated by random noise processes due to non-linearity of the system (Krynski and Zanimonskiy, 2002).

GPS solutions based on processing of as long as 24h sessions, that are common for establishing and maintaining geodetic reference frame and for geodynamic applications, are considered as ones smoothed off for daily and sub-daily periodic biases. The use of shorter observing sessions with preserving high quality of GPS positioning as well as the improvement of real-time GPS positioning performance requires the investigation of periodic biases,

their detection, their source specification and an attempt towards their modelling.

Due to a large amount of information contained in time series of GPS solutions based on overlapped sessions it becomes possible to apply statistical tests to detect outliers. Numerous sudden changes (jerks) in satellite configuration occur with a period of one sidereal day. They cause specific variations in time series of the components of computed vectors from GPS data with periods significantly smaller than one sidereal day, i.e. even of the order of 1h. Variations in such a time series correspond rather to a chaotic process than a random one. Jerks can be suppressed by optimising the length of overlapping sessions and eliminating the disturbing results (Krynski and Zanimonskiy, 2002; Cisak *et al.*, 2002).

In spite of jerks in GPS solutions the continuous change of satellite constellation causes smooth changes of parameters of measuring process, i.e. signal to noise ratio, atmospheric delays, multipath, orbit corrections, etc. High regularity of changes in satellite constellation makes all those variations periodic with a half of sidereal day period. Spectral and correlation analysis of time series of GPS solutions shows the existence of such period (Krynski *et al.*, 2002). Periodic terms with periods of half of sidereal day and one sidereal day occur in informative parameters such as vector components as well as in non-informative parameters, like standard deviations of GPS solutions provided by processing software, cross-correlation coefficients of vector components, number of single measurements taken to the solution, etc.

A careful estimation of an optimum length of a session used to calculate positions from GPS data is needed due to jerk type variations in GPS solutions corresponding to a satellite rising or even more distinguishably to its descending as well as to ionospheric storms. The optimum length of a session does not necessarily correspond to longer ones. With the increase of the session length an internal accuracy of the output data increases but at the same time the increase of spectral leakage is observed. Thus the extension of a session length used for computing GPS data reduces the estimated uncertainty of the solution but it simultaneously decreases Nyquist frequency. The sum of those two counteracting effects depends also on spectrum of noise and the signal itself. The increase of Nyquist frequency can be accomplished by using overlapping sessions. Correlation accompanying time series of solutions obtained from overlapping GPS sessions is significantly smaller than the one in the classical time of a random process. For example, the correlation coefficient in time series based on solutions from the sessions with 87% overlap is at the level of 0.5 (Krynski *et al.*, 2002) while such a coefficient for a wideband random process reaches 0.5 in case of 50% overlap (Harris, 1978).

Predictability of the reaction of the GPS measuring system (both receiver and processing software) on disturbances and inadequacy of models used is difficult due to user's limited access to the algorithms applied to data processing.

That reaction could, however, be viewed experimentally by statistical and correlation analysis of time series of GPS solutions.

Numerical experiments

The problem of reliable accuracy estimation of GPS positioning can be investigated using time series of GPS solutions obtained from sessions of different lengths for vectors of different length, located in different geographic regions. Practical needs, potentiality of accessible data processing infrastructure, and the experience gained in GPS research contributed towards making the choice of GPS data for processing and determining its strategy for numerical experiments.

As an example, GPS data provided by two EUREF Permanent Network Stations BOGO and JOZE from 2001 was used to generate time series of BOGO-JOZE vector (42 km length) components with the Bernese v.4.2 and Pinnacle software. With the Bernese software the GPS solutions were obtained from processing 1h, 2h, 3h, 4h, and 6h sessions over 19 days in August, with overlap (1h shift), 3h sessions with 2.5h overlap (30m shift), and 24h sessions with 23h overlap over 4 months (February-May). GPS solutions were obtained with Pinnacle from processing 2h - 28h sessions with 1h time resolution (1h shift), over 15 days in August. Chosen data represent two different periods of seasonal atmospheric dynamics in Europe, i.e. winter-spring corresponds to quiet atmosphere while summer to a disturbed one. Data set from the Antarctic stations used covered the period of extremely active ionosphere (October and November 2001) as well as the period of quiet ionosphere in July 2001. Time series of GPS solutions generated were then the subjects of statistical analysis. The dispersion of GPS solutions as well as their averaged combinations together with their precision estimates was analysed. The conceptual scheme of forming groups of GPS solutions for further statistical analysis is shown in Fig. 1.

Dispersion of GPS solutions grows with the size of sample, i.e. with a number of solutions that form the group investigated; that also corresponds to the length of data window used. On the other hand the dispersion of the average solution from the group of sessions decreases with growing number of sessions in the group investigated. The plots illustrating those dispersions for vertical component of the vector calculated with the Bernese software using 3h sessions with 0.5h shift over 3 months are given in Fig. 2a and Fig. 2b, respectively.

In both cases shown in Fig. 2, the change of the variation rate of dispersion is observed around data window of 12h. For longer windows the change of the variation rate of dispersion becomes substantially less significant. The mechanisms that affect GPS solutions obtained from sessions shorter than 12h differ from those observed in the solutions from longer sessions. Solutions from sessions shorter than 12h are mainly affected with noise and periodic biases due to varying GPS satellite constellation.

Fig. 2b also shows that vertical component of 42 km vector can be determined from 12h GPS data with accuracy of 6-7 mm at one sigma level.

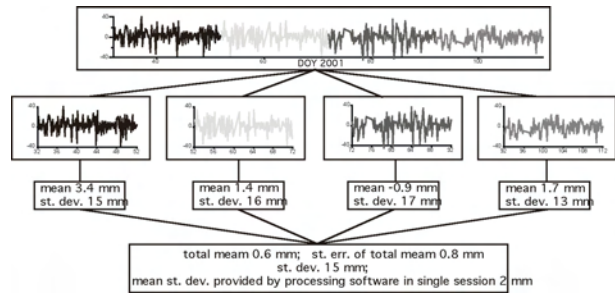


Fig. 1. The scheme of forming groups of GPS solutions and estimating their statistics

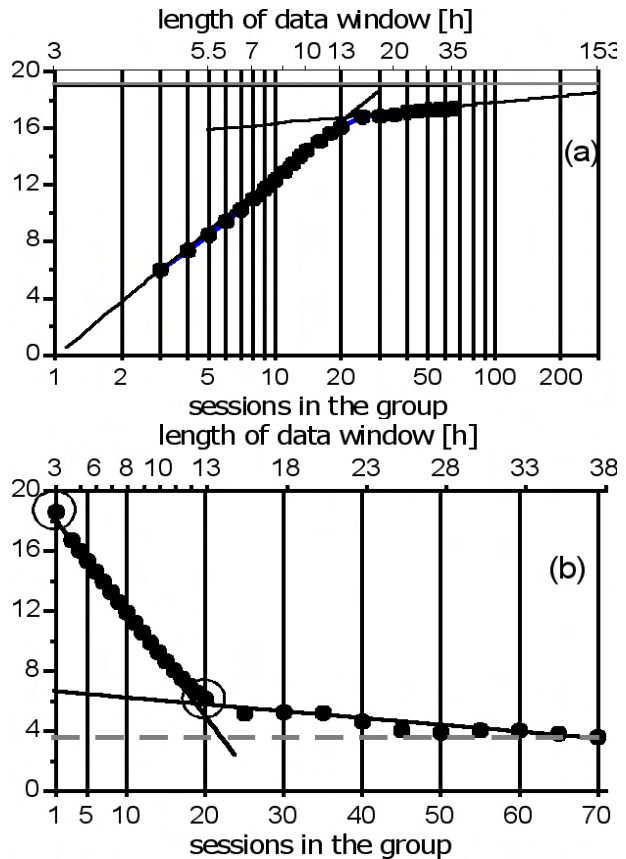


Fig. 2. The rms of vertical component from single sessions in the group of n sessions (a) and rms of average solutions in the groups of n sessions (b) versus the length of data window. Grey line at (a) corresponds to the rms in 3 months long group of sessions. Dashed line at (b) corresponds to the accuracy (3_level) of average solution from 3 months data

The increase of the length of session (data window) used to generate GPS solutions, results in reduction of dispersion of those solutions, mainly due to averaging noise and periodic biases. Time series of GPS solutions based on longer sessions is much smoother as compared with the one derived from short sessions. The effect of such a smoothing procedure could be simulated by combining and averaging GPS solutions obtained using short data window. The effect of smoothing GPS-derived vertical

component of the vector obtained from 3h data window, by applying running average with 12,5h window may be seen by comparison of Fig. 3a and Fig. 3b, respectively.

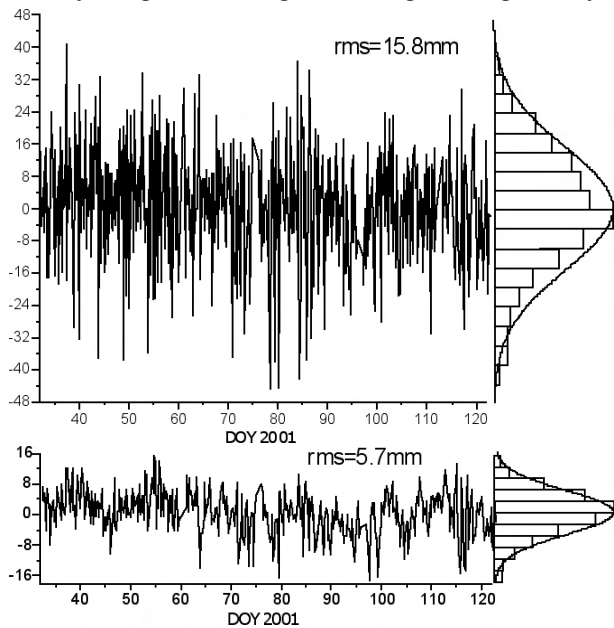


Fig. 3. Time series of vertical component of the vector obtained from processing 3h sessions with 30m shift (a), and running average of vertical component of the vector obtained from processing 3h sessions with 30m shift with a window of 12.5h (averaging current groups of 20 solutions from single sessions) (b)

The results shown so far indicate the external accuracy estimate of GPS solutions that is based on analysis of repeatability with use of regular time series of high temporal resolution. Such an accuracy estimate does not coincide with standard deviations provided by GPS processing software that reflect an internal accuracy of the system. Short period biases, including non-modelled effects, some with unstable amplitudes, that affect GPS solutions are as systematic-type terms not reflected in uncertainty estimation. Therefore, calculated uncertainty is usually much too optimistic as the accuracy estimate. Comparison of external with internal accuracy of determination of the length and vertical component of the vector obtained using the Bernese and Pinnacle software from sessions of different length with 1h shift, are given in Fig. 4 and Fig. 5, respectively.

The dispersion of GPS solutions obtained using the Bernese software is larger than that from the Pinnacle software, when short sessions were processed. That phenomenon is more distinct in case of vector length than of the vertical component. In spite of large dispersion of GPS solutions that might be explained by the use of QIF strategy for processing data for 42 km vector with the Bernese software, the software-provided standard deviations of the solutions obtained are at the very low level. That discrepancy is particularly distinguished for solutions based on short sessions. Both height difference and the length of a vector examined was determined with the accuracy of about 5 cm (one sigma level) from 2h

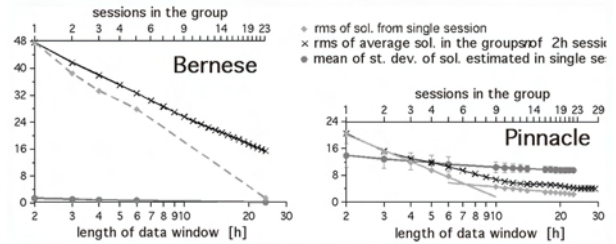


Fig. 4. Standard deviations of the GPS-derived vector lengths provided by processing software and estimated by statistical analysis of time series of GPS solutions.

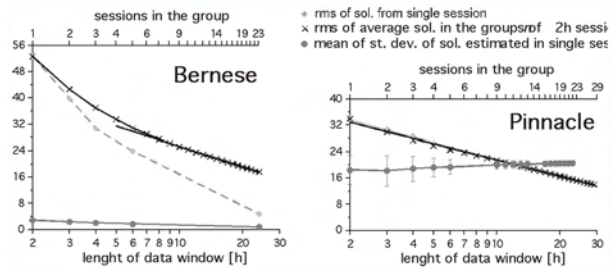


Fig. 5. Standard deviations of the GPS-derived vertical component provided by processing software and estimated by statistical analysis of time series of GPS solution

sessions while precision of the solution provided by the Bernese software was at the level of single millimetres. The discrepancy between the external and internal estimate of accuracy of GPS solutions decreases with increase of session length while their ratio remains the same. In case of solutions based on 24h sessions it drops down to the level of a few millimetres although their internal accuracy estimated remain a few times better than the external accuracy.

The effect of noise and periodic biases on GPS solutions can also be reduced by averaging the solutions over the groups of sessions, e.g. the mean of n, e.g. 2h sessions, that form the group. Such simple averaging does not remove all effects that are eliminated when processing with the Bernese software one session of length corresponding to the length of the respective group of short sessions. The external accuracy based on analysis of groups of sessions is thus overestimated although its trend remains similar to the one related to single sessions.

For GPS solutions obtained using the Pinnacle software that is less sophisticated in terms of GPS observations modelling then the Bernese one, the main trends for the external accuracy getting improved with growing session length are preserved. Different image has, however, the mutual relationship of the external and internal accuracy. The internal accuracy estimate given by Pinnacle is more realistic then in case of the Bernese software. A vertical component of a vector examined was determined with the accuracy of about 3.5 cm (one sigma level) from 2h sessions while precision of the solution provided by the Pinnacle software was about 2 cm. For the vector length the external and internal accuracy was 2 cm and 1.5 cm, respectively. Moreover, for a certain length of session, internal accuracy coincides with the external one. With further growing session length the internal

accuracy of the solutions becomes overestimated. Such a singularity corresponds to 12h and 4h sessions in case of vertical component and vector length determination, respectively.

GPS solutions obtained using the Pinnacle software, averaged over the groups of sessions, practically coincide with the ones corresponding to respective single sessions. It particularly concerns vertical component.

The discrepancy between the external accuracy and internal consistency of GPS solutions obtained using the Bernese software was investigated for numerous vectors of European Permanent Network of length from a few tens to a few hundred kilometres and for some vectors of length up to a few thousand kilometres in Antarctic (Cisak et al., 2003a, 2003b). 3h and 24h GPS sessions covering 4 months of 2001 were processed. The correlation between two accuracy estimates, the external and the internal one is given in Fig. 7. Internal accuracy differs from the external one by a scale factor of about 7 and 10 for a vertical component and vector length, respectively.

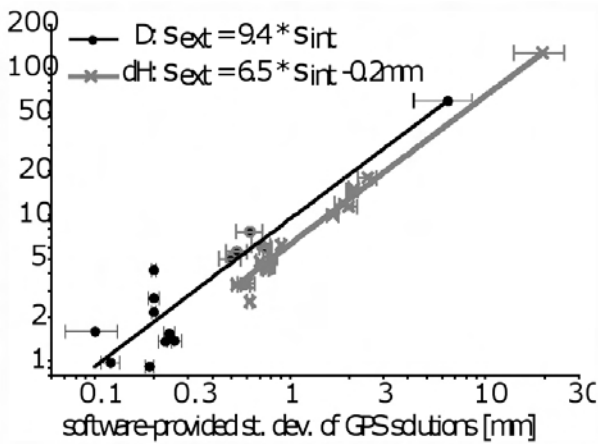


Fig. 6 Correlation between the external accuracy and the internal accuracy of GPS solution provided by the Bernese software

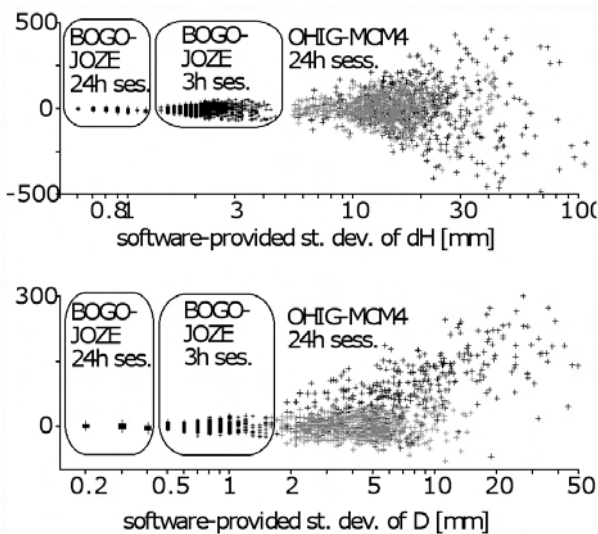


Fig.7 Deviations from average values of vectors components vs. internal accuracy of GPS solution

The observed simple functional relationship between the external and internal estimate of accuracy was fulfilled for the vectors of different length (from a few tens to a few thousand of kilometres) from different geographical regions (mid- and high latitudes).

Analysis in detail of the relations of the external and internal estimate of accuracy of GPS solutions is not satisfactorily effective due to the poor discretisation of the software-provided standard deviation that are usually expressed by numbers consisting of one or two digits. Large random errors of GPS solutions present in cases of short observation sessions processed, long vectors calculated, poor satellites configuration visible or ionospheric storms occurred, make the discretisation effect negligible.

The OHIG-MCM4 vector as a long one (3.9 thousand kilometres) and as located at high latitudes (Antarctic) is a good example of coincidence of a number of sources of random errors. Similar effects are observed in the solutions for BOGO-JOZE vector (42 km) based on 3 h sessions. Deviations from the mean for vectors components versus internal accuracy of GPS solutions provided by the Bernese software are shown in Fig. 7.

The larger software-provided standard deviation of GPS solutions the larger is the dispersion of the vector components estimated. GPS solutions for a long vector length may be separated onto two subsets (grey and black marks in Fig. 7). One of them evidently contains a bias. It is possible to separate subsets heuristically by means of analysis of the results in the stacked time domain. Dispersion of vertical component and vector length as well as software-provided standard deviation of the estimated length of the vector versus time of day corresponding to the beginning of 24h session are shown in Fig. 8.

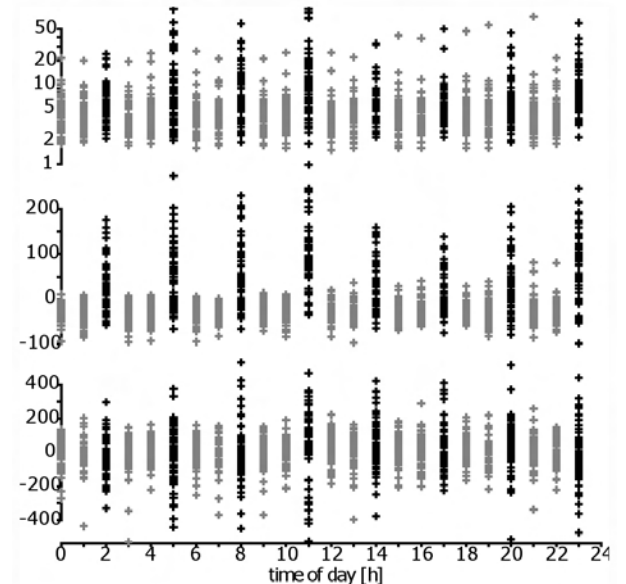


Fig. 8 Dispersion of vertical component and vector length as well as software-provided standard deviation of the estimated length of the vector versus time of day corresponding to the beginning of 24h session (OHIG-MCM4 vector)

The results in Fig. 8 show the non-uniformly weighted data (e.g. due to the choice of reference satellite) in diurnal sessions. A third part of GPS solutions obtained for OHIG-MCM4 vector components (black marks in Fig. 7 and Fig. 8) are non-acceptable due to biases in vector length estimated. Uniform weighting in processing GPS observations from 24h sessions could substantially reduce or even eliminate from GPS solutions the influence of changes of satellites configuration of diurnal and half-diurnal periods.

Significant differences in systematic and random errors in vector length, in the numbers of observations and ambiguities resolved, as well as in random errors in vertical component between two subsets examined are observed (Fig. 9). Bias in the vector components and their uncertainty estimated using GPS data from one subset exceeds maximum dispersion obtained. It results in discrepancy of constant sign between the corresponding parameters determined from two data sets considered. The reasons and mechanisms of generation of asymmetry in distribution of results require further investigation. Such differences may occur due to the errors generated in the process of ambiguity resolution. Those errors can be amplified by poor configuration of visible satellites. The “configurationally induced” problem of ambiguity resolution is in particular frequently faced when processing GPS data from the stations in high latitudes, in particular in

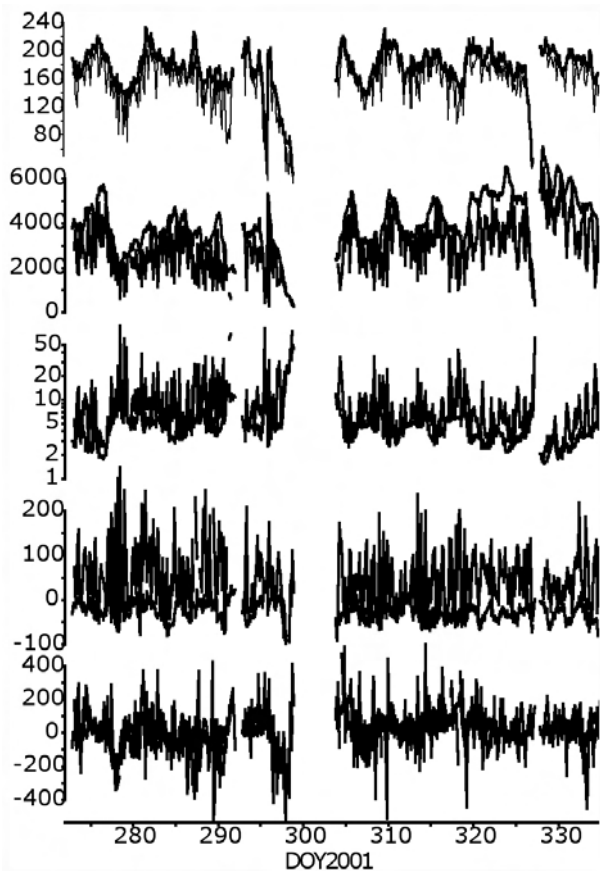


Fig. 9 Time series for OHIG-MCM4 vector vertical component, its length, number of single differences used and number of ambiguities resolved

Antarctic. Therefore, polar regions are considered suitable test areas for advanced analysis of GPS positioning.

Similar, “ionosphericly induced” problem of ambiguity resolution was already reported (Cisak *et al.*, 2003a; 2003b). The problems addressed above can also affect GPS positioning at mid-latitude permanent GPS stations, but their effect is smaller and its separation becomes more difficult. Mutual analysis of time series of both fix and float GPS solutions is a powerful tool for studying such problems, using for example a wide range of data provided by EPN stations.

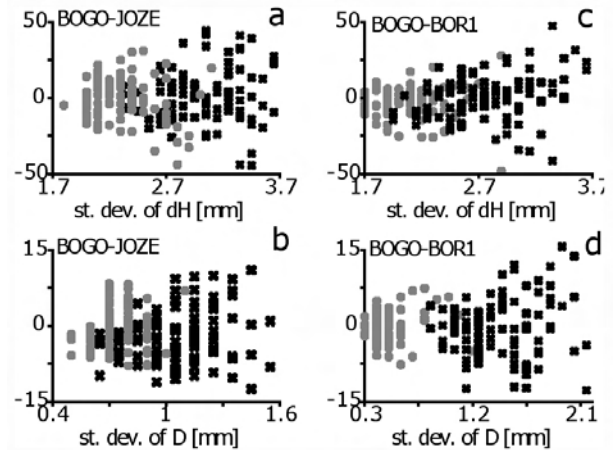


Fig. 10. Dispersion of lengths and vertical components of the vectors vs. internal accuracy of GPS solutions (fix - grey marks, and float - black marks)

Dispersion of the lengths and vertical components of BOGO-JOZE and BOGO-BOR1 vectors versus internal accuracy of GPS solutions (fix - grey marks, and float - black marks) are shown in Fig. 10. No essential difference in solutions and their error estimates for vectors of 42 and 250 km length is observed. On the other hand no significant biases were detected and the larger standard deviations estimated the larger are random errors.

Strategy of GPS solution quality analysis

The strategy developed for detecting and modelling biases in time series of GPS solutions is given in Fig. 11.

Temporal resolution of a series of GPS output solutions is determined by a sampling rate that corresponds to the length of session when data is processed in consecutive blocks. The longer the processed GPS sessions the smoother become solutions and consequently time series obtained. Smoothing obviously reduces random effects but also some periodic biases. Solutions based on shorter sessions are thus affected by larger biases than those based on longer ones. To study biases in GPS solutions the examination of time series with sufficient temporal resolution is required. Thus time series of GPS solutions obtained from short sessions is preferable despite of increased noise level with shortening the length of session processed. Shortening the sessions is, however, limited by the length of the vector determined. Therefore, in order to increase temporal resolution of time series the overlapped sessions need to be processed. Overlapping the sessions

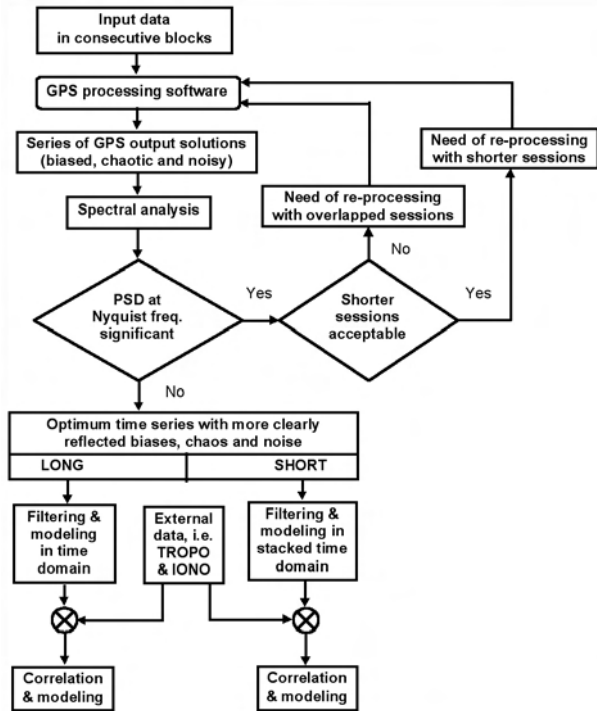


Fig. 11 Flowchart of the strategy of GPS solutions quality analysis

causes an increase of correlation between consecutive GPS solutions that has to be carefully considered when estimating statistical parameters of such time series. It allows, however, efficiently detect and separate chaotic effects from biases. Power spectrum density at Nyquist frequency can be used as an indicator of need of a further increase of temporal resolution of a series by processing either shortened sessions or more overlapped sessions. Time series, optimal with respect to the structure of investigated biases, consist of GPS solutions obtained from optimum session length and optimum sampling time. Such series reflect very clearly periodic biases as well as chaotic terms. Therefore they are suitable to detect and estimate periodic biases. Similar strategy with four hours window stepped by 30 minutes, followed by a running average procedure, was used for investigation of the vertical shift caused by Earth tides (Neumeyer *et al.*, 2002).

Long time series can be directly processed for filtering noise and modelling periodic biases. In case of short time series stacked solutions need to be calculated over e.g. one-day period and then filtered and processed to model biases. Finally the models could be correlated with the external data, e.g. troposphere or ionosphere parameters in order to separate biases and find their sources.

Conclusions

A dispersion of GPS-derived vector components that is considered as an external accuracy estimate does not coincide with processing software-provided estimated accuracy of vector components determination that is the internal accuracy estimate. The discrepancy between externally and internally estimated accuracy

was investigated using statistical analysis of time series of vector components obtained with the Bernese and Pinnacle software. Internal accuracy provided by the Bernese software differs from the external one, in the case investigated, by a scale factor of about 7 and 10 for a vertical component and vector length, respectively. Internal accuracy estimation provided by the Pinnacle software can be considered as the acceptable rough estimate of accuracy.

Accuracy and precision of GPS solutions based on data from permanent stations or from long-term geodynamics campaigns, especially in polar regions, need to be estimated by investigating time series of overlapping solutions using the tools of statistical analysis. The described strategy of quality analysis of GPS solutions besides their filtering allows for estimation of biases and chaotic effects. That procedure is not suitable for estimation of accuracy of GPS solutions obtained from single, short time occupation of sites. The majority of noise can be filtered using simplified statistical analysis of overlapped solutions based on sub-intervals of the observed session. Biases and jerks, however, can only be roughly estimated externally using the results of extended statistical analyses.

Acknowledgements

The research was supported by the Institute of Geodesy and Cartography in Warsaw and was partially financed by the Polish State Committee for Scientific Research (grant PBZ-KBN-081/T12/2002). The authors express special gratitude to Mrs. M. Mank and Mr. L. Zak from the Institute of Geodesy and Cartography, Warsaw, as well as to Dr. P. Wielgosz from the University of Warmia and Mazury, Olsztyn, for processing GPS data.

Bibliography

- Bruyninx C. (2001): Overview of the EUREF Permanent Network and the Network Coordination Activities, *EUREF Publication*, Eds. J. Torres, H. Hornik, Bayerischen Akademie der Wissenschaften, München, Germany, 2001, No 9, pp. 24-30.
- Cisak J., Kryński J., Zanimonskiy Y.M., (2002): *Variations of Ionosphere Versus Variations of Vector Components Determined from Data of IGS Antarctic GPS Stations – New Contribution to the GIANT Project* “Atmospheric Impact on GPS Observations in Antarctic”, Paper presented at the AGS-02, Wellington, New Zealand, http://www.scar-ggi.org.au/geodesy/ags02/cisak_ionosphere_gps.pdf
- Cisak J., Kryński J., Zanimonskiy Y.M., Wielgosz P., (2003a): *Variations of Vector Components Determined from GPS Data in Antarctic*. Ionospheric Aspect in New Results Obtained within the Project “Atmospheric Impact on GPS Observations in Antarctic”, Paper presented at the scientific conference, 22-23 January 2003, Lviv, Ukraine.
- Cisak J., Kryński J., Zanimonskiy Y., Wielgosz P., (2003b): *Study on the Influence of Ionosphere on GPS Solutions*

- for Antarctic Stations in the Framework of the SCAR Project, "Atmospheric Impact on GPS Observations in Antarctic", Paper presented at the 7th Bilateral Meeting Italy-Poland, Bressanone, Italy, 22-23 May 2003
- Dubbini M., Gandolfi S., Gusella L., Perfetti N., (2003): *Accuracy and precision vs software and different conditions using Italian GPS fiducial network (IGFN) data*, Presented at 7th Bilateral Geodetic Meeting Italy-Poland, Bressanone, Italy, 22-23 May 2003.
- Harris F.J., (1978): *On the Use of Windows for Harmonic Analysis with the Discrete Fourier Transform*, Proc. IEEE, Vol. 66, January 1978, pp. 51-83.
- King M., Coleman R., Nguyen L.N., (2002): *Spurious Periodic Horizontal Signals in Sub-Daily GPS Position Estimates*, *Journal of Geodesy*, Vol. 77, No 1-2, May 2003, pp. 15-21.
- Krynski J., Zanimonskiy Y., Wielgosz P. (2000): *Short Time Series Analysis of Precise GPS Positioning*, Presented at the XXV General Assembly of European Geophysical Society, Millenium Conference on Earth, Planetary and Solar System Sciences, Nice, France, 25-29 April 2000.
- Krynski J., Zanimonskiy Y., (2001): *Contribution of Data from Polar Regions to the Investigation of Short Term Geodynamics. First Results and Perspectives*, *SCAR Report, No 21*, January 2002, Publication of the Scientific Committee on Antarctic Research, Scott Polar Research Institute, Cambridge, UK.
- Krynski J., Cisak J., Zanimonskiy Y.M., Wielgosz P., (2002a): *Variations of GPS Solutions for Positions of Permanent Stations – Reality or Artefact*, Symposium of the IAG Subcommission for Europe (EUREF) held in Ponta Delgada, Portugal, 5-7 June 2002, *EUREF Publication No 8/2*, Mitteilungen des Bundesamtes für Kartographie und Geodäsie, Frankfurt am Main (in press).
- Krynski J., Zanimonskiy Y., Wielgosz P. (2002b): *Modelling biases in GPS Positioning Based on Short Observing Sessions*, Presented at the XXVII General Assembly of European Geophysical Society 2002, Nice, France, 21-26 April 2002.
- Krynski J., Zanimonskiy Y., (2002): *Quality Structure of Time Series of GPS Solutions*, Proceedings of the NKG General Assembly, 1-5 September 2002, Espoo, Finland, pp. 259-264.
- Neumeyer J., Barthelmes F., Combrink L., Dierks O., Fourie P., (2002): *Analysis Results from the SG Registration with the Dual Sphere Superconducting Gravimeter at SAGOS (South Africa)*, *BIM 135*, 15 July 2002, Paris, pp. 10607-10616.
- Poutanen M., Koivula H., Ollikainen M. (2001): *On the Periodicity of GPS Time Series*, Proceedings of IAG 2001 Scientific Assembly, 2-7 September 2001, Budapest, Hungary.
- Teunissen P.J.G. (2002): *The Parameter Distributions of the Integer GPS Model*, *Journal of Geodesy* (2002), Vol. 76, No 1, pp. 41-48.

Application of the Planetary Geodesy Methods (The Geoid Theory) for the Reconstruction of the Earth's Interior Structure in the Western Antarctic

Rudolf Greku, Ksenya Bondar, Victor Usenko

Institute of Geological Sciences, National Academy of Sciences of Ukraine,

Kiev, 55B, Gonchara St., 01054, Kyiv, Ukraine

e-mail: satmar@svitonline.com

Abstract

The algorithm for calculation of differential geoid heights and anomalous harmonic densities inside the Earth is represented in the paper. Expansion of external gravitational potential in series of spherical functions is used. The application of geopotential topography and anomalous harmonic densities for studying of structural features of regional deep sections is illustrated. The structure of the Scotia Arc Region with a technique named by us as the gravimetric tomography method is considered along typical latitudinal and longitudinal cross-sections, and also on maps of the differential geoid for different ranges of spherical harmonics.

1. Theoretical background

Density of the Earth's interior can be presented as a sum of normal and anomalous components:

$$\rho = \rho_1 + \rho_a,$$

where normal density ρ_1 determines normal gravity potential of the Earth; disturbing potential is caused by anomalous density ρ_a .

The global gravity models describe the disturbing potential of the Earth which depends on spherical coordinates of the point on its surface. It can be represented as Newton's integral

$$V(r, \theta, \lambda) = G \iiint_V \frac{\rho}{l} dv,$$

where G - gravitational constant, l - distance from the investigated point to the surface of the Earth, v - elementary volume. So, there is a linear dependence between ρ_a and V, i.e. $V = N \rho_a$ where N is a linear operator.

Hence, the inverse gravitational problem can be formulated

in the following way:

$$\Delta V = N^{-1}V,$$

the operator N^{-1} is unique if V is determined in the whole 3 dimensional space [Moritz, 1990]. The kernel of the operator N^{-1} consists of set of possible distributions of density ρ_0 inside closed contour S (within the Earth), which generate ground external potential.

The uniquely defined inverse Newton's operator provides harmonic density ρ_0 .

$$\Delta V = N^{-1}V.$$

Thus, the solution could be found in the way of summation of definite harmonic density and the density of ground potential ρ_0 .

$$\rho_a = \rho_0 + \rho_h$$

The densities of ground potential characterize features of spherical stratification inside the Earth. Local heterogeneity is described by anomalous harmonic density ρ_h .

2. The algorithm for calculation of the disturbing potential (or geoid height)

The geoid height above reference ellipsoid is found from the well-known formula

$$\zeta = R \sum_{n=2}^{\infty} \sum_{m=0}^n (c_{nm} \cos m\lambda + s_{nm} \sin m\lambda) P_{nm}(\cos \hat{A}),$$

where $R \approx 6371$ km - radius of the Earth, c_{nm} and s_{nm} - normalized coefficients of external spherical harmonics of gravity potential, λ - longitude of the investigated point, \hat{A} - polar distance of the investigated point, $P_{nm}(\cos \hat{A})$ - Legendre polynomial, n - number of harmonics to the 360th inclusive.

The formula taken from [Shabanova, 1962] was used for calculation of normalized spherical functions:

$$P_{nm}(\cos \hat{A}) = \cos \hat{A} \sqrt{\frac{4n^2 - 1}{n^2 - k^2}} P_{n-1,m}(\cos \hat{A}) - \sqrt{\frac{2n-1}{2n-3} \cdot \frac{(n-1)^2 - m^2}{n^2 - m^2}} P_{n-2,m}(\cos \hat{A})$$

The necessary set of formulae for calculation of any spherical function can be received on the base of following ones

$$P_{00}(\cos \hat{A}) = 1,$$

$$P_{11}(\cos \hat{A}) = \sqrt{3} \sin \hat{A},$$

$$P_{10}(\cos \hat{A}) = \sqrt{3} \cos \hat{A},$$

$$P_{nm}(\cos \hat{A}) = \sin \hat{A} \sqrt{\frac{2m+1}{2m}} P_{m-1,m-1}(\cos \hat{A}), m > 1$$

3. The algorithm for calculation of anomalous harmonic densities

The solution of the inverse gravity problem is given by Moritz [1990] under condition that distribution of density is a continuous function which can be approximated uniformly with a system of polynomials.

The density as a function of spherical coordinates can be expanded in series of spherical harmonics

$$\rho(r, \theta, \lambda) = \sum_{n=0}^{\infty} \sum_{m=0}^n (a_{nm} \cos m\lambda + b_{nm} \sin m\lambda) P_{nm}(\cos \theta) = \sum_{n=0}^{\infty} \sum_{m=0}^n f_{nm}(r) Y_{nm}(\theta, \lambda)$$

The coefficients f_{nm} ($= a_{nm}$ or b_{nm}) are arbitrary and can be represented as polynomials

$$f_{nm}(r) = \sum_{k=0}^N x_{nmk} r^k$$

Having excluded a general solution, which corresponds to the densities of ground potential, the expression for anomalous harmonic densities as a series of internal spherical harmonics is received

$$\rho_h(r, \theta, \lambda) = \sum_{n=2}^{\infty} \sum_{m=0}^n x_{nm} r^n Y_{nm}(\theta, \lambda),$$

where $x_{nm} = \frac{(2n+1)(2n+3)}{4\pi GR^{2n+3}} V_{nm}$, V_{nm} - coefficients of external gravity potential, $V_{nm} (= c_{nm} \cdot GMR^n \text{ or } s_{nm} \cdot GMR^n)$, M - mass of the Earth.

Thus, external spherical harmonics are used for determination of internal spherical harmonics. The internal spherical harmonics are used to receive distribution of positive and negative density inhomogeneities, which does not change external gravity potential as their total mass is equal to zero.

The final formula is

$$\rho_h = \sum_{n=2}^{\infty} \sum_{m=0}^n \frac{M(2n+1)(2n+3)}{4\pi R^{n+3}} \cdot r^n (c_{nm} \cos m\lambda + s_{nm} \sin m\lambda) P_{nm}(\cos \theta)$$

Corresponding number of harmonics n is taken to calculate the density ρ_h on the depth $(R-r)$.

4. Estimation of the depth of disturbing layer according to the number of harmonic

The obtained above density anomalies obviously are situated in different depths. However the mathematical methods used in physical geodesy though suppose but have no evident connection with the real geological structure of the Earth. Therefore a following question is remained: what layers of the Earth are responsible for disturbing gravitational potential.

In our method an assessment of the disturbing layer's depth is computed by a known harmonic function in physical geodesy in the case of the potential of the internal masses confined by a sphere

$$\frac{1}{r} = \sum_{n=0}^{\infty} \frac{\rho^n}{R^{n+1}} P_n(\cos \psi)$$

where r is the distance from the sphere surface down to the disturbing mass, ρ is the distance from the center of the sphere up to the disturbing mass, R is the radius of the sphere, $P_n(\cos \psi)$ is the Legendre polynomial of n^{th} degree, ψ is the central angle between R and ρ .

Calculations was carries out from $n_{\min} = 2$. At the right part of the expression the normalizing coefficient $(2n+1)^{1/2}$ was considered. If $\psi = 0$, $P_n(\cos \psi) = 1$ for any n , and $r = R - \rho$. Under this condition for specified values of r , ρ and R corresponding n was found.

Obviously, for large n the series

$$\frac{\rho^n}{R^{n+1}}$$

converge weakly. That is why restrictions are included into the procedure of calculation. Maximal degree n_{\max} is defined under condition

$$r - \frac{R}{\sum_{n=0}^{n_{\max}} \left(\frac{\rho}{R}\right)^n} \leq 0.1r$$

where coefficient 0.1 means 10% error from r.

Relationship between harmonic degrees n and depths r of disturbing layers is shown on the bilogarithmic diagram (Fig. 1). Main boundaries of the lithosphere are shown in accordance with the Bullard's density model of the Earth. The program allows to compute values of the disturbing gravity potential in terms of heights of the geoid, values of harmonic anomalies in units of g/cm3 and values of upper cover depths of disturbing layers of the Earth. Spherical coefficients of two geoid models OSU91A and EGM96 are used.

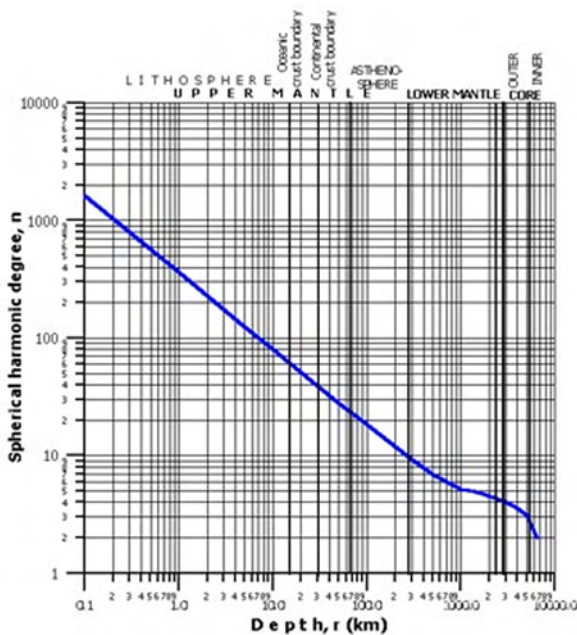


Figure 1. Relationship between harmonic degrees n and depths r of the disturbing layers of the Earth. Value n is the sum of harmonics in a range from degree 2 up to n. Depth r corresponds to upper cover of the disturbing layer, which thickness is considered from the center of the Earth

5. Examples of density structure in the Scotia Arc region

Deep structure and geodynamics of the Scotia Arc and adjacent provinces within limits of 48°S-66°S and 80°W-10°W are submitted with the EGM96 gravity geoid model. The distribution of density inhomogeneities of the Earth is displayed along the Scotia Sea's central 58°S latitudinal vertical cross-section (Fig. 2) and on 100 km and 1 km lateral levels with the spatial resolution of 30 km also (Fig. 3).

The images of differential anomalies (relatively of homogeneous deep layers) as three-dimensional surfaces show a detailed distribution of masses in the upper layers of the lithosphere, geometry and sizes of density inhomogeneities, their displacement in depth under influence of dynamic processes, and correlation of subsurface bodies with the bottom topography also.

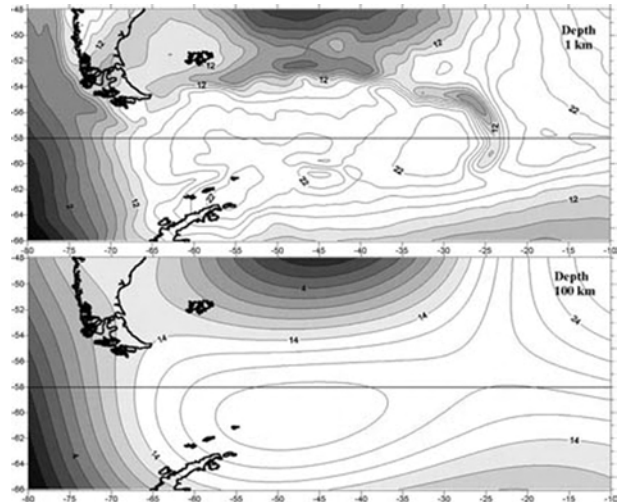


Figure 2. Maps of differential geoids topography corresponding disturbing layers with indicated depths of the upper cover. Lighter tint is more dense structure. The area of increased density is noted in depth of 100 km with epicenter 50°S, 47°W. It is a root part of the really Scotia body. On smaller depths (1 km) a structural differentiation of the Scotia Sea and correlation with the bottom relief are increased.

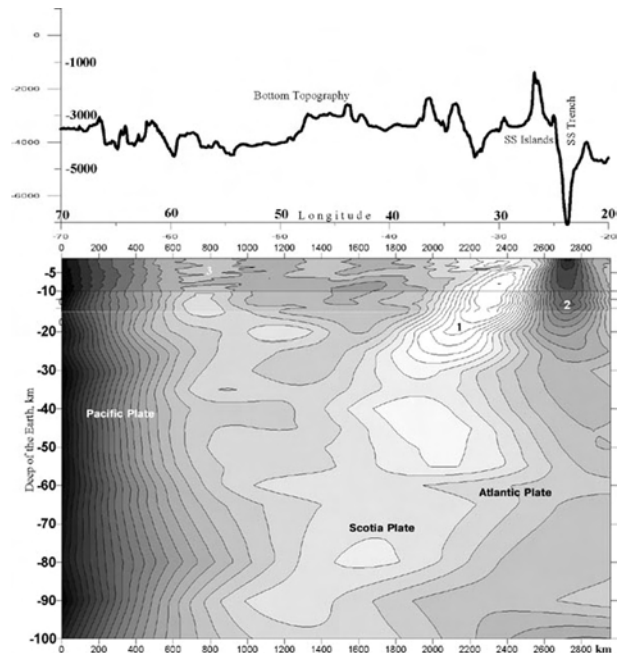


Figure 3. Vertical cross-section of the geopotential along 58°S latitude.

The roots of the South Sandwich Island ridge (1) are sloped to the Scotia Sea side and are immersed into depths 25-30 km. The SS Trench (2) is traced up to depth of 20 km. A fragment (3) of a joint area of the Shackleton F.Z. and the Western Scotia Ridge is observed at 57°W.

References

Moritz H (1990) The Figure of the Earth. Theoretical Geodesy and the Earth's Interior. Wichmann, Karlsruhe.

Shabanova A I (1962) Calculation on ECVM Ural-1 of characteristics of gravity field applying gravity

anomalies in spherical functions (in Russian) J CNIIGAIK 145: 77-81.

Results of GPS, Ground Photogrammetry, Echosounding and ERS Interferometric Surveys during Ukrainian Antarctic Expeditions

Rudolf Greku(1), Gennady Milinevsky(2), Yuriy Ladanovsky(3), Pavel Bahmach(3), Tatyana Greku(1)

(1) Institute of Geological Sciences, National Academy of Sciences of Ukraine, Kiev, 55B, Gonchara st, 01054, Kyiv, Ukraine, e-mail: satmar@svitonline.com

(2) Ukrainian Antarctic Center, Kyiv/Ukraine; antar@carrier.kiev.ua

(3) ECOMM Co, 18/7, Kutuzov st., 01133, Kyiv, Ukraine, lada@ecomm.kiev.ua

Abstract

The region of Ukrainian Antarctic geodetic and topographic surveys includes the Argentine Archipelago where the Vernadsky/Faraday Ukrainian Antarctic Station is located and an adjoining part of the Antarctic Peninsula. Following works in this area are carried out under the auspices of the Ukrainian Antarctic Center within the State Program of the Ukrainian Antarctic Research for the SCAR's GIANT, ANTEC and IBCSO Projects:

- Seasonal many days GPS observations at the "SCAR GPS 2002" site on Galindez Island;
- Restoration of coordinates of the British triangulation stations and creation of new network on islands;
- Large-scale topographic mapping of islands and ground photogrammetry survey;
- Echosounding of the Argentine archipelago's seabed in the shallow water unsurveyed areas;
- Mapping of the Galindez ice cap and ice streams of the Antarctic Peninsula with the ERS radar interferometry;
- Determination of the Bellingsausen sea geoid with the altimeter data for geological purposes.

The main goal of these works consists in following: creation with the GPS survey of a precision geodetic network and determination of geodynamic characteristics of the region, determination massbalance and dynamics of the ice cover

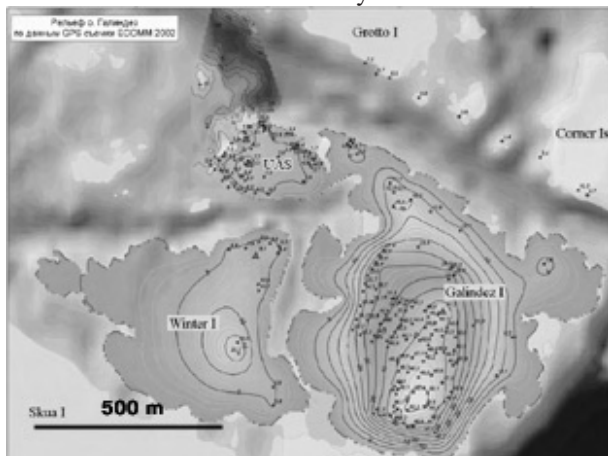


Figure 1. Topographic map of the Galindez (Ukrainian Antarctic Station) and Winter Islands by the GPS survey at geophysical polygons. Contour isoline: 5m

by the satellite radar interferometry, modelling of a deep structure of the lithosphere with the altimeter data, creation of the "Vernadsky-Argentine Islands" GIS.

Seasonal continuous GPS observations

Observations with dual frequency Trimble 4700 receiver were carried out during two weeks in 2002 and 2003 to monitor the physical stability of the main station and for the estimation of the regional tectonic stability of the area. Four IGS GPS stations were used for processing of our measurements by the Space Geodesy Analysis Centre (AUSPOS), Australia. Differences between coordinates are: 3.1 mm in latitude, 6.4 mm in longitude, 5.0 mm in height. RMS were from 3 mm to 7 mm. Horizontal vector of the ground mark displacement during one year is 7.2 mm at azimuth 64.5°.

Coastal GPS survey

Local network of GPS sites was created in an approximate 10-15 km radius around the main observing station and relatively the "SCAR GPS 2002" site. More than 300 GPS points had determined for positioning of different geophysical measurements on islands. They are different objects on the Vernadsky station (meteorological and geophysical pavilions, masts and antennas), British triangulation stations, tidal gauge, fixed points for the stereophotogrammetric survey, and points of geomagnetic, geological and biological samples. 30 points are fixed in rock and can be used for repeated observations and expansion of a local geodetic network. One of results is shown in Fig. 1 as a topographic map of the Galindez Island by the GPS measurements.

Ground Photogrammetry for mapping of the Galindez Island ice cliff

Stereophotogrammetric survey of the coastal line and ice cliff were carried out by a Sony DSC-F717 digital camera on a boat. 70 overlapping images were made for the Galindez and Winter Islands along length of 1000 m (Fig. 2). Coordinates of the reference marks (x) were determined by GPS. Comparison of the topographic data allows to estimate a seasonal changeability of the ice cap by layers with high accuracy.

Now the processing of stereopairs is implemented with the



Figure 2. Fragment of a photomontage shows the southeast coast of the Galindez Island with the cliff of the island ice cap (height approximately 50 m).

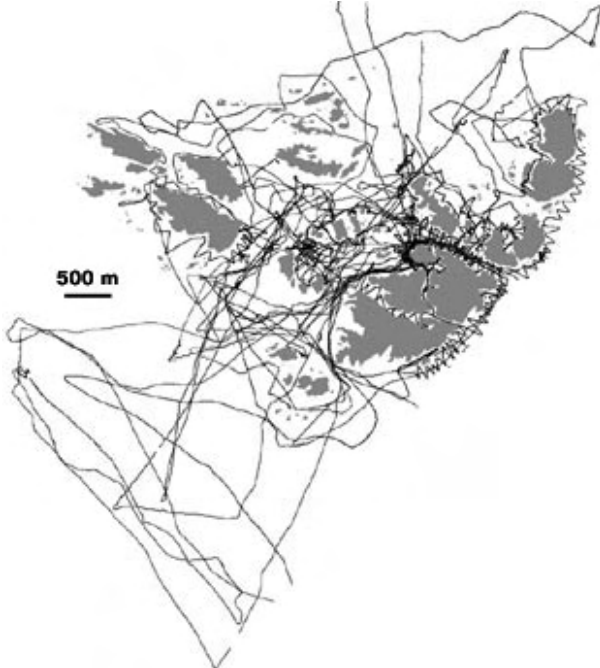


Figure 3. Boat echosounding survey during season expeditions 1998-2003.

DEM with 20 m resolution and an electronic map of the bottom topography were constructed (Fig. 3). On this base different morphometric and geomorphological maps (slope, aspect, curvature, ridge and channel directions) were created with the LandSerf software (Lester Univ., UK). Depths within the archipelago are not more than 70 m. The general nature of the bottom is rock with thin mud and sand sediments distributed in morphological traps. ERDAS software. These field works have been carried out in collaboration with the Lviv Polytechnic University

Research of the Archipelago's bottom topography

The archipelago of the Argentine Islands is located on the western shelf of the Antarctic Peninsula. It is separated from the Peninsula by deep (more than 300 m) and wide (7 km) Penola strait. The archipelago is tectonic mesoblock, which is broken at smaller fragments by system of fractures.

Echo-sounding and geological sampling on the equipped boat were carried out in the internal water between islands of the archipelago during March - April 1998 and then added in 2002 and 2003 (Fig. 2). Total tracks extension is 400 km approximately. Depths and co-ordinates were recorded with two second period (or 5 m distance approximately). Depth accuracy is not worse than 0.1 %. Depths are corrected for the tidal level.

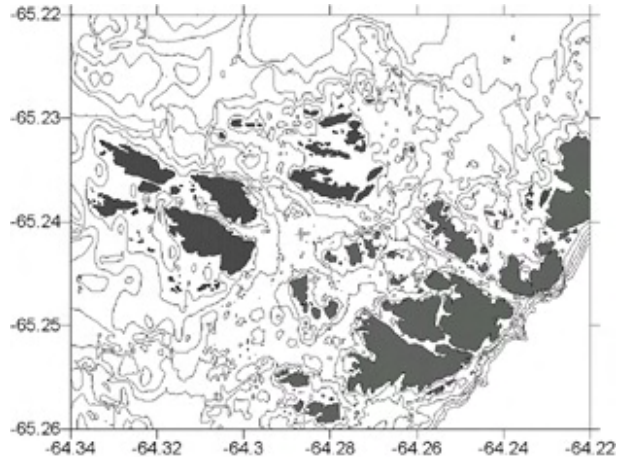


Figure 4. Bathymetric map of the Argentine Archipelago's sea-bed with the season Ukrainian expeditions (1998-2003). Contour interval is 10 m

Topography of the Flask Glacier (Antarctic Peninsula with the interferometry technique by the ERS SAR images

12 radar ERS1/2 images (including the Tandem mission) for the same area of the Graham Land on area 100x100 km are received. These images are used for investigation of variability of the ground and ice cover topography for period 1996-2003, and for geological, oceanological and ecological researches also.



Figure 5. ERS-2 image of 27.02.96 for the Flask Glacier flowing from the Bruce Plateau (1700 m) to the Weddell Sea;

A – area of the fragment is 36km x 32km
 B - amplitude image of the fragment distinguished from A for interferometry processing, area is 7 x 15 km

C - phase interferogram by two Tandem images
 D - 3D image by DEM from the interferogram
 Topographic-geodetic works in a complex with other

researches at the Vernadsky station (seismology, geomagnetism...) will be an important contribution to a fundamental area of studying of geodynamic processes.

Crustal Motion in East Antarctica Derived from GPS Observations

M. Jia, J. Dawson, G. Luton, G. Johnston, R. Govind, J. Manning

Geoscience Earth Monitoring Group, Geoscience Australia, Canberra, Australia

Abstract

Eight years of continuous permanent GPS data and three years of GPS campaign data are used to provide current estimates of crustal motion in Antarctica within the International Terrestrial Reference Frame 2000 (ITRF2000) (Altamimi *et al.* 2002). Crustal motions derived for this paper are compared with published results from several groups. The crustal motion estimates are consistent with that provided by other groups in the horizontal components but not in the vertical component.

1 Introduction

Current-day velocities of crustal deformation in Antarctica are important indicators for many geodetic and geophysical studies, including plate motion, intra-plate tectonics, Antarctic post glacial rebound and absolute sea level change. GPS geodesy has the potential to measure velocities of the crust directly over periods of maybe a few years, especially in horizontal components, as demonstrated by Dietrich *et al.* (2001) and Sella *et al.* (2001).

In this paper, almost eight years of continuous permanent GPS data and three years of GPS campaign data, for a total of 50 sites in the Antarctic and Australian regions are analysed with three strategies (A, B and C). Solution A is a combination of the Geoscience Australia's IGS RNAAC (Regional Network Associate Analysis Centre) solutions as submitted to the IGS from 1996 to present. Solution B is a combination of the re-processed daily regional solutions only using data observed during the Geoscience Australia Antarctic campaigns of 2001, 2002 and 2003. While solution C is a combination of re-processed daily regional solutions from continuous permanent GPS data from 1995 to 2001 in Antarctica and Australia region.

The crustal velocities in Antarctica relative to ITRF2000 are derived. These results are compared with that provided by several other groups and some conclusions are drawn from this analysis and comparison.

2. Data

This research uses GPS data collected from both continuous GPS networks operated by Geoscience Australia (formerly, AUSLIG) and also other organizations, and additionally includes Antarctic summer campaign data as well.

Continuous GPS sites around this region have gradually increased since 1989. Up to now more than 40 such GPS sites are available around this region. However due to inconsistent hardware and software description

and availability of reliable precise IGS orbital products, only the data after 1995 are used in this paper. Data from another 33 Antarctica sites, which were collected during three summer campaigns are also used. Seven Antarctica sites, which have at least a three-year time span of GPS data, are shown in Figure 1. The occupation and duration history of all sites are listed in Table 1.

3. Data Processing

Three data processing strategies (A, B and C) are reviewed in this paper. The Bernese GPS Software Version 4.2 (Hugentobler, *et al.*, 2001) is used in the daily data processing for all three strategies.

3.1 Weekly Combined Regional IGS RNAAC Solutions (Strategy A)

In the case of processing Strategy A the GPS data from the 16 Australia regional sites (including the Australian Antarctic sites) are processed and combined into weekly SINEX files and stored as products of the IGS RNAAC. The data spans the period 1 January 1996 to 31 July 2003. IGS final orbital and the Earth rotation parameters are used. This data has not been re-processed and the computed solution strategy is not consistent over the period of the solution but generally reflects the IGS standard at the time of computation (around 30 days after observation). For historical reasons ionosphere free floating solutions are used as final solutions.

3.2 Reprocessed Daily Solutions (Strategy B and C)

For processing strategy B and C the GPS data are processed on a daily basis using the Bernese Processing Engine (BPE) of the Bernese GPS Software Version 4.2. Dual-frequency carrier-phase and code data are used. RINEX file sizes less than 70% of normal size are excluded. Code measurements are only used for receiver clock synchronisation. The elevation cut-off angle is 10° with elevation-dependant data weighting. The data sampling rate is 30 seconds for strategy B and 180 seconds for strategy C. Standards and procedures for the data processing are briefly summarised as follows:

- Precise satellite orbits and the Earth rotation parameters provided by the IGS are used for the daily data processing.
- All stations are corrected for site displacement due to solid Earth and pole tides (McCarthy, 1996) and ocean tidal loading using GOT00.2 model provided by Scherneck (www.oso.chalmers.se/~loading).

REPORT OF THE FIFTH SCAR ANTARCTIC GEODESY SYMPOSIUM

Table 1 Site occupations used in this analysis

(* denotes continuous occupation, numerical values for sites A351 denote occupation days for that year's campaign)

Site	1995	1996	1997	1998	1999	2000	2001	2002	2003	Span(years)
Antarctic plate										
A351							17	45	46	3
CAS1	*	*	*	*	*	*	*	45	50	9
DAV1	*	*	*	*	*	*	*	45	50	9
DUM1				*	*	*	*			4
KERG	*	*	*	*	*	*	*	45	50	9
MAW1	*	*	*	*	*	*	*	45	50	9
MCM1	*									
MCM4	*	*	*	*	*	*	*	45	50	9
Australia plate										
ALIC	*	*	*	*	*	*	*			7
AUCK	*	*	*	*	*	*	*			7
BUR1				*	*	*				3
CEDU	*		*	*	*	*	*			7
COCO	*	*	*	*	*	*	*			7
DARW	*	*	*	*	*	*	*			7
DST1		*	*	*	*	*	*			6
GRIM	*	*	*	*	*					5
HIL1			*	*	*	*	*			5
HOB2	*	*	*	*	*	*	*			7
JAB1			*	*	*	*	*			5
KARR	*	*	*	*	*	*	*			7
KOUC					*	*	*			3
NOUM				*	*	*	*			4
PERT	*	*	*	*	*	*	*			7
STR1				*	*	*	*			4
SUVA					*	*	*			3
TID1		*	*	*	*	*	*			6
TOW2	*	*	*	*	*	*	*			7
WEL1	*	*	*							3
YAR1	*	*	*	*	*	*	*			7
Eurasia plate										
BAKO				*	*	*	*			4
BINT					*	*	*			3
GETI				*	*	*	*			4
NTUS			*	*	*	*	*			5
Pacific plate										
CHAT	*	*	*	*	*	*	*			7
FALE				*	*	*	*			4
KWJ1		*	*	*	*	*	*			6
MAC1	*	*	*	*	*	*	*			7

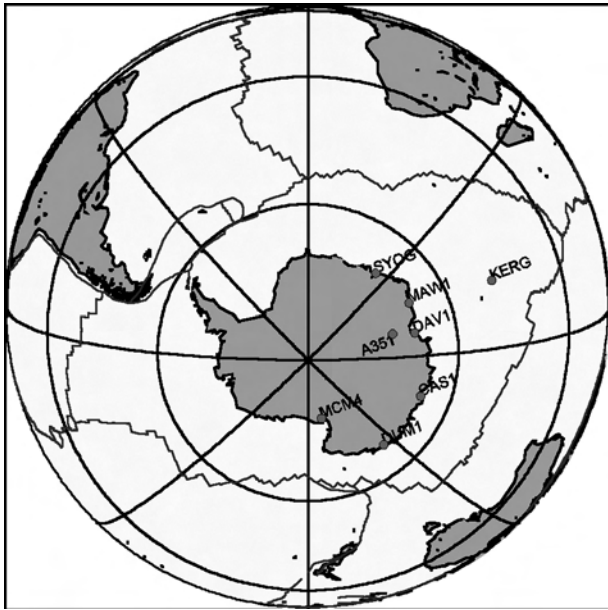


Fig. 1 Antarctica GPS sites, which have at least three-year time span of GPS data

- The IGS_01 antenna phase centre variation models (igsceb.jpl.nasa.gov/igsceb/station/general/igs_01.pcv).
- Carrier phase preprocessing is conducted on a baseline by baseline mode using triple differences. Checking simultaneously different linear combinations of L1 and L2, cycle slips are fixed in most cases. If cycle slips cannot be fixed reliably, bad data points are removed or new ambiguity parameters are set up. In addition, a data screening step in a baseline by baseline mode on the basis of weighted post-fit residuals is performed and outliers are marked and are not used for the final processing.
- Ionosphere delay estimation using geometry-free combination L4 to support ambiguity resolution.
- Estimation of tropospheric delay and floating coordinates using ionosphere-free combination L3 to support ambiguity resolution.
- Ambiguity resolution in a baseline by baseline mode using L1 and L2 phase data with stochastic ionospheric constraints and with floating coordinates, ionospheric and tropospheric delay supporting.
- Estimation of coordinates and tropospheric delay (at a 1-hour interval for each station) and generating of the daily Normal Equations (NEQ) with and without tropospheric parameters and results in the international standard Software Independent Exchange (SINEX) format.
- Weekly sets of troposphere estimates are re-computed on the NEQ level using weekly combined coordinates for the study of long-term change of integrated water vapour.

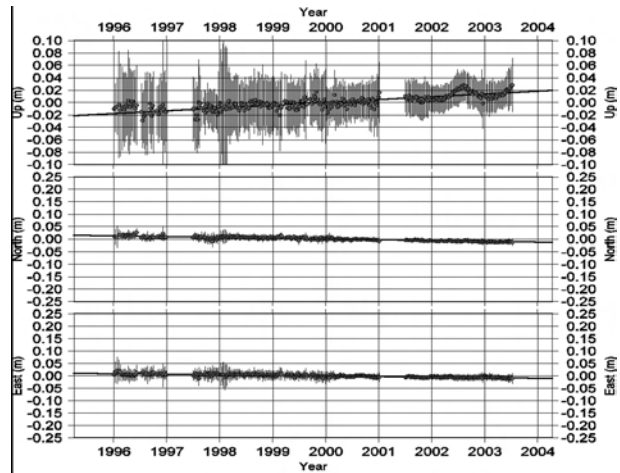


Fig.2 Coordinate time series for site MAW1 (strategy A)

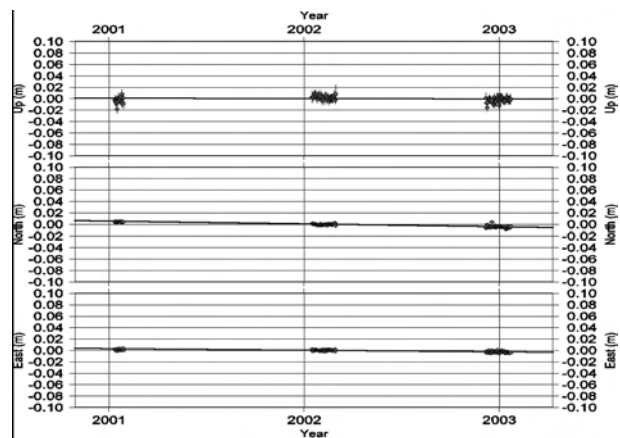


Fig. 3 Coordinate time series for site A351 (strategy B)

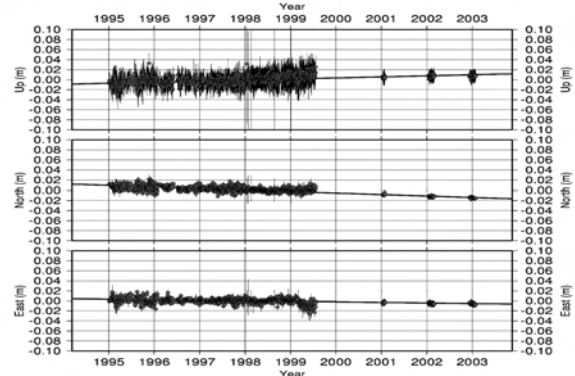


Fig.4 Coordinate time series for site MAW1 (strategy C)

4. Data Analysis

Crustal velocity estimates are based on a weighted least squares line fit of the weekly position estimates for strategy A, and to the daily position estimates for the strategies B and C. Twelve IGS core stations around this region comprise the reference network. The reference stations, which are constrained to their ITRF2000 values with weighted constraints on Net-Translation/Net-Rotation/Net-Scale change and their rates, are listed in bold letters in Table 1. Incorrect antenna heights are corrected using Bernese GPS Software Version 4.2. Outliers, defined as both points that lie off the best fit line by more than 3 times

Table 2 Estimated velocities and their standard deviations for the three solution strategies

Site	Solution	Velocity (mm/yr)			Velocity standard deviation (mm/yr)		
		East	North	Vertical	East	North	Vertical
CAS1	A	2.6	-9.7	2.2	0.6	0.4	1.5
	B	2.1	-9.5	4.0	0.2	0.2	0.2
	C	3.1	-9.4	5.0	0.2	0.2	0.3
DAV1	A	-0.8	-5.4	3.5	0.4	0.4	1.1
	B	-1.3	-5.6	3.0	0.3	0.2	0.7
	C	-0.4	-5.2	1.6	0.2	0.2	0.3
KERG	A						
	B	6.0	-2.7	5.0	0.2	0.2	0.1
	C	8.0	-4.1	4.2	0.2	0.2	0.3
MAW1	A	-2.2	-3.1	4.3	0.5	0.4	1.1
	B	-1.9	-2.5	3.5	0.3	0.2	0.5
	C	-1.1	-2.9	2.1	0.2	0.2	0.3
MCM4	A						
	B	6.3	-10.0	-1.1	0.5	0.4	2.0
	C	8.3	-11.5	10.0	0.2	0.2	0.4
A351	A						
	B	-2.9	-4.7	-0.5	0.3	0.3	1.0
	C	-2.3	-5.1	-0.9	0.8	0.6	3.2

the standard deviation and points whose residuals are larger than 3cm for vertical component, and 2cm for horizontal components, are not used in the final combined solutions. In this paper, velocity error estimates account for only white noise and parameters of annual and semi-annual signals are not estimated due to the use of limited campaign data. Therefore, the estimated standard deviations for velocities may be not very reliable at this stage.

Typical time series plots are shown in Figure 2 for strategy A, in Figure 3 for strategy

B and in Figure 4 for strategy

C. The estimated velocities and their standard deviations for the three solution strategies are listed in Table 2.

5. Comparison Of Results

The crustal motion velocities derived from GPS are compared with that from other groups. The results of comparisons are listed in Table 3. The NUVEL1A-NNR values are from DeMets *et al*, 1990 and DeMets *et al.*, 1994. The ITRF2000 values are from Altamimi, 2002. The JPL values are from JPL, 2003. The IGS (weekly) MIT values are from Herring, 2003. The SOPAC values are from Bock, 2003. Table 3 shows that the velocities in horizontal directions from all groups are compatible. The RMS velocity differences are generally less than 1mm/yr and have a maximum RMS of 1.2 mm/yr. On the other hand, the velocities in vertical direction show greater variability than that in the horizontal directions. When the likely outliers (indicated in bold) are included the maximum RMS is 8.1 mm/yr and the all RMS values are larger than 3 mm/yr. When the likely outliers are excluded then all the RMS values are less than 2 mm/yr. Further analysis of the relative motions between plates and intra-

plate deformation analysis are beyond of the scope of this paper and will be discussed in the future.

Summary

Three solution strategies have been used to derive current crustal motion velocities in Antarctica. All results in horizontal directions from the three solution strategies are compatible with that from others. Significant inconsistency in vertical component between different groups exists. Likely outliers in the vertical component are visible for all sites between the IGS (WEEKLY) MIT estimates and all other solutions. Another likely outlier appears between the MCM4 solution C and other solutions, the explanation of which is not clear at this stage. Further analysis of MCM4 in time will provide more conclusive estimates of velocity and perhaps time series discontinuity. Much longer time data spans, more accurate loading corrections and velocity estimation models, which take into account annual and semi-annual signals, may be needed to derive reliable results in the vertical component.

Acknowledgments

The authors are grateful to the IGS community for the IGS products and data used in this analysis, and to Paul Digney for his contribution to the Antarctic field activities. This research was supported by the Australia Antarctic Division (ASAC proposal 1159).

References

Altamimi Z., Sillard P., and Boucher C., 2002, ITRF2000: A New Release of the International Terrestrial Reference Frame for Earth Science Applications, *J. Geophys. Res.* 107, ETH 2-1 to ETG 2-19.

SCAR WORKING GROUP ON GEODESY AND GEOGRAPHIC INFORMATION

Table 3 Velocity comparisons (- denotes velocity unavailability. Bold values show likely outliers and values for mean and RMS differences in the vertical are calculated excluding these outliers).

Site	Solution	Velocity (mm/yr)		
		East	North	Vertical
CAS1	NUVEL1A-NNR	2.0	-8.7	-
	ITRF2000	2.6	-9.6	3.7
	JPL	2.7	-11.2	4.6
	SOPAC	1.9	-9.9	3.5
	IGS (WEEKLY) MIT	2.0	-9.6	-6.8
	IGS (WEEKLY) Official	2.6	-10.2	2.8
	A	2.6	-9.7	2.0
	B	2.1	-9.5	4.0
	C	3.1	-9.4	5.0
	MEAN	2.5	-9.9	2.4
	RMS	0.4	0.6	3.5
	DAV1	NUVEL1A-NNR	-2.2	-2.9
ITRF2000		-1.5	-4.8	4.3
JPL		-1.7	-5.6	1.7
SOPAC		-2.0	-4.9	3.1
IGS (WEEKLY) MIT		-1.7	-5.0	-8.5
IGS (WEEKLY) Official		-1.6	-5.9	2.4
A		-0.9	-5.5	3.6
B		-1.3	-5.6	3.0
C		-0.4	-5.2	1.6
MEAN		-1.4	-5.3	1.4
RMS		0.5	0.4	4.1
KERG		NUVEL1A-NNR	6.4	-1.3
	ITRF2000	6.0	-3.1	5.0
	JPL	4.5	-4.3	0.9
	SOPAC	5.8	-3.7	4.9
	IGS (WEEKLY) MIT	5.9	-2.5	-7.6
	IGS (WEEKLY) Official	5.6	-3.6	4.1
	A	-	-	-
	B	6.0	-2.7	5.0
	C	8.0	-4.1	4.2
	MEAN	5.9	-3.4	2.3
	RMS	1.0	0.7	4.6
	MAW1	NUVEL1A-NNR	-2.1	0.3
ITRF2000		-2.3	-2.6	2.8
JPL		-2.8	-4.7	0.4
SOPAC		-2.0	-3.0	1.1
IGS (WEEKLY) MIT		-2.3	-2.8	-15.0
IGS (WEEKLY) Official		-2.9	-3.5	0.8
Dietrich <i>et al.</i> (2001)		-3.0	-5.0	-
A		-2.3	-3.2	4.5
B		-1.9	-2.5	3.5
C		-1.1	-2.9	2.1
MEAN		-2.2	-3.4	-1.1
RMS		0.6	0.9	6.1

REPORT OF THE FIFTH SCAR ANTARCTIC GEODESY SYMPOSIUM

MCM4	NUVEL1A-NNR	7.5	-11.7	-
	ITRF2000	9.7	-11.7	0.8
	JPL	10.0	-11.9	-1.1
	SOPAC	8.7	-11.6	2.5
	IGS (WEEKLY) MIT	9.2	-10.9	-16.8
	IGS (WEEKLY) Official	9.1	-12.0	1.7
	A	-	-	-
	B	6.3	-10.0	-1.1
	C	8.3	-11.5	10.0
	MEAN	8.7	-11.3	-0.6
	RMS	1.2	0.7	8.1
A351	NUVEL1A-NNR	-4.3	-2.3	-
	ITRF2000	-	-	-
	JPL	-	-	-
	SOPAC	-	-	-
	IGS (WEEKLY) MIT	-	-	-
	IGS (WEEKLY) Official	-	-	-
	A	-	-	-
	B	-2.9	-4.7	-0.5
	C	-2.3	-5.1	-0.9
	MEAN	-2.6	-4.9	-0.7
	RMS	-	-	-

- Bock Y., 2003, Global Time Series, web site: <ftp://garner.ucsd.edu/pub/timeseries/>
- DeMets C., Gordon D., Argus D.F. and Stein S., 1990, Current plate motions, *Geophys. J. Int.* 101, 425-278.
- DeMets C., Gordon D., Argus D.F. and Stein S., 1994, Effect of recent revisions to the geomagnetic reversal time scale on estimates of current plate motions, *Geophys. Res. Lett.*, 21, 2191-2194.
- Dietrich-R; Dach-R; Engelhardt-G; Ihde-J; Korth-W; Kutterer-H-J; Lindner-K; Mayer-M; Menge-F; Miller-H; Mueller-C; Niemeier-W; Perlt-J; Pohl-M; Salbach-H; Schenke-H-W; Schoene-T; Seeber-G; Veit-A; Voelksen-C, 2001, ITRF coordinates and plate velocities from repeated GPS campaigns in Antarctica; an analysis based on different individual solutions. *Journal of Geodesy.* 74; 11-12, Pages 756-766. 2001.
- Herring T., 2003. Global Time Series, web site: http://www-gpsg.mit.edu/~tah/MIT_IGS_AAC/index2.html
- Hugentobler U., Schaer S. and Fridez P., 2001, Bernese GPS Software Version 4.2. Astronomical Institute, University of Berne.
- McCarthy, 1996, IERS Technical note No. 21: IERS Conventions (1996)
- Sella-Giovanni-F; Mao-Ailin; Dixon-Timothy; Stein-Seth, 2001, REVEL; a new global plate velocity model and changes in plate velocities over the last 25 ma. Abstracts with Programs - *Geological Society of America.* 33; 6, Pages 397. 2001.
- JPL (Jet Propulsion Laboratory), 2003, GPS Time Series, web site: <http://sideshow.jpl.nasa.gov/mbh/series.html>

**Recent Geodynamics of the Earth's Crust in the Region of Antarctic Station
"Academic Vernadsky"
Due To Results Of Tectonomagnetic Investigations**

Valentyn Maksymchuk, Yury Gorodysky, Ihor Chobotok, Valentyna Kuznetsova

Carpathian Branch of the Institute of Geophysics of NAS of Ukraine, Naukova str. 3-b,

Lviv, 79060 Ukraine

E-mail: depart10@cb-igph.lviv.ua

Abstract

The studying of the tectonic activity in the region of location of "Academic Vernadsky" station (64°15', 65°15') is actual since near the station the large regional deep faults were revealed. The important feature of the Antarctic

station location is that archipelago Argentine islands lies in the subduction zone of Eastern-Pacific and Antarctic plates and thus under influence of intense tectonic stresses.

Tectonomagnetic investigations in the region of the

Antarctic station “Academic Vernadsky” were initiated in 1998. In 2001 and 2002 these works were repeated. They were aimed at the study of the recent geodynamics of the region, detection of active deep faults and glacier motion study. The tectonomagnetic method is based on the study of the anomalous magnetic field temporal variations, caused by various physical-chemical processes in the Earth’s lithosphere. The methodology presupposes laying of long-term points and profiles, at which repetitive observations of geomagnetic field F are performed at the temporal interval. In addition the parameter of DDF- anomalous geomagnetic field F variation is determined for the period of time between the cycles of observations.

The tectonomagnetic works were carried out over the profile Barñhany-Rasmussen of the length 11 km, on which 7 tectonomagnetic points had been set up and three cycles of observations had been performed. The profile crosses crosswise the strike the main rock-forming complexes in the west-east direction. A mean-square error of the survey was about 0.7 nT.

As a result of these observations were determined that anomalous magnetic field temporal variations (DDF-

anomalies) have the values from some few to about 15 nT. The morphology of DDF field have certain regularities, which can be seen for period 1998-2001 and for period 1998-2002 (the total changes), as well. The eastern part of the profile is characterized by rather low positive values of DDF with the extremum +2.6 nT. The DDF of the western part is noticeably more anomalous: from -3,5 nT to -15 nt. Another peculiarity of DDF curves consist in similarity between DDF for 1998-2001 and total DDF.

Evident correlation between the static field DFa and DDF allow us to conclude that observed anomalies DDF may be of double nature: a part of it is a result of magnetisation effect under influence of secular variation, another part may be caused by piesomagnetic effect on account of crust stressed state changes.

By the help of mathematical modelling we made the quantitative evaluations of observed tectonomagnetic anomalies. Due to these evaluations the Earth’s crust rocks in the region of archipelago stay under expend horizontal stresses of sublatitudinal elongation. The values of these stresses variations may be about several bar per year.

Antarctic Geodesy

Gravity Studies of the Western Antarctic Region – New Possibilities in Geophysical Modelling.

Yu.V. Kozlenko, I.N. Korchagin, V.D. Solovjov

Institute of Geophysics of National Academy of Science of Ukraine

E-mail: valsolov@igph.kiev.ua.

Abstract

Knowledge of gravity anomalies space distribution has a great value to understanding their relationships with geology and major crust features of different tectonic elements of the West Antarctic region that is rather poorly studied now. That is why there is a necessity to use different gravity measurements- high resolution satellite models in conjunction with shipboard, airborne and land based gravity- for 3D geophysical modelling. Usually short-wave anomalies show obvious correlation with the geology of outcrops which consist of Mesozoic plutons of diverse composition emplaced in metamorphic rocks and members of the Antarctic Peninsula Volcanic Group.

Simultaneous analysis of remote altimeter, marine on-board and land base gravity measurements allows to elaborate some criterious of geological objects density models construction in wide depth’s values- from near surface local structures to large-scale upper mantle heterogeneities.

First experience of such works becomes available during “Ernst Krenkel” Expeditions where a possibility to compare the observed on-board marine gravity anomalies with satellite altimeter data was realized. It was noted that close relationship between the local bottom relief features and calculated Geosat altimeter data was not existed. Both types of measurements are confirmed to anomalies with total length that is more than 20 km.

It is known that the Antarctic land base gravity data sets are characterized by standard errors estimated about 2,5 mGal for Free-air anomalies in the previous works. New results of such measurements are not published and realization of international program to compile Antarctic gravity data south of 60°S is not finished. Now it is necessary to compile different gravity anomalies data into a digital database and prepare the anomaly map for the Vernadsky station region.

AGS '03
List of Participants

Name	Country	E-mail
Philip E O'Brien	Australia	Phil.O'Brien@ga.gov.au
Gary Johnston	Australia	Gary.Johnston@ga.gov.au
Alessandro Capra	Italy	alessandro.capra@mail.ing.unibo.it
Pierguido Sarti	Italy	pierguido.sarti@itis.mt.cnr.it
Hans Werner Schenke	Germany	hschenke@awi-bremerhaven.de
Jerry Mullins	USA	jmullins@usgs.gov
Richard Sanchez	USA	rsanchez@usgs.gov
Jan Cisak	Poland	jcisak@astercity.net
Jan Krynski	Poland	krynski@igik.edu.pl
Andrzej Krankowski	Poland	kand@moskit.uwm.edu.pl
E Dongchen	P.R. China	edc1939@public.wh.hb.cn
Li Fei	P.R. China	zskai@hp827s.wtusm.edu.cn
Zhang Shengkai	P.R. China	zskai@hp827s.wtusm.edu.cn
Hannu Koivula	Finland	hannu.koivula@fgi.fi
Alexander Yuskevich	Russia	aerogeodezia@actor.ru
Jurij Shagimuratov	Russia	pcizmiran@gazinter.net
Vladimir Berk	Russia	
Yurij Bobalo	Ukraine	bobaloyu@polynet.lviv.ua
Petro Zazulyak	Ukraine	ssavchuk@polynet.lviv.ua
Valeri Lytvynov	Ukraine	antarc@carrier.kiev.ua
Gennadi Milinevski	Ukraine	antarc@carrier.kiev.ua
Svetlana Kovalenok	Ukraine	antarc@carrier.kiev.ua
Rudolf Greku	Ukraine	satmar@svitonline.com
Ivan Makarenko	Ukraine	lepetjuk@geomatka.kiev.ua
Anatolij Bondar	Ukraine	lepetjuk@geomatka.kiev.ua
Valentyn Maksymchuk	Ukraine	depart10@cb-igph.lviv.ua
Yurij Horodyskyj	Ukraine	jorgorod@cb-igph.lviv.ua
Yevgen Zanimonsky	Ukraine	yzan@poczta.onet.pl
Fedir Zablotskyj	Ukraine	fzablots@polynet.lviv.ua
Lyuba Yankiv-Vitkovska	Ukraine	luba_y@ukr.net
Yaromyra Kostetska	Ukraine	
Volodymyr Glotov	Ukraine	v_glotov@ukr.net
Kornelij Tretyak	Ukraine	kornel@polynet.lviv.ua
Alexander Marchenko	Ukraine	march@pancha.lviv.ua
Zoryana Tartachynska	Ukraine	march@pancha.lviv.ua
Fedir Kuzyk	Ukraine	fzablots@polynet.lviv.ua
Roman Demus	Ukraine	fzablots@polynet.lviv.ua
Alexandra Zablotska	Ukraine	fzablots@polynet.lviv.ua
Natalya Dovhan	Ukraine	fzablots@polynet.lviv.ua

Antarctic Geodesy: Recent Work and Future Prospects
AGS'03
5th International Antarctic Geodesy Symposium
Lviv, Ukraine, September 15-17, 2003
PROGRAM

Monday, 15th September 2003

- 9:00-10:00** Registration of the Symposium participants (Assembly Hall of the University "Lviv Polytechnic", S.Bandera str.,12)
- 10:00-11:30** Plenary session,
Chairman Fedir Zablotskyj
- 10:00-10:30** Presentation of the Symposium participants.
Welcomes from the University Administration of "Lviv Polytechnic", SCAR Geoscience SSG, Ukrainian Antarctic Center, Public Geodetic Service of Ukraine;
- 10:30-11:00** *Valery Lytvynov, Gennadi Milinevsky, Svetlana Kovalenok, Elena Chernysh, Rudolf Greku*
Ukraine National Antarctic Program: geodesy activity
- 12:00-13:00** Walking-tour of the University "Lviv Polytechnic"
- 14:00** **Session 1: 2002/2003 Austral Summer Geodesy Activities** *Chairman Jerry Mullins*
- 14:00-14:20** *John Manning, Gary Johnston* Geodesy during the PCMEGA2002/2003 summer season
- 14:20-14:40** *Larry Hothem* U.S. Geodetic Activities in Antarctica - an Update
- 14:40-15:00** *Hannu Koivula, Jaakko Makinen* Geodetic activities at Finish Antarctic research station Aboa
- 15:00-15:20** *Andrzej Pachuta* An outline of polar expeditions of the scientists from Warsaw University of Technology
- 15:20-15:40** *Hans Werner Schenke* Actual and planned activities in geodesy and bathymetry
- 15:40-16:00** *Olexandr Dorozhynskyy and Volodymyr Glotov* Photogrammetrical investigations of the Antarctic coast
- 16:20** **Session 2: Atmospheric impacts on GPS observations in Antarctica** *Chairman Jan Cisak*
- 16:20-16:40** *Alexander Prokopov, Yeugenij Remyev* Troposphere delay modeling for GPS measurements in Antarctica
- 16:40-17:00** *Jan Cisak* Overview of the research on the atmospheric impact on GPS observation in polar regions
- 17:00-17:20** *Fedir Zablotskyj, Olexandra Zablotska and Natalya Dovhan* An analysis of contribution of the troposphere and lower stratosphere layers to forming of the tropospheric delay wet component
- 17:20-17:40** *Alexander Prokopov, Alla Zanimonska* The Second Order Refraction Effects for GPS Signals Propagation in the Ionosphere
- 17:40-18:00** *I. Shagimuratov, A. Krankowski, L. W. Baran, J. Cisak, G. Yakimova* Storm-time structure and dynamics of the ionosphere obtained from GPS observations
- 18:00-18:20** *I. Shagimuratov, L. W. Baran, A. Krankowski, J. Cisak, I. Epishov* Development of TEC fluctuations in Antarctic ionosphere during storm using GPS observations
- 18:20-18:40** *P. Wielgosz, I. Kashani, D. Grejner-Brzezinska, J. Cisak* Regional Ionosphere Modeling Using Smoothed Pseudoranges
- 18:40-19:00** *Svetlana Kovalenok, Gennadi Milinevsky, Vladimir Glotov, Korniliy Tretjak, Rudolf Greku, Yury Ladanovsky, Pavel Bahmach* Argentine Island ice cap geodesy survey for climate change investigation
- 19:00** Ice-breaker party

Tuesday, 16th September 2003

- 9:00** **Session 3: Local and Regional geodetic networks; past and future** *Chairman Larry Hothem*
- 9:00-9:20** *E Dongchen, Zhou Chunxia, Liao Mingsheng* Application of SAR Interferometry in Grove Mountains, East Antarctica
- 9:20-9:40** *E Dongchen, Zhang Shengkai, Jiang Weiping* The Establishment of GPS Control Network and

REPORT OF THE FIFTH SCAR ANTARCTIC GEODESY SYMPOSIUM

- Data Analysis in the Grove Mountains, East Antarctica
- 9:40-10:00** *Richard D. Sanchez* Positional Accuracy of Airborne Integrated Global Positioning and Inertial Navigation Systems for Mapping in Glen Canyon, Arizona
- 10:00-10:20** *A.Capra, F. Mancini, M. Negusini, G. Bitelli, S. Gandolfi, P. Sarti, L. Vittuari, A. Zanutta* VLNDEF network for deformation control and as a contribution to the Reference Frame definition
- 10:20-11:00** *Larry Hothem* Experiences with Remote GPS Observatories in Southern Victoria Land
- 11:20 Session 4: Local and Regional geodetic networks; past and future** *Chairman E Dongchen*
- 11:20-11:40** *Larry Hothem* LIDAR Data and Comparisons with Other Measurements
- 11:40-12:00** *P.Sarti, J.Manning, A.Capra, L.Vittuari* A project on local ties and co-locations in Antarctica
- 12:00-12:20** *Alexander Yuskevich* Accomplishment of topographic-geodetic research works in Antarctica
- 12:20-12:40** *Yevgen Zanimonskiy* On the Randomization of GNSS Solutions
- 12:40-13:00** *Kornylj Tretyak* Optimization of geodynamic network on the Argentina Islands neighbouring to Vernadsky antarctic station
- 14:00 Session 5: Antarctic Gravity and Sea level monitoring** *Chairman Alessandro Capra*
- 14:00-14:20** *G. Bitelli, A. Capra, F. Coren, S. Gandolfi, P. Sterzai* Geoid estimation on Northern Victoria Land
- 14:20-14:40** *Alexander Marchenko, Zoryana Tartachynska, Alexander Yakimovich, Fedir Zablotyskiy* Gravity anomalies and geoid heights derived from ERS-1, ERS-2, and TOPEX/POSEIDON altimetry in the Antarctic Peninsula area
- 14:40-15:00** *Gennadi Milinevsky* Tidal observations at Faraday/Vernadsky Antarctic Station
- 15:00-15:20** *Krynyski J., Cisak J., Zanimonskiy Y.* Contribution of data from polar regions to the investigation of GPS positioning accuracy and short-term geodynamics. Current results and perspectives
- 15:20-15:40** *Rudolf Greku, Ksenya Bondar, Victor Usenko* Application of the Planetary Geodesy Methods (the Geoid Theory) for the Reconstruction of the Earth's Interior Structure in the Western Antarctic
- 16:00-18:30 City-tour "By streets of the old Lviv"
- 19:30-22:00 Opera – house

Wednesday, 17th September 2003

- 9:00 Session 6: The SCAR Antarctic Neotectonics program** *Chairman Phil O'Brien*
- 9:00-9:20** *Gary Johnston* The determination of tectonic motion from long occupation of GPS in East Antarctica
- 9:20-9:40** *Valentyn Maksymchuk, Yury Gorodysky, Ihor Chobotok, Valentyna Kuznetsova* Recent Geodynamics of the Earth's Crust in the Region of Antarctic Station Akademik Vernadsky due to Results of Tectonomagnetic Investigations
- 9:40-10:00** *Yu.V. Kozlenko, I.N. Korchagin, V.D. Solovjov* Gravity studies of the western Antarctic region – new possibilities in geophysical modeling
- 10:20 Session 7: GIANT Program activities** *Chairman Gary Johnston*
- 10:20-10:40** *Phil O'Brien* The New SCAR - What should we do next?
- 10:40-11:00** *John Manning, Gary Johnston* Overview of the GIANT program
- 11:00-11:20** *Gary Johnston* The creation of a project to improve the stability of the Antarctic Reference Frame within ITRF
- 11:20-11:40** *Gary Johnston* The sub project of high precision local ties between collocated techniques in Antarctica (ex VLBI-GPS, GPS-DORIS, GPS-GLONASS, GPS –tide gauge benchmarks, tide gauge calibration and ties to coastal benchmarks)
- 11:40-12:30** Proposals for the International Polar Year 2007
Proposals for an AGS04 meeting
Closing the Symposium

Antarctic Geodesy Symposium 2003**Monday, 15 September 2003**

Ukraine National Antarctic Program: geodesy activity	Lytvynov
Evolution of the SCAR GIANT program	Manning
Geodesy activities in the Prince Charles Mountains	Johnston
U.S. Geodetic Activities in Antarctica - an Update	Hothem
Geodetic activities at Finish Antarctic research station Aboa	Koivula
An outline of polar expeditions of the scientists from Warsaw University of Technology	Pachuta
Actual and planned activities in geodesy and bathymetry	Schenke
Photogrammetric investigations of the Antarctic coast	Dorozhynskyy
Troposphere delay modeling for GPS measurements in Antarctica	Prokopov
Overview of the research on the atmospheric impact on GPS observation in polar regions	Cisak
An analysis of contribution of the troposphere and lower stratosphere layers to forming of the troposphere delay wet component	Zablotskiy
The Second Order Refraction Effects for GPS Signals Propagation in the Ionosphere	Prokopov
Storm-time structure and dynamics of the ionosphere obtained from GPS observations	Shagimuratov
Development of TEC fluctuations in Antarctic ionosphere during storm using GPS observations	Shagimuratov
Regional Ionosphere Modeling Using Smoothed Pseudoranges	Wielgosz
Argentine Island ice cap geodesy survey for climate change investigation	Kovalenok
On the influence of the Solar activity on the results of GPS measurements	Kostetska

Tuesday, 16 September 2003

Application of SAR Interferometry in Grove Mountains, East Antarctica	Dongchen
The Establishment of GPS Control Network and Data Analysis in the Grove Mountains, East Antarctica	Dongchen
Positional Accuracy of Airborne Integrated Global Positioning and Inertial Navigation Systems for Mapping in Glen Canyon, Arizona	Sanchez
VLNDEF network for deformation control and as a contribution to the Reference Frame definition	Capra
Experiences with Remote GPS Observatories in Southern Victoria Land	Hothem
LIDAR Data and Comparisons with Other Measurements	Hothem
A project on local ties and co-locations in Antarctica	Sarti
Accomplishment of topographic-geodetic research works in Antarctica	Yuskevich
On the Randomization of GNSS Solutions	Zanimonskiy
Optimization of geodynamic network on the Argentina Islands neighboring to Vernadsky Antarctic station	Tretyak
Geoid's estimation on Northern Victoria Land	Bitelli
Gravity anomalies and geoid heights derived from ERS-1, ERS-2, and TOPEX/POSEIDON altimetry in the Antarctic Peninsula area	Marchenko
Tidal observations at Faraday/Vernadsky Antarctic Station	Milnevsky
Contribution of data from polar regions to the investigation of GPS positioning accuracy and short-term geodynamics. Current results and perspectives	Krynski
Application of the Planetary Geodesy Methods (the Geoid Theory) for the Reconstruction of the Earth's Interior Structure in the Western Antarctic	Greku
Results of the GPS, Ground Photogrammetry, Echosounding and ERS Interferometric Survey	Greku

Wednesday, 17th September 2003

The determination of tectonic motion from long occupation of GPS in East Antarctica	Johnston
Recent Geodynamics of the Earth's Crust in the Region of Antarctic Station Akademik Vernadsky Due to Results of Tectonomagnetic Investigations	Maksymchuk
Gravity studies of the western Antarctic region – new possibilities in geophysical modeling	Kozlenko
The New SCAR - What should we do next?	O'Brien
The sub project of high precision local ties between collocated techniques in Antarctica (ex VLBI-GPS, GPS-DORIS, GPS-GLONASS, GPS –tide gauge benchmarks, tide gauge calibration and ties to coastal benchmarks)	Johnston